OPTICS OF PHOTONIC CRYSTALS AND THEIR POTENTIAL APPLICATIONS

THESIS

SUBMITTED FOR THE AWARD OF THE DEGREE

OF

Doctor of Philosophy

IN

APPLIED PHYSICS

Submitted by

ASISH KUMAR

Enrollment No. 404/14

Under the Supervision of

Dr. KHEM BAHADUR THAPA

DEPARTMENT OF APPLIED PHYSICS

SCHOOL FOR PHYSICAL SCIENCES

BABASAHEB BHIMRAO AMBEDKAR UNIVERSITY

(A CENTRAL UNIVERSITY)

LUCKNOW-226025, U.P. (INDIA)

2020

Dedicated to My Parents

DECLARATION

I declare that the thesis entitled **"OPTICS OF PHOTONIC CRYSTALS AND THEIR POTENTIAL APPLICATIONS"** has been prepared by me under the supervision of **Dr. Khem Bahadur Thapa**, Department of Applied Physics, School for Physical Sciences, Babasaheb Bhimrao Ambedkar University, Lucknow. No part of this thesis has formed the basis for the award of any degree, diploma or fellowship previously. Further, I declare that the material embodied in the present work is based on original research work and the indebtedness to others has been duly acknowledged at relevant places. This is also declared that the thesis is essentially free from all kinds of plagiarism.

Kumar

(**Asish Kumar**)

Department of Applied Physics, School for Physical Sciences,
Babasaheb Bhimrao Ambedkar University, Vidya Vihar,
Raebareli Road, Lucknow-226025, U.P., India.

Date: 26/08/2020
Place: Lucknow

CERTIFICATE

This is to certify that the thesis titled **"OPTICS OF PHOTONIC CRYSTALS AND THEIR POTENTIAL APPLICATIONS"** submitted by **Mr. Asish Kumar** is an original research work and has not been previously submitted in part or full for the award of any other degree or diploma to this or any other university or institutions.

The thesis submitted to the Babasaheb Bhimrao Ambedkar University, Lucknow satisfies all the requirements as stipulated in the *Doctor of Philosophy (Ph.D.) regulations -1999 as amended in 2013* and it is fit for submission and evaluation for the award of the degree of Doctor of Philosophy of the University.

Date: 26/08/2020

(Supervisor)

Dr. Khem B.Thapa
Assistant Professor
Department of Applied Physics
Babasaheb Bhimrao Ambedkar University
(A Central University) Lucknow-226025

(Head of the Department)

विभागाध्यक्ष
Head
भौतिकी विभाग
Deptt. of Physics
बाबा साहेब भीमराव अम्बेडकर विश्वविद्यालय
Baba Saheb Bhimrao Ambedkar University
लखनऊ - 226025 उ0 प्र0, भारत
Lucknow - 226025, U.P., India

ACKNOWLEDGEMENT

It is my firm belief that any major research work to result in a positive outcome including a worthy thesis requires the culmination of several factors such as a meaningful subject which can motivate a determined researcher to take up the challenge, a learned and sincere guide in the form of friend, relative and colleague who selflessly encourage and help the researcher throughout the research. I had the honour and privilege to have **Dr. Khem Bahadur Thapa** as an excellent guide. I take this opportunity to place on record my heart felt and sincere gratitude and deep indebtedness to him without whose guidance this work could not have been meaningfully concluded. I also owe my sincere thanks and sense of deep gratitude to **Prof. Bal Chandra Yadav**, Head, Department of Physics, School of Physical & Decision Sciences, Babasaheb Bhimrao Ambedkar University, for providing necessary facilities in the department in a very kind behavior.

I am extremely thankful to my teachers **Prof. Devesh Kumar, Dr. Ramesh Chandra**, **Dr. Anil K. Yadav**, **Dr. Devendra Singh** for their valuable suggestions and encouragements which have been a great asset to me during the entire course of study. I owe my deep gratitude towards them for their constant motivation and moral support. I feel myself blessed to have such teachers. Also, I am thankful to staff members at Babasaheb Bhimrao Ambedkar University especially **Department of Physics (DOP).**

I am highly thankful to **Prof. S. P. Ojha**, Former Vice-Chancellor CCS University Meerut and Former Head, Banaras Hindu University, Varanasi, **Dr. Narendra Kumar**, Senior Assistant Professor & Coordinator, Department of Physics, CASH, Mody University of Science and Technology, Laksmangarh-332311, Sikar (Raj.) for his valuable suggestions and encouragements. Also, I am highly grateful to **Dr. Asheesh Kumar** and **Mr. Ajeet Singh**, Department of Physics, BBAU Lucknow for his constant support and providing help at the hour of need. Without his support, the thesis cannot be in its present form. I am highly thankful to **Shri Balan G,** BBAU for his moral support and encouragement.

I am also thankful to my seniors **Dr. Jitendra Kumar, Dr. Deep Kumar, Dr. Samiksha Sikarwar, Dr. Rajkamal Shastri, Dr. Surya Pratap Goutam, Dr. Yashkaur Singh, Dr. Ratindra Gautam, Dr. Utkarsh Kumar, Vikas Kumar**

Verma, Dr. Prabal Pratap Singh, Dr. Mahesh Kumar, Ms. Priyanka Chaudhary and Mr. Diptarka Roy for his valuable suggestions and encouragement.

I am also thankful to our research group members **Mr. Krishan Pal, Ms. Abhisikta Bhaduri, and Mr. Pawan Singh** for his supporting every moment of my journey.

I would like to acknowledge the contribution of my friends and colleagues, **Mr. Shyam Sundar, Mr. Prashant Priya Chandra, Mr. Ujjwal Chaudhary, Mr. Ravi Pratap Jauhar, Er. Atul Kumar Verma, Mr. Guddu, Mr. Arun Kumar, Mr. Soumya Vishwas, Mr. Kuldeep Kumar, Mr. Sudhir Kumar, Dr. Dinesh Verma, Mr. Pintu Yadav, Dr. Dileep Yadav, Mr. Aman Pervan, Mr. Subhash Bhargva, Mr. Bhanu Pratap, Mr. Saroj Kumar, Er. Vishal Saxena, Mr. Mahendra Kumar, Mr. Sudhakar Pushkar, Mr. Shakti Singh and Ms. Shivani Chaudhary** for a joyful and healthy environment around me to work.

Finally, I would like to pay my highest regard to my grandparents **Smt. Parwati Devi** and **Late Shri Dalla Ram**. I owe my indebtedness towards my parents **Shri Chunni Lal** and **Smt. Suhela Devi** for their love, support and sacrifice from the very first day of my journey of life. Also, I am highly thankful to my pride, my younger brothers **Mr. Alok Gautam, Mr. Pushpendra Kumar, Mr. Akash Deep Gautam,** and my younger sister **Ms. Anshu Lata Gautam** for his unconditional love and support. I am highly thankful to my friend **Ms. Archana Gautam** for unconditional love and support at every moment of my struggle.

I am highly thankful to my well wishers **Shri Prem Praksh, Smt. Prabha Verma, Dr. Anil Kumar, Shri Kshetra Pal, Shri Mauji Lal Gautam, Shri Ashok Bharti, Shri Arjundev Bharti, Shri Balveer Singh, and Shri Sumendra Kumar Singh** for moral support and encouragement.

Last but not the least, my final words of thanks will be for Almighty God, for his countless blessings, mercy and companionship through all turmoil of my life.

Kumar.

Asish Kumar
(Ph.D. Scholar)

LIST OF PUBLICATIONS

Part of the thesis published and communicated in the refereed journals:

1. **Asish Kumar**, N. Kumar and K. B. Thapa, Tunable broadband reflector and tunable narrowband filter of a dielectric and magnetized cold plasma photonic crystal, Eur. Phys. J. Plus 133 (2018) 250-8.
2. **Asish Kumar**, K. B. Thapa and S. P. Ojha, A tunable broadband filter of ternary photonic crystal containing plasma and superconducting material, Ind. J. Phys. 93(6) (2018) 791-798.
3. **Asish Kumar**, K. B. Thapa, Multichannel filter application of a magnetized cold plasma defect in periodic structure of ZnS/TiO_2 materials, Opt. Quant. Electron 51(11) (2019) 355-14.
4. **Asish Kumar**, K. B. Thapa and A. K. Yadav, Enhancement of absorption property of one-dimensional ternary periodic structure containing plasma based hyperbolic material for the application of microwave devices, J. Mag. Mag. Mater 93 (2019) 165371-9.

Work not included in thesis

1. **Asish Kumar**, N. Kumar, G. N. Pandey, D. Singh and K. B. Thapa, Metamaterial-plasma based hyperbolic material for sensor, detector and switching application at microwave region, J. Phys.: Cond. Mat. 32 (2020) 325701-13.
2. **Asish Kumar** and K. B. Thapa, Study of optical property of defect mode in one dimensional double negative photonic crystal with plasma, Adv. Sci. Eng. Med. 10(7-8) (2018) 837-841.
3. **Asish Kumar**, P. P. Singh and K. B. Thapa, A new idea for broadband reflector and tunable multi-channel filter of one dimensional symmetric photonic crystal with magnetized cold plasma defects, AIP Conf. Proc. 1953(1) (2018) 060043-4.
4. **Asish Kumar**, K. B. Thapa and G. N. Pandey, Tunable optical properties of Hyperbolic meta-material, AIP Conf. Proc. 2142(1) (2019) 050002-3.
5. **Asish Kumar**, P. Singh, K. Pal, N. Kumar and K. B. Thapa, Broadband reflector of 1D photonic crystal containing TiO_2/SiO_2 material at visible region, AIP Conf. Proc. 2220(1) (2020) 020068-4.

6. **Asish Kumar**, K. B. Thapa, N. Kumar and A. K. Yadav, Tunable Broadband Reflector in a One-Dimensional Meta-Photonic Crystal with Symmetrically Introduced Magnetized Cold Plasma as Defect, Book chapter, Advances in Photonic Crystals and Devices, CRC Press, Taylor & Francis USA 2019.
7. N. Kumar, A. K. Poonia, **Asish Kumar**, K. B. Thapa, G. N. Pandey, B. Suthar, Analysis of the impact of graphene coating on reflectivity of a silicon substrate for optoelectronic devices, AIP Conf. Proc. 2220(1) (2020) 020038.
8. **Asish Kumar**, P. Singh, K. B. Thapa, Study of super absorption properties of 1D graphene and dielectric photonic crystal for novel applications, revised in Opt. Quant. Electron 2020.

Papers presented in International Conferences/Proceedings

1. A workshop on **"Recent Advances and Fundamentals of Nanomaterials for Applications in Photonics (RAFNAP-2017)"** during February 15-19, 2017 organized by Department of Physics, National Institute of Technology, Durgapur (West Bengal) INDIA.

2. **Presented Poster in "4th Lucknow Science Congress (LUSCON-2017)"** during March 03-04, 2017 held in BBA University, Lucknow (U.P.) INDIA.

3. A workshop on "**Laser and its Applications (LAP-2017)"** during March 27-31, 2017, held in Motilal Nehru Institute of Technology, Allahabad (U.P.) INDIA.

4. **Presented Poster in** "**International Conference on Nanoscience and Nanotechnoloy (ICNN-2017)"** during September 22-24, held in Babasaheb Bhimrao Ambedkar University, Lucknow (U.P.) INDIA.

5. **Presented Poster** in "**International Conference on Condensed Matter & Applied Physics (ICC-2017)"** during November 24-25, 2017 held in Govt. Engineering College, Bikaner (Rajasthan) INDIA.

6. **Presented Poster** in "**Student Conference on Optics and Photonics (SCOP-2018)"** during October 4-6, 2018 held in Physical Research Laboratory, Ahmadabad (Gujrat) INDIA.

7. **Delivered Oral Presentation** in **"3rd International Conference on Condensed Matter & Applied Physics**" during February 7-9, 2019 held in Ambalika Institute of Technology, Lucknow (U.P) INDIA.

8. **Delivered Oral Presentation** in three day workshop on "**Computational Physics in Applied Research**" during July, 25-27, 2019 held in Gautam Buddha University, Gautam Buddha Nagar (Gr. Noida) (U.P) INDIA.

ABSTRACT

Photonic crystals (PCs) are a periodic pattern of the dielectric constants with thicknesses from micro to nanometer. If the periodic arrangement of the PCs is of the order of the wavelength of light or Electromagnetic Wave (EMW), then light or EMW cannot propagate through the PCs for some of range of wavelengths called *Photonic Band Gap* (PBG). The PBG is a unique property of photonic crystals and it is strongly dependent on refractive index contrast, scalability, periodicity, and symmetry and unit cell of internal structure of the binary or ternary periodicity of the materials. The occurrence of PBG is the interference of the waves at the interfaces and the localization of light occurs due to existence of the resonance. The manipulating and controlling the flow of light or EMW of the PBG, the photonic crystals have the great applications in research of the optical engineered materials. The photonic band gap material shows the dispersion relation for the periodic structure. The dispersion relation of the photonic crystals is correspondent to the Fresnel's reflection coefficients. The study of optical properties of the periodic structured materials or photonic band gap materials belongs to the optics of photonics. Therefore, the reflectance, transmittance and absorption of the periodic structured materials or photonic band gap materials are studied for their applications in designing the optical devices.

In modern optics, One-Dimensional Photonic Crystals (1-D PCs) offer the very interesting applications in the fields of photonics and optical engineering. The one-dimensional photonic crystals are used to fabricate the optical filters, optical switches, optical logic gates, optical storage devices, microwave absorber, sensor, detectors, resonance cavities, laser applications, high-reflecting devices, omni-directional mirrors, optoelectronic circuits etc. Due to the advancement of thin film technology as well as the concept of quantum dot, the study of the 1D-PCs has become more interesting among the researchers and industrialists.

Chapter 1 contains the development of periodic structure and type of periodic structure and discussed in detail the applications of such periodic structure in the optical science community. The basic theme of the introduction of thesis is to introduce theories for optical calculations, fabrication techniques and applications of the periodic structures. Such periodic structures are known as the photonic crystals.

Especially one-dimensional photonic crystals are also taken into consideration and discussed in detail.

Chapter 2 covers the theory and methodology for photonic crystals where Maxwell's equations for optical materials are solved for optics of photonics. The different methods are discussed in deals to solve the photonic band gap and the optical properties of the photonic crystals. In the entire thesis, the well-known simple Transfer Matrix Method (TMM) has been used to study of band structure, transmission, reflection and absorption spectra of the 1-D PCs containing metals, dielectrics, semiconductors, plasma, magnetized cold plasma, superconductor materials etc.

In Chapter 3, the band structure and transmission spectra versus frequency curve of dielectric/magnetized cold plasma periodic structure have studied theoretically with variation of varying the plasma density and the effective collision frequency of the magnetized cold plasma for right hand polarization and left hand polarization structure. The positive and negative values of applied magnetic field demonstrate the right hand polarization and left hand polarization, respectively. On variation of variable parameters of the magnetized cold plasma, the optical constant and the optical property of the material are also changed. On the basis of our calculated results of the right hand polarization and left hand polarization structure, a new idea for formation of the broadband reflector and narrow tunable filter at lower and higher frequency ranges was investigated. Hence, the one-dimensional photonic crystals with dielectric/magnetized cold plasma may be used to design of tunable photonic devices.

Chapter 4 covers the theoretically calculations of the transmittance of ternary photonic crystal containing the dielectric/Magnetized Cold Plasma (MCP)/high temperature superconducting material against frequency (GHz) with varying the incident angle, the applied magnetic field, the electron density of the magnetized cold plasma, the temperature of superconducting material and also the thickness of the magnetized cold plasma and superconducting material for the right hand polarization/the left hand polarization structure.The calculated results have proposed an innovative idea to design the broadband reflector or the high pass filter and the narrow tunable filter of the ternary photonic crystal containing the magnetized cold

plasma and the superconducting material under certain the transverse magnetic field and the operating temperature.

Chapter 5 contains a detailed analysis of the transmittance of symmetric and asymmetric one-dimensional periodic structure containing zinc sulfide and titanium dioxide with one or two defect of magnetized cold plasma layer versus frequency (GHz). The transmittance of two MCP layer inserted in symmetric periodic structure with variation of electron density of plasma as well as thickness of ZnS and TiO_2 material have found better response as comparison to one layer defect in same periodic structure. The calculated results have suggested a simple and innovative idea to fabricate the tunable multichannel filter at microwave region.

Chapter 6 includes a detailed discussion on the parallel and the perpendicular permittivity of hyperbolic meta-material, where the permittivity has analyzed theoretically with the variation of filling fraction and effective collision frequency. The real part of the parallel and the perpendicular permittivity of Hyperbolic Meta-material (HMM) have the metallic and dielectric behaviors at certain frequency range. The absorption of one-dimensional ternary periodic structure containing dielectric, silicon dioxide and hyperbolic material have studied with varying incident angle, filling fraction, electron collision frequency as well as the thicknesses of dielectric material. The study of the absorption property of the ternary periodic structure containing hyperbolic materials are very pioneering results to design the optical switch, logic gate, sensor as well as the absorber at microwave region.

Chapter 7 summarizes the work done included in the whole thesis and outlines the conclusion and future prospects.

PREFACE

Over the past few decades, the development of optics and photonics of periodic structure of different material to analyze the physical, chemical and biological processes in unprecedented detail. During our research work, we have involved the study and development of theory of the interaction of Electromagnetic Wave (EMW), especially light with matters. The fundamentals of EMW and its interaction with matter can be classified by classical electrodynamics and quantum electrodynamics. These theories are able to explain all electromagnetic phenomena. These provide a firm of basis for contemporary physics and also generate a vast range of technology applications. Now, the interaction between EMW and matter is controllable using photonic crystals or photonic band gap structure a remarkable investigation realized by combination of optical physics and micro fabrication technique. The research concerns mostly the analytical study of the optical properties of the one-dimensional periodic multilayered structure of dielectric/Magnetized Cold Plasma (MCP), dielectric/MCP/superconductor, zinc sulfide (ZnS)/MCP/titanium dioxide (TiO_2) and dielectric/silicon dioxide (SiO_2)/hyperbolic material etc. Using Transfer Matrix Method (TMM) and Bloch's theorem, we have obtained the band structure, reflectance, transmittance and absorption spectra of the one-dimensional photonic crystals. The study of band structure and transmittance of the photonic crystals containing different material having different parameters and material thickness ratio have shown the remarkable optical behavior. Such studies may give insight into the optics of periodic structure. The development of the one-dimensional photonic crystals can be utilized to study the optics of nano scale materials and photonics. The one-dimensional photonic crystals may be widely applicable for manufacturing the optical and photonic devices due to easy fabrications.

LIST OF FIGURES

TABLE OF CONTENTS

Chapter 1
Introduction

Chapter-1

Introduction

1.1 Introduction to optics behind photonics

In this chapter, we have elaborated the optics of materials; further the optics of photonic has been presented in detail by investigating the optical properties of periodic materials using the simple laws and concepts of optics. Finally, the potential application of periodic structure of different materials has been given in detail. The investigated property of photonic crystals has been discussed for potential applications of photonics and it is explained one by one.

1.2 Optics

In our daily life, we perceive the beauty of the Nature through our eyes when the light, Electromagnetic Wave (EMW), is scattered, reflected, diffracted etc. In simple way, especially light and infrared radiation, the electromagnetic wave interacts with matter and this phenomenon/process can be well understood by the well known branch of physics, which is called *Optics*. Hence, the optical instruments are accustomed to gather information of electromagnetic radiation during the interaction of light. Optics primarily deals with the study of sight. The study of interaction of light with object is related with optical density or refractive index or optics of the material. So, the optics is an excellent branch of physics in which the behavior and properties of EMW during its wave interactions with matter and this study of optics is generally used in the development of optical instruments. X-rays, microwaves, and radio waves are other forms of electromagnetic radiation, which are similar to the light and infrared radiation [1]. Most of the optical phenomenon can be accounted for the classical electromagnetic description of light.

The classical optics is characterized into two categories: (1) Geometrical optics, also called ray optics and (2) Physical optics, also called wave optics. These have been discussed below:

1.2.1 Geometrical optics

Geometrical optics describes the wave propagation of light in forms of rays which travel in straight line and whose paths are governed by the laws of reflection and refraction at interface between two medium. These waves were discovered

empirically as far back in 984 AD and have been used for the design of optical components and instruments [2].

In the Universe, every material has unique property for the electromagnetic radiation that is called optical density or refractive index (n). The refractive index is the ratio of speed of light in vacuum to the velocity of light in the given medium. The refractive index is expressed in the given form:

$$n = \frac{c}{v} \tag{1.1}$$

where n is a refractive index of the material, c and v are the velocity of light in vacuum and medium, respectively. This refractive index of the medium has optical property and this property also defines how light propagates in the medium.

Now, the question arises that how the light propagates in a medium, and researchers consider that light propagates in a medium which is called ether. In 1864, Maxwell came up with a new idea of electromagnetism, where the electricity and the magnetism are unified with the well known Maxwell's equations. Maxwell's equations came to existence after the discovery of Coulomb, Oersted, Ampere, and Faraday etc. For electricity and magnetism, the discovery of these laws for understanding the electromagnetic radiation this was the greatest achievement by Maxwell in that period. By solving Maxwell's equations, first time he arrived at the most important conclusion that light is an electromagnetic wave.

1.2.2 Wave optics

Physical optics is a broader model of light, which includes the wave effects such as diffraction and interference that cannot be accounted for geometric optics. Historically, the ray model of light was first developed by the wave model of light. As discussed earlier that Maxwell summarized the theory of Electromagnetic Waves (EMW) in a mathematical fashion and explained their propagation nature when they travel through a medium. He derived a close relationship between optics and electromagnetism [3]. The optical density or refractive index of the material with the parameters of materials is given as:

$$n^2 = \varepsilon_r \mu_r \tag{1.2}$$

where ε_r, μ_r are the relative electric permittivity and magnetic permeability of the material [4]. Based on the wave optics concept the laws of reflection, refraction, interference, diffraction, and polarization of light are well defined and the optical density is important parameter for the optical properties of materials. It means that the optics of materials or optical properties of the materials are very important to study the behavior of interactions of materials with light. Besides this, the concept of modern optics is also important to describe the transition of electromagnetic radiation.

1.2.3 Modern optics

The dual behavior of the light is shouted as quantized energy of Electromagnetic Wave (EMW), which is called photon, where photon is a basic unit of light or electromagnetic radiation. The photons are the quantized energy of electromagnetic radiation, where the quantized energy levels of atoms and the spectrum of discharge emission from hydrogen take place in a particular optical radiation. The behavior of interaction between light and matter creates the development of quantum mechanics. However, the subfield of quantum mechanics deals with light-matter interaction was considered as a research into matter rather than light, and the researchers spoke about the atomic physics and quantum electronics in 1960. Laser and its application of this field of science has become an active field, and the quantum mechanics underlying the laser's principle was studied now with more emphasis on the properties of light called *quantum optics*. Quantum optics deals with the properties and application of quantum mechanics to the optical systems. Optical science is the branch of quantum optics and studied in many related disciplines including astronomy, various engineering fields, photography, and medicines.

In general, the practical applications of optics are found in variety of technologies and everyday life, including mirrors, lenses, telescope, microscope, lasers and fiber optics [5-7]. The properties of mirrors, lasers and fibers are analyzed with the concept of periodic structure. So, we now discuss the concept and development of periodic structure.

1.3 Basic introduction of periodic structure

In 1887, Lord Rayleigh [8] investigated first time a purely periodic system extending to infinity in one dimension and found that the structure exhibits a range of wavelengths, forbidden to propagate inside this periodic structure. In 1930, condensed

matter physicists realized that a forced electron belongs to some intervals of permitted energies, where forbidden energy bands occur due to periodic potential of the atomic lattice. An excellent property of the periodic structure is to control the propagation of wave due to existence of the forbidden gaps. In 1946, Brillouin [9] found the discontinuities in the relation between the frequency (ω) and the wave vector ($\vec{K}$) for any wave propagating in a periodic medium. These discontinuities are called the frequency gaps in the dispersion relation $\omega = f(\vec{K})$. Later in 1958, Slater [10] described the actual condition behind the occurrence of forbidden gaps. In this forbidden gap, the wave vectors are purely imaginary in periodic dielectric materials and an imaginary wave vector corresponds to damping of the wave in the crystal. Thus, the electromagnetic waves having the energies within the gap could not be transmitted through the bulk of such crystals.

For the past six decades, semiconductor physics has revolutionized the electronic industry and has played a crucial role in every aspect of modern technology due to the invention of the Si-based transistor devices. Success of electronics occurs in the semiconductor materials. The electronic devices based on semiconductor technology are one of the most common objects around us. Semiconductor crystals have a periodic arrangement of atoms occurring naturally in them. All these developments are occurred due to the manipulation of forbidden band gaps of the semiconductor materials. So, it is necessary to develop the new materials and concepts with increased optical functionality for a variety of applications.

In the past years, lots of researchers have recommended that they may now be able to achieve similar things with light. In order to realize the advanced optical elements needed for networks, new approaches for the manipulation of photons will have to be developed. This objective is achieved by a new type of materials known as photonic crystals which is an optical analogue of the electronic semiconductors [11]. The importance of the structure for electromagnetic properties was first pointed out by the Yablonovitch [11] and John [12] by drawing analogies between the behavior of light and electron. Yablonovitch [11] introduced the forbidden gap for controlling the spontaneous and stimulated emission of light in 3-D periodic dielectric materials; and John introduced the gaps to induce the Anderson localization of light waves in the super lattices. After these investigations, the optical community generalized a new

term in optics which is known as a photonic crystal and such photonic crystal bears the Photonic Band Gap (PBG) that will discuss in the next section.

1.4 Photonic crystal

Photonic crystal (PC) is a periodic arrangement of dielectric materials that exhibits strong interaction with electromagnetic wave. It is composed of a multilayer stack of alternating high and low optical constants of dielectric materials. Strong interaction occurs with electromagnetic wave in a material due to interference of the reflected and refracted light at all interfaces inside the materials. The complex pattern of superimposing beams will reinforce or cancel out one another. With reference to the wavelength of light, the direction of incidence, the refractive index, size and arrangement of the building stacks are defined. Due to this, one can find a frequency band for which the propagation of light is forbidden in a certain direction. The forbidden frequency region is called photonic band gap [13, 14].

Photonic crystal (PC) structure can be seen in the Nature in the skins and furs of small creatures. For example, the butterfly wing of the mitouragrynea produces a greeny blue iridescent reflection depending on the angle from which it is viewed. Some Mexican and Australian opal gemstones (minerals), whose surfaces are present in periodic stacks of the silica particles, are the other visible examples.

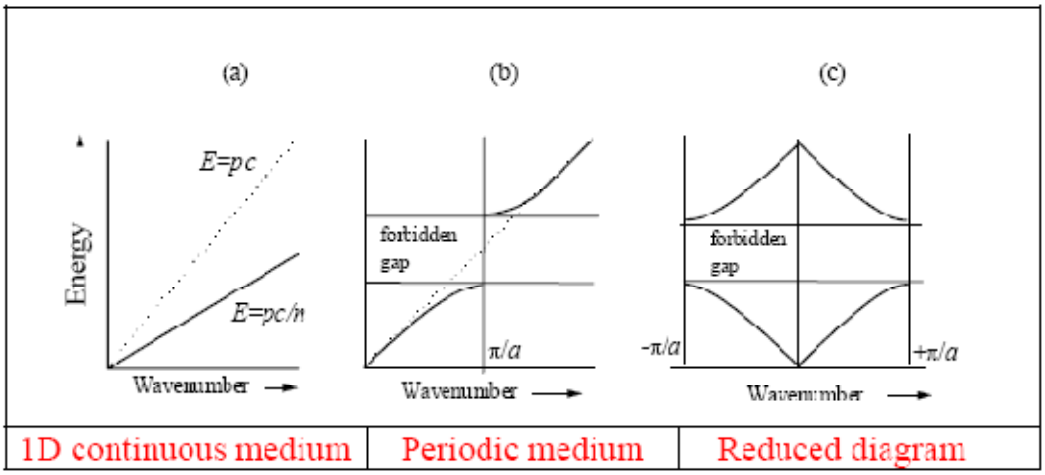

Figure 1.1: Photonic band structure in 1-D and Brillouin zones for electromagnetic waves [13, 14]

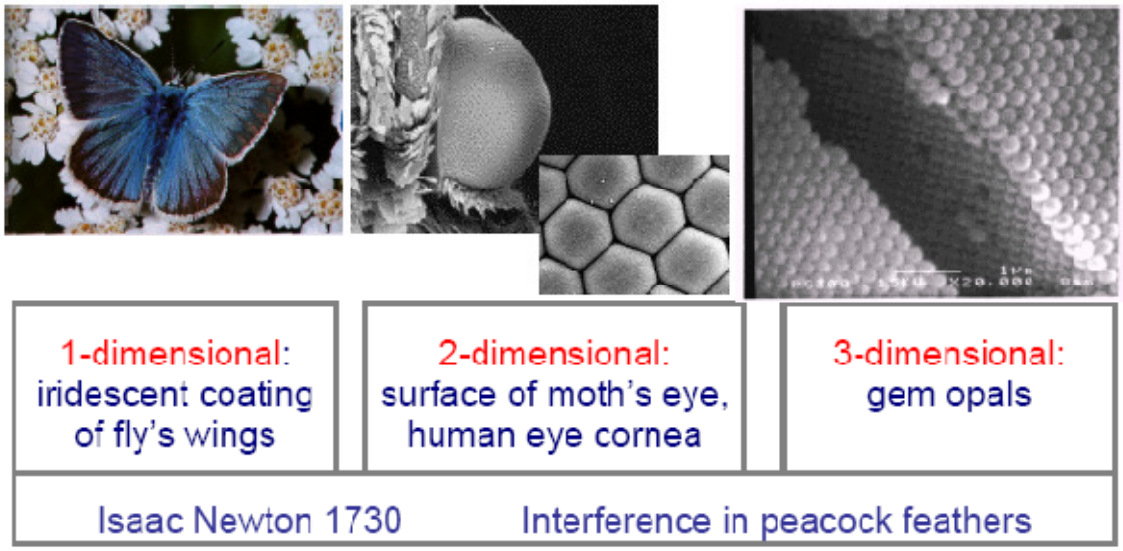

Figure 1.2: Natural photonic crystals [13, 14]

The electromagnetic wave can be controlled using periodic structure, because such periodic structure exhibits an excellent property of band gap, which is called photonic band gap. The photonic band gap can be tuned by varying the variable parameters of the material. Now, we will discuss the formation of photonic band gap in the next section.

1.5 Origin of the Photonic Band Gap (PBG)

Photonic crystal basically does not have the continuous symmetry, like the system of atoms. They have shows discrete translational symmetry. Thus, these crystals are not invariant under certain condition of translations of any distance, but only under distances that are multiple of a fixed step length. This basic step length is also called the *lattice constant* 'a', and the basic step vector is called primitive lattice vector 'a', because of this symmetry, $\varepsilon(\mathrm{r}) = \varepsilon(\mathrm{r} + \mathrm{R})$. By repeating this translation, we can see that $\varepsilon(\mathrm{r}) = \varepsilon(\mathrm{r} + \mathrm{R})$ for any R that is an integral multiple of a. The dielectric unit that is repeated over and over is known as the unit cell. We have see that the behavior in electromagnetic wave interaction with single layer without any band as shown in Figure 1.3 (a). Similarly, when electromagnetic wave interaction with the multilayer periodic structure takes place then some part of light will be reflected and some will be transmitted from the interface and it forms the interference due to surface wave at the interfaces, and hence forms a forbidden range which is called *Photonic Band Gap* (PBG) as shown in Figure 1.3 (b). The same phase of surface wave forms the high

intensity and opposite phase shows the nearly zero intensity as shown in Figure 1.3 (c).

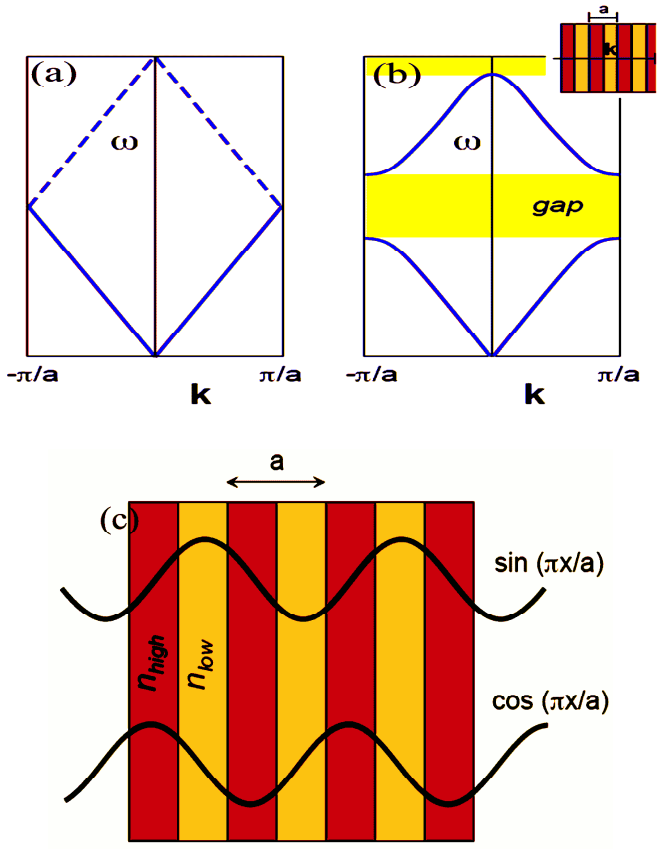

Figure 1.3: Shows (a) No gap (b) Photonic band gap and (c) Propagation of light in 1-D periodic structure

The basic theory of discrete periodicity in a certain direction leads to a dependent of H for that direction that is simply the combination of plane waves, modulated by a periodic function because of the periodic lattice as:

$$H(r) = e^{ik_r \cdot r} u_k(r) \tag{1.3}$$

where $u_k(r)$ is periodic in the real space lattice. This result is commonly known as Bloch's theorem and the form of above equation is known as Bloch state. The wave vectors k_r that differ by integral multiples m of $2\pi/a$, while not different from a physical point of view. In fact, all modes with the wave vector are of the form $k_r + m(2\pi/a)$ where m is an integer, and they form a degenerate set and leave the state unchanged. Thus the mode frequencies also periodic in k_r: $\omega(k_r) = \omega(k_r + m(2\pi/a))$. In fact, we only require to consider that k_r is exists in the

range $-\pi/a \le k_r \le \pi/a$. This range of non-redundant values of k_r is called the Brillouin zone.

$$\nabla \times \left(\frac{1}{\varepsilon_r} \nabla \times \psi \right) + \left(\frac{\omega(k)}{c} \right)^2 = 0 \tag{1.4a}$$

where, ψ is electromagnetic field wave.

By substituting the Bloch state in the Master equation (1.4a), we can obtain a reduced form of Master equation:

$$(ik + \nabla) \times \left(\frac{1}{\varepsilon(r)} (ik + \nabla) \times u_k(r) \right) = \left(\frac{\omega(k)}{c} \right)^2 u_k(r) \tag{1.4b}$$

The Master Eq. (1.4b) can be numerically solved for all k in the first Brillouin zone, resulting in an infinite set of modes with discretely spaced frequencies labeled with the band index 'n'. In this way, we can find an arrangement at the description of the modes of the photonic band gaps $\omega_n(k)$ of the crystal: where they are a family of continuous functions, indexed in the order of increasing frequency by the band number. The information contained in these functions is called the band structure of the photonic crystal. The optical properties of the crystals can be obtained by studying the band structure of a crystal. The band structure of 1-D photonic crystal is equivalent to the reflection coefficient of considered structure. The reflectance, transmittance and absorption spectra of the one dimensional periodic structure/photonic crystal are showed with the help of transfer matrix method in the upcoming chapters.

The Figure 1.4 shows the equality between electrons in crystalline solids and photons in photonic crystals. The energy dispersion relation for an electron in free space shows parabolic with no gaps. When electron is under influence of a one-dimensional (1-D) periodic potential, energy gaps are found and electrons with energies therein have localized (non-propagating) wave functions as opposed to electrons in allowed bands which have extended (propagating) wave functions. Similarly, a One-Dimensional (1-D) periodic dielectric medium will be present frequency regions, where propagating photons are not allowed and will find it impossible to travel through the crystal structure. One unique difference between electrons and photons

rests on the different nature of their associated waves. Electrons are scalar waves, while photons are in vectorial forms. This implies that polarization must be taken into account while dealing with photons.

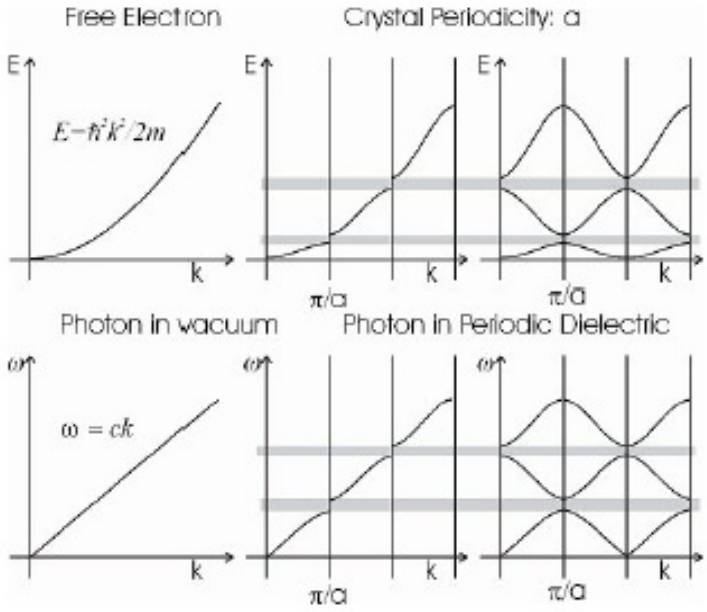

Figure 1.4: Energy dispersion relations for free electron (left) and electron in a 1-D solid (right), and for free photon (left) and photon in a 1-D photonic crystal (right) [14]

It means that the periodicity of the materials with high refractive index contrast has the photonic band gap where photons can be manipulated with such periodic medium. The periodic materials can be arranged in three ways: One-Dimensional (1-D), Two-Dimensional (2-D) and Three- Dimensional (3-D), which will be discussed in the next section.

1.6 Types of photonic crystal

Photonic Crystals (PCs) are divided as one-dimensional (1-D), two-dimensional (2-D) and three-dimensional (3-D) crystals according to the dimension of the multilayer.

1.6.1 One-Dimensional (1-D) Photonic Crystal (PC)

1-D PC consists of alternating layers of the different materials having low and high refractive index and the dielectric constant is modulated along only in one direction, as shown in Figure 1.5 [8]. 1-D photonic crystal can be fabricated easily and cheaply on a desirable wavelength scale. One-dimensional photonic crystal can be used as omnidirectional totally reflecting mirrors, frequency filters, microwave antenna

substrates, enclosure coatings of waveguide, etc. Its applications depend on the considered periodic structure, materials and frequency regions [15, 16].

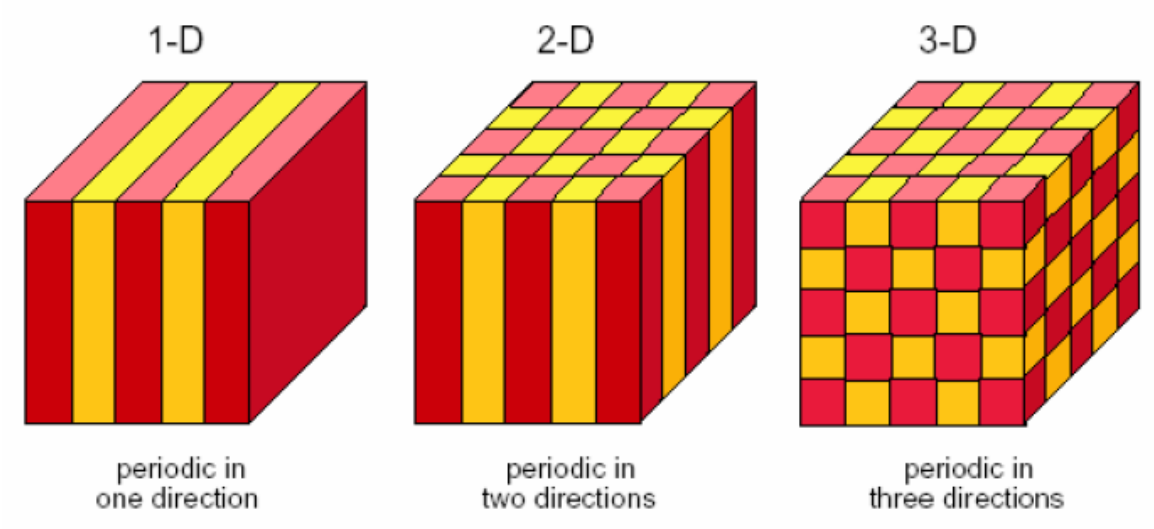

Figure 1.5: Schematic diagram of photonic crystals periodic in one-, two-, and three-dimensions, where the periodicity of the material structure of the crystals

1.6.2 Two-Dimensional (2-D) photonic crystal

In the 2-D photonic crystals, the dielectric constant of the materials is periodic in one plane and extended to infinity in the third direction. These include quadratic, hexagonal and honeycomb types of lattices, as shown in Figure 1.5. The 2-D PCs are less difficult to fabricate in comparison to the three-dimensional dielectric arrays. Some observation of fundamental phenomenon, such as Anderson localization of light, may be found easier in 2-D structures [17]. In a 2-D dielectric array, two orthogonally polarized waves, one with its E-field polarized in the 2-D-plane (TE-mode) and the other with its E-field polarized perpendicular to the 2D-plane (TM-mode) have very different dispersions [18]. Because of this a "complete photonic band gap" i.e. a frequency region in which the propagation of EM wave is completely forbidden for all-directions of propagation and polarization, is less likely to form. Reason for this is the band gap formation for individual polarization is unlikely to overlap.

1.6.3 Three-Dimensional (3-D) photonic crystal

In the 3-D PBG structures, refractive index modulation is periodic along the entire three dimensions. These types of materials assist complete localization of electromagnetic wave and provide complete inhibition of spontaneous emission of

light from atoms, molecules and other excitations. Such feedback effects have important consequences on laser action from a collection of atoms. The 3-D photonic crystals, such as the inverse opals, exhibit frequency ranges over which the ordinary linear propagation is forbidden irrespective of the direction [19, 20].

The photonic crystals have the periodic arrangement of the materials. So, the material's properties and the crystal properties have to affect the property of the photonic crystals, which will be discuss the next section.

1.7 Properties of photonic crystals

The optical features of photonic crystal will depend on several parameters they are:

1.7.1 Refractive index contrast (δ)

It is defined as the ratio of refractive index between the high dielectric constant materials to that of the low dielectric constant material.

1.7.2 Lattice parameter (a)

It is the separation of distance between scattering building blocks of periodicity. The operating range of wavelength of the photonic crystal is directly proportional to the lattice parameter. The lattice parameter is depending on the unique property of photonic crystal that is photonic band gap.

1.7.3 Filling fraction (f)

It is ratio between the volumes occupied by the material with respect to the total volume of the composite material. Composite is mixture of two materials and the filling fraction is very important property to study the optical property of composite material because the optical density/refractive index is changed.

1.7.4 Symmetry of the structure

The position of the building blocks of the photonic crystals will set the symmetry of the lattice. Symmetry can be used to calculate strong point in the structure as well as in defect in a periodic structure.

1.7.5 Topology

It may be changed by interpenetrating the structure or isolating them Economou [20] and Sigalas [20] published a basic idea about topologies in photonic crystals for explaining the theory of PBG.

1.7.6 Scalability

This can be used to change the size and scale of the building blocks for electromagnetic region. The building block formation occurs in this concept.

Based on the study of the photonic crystals or photonic band structure materials and their properties, a literature review on one-dimensional photonic crystal has been studied.

1.8 Literature survey

Researchers have shown much attraction in the direction of optics of photonic crystals after the proposed the papers in 1987 [11, 12]. The growth and development of this research field can be seen with exponentially an increase in published papers on photonic crystals. At present moment, there are no sign shown about the saturation of this field. Here, a brief summary of the optics and the photonic crystals with different dielectrics and metallic materials and others material is discussed. As earlier discussion the interaction of light with ordered dielectric structures had already been studied in the optical region. The calculated results of light diffraction experiments of colloidal particles with diameters close to the optical wavelength were attributed to Bragg's reflection of visible light in the first half of the 20^{th} century [21]. Ohtaka [22] published a dynamical theory of the diffraction for visible and ultraviolet light in 1979, in which he studied that the interaction of light with a dielectric structure in a three-dimensional lattice. This tool widely used for energy band calculations in semiconductors. He also looked into account regarding the full vector of photons and did not use as a scalar approximation. Ohtaka [22] developed his theory borrowing many aspects from semiconductors. For this reason, his work was remained unknown for many years. Besides, he modeled the systems in that paper, has also had a tremendous importance as photonic crystals.

On May 18^{th} 1987, two independent research works appeared in the same issue of the journal "Physical Review Letters". The first one, published by Yablonovitch [11], dealt with the possibility of inhibiting spontaneous emission of radiation using a three-dimensional structure. This lattice has a region of forbidden energy states for photons shows photonic band gap. Second one, John [12] discussed the strong Anderson localization [23] of photons in disordered dielectric super lattices. The disordered super lattice within a lattice trapped the Electromagnetic (EM) radiations

where certain energy states were forbidden for photons. These two works are considered as the origin of the "photonic crystals or photonic band gap materials".

In 1989, John published another research work where he proposed that an fcc structure shows a complete PBG between the second and third energy band [24]. After that, 1990 was a very exciting year for the concept of photonic crystals. At the starting of this year, Satpathy et al. [25] and Leung et al. [26] published implementation of the plane wave method with the scalar approximation for the analysis of photonic bands. These theoretical and experimental data [27] showed excellent agreement. These events lead to the editor of the well-known journal "Nature" to assure that "Photonic Crystals bites the dust" [27]. Ho et al. [28] demonstrated that although fcc lattices with spherical atoms did not show the "missing" gap, but a diamond structure could do it. Later, Yablonobitch et al. [29] submitted another work in which a structure based on an fcc lattice with non-spherical atoms, that is presented a complete PBG and such structure was called "Yablonovite".

Sözüer et al. [30] proposed the plane wave method to analyze the behavior of higher energy bands in 1992. They showed a complete PBG which was formed for an fcc lattice of air holes in the semiconductor between the 8^{th} and 9^{th} bands. In 1994, a newly proposed woodpile or layer-by-layer structures followed with the diamond symmetry presented a complete Photonic Band Gap (cPBG) between the 2^{nd} and 3^{rd} bands. Yablonovite structure had been fabricated in the microwave regime at the end of 1994. At the fabrication part, two groups at Sandia Labs (USA) and Kyoto University (Japan), independently fabricated four-layer crystals based on the woodpile or layer-by-layer structures at the end of 1998. Such type of periodic structure showed the band gap effects at the mid-infrared wavelengths [31, 32]. In 1997, Velev et al. [33] succeeded to obtain the first inverse structure. In 1996, Lin et al. [34] observed that photons were strongly dispersed in 2-D crystals when their frequencies were close to the band gap edges. Kosaka et al. [35] showed experimental evidences of novel anomalous dispersion phenomena and explained on the basis of dispersion and group velocity.

In 1999, Fleming and Lin [36] presented the first photonic crystal working in the Near Infra-Red (NIR) range. After one year, Noda et al. [37] fabricated an eight layer crystal by the wafer fusion method. In 1999, the first artificial opals with the appropriated periodicity were obtained [38] and an inverse opal of silicon was

presented in 2000 by Painter et al. [39]. The research work on photonic crystal was now shifting towards negative index materials. In 1999, Pendry et al. [40] showed that how a negative μ material with the metal could be created using Split Ring Resonators (SRR). A boost came to this field, when negative refraction was experimentally verified by Shelby et al. [41] in their composite material, which was made of wire array and SRR. Furthermore, Pendry in 2000 [42] proposed that a negative index medium could be used to make a perfect lens. Negative refraction in photonic crystals had also been demonstrated [43]. A new type of photonic gap obtained by stacking alternating layers of ordinary (positive-index) and negative-index materials was proposed in 2003 by Li et al. [44]. In 2006, Panoiu et al. [45] demonstrated that photonic super lattices consisting of a periodic distribution of layers of materials with positive index and photonic crystal slabs at the operating frequency had negative effective index and presented a photonic band gap. Ricci et al. [46] experimentally demonstrated the properties of low loss superconducting materials; and Peminov et al. [47] realized experimentally about the negative refraction in ferromagnetic superconductor supper lattices at millimeter waves.

The nonlocal investigations have been founded for the exciton-photon coupling in one-dimensional photonic crystal containing of two kinds of slabs. The lower branch of the excitonicpolariton for this system is found to split into many bands separated by small band gaps [48]. The spontaneous emission of an atom embedded in a one-dimensional photonic crystal or super lattice was shown using a classical electrodynamics theory of radiation. The emission spectrum was shown to have an oscillatory behavior which follows the photonic band structure [49]. The light scattering induced optical binding of one-dimensional (1-D) dielectric photonic crystals was studied and it showed that light can induce self-organization of dielectric slabs into stable photonic crystals, with its lower band edge coinciding with the incident light frequency [50]. A theoretical analysis of the effects of dissipation on the propagation of light waves through a multilayer periodic mirror constructed from resonant absorbing atoms was presented [51]. The temporal development of extended nonlinear modes of a one-dimensional periodic structure during the build-up the nonlinearity was investigated. The experimental results were compared with numerical calculations which make use of the Floquet-Bloch approach, and the finite difference approximation [52].

The Electromagnetic Density of Modes (EDOMs) in one-dimensional photonic crystal for electric and magnetic field polarizations was analyzed. Two methods of computational technique were presented to analyze the EDOM in the lower-index layer and described the possibility of using the EDOM to establish the population inversion, which may be useful for higher-frequency lasers (e.g., X-rays) and to control any radiative processes [53]. The formulation of band structure, reflection and the transmission coefficients had been calculated by using the simple transfer matrix method. The equation of the structure revealed the existence of gaps, which is analogous to the Kronig-Penney model in the electronic band-structure problem [54]. The Maxwell's equations were calculated in an analytic manner using the Eigen-modes for the empty lattice case and compact formulas for transmittivity of the incident wave; and excitation efficiency of waveguide modes was obtained [55]. This band gap had been obtained using quite simple expressions. The band gap edges were derived for an infinite number of gaps, for both polarizations at arbitrary incident angle for the design of photonic crystal devices [56]. The effect of the polarization state and the non-perpendicular incidence of the electromagnetic wave were taken into account by: introduction of an effective excitonic susceptibility, an effective optical width of the quantum wells [57].

The wave propagation in a One-Dimensional Metal/Dielectric Photonic Crystal (1-D MDPC) containing the alternating metallic and dielectric materials had been analyzed by using the transfer matrix method in terms of the electron density, the thickness of the metallic layer, different kinds of metals, and the plasma frequency [58]. TMM for the resonant modes in nanometal/dielectric multilayer described the splitting of resonant modes [59]. Electromagnetic wave transmission at THz in a one-dimensional superconducting metallic-dielectric super lattice had been theoretically investigated [60]. Optical properties multilayer structure composed of superconducting and dielectric films were studied [61]. A terahertz multichannel transmission filter achieved within the photonic pass band. This structure possessed the comb-like resonant peaks in transmission spectrum at low temperature [62]. On comparison of all-dielectric binary photonic crystal, the photonic band gap in ternary metal-dielectric photonic crystal had been significantly enlarged. All the theoretical analyses made were based on TMM together with the Drude model of metals [63].

A theoretical analysis of the optical properties of the defect modes in a one-dimensional defective periodic structure was analyzed. Two defective PCs stacked in symmetric and asymmetric geometries had been considered for TE and TM modes [64]. To theoretically analysis of optical properties of the defect mode in a 1-D lossy symmetric defective photonic crystal containing two magnetized cold plasma defect layers using characteristic matrix method [65]. The theoretical investigation of the tunable Photonic Band Structure (PBS) for an extrinsic Plasma Photonic Crystal (PPC) was analyzed. The extrinsic PPC was a bulk cold plasma layer, which had been influenced by an externally periodic static magnetic field [66].

Electromagnetic wave propagation through one-dimensional lossy photonic crystals composed of negative and positive refractive index material layers with symmetric and asymmetric geometric structures with a defect layer at the center of the structure were investigated [67]. Transmittance properties of a one-dimensional superconductor dielectric Photonic Crystal (PC) had been analyzed and focused on the cutoff frequency [68]. Using the two-fluid model, the transmission characteristics of the one-dimensional photonic crystal had been investigated. The structure of one-dimensional photonic crystal composed of low-temperature superconductor material (NbN) and double-negative meta-material layers [69] was investigated. The transmission properties of one-dimensional dielectric–semiconductor meta-material Photonic Crystals (PCs) at Terahertz (THz) range had been theoretically studied. The numerical results showed the appearance of cutoff frequency within THz range, where the thicknesses of the constituent's materials and the filling factor had a significant effect on the cutoff frequency [70]. The transmission characteristics of one-dimensional photonic crystals containing a defect layer of nano-composite material were analyzed in infrared radiation. The structure had been many applications such as narrow band filters and among optoelectronic applications [71]. Optical properties of the defect mode in a periodic structure of magnetized cold plasma had been doped by semiconductor and found variation in electric permittivity for both right- and left-hand polarized transversal magnetic waves [72]. The optical properties of narrow transmission mode within the reflection band in one-dimensional symmetric defective photonic crystal containing double negative meta-material and high temperature superconductors had been investigated. The obtained result showed that two modes

for smaller thickness of double negative layer were affected only a single mode for larger thickness [73].

The microwave magnetic-field tunable filtering properties in a multichannel filter based on one-dimensional finite magnetized Plasma Photonic Crystal (PPC) had been investigated. The considered periodic structure had a structure of air/$(AB)^N$/air, where A is a dielectric layer, B is a plasma layer, and N is the number of periodicity. The effect of the magnetic field had caused the channel frequencies, which are being blue-shifted or red-shifted depending on the orientations of the applied magnetic field [74]. Terahertz unidirectional resonant absorption in a finite one-dimensional defective superconducting photonic crystal was theoretically investigated [75]. Transmittance characteristics of one-dimensional defective photonic crystal had been analyzed by using TMM for the microwave radiations based on the fundamentals. The defect layer was magnetized plasma. The numerical results showed the appearance of defect peaks inside the PBG. Therefore, the proposed structure had the corner stone for many applications in microwave regions [76].

The development of a photonic biosensor was proposed, which was based on a one-dimensional photonic crystal. Different types of cancer cell detection methods had been developed by introducing a defect layer in the photonic crystal using cancer cells. The sensing mechanism of the present cancer sensor was based on varying the refractive index, which led to shift in the transmission or the reflection spectrum [77]. Photonic sensing is a new technology and accurate measurement for bio-sensing applications. The proposed blood sugar biosensor in the visible region using a defective One-Dimensional Photonic Crystal (1-D-PC) had been analyzed, where the adopted structure was Air/$(SiO_2/Si)^5/SiO_2/D/SiO_2/(SiO_2/Si)^5/SiO_2$ with substrate SiO_2. The defect layer (D) had filled with blood sugar solution with different concentrations. The transmission spectrum had been calculated numerically by using TMM. The obtained results indicated that the proposed structure has higher performance as a blood sugar sensor than many previously reported data [78]. Transmittance characteristics of the one-dimensional metallic-dielectric photonic crystals in UV regions had been investigated. The current design provided a very narrow pass band filtering feature to act as a multilayer Fabry–Pérot resonator in UV short wavelength regions without introducing a defect layer inside the periodic structure [79].

On the basis of the literature review, we now select some special materials for the study of the photonic band gaps offered by them, that is, we consider the one dimensional periodic structure/one-dimensional photonic crystals. As discussed earlier, we have chosen one-dimensional photonic crystals of binary or ternary periodic structures with periodic composite of dielectric/metal/plasma and others like superconductor/meta-material.

1.9 One-dimensional periodic structure with different dielectric materials

Different types of dielectric and metallic periodic structures with crystal parameters, refractive index contrast and scalability have been considered in the present thesis. Besides this, we have considered dielectric, semiconducting, plasma, and superconductor and magnetized cold plasma material as the constituent for a one-dimensional periodic structure. The following types of one- dimensional photonic crystals are considered in this thesis.

1.9.1 Plasma and plasma photonic crystals

Plasma is a hot ionized gas consisting of equal number of positively charged ions and negatively charged electrons. The characteristics properties of plasma are different from those of ordinary neutral gases. A non-thermal plasma or cold plasma or non equilibrium plasma is plasma which is not in thermodynamic equilibrium because temperature of electron is much hotter than the temperature of heavy species like ions and neutrals. Such type of material is called plasma. We discuss the unique property of plasma when magnetized it at lower temperature.

Plasma based one-dimensional periodic structure of dielectric/plasma is known as plasma photonic crystal. First time, the one-dimensional plasma photonic crystal is considered as plasma and dielectric periodic structure, which was proposed by Hojo et al., Plasma Research Centre, Japanin 2004 [80]. As we know that the plasma is the fourth state of matter, the dielectric constant of such plasma for the frequency (ω) is represented by: $\varepsilon(\omega) = 1 - \frac{\omega_p^2}{\omega^2}$, where ω_p is the plasma frequency and it depends on the plasma density. For the electromagnetic wave transmission in one-dimensional multilayer-plasma, the EM waves are generally reflected when waves are launched into a plasma layer. However, it is well known that the waves can be perfectly transmitted without receiving reflections, if certain condition is satisfied. This is

called the Febry-Perot resonance. This phenomenon can be realized for an under dense plasma layer $\omega > \omega_p$. The reflection less transmission can be possible for multilayer plasma if $\omega = \omega_p$. This should be considered as Febry-Perot resonance [81, 82]. Shiveshwari and Mahto [83] studied the photonic band gap effect in plasma/dielectric photonic structure. The periodic structure of dielectric material, that is, Photonic Crystals (PCs) which have attracted much interest in the field of solid state and optical physics [84, 85]. This leads to a variety of possible applications such as the inhibition of spontaneous emission [11], the low loss waveguide with sharp bands [86], narrow band filters, frequency converters and strong field enhancement related to group velocity, mode frequencies near the band edges, etc. [87].

The plasma photonic crystal specially and dynamically controlled micro plasma with periodicity in one, two and three-dimensions plays a significant role in changing the refraction of electromagnetic waves. Whereas, the conventional photonic crystals are composed of solid materials including dielectrics, metals, etc. and the unique characteristics of photonic crystals, band gap and negative refraction, have been observed, which cannot be accomplished in bulk materials [88, 89]. The unique property of plasma occurs when plasma is placed in the presence of magnetic field, such type of plasma called magnetized plasma. This is discussed in the next section.

1.9.1.1 Magnetized cold plasma

During the some previous years, magnetized cold plasma has attracted lot of researchers due to abnormal behavior of plasma. If the external magnetic field is introduced in the plasma then it acts as magnetized cold plasma; and shows unique behavior due to positive and negative directions of magnetic field. If the electromagnetic wave propagation in positive and negative magnetic field directions, the propagation of magnetic field wave in the magnetized cold plasma also shows the right hand and left hand polarization, respectively. Magnetic field is very important parameter for the magnetized plasma; and the gyro-electric frequency is also affected parameter for magnetized plasma [90, 91]. Due to unique property of magnetized cold plasma, we have studied the magnetized cold plasma based periodic structure, and analyzed the optical property with variation of variable parameters, which will be discussed in Chapters 3-5.

1.9.2 Superconducting photonic crystal

Superconducting materials are known to exist with zero resistance at very low temperature below critical temperature; where Onnes [92] came with his discovery in 1911. Since 1986, superconducting behavior has been demonstrated near the temperature of liquid nitrogen, so called high temperature superconductors, which created the applications of superconductor more practically [93, 94]. Since, the discoveries of high temperature superconductivity in certain ceramic materials, the applications of these materials were explored extensively in the design of practical devices. In particular research on the fabrication and use of high temperature superconductors in thin film technology has been carried out extensively. Additionally, a large amount of researchers had been accomplished in the use of pulse laser to break quasi-particle bonds in High Temperature Superconductor (HTS) by lowering the transition temperature and including the transition from the superconducting state to the normal states. The superconductor material exhibited markedly different optical properties in the superconducting state to the normal state. If the infrared pulsed laser (1.06μm wavelength) was incident to illuminatory Yttrium Barium Copper Oxide (YBCO) thin films with intensity above critical value, then thin film switches from the superconductor to the normal state and recovers on the order of 1μs. Thus, when an HTS switches from superconducting to normal, its optical properties were changed. If HTS thin film was incorporated in the periodic structure, then the transmittance characteristics of the resulting structure became the reflected the optical properties of the HTS [95-99].

The transmission properties of a high critical temperature superconductor-dielectric multilayer photonic crystal structure had been studied and demonstrated that superconductivity was rapidly quenched (transition temperature on the order of 10^{-9} sec) when the radiation intensity was reduced below the critical value [100]. Superconductors undergo a change in optical properties in terms of index of refraction, dielectric function, dispersion relation, transmittance and reflectance as the transition is made between the Superconducting (S) and Normal (N) state, even if the degree to which the dielectric function differ between the S-state to N-state varies with normalized frequency. The change in optical properties in a high temperature superconductor thin film is though a small, can produce a pronounced switching effect, if the HTS was incorporated as one of the constitutes materials in photonic

band gap structure. The time dependent Ginzberg London theory to model the change in the dielectric functions as YBCO undergoes the S/N state. In our study, we have theoretically discussed the property of binary and ternary multilayer structure of dielectric/magnetized cold plasma/high temperature superconductor in Chapter-4.

1.9.3 Dielectric and semiconducting photonic crystal

Dielectric and semiconducting periodic structure is known as dielectric and semiconducting photonic crystal. Dielectric and semiconducting coating of thin films of materials occurs due to either the strong ionic or the direct covalent bond. For most of the cases, they are range from transparent to visible and infrared light rays. The interaction of the electromagnetic radiation with these films is treated by applying boundary conditions to solve in the Maxwell's equations at the boundary between different media. In the direction of optical coating, the wavelength of the light is always very much larger than inter atomic dimensions. Thus, for the interaction of light with matter and the study of optical properties, each layer can be described macroscopically in terms of phenomenological parameters, so called optical constants or optical parameters. The optical constant has real and imaginary parts for a complex refractive index. The real part of refractive index shows the ratio of the velocity of light in vacuum to light in medium and the imaginary part is an attenuation coefficient or decaying wave measuring the absorption of light with distance as discussed earlier. Using Maxwell's equations, it is possible to relate these frequency dependent constants to other optical parameters such as the dielectric constant and the conductivity. The periodic materials are composed of charged particles: bound and conduction electrons, ionic cores, and impurities etc. These particles move differently with oscillating electric fields, giving rise to polarization effects. At visible and infrared light frequencies, the contribution of polarization comes from the displacement of electron cloud, which produces an induced dipole moment. These parameters describe the optical effects, i.e. dielectric constant, dielectric susceptibility, and the conductivity that can be treated as scalars for isotropic material.

Generally, dielectric and semiconducting coating materials are considered as non-magnetic, and have no extra charge other than those bound in atoms [101]. The main absorption process in semiconductor and dielectrics originates from the interaction of light with electrons [102-104]. If the photon has the frequency such that its energy matches the energy needed to excite an electron to higher allowed states, then the

photon may be absorbed. The electron may be an ion core electron or a free electron in the solid. If the energy of the incoming photon does not match the required excitation energy, no excitation occurs the material is transparent to such radiation. In non-metal solids, there is need of minimum energy separating the highest filled electron states (valence band) and the lowest empty ones (conduction band), known as the energy band gap. Electron transitions from band to band composite the strongest source of absorption. In dielectrics, such as glass, quartz, some salt, diamond, many metal oxides and most plastic material, no excitation resonances exist in the visible spectrum, because the valence electrons are so tightly bound that photons with energy in the ultraviolet are necessary to free them. Ideally, photons having energy smaller than the band gap are not absorbed. Both effects are derived from the existence of large density of free electrons which are able to move so freely that no electric field may propagate within the solid. The reflecting properties of metals find numerous optical applications as in mirrors. The optical properties of semiconductor lie between the metals and insulating dielectrics. Semiconductors are normally transparent in the near infrared and absorbing in the visible spectrum, whereas the absorption in dielectrics is strongest in the ultraviolet [101]. The optical properties of dielectric and semiconducting material based periodic structure with defect of magnetized cold plasma are analyzed in detail in Chapter-5.

1.9.4 Meta-material photonic crystal

The meta-materials photonic crystal is a periodic structure containing meta-materials. Meta-materials are artificially composite materials whose internal structure generates the Electromagnetic (EM) wave properties in artificial environments that do not occur in natural environments. “Meta” word is comes from the Greek word “μετά” which means beyond the Nature [105, 106]. Generally, an artificial engineered structure is also a periodically or randomly distributed structured material. The size and spacing of meta-material is much smaller than wavelength of incident EM wave. For the existence of meta-material, the characteristic scale (α) is related with $\alpha < \left(\lambda/_{10}\right)$ where λ is the wavelength of incident EM wave. The condition belonging to the meta-materials is the sub-wavelength feature that controls the macroscopic electromagnetic properties.

Meta-material is a so hot topic in photonic crystals due to their wide applications including sub-wavelength, imaging [107-110], hyper lens [111] and optical cloaking [112, 113]. Recent development in nanofabrication technologies allow for producing several meta-material systems, where the dielectric permittivity and magnetic permeability tensor can be designed and engineered at our will. As we discussed meta-materials are the periodic arrangements of metal or dielectric material, where the arrangement follows the sub wavelength condition. Meta-materials derive their properties of the base materials as well as the designed periodic structure. These materials occur in the precise shape, size, orientation and arrangement and give their unique properties capable to manipulating EM wave by blocking, absorbing, enhancing to achieve that go beyond which is not possible with conventional materials. In these realizations, one type of the meta-material is attractive for among the researchers, which is known as *hyperbolic meta-material*.

As we know that the complex refractive index of the materials is characterized by [114]:

$$\tilde{n}=n(\lambda)+ik(\lambda) \tag{1.5}$$

where n(λ) is the real part of the complex refractive index, also called optical constant. The imaginary part of the Eq. (1.5) shows the absorption coefficient or decaying wave [115]. The complex refractive index depends on the wavelength of the incident EM wave. If the complex number is real at some wavelength, it means that the electromagnetic wave passes through the periodic structure without being absorbed (k(λ)=0), the medium is transparent for this wavelength. According to Maxwell's equations, the complex refractive index for all optical media can be described by only two parameters, i.e., electric permittivity, and magnetic permeability, which is wavelength dependent.

$$n^2(\lambda)=\varepsilon(\lambda)\mu(\lambda) \tag{1.6}$$

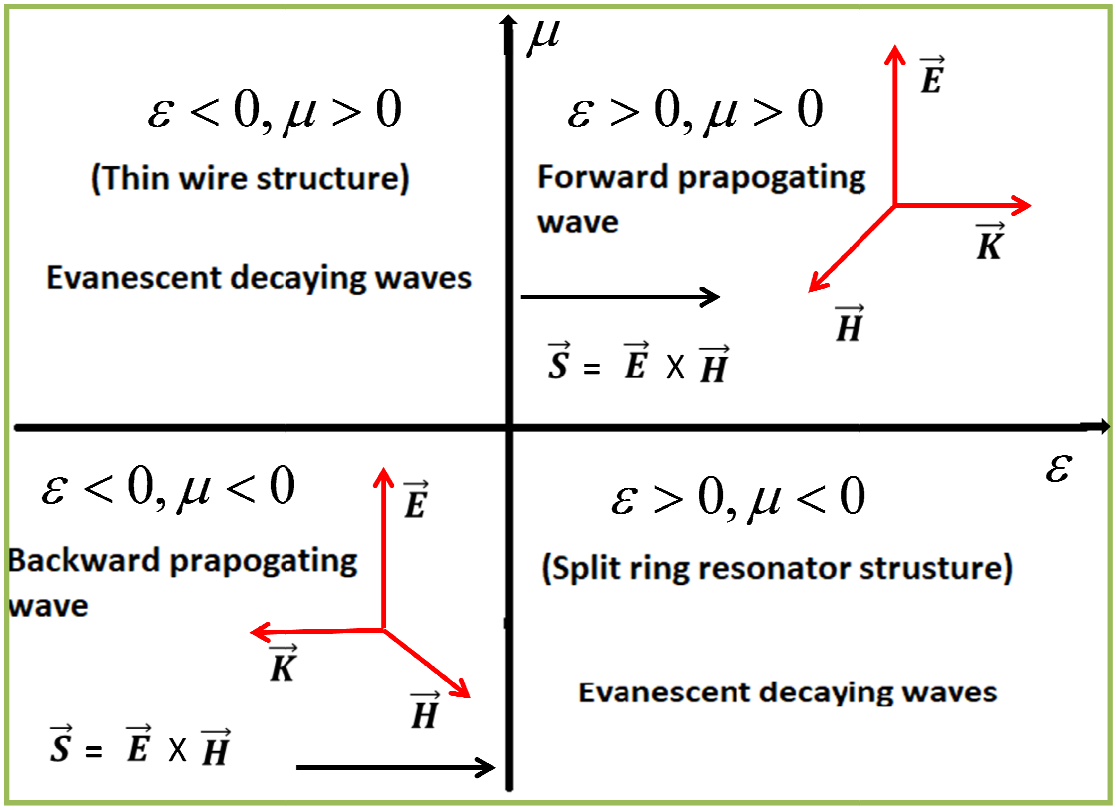

Figure 1.6: Classification of materials in the x-axis of electric permittivity and y-axis of magnetic permeability

The electric permittivity and the magnetic permeability of the material are the two parameters for the EM wave properties through the mediums [116, 117]. The classification of meta-materials can be well understood and portrayed on four quadrants on the basis of behavior of electric permittivity and magnetic permeability of the material, which is shown in the Figure 1.6. In quadrant 1 of the Figure 1.6 shows both the electric permittivity and magnetic permeability of the material as positive is called Positive Index Material (PIM) or Double Positive (DPS) material. In quadrant 2 of the Figure 1.6, negative for the electric permittivity of the material and positive for magnetic permeability of the material is called Single Negative (SNG) material or ε-Negative (ENG) material. In quadrant 3 of the Figure 1.6, the electric permittivity and magnetic permeability of the materials has the negative behavior at certain frequency range and such materials are called Double Negative (DNG) material which did not occur in nature, is called *meta-material*. At last quadrant 4 of the Figure 1.6, the electric permittivity of the material is positive and magnetic permeability of the material is negative is also called the single negative (SNG) material or μ-negative (MNG) material. In 1968, first time Veselago had given the

concept for the electric permittivity and magnetic permeability of the material both become negative simultaneously for the wave propagation in the medium and coined the name of such medium as negative refractive index of the material [118]. Such unique material having negative refractive index really arise interesting materials for researchers in the early 2000's when Smith and Pendry laid forward again the proposal of negative index refraction and its applications in perfect lenses [119] as well as cloaking devices [120]. Recently, hyperbolic meta-materials are developed in the field of meta-materials.

1.9.5 Hyperbolic meta-material

After the pioneer work of Veselago and Pendry on meta-materials, various nanostructures [116-118] were demonstrated to discuss the optical properties unobtainable from natural media. Among the various meta-material proposed in the past decades, hyperbolic meta-materials were significantly noticed, due to their ability of presenting sub-wavelength, resolution, imaging and manipulating the near field of a light emitter or a light scatter. Near field is defined by the distance, the distance is relatively shorter than the wavelength of light. The propagation properties of Hyperbolic Meta-materials (HMMs) are originated from the concept of several surface Plasmon modes [121-124]. A surface Plasmon is a collective oscillation of electrons, which is confined to the interface between a metal and dielectric and propagates along this interface. If the sizes of metal particles are in the order of nanoscales, the localized surface Plasmon's are excited at the surface of the metal when incident light interact with localized light. The concept of material of the hyperbolic behavior originates from the optics of crystals. In such media, the constitutive relations connecting the electric displacement, **D,** and the magnetic induction, **B,** to the electric and magnetic fields **E** and **H** can be written as;

$$\overline{D} = \varepsilon_0 \overline{\overline{\varepsilon}} E \tag{1.7}$$

$$\overline{B} = \mu_0 \overline{\overline{\mu}} H \tag{1.8}$$

where ε_0, μ_0 are the electric permittivity and magnetic permeability in vacuum and $\overline{\overline{\varepsilon}}$, $\overline{\overline{\mu}}$ are relative permittivity and relative permeability tensors with $\overline{\overline{\mu}}$ is unit tensor for the non-magnetic media. In diagonalization of $\overline{\overline{\varepsilon}}$ for hyperbolic material, we assume

an anisotropic medium with uniaxial dielectric tensor components that are approximated as follows [125]:

$$\overset{=}{\varepsilon} = \begin{bmatrix} \varepsilon_{xx} & 0 & 0 \\ 0 & \varepsilon_{yy} & 0 \\ 0 & 0 & \varepsilon_{zz} \end{bmatrix} \tag{1.9}$$

The three-diagonal components are positive and dependent, in general, on the angular frequency ω. The principle axes of the crystal are $\varepsilon_{xx} \neq \varepsilon_{yy} \neq \varepsilon_{zz}$ for biaxial, $\varepsilon_{xx} = \varepsilon_{yy} \neq \varepsilon_{zz}$ for uniaxial and $\varepsilon_{xx} = \varepsilon_{yy} = \varepsilon_{zz}$ for isotropic.

To determine the dispersion relation of light in a medium, which is described by Eq. (1.9), we have considered the two Maxwell's equations in the absence of source, as follows:

$$\nabla \times E = -\frac{\partial B}{\partial t} \tag{1.10}$$

$$\nabla \times H = \frac{\partial D}{\partial t} \tag{1.11}$$

where **D** and **B** are as in the Eq. (1.7) and Eq. (1.8), respectively. The plane wave expressions for both fields can be given by $E = E_0 e^{i(\omega t - k.r)}$ and $H = H_0 e^{i(\omega t - k.r)}$, where k is wave vector. By inserting the **D** and **B** in the Eq. (1.10) & Eq. (1.11), we obtain;

$$k \times E = \omega \mu_0 H \tag{1.12}$$

$$k \times H = -\omega \varepsilon_0 \overset{=}{\varepsilon} E \tag{1.13}$$

By taking curl of the k and substitution of Eq. (1.12) into Eq. (1.13), the Eigen value problem of electric field;

$$\vec{k} \times \left(\vec{k} \times \vec{E} \right) + \omega^2 \mu_0 \varepsilon_0 \overset{=}{\varepsilon} \vec{E} = 0 \tag{1.14}$$

This can be rewritten in matrix form when permittivity tensor is inserted and is called the dispersion relation:

$$\begin{pmatrix} k_0^2 \varepsilon_{xx} - k_y^2 - k_z^2 & k_x k_y & k_x k_z \\ k_x k_{yz} & k_0^2 \varepsilon_{yy} - k_x^2 - k_y^2 & k_y k_z \\ k_x k_z & k_y k_z & k_0^2 \varepsilon_{zz} - k_x^2 - k_y^2 \end{pmatrix} \begin{pmatrix} E_x \\ E_x \\ E_x \end{pmatrix} = 0 \tag{1.15}$$

where $k_0 = \frac{\omega}{c}$ is the magnitude of wave vector and $c = \frac{1}{\sqrt{\varepsilon_0 \mu_0}}$, c speed of light in vacuum. The optical axis is oriented along the z direction for hyperbolic media is given $\varepsilon_{xx} = \varepsilon_{yy} = \varepsilon_\perp$ and $k_\perp = \sqrt{k_x^2 + k_y^2}$. The imposition of nontrivial solution to Eq. (1.15) leads to the new dispersion relation [125]:

$$\left(k_\perp^2 + k_z^2 - \varepsilon_\perp k_0^2\right)\left(\frac{k_\perp^2}{\varepsilon_{zz}} + \frac{k_z^2}{\varepsilon_\perp} - k_0^2\right) = 0 \tag{1.16}$$

In the above Eq. (1.16), we have two terms in the k-space, which are equal to zero and these equations have been resembled to a spherical and an ellipsoidal iso-frequency surface: the term $(k_\perp^2 + k_z^2 - \varepsilon_\perp k_0^2)$ is described as the wave polarized in the xy-plane (ordinary or TE wave), the terms $\left(\frac{k_\perp^2}{\varepsilon_{zz}} + \frac{k_z^2}{\varepsilon_\perp} - k_0^2\right)$ is resembled to the wave polarized in the plane containing the optical axis (TM wave or extraordinary wave).

The condition substantially changes if we assume an extreme anisotropy, namely when one between $\varepsilon_\perp$ and ε_{zz} is negative. Media with such an optical signature are termed an indefinite from the point of view of mathematics [126], since their permittivity tensor represents an indefinite non-degenerate quadratic form, and exhibits a number of unconventional properties. Permittivity components with an opposite sign result in hyperbolical iso-frequency surface for the extraordinary polarization and hence it is the physical denomination of hyperbolic material. As consequences, waves with arbitrarily large wave vector retain a propagating nature while in isotropic materials they become evanescent due to the bounded iso-frequency contour [127]. The choices of $\varepsilon_\perp > 0$, $\varepsilon_{zz} < 0$ correspond to a twofold hyperboloid for hyperbolic medium is called dielectric (with reference its behavior in xy-plane) [128] or called Type I (dielectric) medium; the choices of $\varepsilon_\perp < 0$ and $\varepsilon_{zz} > 0$ describe a one fold hyperboloid for hyperbolic medium, is namely called a metallic or called Type II (metallic) medium [129].

Furthermore, we have studied in literature reviewed that the photonic band gaps of the periodic structures or photonic crystals with different materials have several applications, which will discuss briefly in next section.

1.10 Applications of photonic crystal

Photonic crystals promise to provide us a range of exciting applications from microwave to X-ray region of electromagnetic wave spectrum with the scale of lattice parameters from millimeter to angstrom scale, respectively.

1.10.1 Tunable narrowband filter and multichannel filter

The filters have lots of applications in the direction of optical communication. Mainly filter operates in a range of frequency or wavelength where light propagates or blocks the one-dimensional photonic crystal of different dielectric materials is called filter. The repeated frequency propagates or blocks and is called the multichannel filter. In the similar way, when we operate the frequency of light pass or block, such type of filter is known as tunable narrowband filter [130, 131].

1.10.2 Perfect Reflector

Metallic mirrors are used for the frequencies in the optical regions. 1-D metallic photonic crystal is simply to fabricate and it can be used as omnidirectional reflector in the optical region [132]. Omni-directional mirror can be used as the walls of laser cavities.

1.10.3 Absorption based device

The absorption of the materials property is eminent in the present scenario for the research community. The optical storage devices are also formed on the basis of absorption spectra in certain frequency ranges. Many researchers have worked on the fabrication of the microwave absorber and made possible to design the periodic structure with the help of dielectric and metallic materials. This fabrication of the metallic and dielectric materials will also simplify the concept of hyperbolic material, and the obtained absorption will be used in microwave region. The obtained absorption of the considered structure is also used to fabricate the optical logic gate, optical data storage and optical switch devices [133, 134].

1.10.4 Light emitting diode

Photonic crystals (PCs) can be used to produce high efficiency light sources [135]. By using a PC as the active material in the Light Emitting Diode (LED), one can forbid all modes of photons except those which would normally escape the crystal. Since spontaneous emission in the other modes is forbidden, so all the energy will

then go into those modes which can escape. Such type of LEDs can take advantage of the high internal quantum efficiency.

1.10.5 Photonic crystal laser

PCs can be used to produce lasers with an extremely low lasing threshold [136, 137]. PCs have the property of suppressing spontaneous emission inside the band gap. It is forbidden to emit photons with these energies for the atoms in the crystal.

1.10.6 Photonic integrated circuit

Much research is going in this field and it shall be some time when integrated photonic circuitry is produced. After that PCs are play a central role. That is why photonic crystals are considered as the new-age crystals that should lead to the entirely optical computer.

1.10.7 Other applications

Photonic crystals without a complete photonic band gap can be designed to obtain super collimators and super lenses [138, 139]. PCs can also be used as antenna substrates, resonant cavities and filters at microwave frequencies. These are some useful applications of photonic crystals in the field of optics and photonics. For fabricating the devices, the periodic structures of the materials are studied theoretically as well as experimentally. In the coming section, we will discuss about the theoretical methods and fabrication techniques for the photonic crystals.

1.11 Theoretical methods

The main theoretical models are based on the Maxwell's equations and used to calculate the optical properties of photonic crystals viz. dispersion relation, photonic band gap, transmittance, reflectance and absorption.

There are six main theoretical methods to calculate the optical properties of photonic crystals and are as follows: (1) The Transfer Matrix Method (TMM) [140], (2) The Finite Difference Time Domain (FDTD) method [141], (3) The Finite Element method [142], (4) The Plane Expansion Wave Method [143], (5) A method based on the rigorous theory of scattering by a set of rods for a two-dimensional crystal, [144] or a set of spheres for a three-dimensional crystal [145], and (6) The study of diffraction gratings [146]. We will briefly discuss those methods which are mostly used to study the optical properties of the periodic structure/photonic crystals.

1.11.1 Transfer Matrix Method (TMM)

The dispersion behavior of propagating wave in one-dimensional periodic structure can be analyzed by using the Transfer Matrix Method (TMM). This method is also known as the translational matrix method [12], based on connection of electric and magnetic field vector at interfaces of the two layers [147-149, 140]. The TMM is well defined in Ref. [12] and this method also works in k-space using Maxwell's equations and applied them on a mesh structure. It is proficient to deals with photonic band gap (PBG) materials of finite thickness using layer-by-layer matrix calculations at each interface of layers. The band structures, reflectivity and transmission coefficients of the binary and ternary layers of one-dimensional photonic crystals can be found by this method easily. Many researchers have used this method [150-153]. Based on the rigorous scattering of light, many groups implemented this method to study the optical properties of finite sized cylinders/spheres based structures [154, 155]. The TMM is also useful with diffraction gratings theory which agrees the calculation of reflection and transmission coefficients of a photonic crystal constituted by a stack of a finite number of infinite grating layers [156]. This method can deal only with an infinitely long cavity as a defect for the structure. But this method is restricted to study new PBG materials that are sophisticated doped structures and active structures.

1.11.2 Plane Wave Expansion Method (PWEM)

The PWEM is very useful and easy to execute on the photonic crystals and it gives the 2-D band structure for the certain direction. The method provides all energies of the propagating and evanescent wave in the appropriate direction. A defect in the infinite photonic crystal be treated using a super-cell. Various consequences have been obtained with this method which gives the band structure in various domains [157-159].

1.11.3 Finite Difference Time Domain (FDTD) method

The FDTD method analyze the periodic structures by the Maxwell equations in time domain form and the simulation data through the FDTD method are almost agree with the experimental measurements [160-162]. A lot of research works on the photonic crystals have been described using this method. To study the transmission through the crystal, an electromagnetic pulse is made to propagate through the material and the output intensity of electromagnetic pulse is measured. After this, a Fast Fourier

Transform (FFT) is applied to both incident and transmitted intensities and the transmission values are recorded. The FDTD method can simulate finite or infinite crystals with different possible conditions. In point of applicability, FDTD make possible to simulate the whole experimental system of photonic crystal. MIT has developed as free and open source software based on FDTD, MEEP for everyone through online copyright permission of educational purpose.

1.11.4 Finite Element Method (FEM)

The Finite Element Method (FEM) is well useful method to be applicable in electrodynamics and such method has the excessive advantage and lot of commercial softwares like as MAFIA, COMSOL, HFSS, etc. are based on this method. In this method, the simulation of the properties of the various crystals e.g. non-doped crystals with inner or outer layers, infinite and finite doped crystals [163].

Overhead mentioned methods are gives higher efficient and accurate results which is in good agreement with experimental observations depending on the type of the problem. The above methods from (1) to (4), as discussed above, help to simulate any doped or non-doped crystals [163, 155, and 156] depending on the flexibility of crystals. Method (5) depends on the type and building block of photonic crystals e.g. parallel cylinders is the building block for 2-D photonic crystals and spheres for 3-D photonic crystals [18, 19]. The methods (1), (4) and (6) simulate only the infinite crystals [15, 16 and 20]; and method (5) simulate only with finite-sized structures [157, 158]. Finally, methods (1), (4) and (6) study the defect structures that can be periodically manner using super-cell. The methods (2), (3) and (5) are worked for the finite structure with a single defect.

Among of all the above mentioned methods, the TMM is only used to analyze the dispersion relation, transmission, reflection and absorption of one-dimensional periodic structure. TMM method is very accurate method for the analysis of one-dimensional photonic crystal and the finding consequence with this method is in a decent promise with the experimental opinion like thin film technology. It is a very simple method to analyze the optical properties of one-dimensional periodic structure of the different materials. The details of the theoretical techniques discussed in Chapter-2 (Theory and Methodology).

1.12 Fabrication methods

Photonic crystals are the periodically arrangements of materials of building blocks. For the arrangements of the appropriate materials in the certain dimensions, a wide range of methods in the fabrication process of the photonic crystals. Depending upon the dimensionality, various methods applied for fabrications and some of them are suitable for the fabrication of 1-D and 2-D photonic crystals and 3-D photonic crystals e.g. Self-assembly methods, lithography, etching methods; dry etching method, wet etching, and holographic method.

1.12.1 Self-assembly method

For the fabrication of three-dimensional photonic crystals, the colloidal self-assembly methods appear to be the most effective process with deals with predesigned building blocks. Generally, theses building blocks are polystyrene nanospheres or mono dispersed silica spontaneously consolidate into a stable conformation [164]. Colloidal method has various techniques depending on the desirable yields. A versatile technique used for the generating colloidal crystals is gravity sedimentation. In the sedimentation process particles are suspended in a solution; settle down to the bottom of the container, as the solvent evaporates. Another example of the self-assemble method is *cell method* [165].

1.12.2 Lithography technique

In the fabrication of two-dimensional photonic crystal, the arrangement of the substrate is important, therefore, lithography technique is employed for the patterning the substrate in the fabrication process. The photolithography method can't be applied in the in optical range for producing photonic band gaps in the photonic crystals considering the smaller size of the lattice having periodicity between 0.2 and 0.7 μm, with sub-0.1 nm. So, alternate standard technique is needed which is electron beam lithography that permits to generate several photonic crystals with enormously high resolution. In this method, wafer is covered with an electron-sensitive material called as resist. The material, used as resist, experiences a significant modification in its chemical or physical possessions, after it is open to an electron beam [166].

1.12.3 Etching method

Etching methods are more favorable techniques for the fabrication of two-dimensional photonic crystals. In this these methods, a lithographic technique is used to leveling

undesirable zones on the semiconductor surface in the planar pattern. Etching method has two types; dry etching method and wet etching method.

1.12.3.1 Dry etching method

Reactive-Ion Etching (RIE) is a promising example of dry etching, which employs reactive ions created by plasma discharge in a fluorine-based (CHF_3, CF_4, CF_6, and SF_6) or chloride-based ($SiCl_4$ and Cl_2) gas. The produced ions are accelerated toward the surface of sample under an electric field. The dry etching method offers a decent switch over the size of pores, but up to a certain limit of maximum etching depth. The method has been used for various semiconductors; AlGaAs, GaAs, and Si. Kl.

1.12.3.2 Wet etching method

Wet/electrochemical etching is an illustration of the wet etching method which is also used for many semiconductors. By electrochemical etching of Si, we can produce macro porous silicon photonic crystal in which a pre-pattern with etch pits shaped on the front of a silicon wafer through lithographic process and appropriate chemical etching with TMAH or KOH solutions. The wafer is etched electrochemically by an HF solution in an electrochemical cell. For the electrochemical etching, nucleation centers begin to develop by the pre-etched pits. Another method is also available to design 2-D photonic crystal with electrochemical method by anodic oxidation of aluminum in acidic solutions, which yield highly ordered porous structure of alumina (Al_2O_3) consisting closely packed columnar cells [167, 168]. The main advantage of electrochemical etching method is that high aspect ratio can be effortlessly produced. The size and density of the pores in alumina structure can be precisely varied by appropriate anodization situation and pre-texturing the surface of aluminium with an arrangement of nano identation using a SiC mold [169]. This porous Al_2O_3 structure can be treated as a template to procedure other photonic media that can be grown in the pores, and Al_2O_3 can subsequently be etched out. The pores filled with polymer may be able to generating a negative replica that can subsequently be used for growth of various periodic patterns [170].

1.12.4 Holographic method

In this method, we used periodic photo in resin structure through the periodically pattern of intensity which deals with the interference of different coherent light waves

[171]. The holographic method had been used before a long time ago but in recent time photo polymerizable media consisting of inorganic and metallic or liquid crystal nanodroplets has used. The holographic method also helps to fabricate an electrically switchable polymer-dispersed liquid crystal which acts as photonic band gap material [172].

1.13 Objective of thesis

The objective of the thesis was to study of unusual optical deviation of the photonic crystals through revising the optics of the diverse materials. After the literature survey on the photonic crystals, we have aimed to study the optical characteristics of the one-dimensional photonic crystal, where 1-DPC is a periodic arrangement of the materials of the different refractive indices having thicknesses order from micro to nano scale. Having huge potential applications of the PCs in the nanoscience and nanotechnology, it is needed to investigate the photonic crystals on the basis of the interaction of the Electromagnetic Wave (EMW) with the matter. As discussed earlier, the light or EMW interaction with matter can be scattered. So, we have theoretically investigated the optical properties of photonic crystals of different materials like dielectric, magnetized cold plasma, high temperature superconductor and hyperbolic material in this thesis.

1.14 Organization of thesis

This thesis has been organized into seven chapters. The content of each chapter have been discussed below in brief:

In **Chapter 1**, we have discussed about the history of optics and why we need the periodic structure and what are the main applications of periodic structure. The development of periodic structure and type of periodic structure which is best for the applications of science society is discussed in detail. This chapter also shows the basic idea of thesis or introduction of thesis in which theories, fabrication, experiments and applications of one dimensional periodic structure are also taken into consideration and discussed.

In **Chapter 2**, the Maxwell's equations for the optics of materials as well as the one dimensional periodic structure have been solved; periodic structure is consists of dielectric, metallic, magnetized cold plasma and high temperature superconducting layer. Different theories and optical properties of these considered materials are also

discussed. In the entire thesis, we have applied the transfer matrix method for the study of band structure and the optical properties; transmission, reflection and absorption spectra of one dimensional periodic structure, where TMM is the key method adopted in several chapters of the present thesis.

In **Chapter 3,** the photonic band structure and transmission spectra of the periodic structure of the dielectric and magnetized cold plasma with different values of the effective collision frequency and magnetic field plasma density of the magnetized cold plasma for Right Hand Polarization (RHP) and Left Hand Polarization (LHP) structure have been studied in the GHz region by applying transfer matrix method. We have proposed a tunable narrow band filter and multichannel filter for RHP structure with enhanced magnetic field of the magnetized cold plasma, and high pass filter of broadband reflector for LHP structure at low magnetic field of the magnetized cold plasma. Besides this, we have theoretically designed a tunable narrow band filter for RHP structure with different values of electron density and broadband reflector or high pass filter for LHP structure, where width increases with the value of electron density of magnetized cold plasma. On the basis of our calculated results considering LHP and RHP structure, we demonstrated an original formulation to obtain a broadband reflector and narrow tunable filter at lower and higher frequency ranges. Thus, the analysis can be useful in designing of tunable photonic devices that can be precise by altering the parameters of the magnetized cold plasma.

In **Chapter 4**, the transmittance of the space ternary photonic crystal of dielectric, magnetized cold plasma, high temperature superconducting material with varying incident angle, magnetic field, electron density, temperature, thickness of the magnetized cold plasma for the right hand polarization or left hand polarization structure in the GHz region are discussed. For the right-hand polarization and the left-hand polarizations, the optical properties of the ternary photonic crystal get affected by the material parameters of the superconducting and the magnetized cold plasma layer. The transmittance of the left-hand polarization ternary photonic crystal shows better conclusions in comparison to compared to right-hand polarization due to the presence of the superconducting layer which has temperature and the magnetic field dependent material parameters. The left-hand polarization ternary photonic crystal with wide band gap may be applicable as the broadband reflector as well as high pass filter applications. The superconducting layer plays a crucial role to form the photonic

band gap of the ternary photonic crystal. Based on the obtained results, we have proposed an innovative idea to design the broadband reflector or the high pass filter and the narrow tunable filter of the ternary photonic crystal containing the superconducting material and magnetized cold plasma under certain the magnetic field in the transverse nature and the operating temperature.

In **Chapter 5**, a detailed analysis of the transmission through the asymmetric and symmetric one dimensional periodic structure (1-DPS) containing zinc sulfide (ZnS) and titanium dioxide (TiO_2) with one or more defect layer of Magnetized Cold Plasma (MCP) layer in the Gigahertz (GHz) frequency regime has been done using transfer matrix method. The transmission of the asymmetric one dimensional periodic structure containing zinc sulfide (ZnS) and titanium dioxide (TiO_2) with one or more defect of magnetized cold plasma layer investigated with varying electron densities, incident angles, and magnetic fields applied on the magnetized cold plasma layer. The transmission property of asymmetric periodic structure embedding two MCP layers shows better response as comparison to one layer defect in same periodic structure with variation of electron density of plasma and the thickness of ZnS and TiO_2 material. The obtained results proposed a simple and innovative idea to design the tunable multichannel filter in the microwave region.

In **Chapter 6** a detailed discussion plasma based hyperbolic meta-material and the on the perpendicular and parallel permittivities of hyperbolic meta-material analyzed theoretically with the varying effective collision frequency and filling fraction. The detailed investigation reveals that the real parts of the perpendicular and parallel permittivities of hyperbolic meta-material express the dielectric and metallic behaviors in the certain frequency regime. The absorption characteristics of a One-Dimensional Ternary Periodic Structure (1-DTPS) consisting of dielectric, silicon dioxide (SiO_2) and hyperbolic material studied with variation of different parameters; incident angle, filling fraction, electron collision frequency and the thicknesses of dielectric (A) material. All the absorption characteristics of the periodic structures have been studied by using the well-known simple transfer matrix method. First, we have calculated the absorption characteristics of the considered one-dimensional structure with varying incident angles (θ). The maximum absorption of the periodic structure has found at incident angle $\theta = 80^0$. The detailed study reveals that the tunable 100% absorption can be obtained due to the filling fraction in the hyperbolic

meta-material which is equivalent to the metallic behavior of effective permittivity of the Hyperbolic Material (HM). The analysis of the absorption of the 1-DTPS containing plasma based hyperbolic materials are very informative and leads to design various optical devices e.g. optical switch, logic gate, sensor as well as the absorber at microwave region.

Chapter 7 summarizes the work done included in the whole thesis and outlines the conclusion and future prospects.

References

[1] McGraw-Hill, Encyclopedia of Science and Technology, 10th Ed. McGraw-Hill Comp., Inc; (2007)

[2] R. Rashed, A pioneer in anaclastics: IbnSahl on burning mirrors and lenses ISIS, 81 (3) (1990) 464-491. (https://www.)stor.org/stable/233423).

[3] J. C. Maxwell, A dynamical theory of the Electromagnetic field, Phil. Trans. R. Soc. Lond.155 (1865) 159-521.

[4] H. D. Young, University Physics: Extended Version, 8th Ed., Addison-Wesley (1992) Ch. 35. (ISBN978-0-201-52981-4).

[5] D. F. Wallsand G. J. Milburn, Quantum Optics, Springer Berlin Heidelberg, (1994). (ISBN978-3-540-28574-8).

[6] A. D. McAulay, Optical Computer Architectures: The application of Optical Concepts to Next Generation Computers, Wiley-Interscience (1991). (ISBN978-0-471-63242-9)

[7] Y. R. Shen, Principles of Nonlinear Optics, Wiley-Interscience, New York (2002). (ISBN: 978-0-471-43080-3).

[8] L. Rayleigh, On the maintenance of vibrations by force of double frequency and on the propagation of waves through a medium endowed with a periodic structure, Philos. Mag., 24 (1887) 145-159; L. Rayleigh, On the reflection of light from a regularly stratified medium, Proc. R. Soc. Lond. 93 (1917) 556-577.

[9] L. Brillouin, Wave propagation in periodic structure, Dover Publications, New York (1953).

[10] J. C. Slater, Interaction of Wave in Crystals, Rev. Mod. Phys. 30 (1958) 197-222.

[11] E. Yablonovitch, Inhibited spontaneous emission in solid state physics and electronics, Phys. Rev. Lett. 58 (1987) 2059-2062.

[12] S. John, Strong localization of photons in certain disordered dielectric super lattices, Phys. Rev. Lett. 58 (1987) 2486-2489.

[13] A. Yariv and P. Yeh, Optical Waves in Crystals Propagation and Control of Laser Radiation, Wiley, New York (1984).

[14] J. B. Pendry, An introduction of Photonic band gap materials, J. Phys. Cond. Mat. 8 (1996) 1085–1108.

[15] D. N. Chigrin, A. V. Lavrinenko, D. A. Yarotsky, and S. V. Gaponenko, A dielectric Bragg mirror: can it be an omnidirectional reflector?, Optics and Photonics News, OSA 10 (12) (1999) 33.

[16] D. N. Chigrin, A. V. Lavrinenko, D. A. Yarotsky, and S. V. Gaponenko, Oservation of total omni directional reflection from a one-dimensional dielectric lattice, App. Phys. A Mater. Sci. Process 68(1) (1999) 25.

[17] M. Plihal, A. Shambrook and A. Maradudin, Two-Dimensional Photonic Band Structures, Opt. Comm. 80 (1991) 199-204.

[18] P. Villeneue and P. Michel, Photonic band gaps in two-dimensional square and hexagonal lattices, Phys. Rev. B 46 (1992) 4969-4973.

[19] A. Blanco, E. Chomski, S. Grabtchak, M. Ibisate, S. John, S. W. Leonard, C. Lopez, F. Meseguer, H. Miguez, J. P. Mondia, G. A. Ozin, O. Toader and H. M. van Driel, Large-scale synthesis of a silicon photonic crystal with a complete three-dimensional bandgap near 1.5 micrometers, Nature 405 (2000) 437-441.

[20] Y. A. Vlasov, X. Z. Bo, J. C. Sturm and D. J. Norris, On-chip natural assembly of silicon photonic bandgap crystals, Nature 414 (2001) 289-294; E. N. Ecolomou and M. M. Sigalas, Classical wave propagation in periodic structure: Cermat versus network topology, Phys. Rev. B 48 (1993) 13434-13439.

[21] P. A. Hiltner, and I. M. Krieger, Diffraction of Light by Ordered Suspensions, J. Phys. Chem. 73 (1969) 2386-2389.

[22] K. Ohtaka, Energy-Band of Photons and Low-Energy Photon Diffraction. Phys. Rev. B 19 (1979) 5057-5068.

[23] P. W. Anderson, Absence of Diffusion in Certain Random Lattices, Phys. Rev.109 (1958) 1492-1506.

[24] S. John and R. Rangarajan, Optimal Structures for Classical Wave Localization – an Alternative to the Ioffe-Regel Criterion, Phys. Rev. B 38 (1988) 10101(R)-10105(R). https://doi.org/10.1103/PhysRevB.38.10101

[25] S. Satpathy, Z. Zhang and M. R. Salehpour, Theory of Photon Bands in 3-Dimensional Periodic Dielectric Structures, Phys. Rev. Lett. 64 (1990) 1239-1242.

[26] K. M. Leung, and Y. F. Liu, Photon Band Structures-The Plane-Wave Method, Phys. Rev. B 41(1990) 10188-10190.

[27] J. Maddox, Photonic Band-Gaps Bite the Dust, Nature 348 (1990) 481-1.

[28] K. M. Ho, C. T. Chan, and C. M. Soukoulis, Existence of a Photonic Gap in Periodic Dielectric Structures. Phys. Rev. Lett. 65 (1990) 3152-3155.

[29] E. Yablonovitch, T. J. Gmitter, and K. M. Leung, Photonic Band-Structure: The Face- Centered-Cubic Case Employing Non-spherical Atoms, Phys. Rev. Lett. 67 (1991) 2295-2299.

[30] H. S. Sözüer, J. W. Haus, and R. Inguva, Photonic Bands: Convergence Problems with the Plane-Wave Method. Phys. Rev. B 45 (1992) 13962-13972.

[31] S. Y. Lin, J. G. Fleming, D. L. Hetherington, B. K. Smith, R. Biswas, K. M. Ho, M. M. Sigalas, W. Zubrzycki, S. R. Kurtz, J. Bur, A three- dimensional photonic crystal operating at infrared wavelengths, Nature 394 (1998) 251-253.

[32] N. Yamamoto, S. Noda, and A. Chutinan, Development of One Period of a Three- Dimensional Photonic Crystal in the 5-0 micro-meter Wavelength Region by Wafer Fusion and Laser Beam Diffraction Pattern Observation Techniques, Jpn. J. Appl. Phys. 37 (1998) L1052-8.

[33] O. D. Velev, T. A. Jede, R. F. Lobo, and A. M. Lenhoff, Porous silica via colloidal crystallization, Nature 389 (1997) 447-448.

[34] S. Y. Lin, V. M. Hietala, L. Wang, and E. D. Jones, Highly dispersive photonic bandgap prism, Opt. Lett. 21(21) (1996) 1771-1773.

[35] H. Kosaka, T. Kawashima, A. Tomita, M. Notomi, T. Tamamura, T. Sato, and S. Kawakami,Super prism phenomena in photonic crystals, Phys. Rev. B 58 (1998) R10096(R)-5.

[36] J. G. Fleming, and S. Y. Lin, Three-dimensional photonic crystal with a stop band from 1.35 to 1.95 microns, Opt. Lett. 24 (1999) 49-51.

[37] S. Noda, K. Tomoda, N. Yamamoto, and A. Chutinan, Full three-dimensional photonic bandgap crystals at near-infrared wavelengths, Science 289 (2000) 604-606.

[38] S. Fan, P. R. Villeneuve, J. D. Joannopoulos, and E. F. Schubert, High extraction efficiency of spontaneous emission from slabs of photonic crystals, Phys. Rev. Lett. 78 (1997) 3294-3297.

[39] O. Painter, A. Husain, A. Scherer, P. T. Lee, I. Kim, J. D. O'brien, P. D. Dapkus, Lithographic tuning of a two-dimensional photonic crystal laser array**,** IEEE Photon. Technol. Lett. 12 (2000) 1126-1128.

[40] J. B. Pendry, A. J. Holden, D. J. Robbins, and W. J. Stewart, Magnetism from conductors and enhanced nonlinear phenomena, IEEE Trans. Microwave Theory Tech. 47 (1999) 2075-2084.

[41] R. A. Shelby, D. R. Smith, and S. Schultz, Experimental verification of a negative refractive index of refraction, Science 292 (2001) 77-79.

[42] J. B. Pendry, Negative refraction makes a perfect lens, Phys. Rev. Lett. 85 (2000) 3966-3969.

[43] P. V. Parimi, W. T. Lu, P. Vodo, J. Sokoloff, J. S. Derov, and S. Sridhar, Negative refraction and Left-Handed Electromagnetism in Microwave Photonic Crystals, Phys. Rev. Lett. 92 (2004) 127401-4.

[44] J. Li, L. Zhou, C. T. Chan, and P. Sheng, Photonic band gap from a stack of positive and negative index materials, Phys. Rev. Lett. 90 (2003) 083901-4.

[45] N. C. Panoiu, R. M. Osgood, S. Zhang and S. R. J. Brueck, Zero- $\bar{n}$ bandgap in photonic crystal superlattices, J. Opt. Soc. Am. B 23 (2006) 506-513.

[46] M. Ricci, N. Orloff and C. M. Anlage, Superconducting meta-materials, App. Phys. Lett. 87 (2005) 034102-3.

[47] A. Peminov, A. Loidl, P. Przyslupski and B. Dabrowski, Negative refraction in ferromagnet superconductor superlattices, Phys. Rev. Lett. 95 (2005) 247009-4.

[48] S. Nojima, Excitonicpolaritons in one-dimensional photonic crystals, Phys. Rev. B 57 (1998) R2057(R)-10.

[49] A. S. Sánchez and P. Halevi, Spontaneous emission in one-dimensional photonic crystals, Phys. Rev. E 72 (2005) 056609-11.

[50] L. Cui, X. Li, J. Chen, Y. Cao, G. Du, and J. Ng, One-dimensional photonic crystals bound by light, Phys. Rev. A 96 (2017) 023833-10.

[51] M. Artoni, G. La Rocca, and F. Bassani, Resonantly absorbing one-dimensional photonic crystals, Phys. Rev. E 72 (2005) 046604-11.

[52] C. E. Rüter and D. Kip, Spectroscopy of nonlinear band structures of one-dimensional photonic crystals, Phys. Rev. A 77 (2008) 013818-10.

[53] C. H. Raymond, T. C. Au Yeung, T. K. Lim, and C. H. Kam, General electromagnetic density of modes for a one-dimensional photonic crystal, Phys. Rev. E 62 (2000) 7405-7409.

[54] S. Mishra and S. Satpathy, One-dimensional photonic crystal: The Kronig-Penney model, Phys. Rev. B 68 (2003) 045121-9.

[55] K. Koshino, Analytic approach to the optical response of one-dimensional photonic crystal slabs, Phys. Rev. B 67 (2003) 165213-8.

[56] I. Nusinsky and A. A. Hardy, Band-gap analysis of one-dimensional photonic crystals and conditions for gap closing, Phys. Rev. B 73 (2006) 125104-9.

[57] M. V. Erementchouk, L. I. Deych, and A. A. Lisyansky, Optical properties of one-dimensional photonic crystals based on multiple-quantum-well structures, Phys. Rev. B 71 (2005) 235335-11.

[58] A. H. Aly, S. W. Ryu, and C. J. Wu, Electromagnetic wave propagation characteristics in a one-dimensional metallic photonic crystal, J. Nonlinear Opt. Phys. Mat. 17(3) (2008) 255-264.

[59] A. H. Aly and S. W. Ryu, Study of Optical Transmission in Nano metallic Photonic Crystal, J. Comput. Theor. Nanosci. 5(4) (2008) 597-601.

[60] A. H. Aly, S. W. Ryu, H. T. Hsu, and C. J. Wu, THz transmittance in one-dimensional superconducting nanomaterial-dielectric superlattice, Mater. Chem. Phys. 113(1) (2009) 382-384.

[61] A. H. Aly, H. T. Hsu, T. J. Yang, C. J. Wu, and C. K. Hwangbo, Extraordinary optical properties of a superconducting periodic multilayer in near-zero-permittivity operation range, J. Appl. Phys. 105(8) (2009) 083917-6.

[62] W. H. Lin, C. J. Wu, T. J. Yang, S. J. Chang, Terahertz multichannel filter in a superconducting photonic crystal, Opt. Exp. 18(26) (2010) 27155-27166.

[63] C. J. Wu, Y. H. Chung, B. J. Syu, and T. J. Yang, Band gap extension in a one-dimensional ternary metal-dielectric photonic crystal, Prog. Electromagn. Res. 102 (2010) 81-93.

[64] C. J. Wu and Z. H. Wang, Properties of defect modes in one-dimensional photonic crystals, Prog. Electromag. Res. 103 (2010) 169-184.

[65] A. Aghajamali, A. Zare, and C. J. Wu, Analysis of defect mode in a one-dimensional symmetric double-negative photonic crystal containing magnetized cold plasma defect, Appl. Opt. 54(29) (2015) 8602-8606.

[66] T. C. King, C. C. Yang, P. H. Hsieh, T. W. Chang and C. J. Wu, Analysis of tunable photonic band structure in an extrinsic plasma photonic crystal, Physica E: Low Dimens. Syst. Nanostruct. 67(5) (2015) 7-11.

[67] A. Aghajamali, M. Hayati, C. J. Wu, and M. Barati, Properties of the defect modes in 1-D lossy photonic crystals containing two types of negative-index-material defects, J. Electromagnet Wave 27(18) (2013) 2317-2329.

[68] A. H. Aly and D. Mohamed, BSCCO/$SrTiO_3$ One Dimensional Superconducting Photonic Crystal for Many Applications, J. Supercond. Nov Mag. 28 (2015) 1699-1703.

[69] A. H. Aly, A. Aghajamali, H. A. Elsayed, and M. Mobarak, Analysis of cutoff frequency in a one-dimensional superconductor-metamaterial photonic crystal, Physica C: 528 (2016) 5-8.

[70] A. H. Aly, W. Sabra, and H. A. Elsayed, Cutoff frequency in metamaterials photonic crystals within Terahertz frequencies, Int. J. Mod. Phys. B 31(15) (2017) 1750123-8.

[71] A. H. Aly, H. A. Elsayed, and C. Malek, Defect modes properties in one-dimensional photonic crystals employing a superconducting nanocomposite material, Optica Applicata XLVIII(1) (2018) 1-12.

[72] C. Nayak, A. Saha and A. Aghajamali, Periodic multilayer magnetized cold plasma containing a doped semiconductor, Ind. J. Phys. 92(7) (2018) 911–917.

[73] S. K. Srivastava and A. Aghajamali, Narrow transmission mode in 1-D symmetric defective photonic crystal containing meta-material and high T_c superconductor, Optica Applicata XLIX(1) 49(1) (2019) 37-50.

[74] T. W. Chang, J. R. C. Chien, and C. J. Wu, Magnetic-field tunable multichannel filter in a plasma photonic crystal at microwave frequencies, Appl. Opt. 55(4) (2016) 943-946.

[75] T. W. Chang, C. H. Huang, D. J. Hou, C. J. Wu, and D. X. Chen, Analysis of unidirectional absorption in a defective superconducting photonic crystal, IEEE Photonics J. 9(4) (2017) 1-9.

[76] A. H. Aly, H. A. Elsayed, A. A. Ameen, and S. H. Mohamed, Tunable properties of one-dimensional photonic crystals that incorporate a defect layer of a magnetized plasma, Int. J. Mod. Phys. B 31(31) (2017) 1750239-9.

[77] A. H. Aly and Z. A. Zaky, Ultra-sensitive photonic crystal cancer cells sensor with a high-quality factor, Cryogenics 104 (2019) 102991-17.

[78] A. H. Aly, Z. A. Zaky, A. S. Shalaby, A. M. Ahmed, and D. Vigneswaran, Theoretical study of hybrid multifunctional one-dimensional photonic crystal as a flexible blood sugar sensor, Phys. Scri. 95(3) (2019) 035510-18. DOI: 10.1088/1402-4896/ab53f5

[79] A. H. Aly, and A. Mehaney, Phononic crystals with one dimensional defect as sensor materials, Ind. J. Phys. 91 (2017) 1021-1028.

[80] H. Hojo, K. Akimoto, and A. Mase, Conference Digest on 28th Int. Conf. Infrared and Millimeter Waves Otsu (2003) 347-348.

[81] H. Hojo and A. Mase, Dispersion relation of electromagnetic waves in one dimensional plasma photonic crystals, J. Plasma Fusion Res. 80(2) (2004) 89-90.

[82] H. Hojo and N. Uchida, K. Hattori, and A. Mase, Beaming of millimeter waves from plasma photonic crystal waveguide, Plasma and Fusion Research: Rapid Communication 1 (2006) 021-2.

[83] L. Shiveshavari and P. Mehto, Photonic band gap effect in one dimensional plasma-dielectric photonic crystal, Solid State Commu. 138(3) (2006) 160-164.

[84] J. D. Joannopoulos, S. G. Johnson, J. N. Winn, and R. D. Meade, Photonic Crystals: Molding the Flow of Light, 2nd Ed. Princeton: Princeton University Press (2008).

[85] R. Fitzpartick, R. D. Hazeltine, and F. L. Waelbroeck, A Graduate Level course, The University of Texas, Austin. (https://www.iaa.csic.es/ebooks/pdf).

[86] A. Mekis, J. C. Chen, I. Kurland, S. Fan, R. Villeneuve and J. D. Jonnapoulos, High transmission through sharp bends in photonic crystal waveguide, Phys. Rev. Lett. 77 (1996) 3787-3790.

[87] K. Sakoda and K. Ohtaka, Optical response of three-dimensional photonic lattice: solution of inhomogeneous Maxwell's equations and their applications, Phys. Rev. B 54 (1996) 5732-5741.

[88] S. Noda and T. Baba (Ed.), Roadmap on photonic crystals, Kluwer Aceadmic, Boston (2003).

[89] D. K. Kalluri, Advanced Electromagnetic computation, 2nd Ed. C.R.C. Press, Taylor & Francis Group, Boca Raton, London, New York (2018).

[90] R. Kumar, Chapter 14, Plasma Photonic Crystal, Book: Photonic Crystals-Innovative Systems, Lasers and Waveguides, Edited by A. Massaro, Intech. Open, UK (2012) (ISBN: 978-953-51-0416-2).

[91] H. G. Booker, Cold Plasma Waves, Springer-Verlag, New York (1984).

[92] H. K. Onnes, The superconductivity of mercury, Comm. Phys. Lab. Univ. Leiden (1911) 122b, reprinted in Proc. K. Ned. Akad. Wet. 14 (1911) 1274.

[93] J. G. Bednorz and K. A. Muller, Possible high T_c superconductivity in the Ba-La-Cu-O system, Z. Phys. B Cond. Mat. 64 (1986) 189-193.

[94] F. Abbas, L. E. Davis and J. C. Gallop, Tunable microwave components based on dielectric nonlinearity by HTS/ferroelectric thin films, IEEE Trans. Appl. Supercond. 5 (1995) 3511-3517.

[95] C. Kittel, Introduction to Solid State Physics, 6th Ed., John Wiley & Sons, New York (1986).

[96] F. Abbas, L. E. Davis and J. C. Gallop, Propagation coefficient in a superconducting asymmetrical transmission line with a buffer layer, J. Appl. Phys. 73 (1993) 4494-4499. https://doi.org/10.1063/1.352790

[97] C. J. Wu, Microwave propagation characteristics of a high temperature superconducting variable spacing parallel plate transmission line, J. Appl. Phys. 89(7) (2001) 3986-3992.

[98] J. E. Nestell, Jr. and R. W. Christy, Optical conductivity of bcc transition metals: V, Nb, Ta, Cr, Mo, W, Phys. Rev. B 21(8) (1980) 2173-7.

[99] W. R. Donaldson, A. M. Kadin, P. H. Ballentine, and R. Sobolewski, Interaction of picosecond optical pulses with high T_c superconducting films, Appl. Phys. Lett. 54 (1989) 2470-3.

[100] C. J. Wu, Transmission and reflection in a periodic superconductor/dielectric film multilayer structure, Prog. Electromag. Res. Symposium, Hangzhou, China (2005) 164-167.

[101] I. Chambouleyron and J. M. Martinez, Chapter-12, Optical properties of dielectric and semiconductor thin films, Handbook of Thin film materials edited by H.S. Nalwa 3 (2002).

[102] R. A. Smith, Semiconductors: 2nd Ed. Cambridge University Press, London (1979).

[103] M. L. Cohen and J. Chelikowsky, Electronic structure and optical properties of semiconductors, 2nd Ed. Springer Series on Solid State Science, 75, Springer Verlag, Berlin, Heidelberg (1989).

[104] E. T. Yu and M. Cardona, Fundamentals of semiconductors: Physics and Materials Properties, Springer-Verlag, Berlin, Heifelberg (1996).

[105] R. S. Kshetrimayum, A brief intro to metamaterials, IEEE Potentials 23 (2004) 44-46.

[106] S. A. Zouhdi, and A. P. Vinogradov, Metamaterials and Plasmonics: fundamentals modeling applications, Springer Science & Business Media (2008).

[107] N. Fang, H. Lee, C. Sun, and X. Zhang, Sub-diffraction-limited optical imaging with a silver super lens, Science 308 (2005) 534-537.

[108] D. O. S. Melville, and R. J. Blaikie, Super-resolution imaging through a planar silver layer, Opt. Express 13 (2005) 2127-2134.

[109] T. Taubner, D. Korobkin, Y. Urzhumov, G. Shvets, and R. Hillenbrand, Near-field microscopy through a SiC superlens, Science 313 (2006) 1595.

[110] Z. Liu, H. Lee, Y. Xiong, C. Sun, & X. Zhang, Far-field optical hyper lens magnifying sub-diffraction-limited objects, Science 315 (2007) 1686.

[111] Z. Jacob, L. V. Alekseyev, and E. Narimanov, Optical hyper lens far-field imaging beyond the diffraction limit, Opt. Express 14 (2006) 8247-8256.

[112] T. Ergin, N. Stenger, P. Brenner, J. B. Pendry, and M. Wegener, Three-dimensional invisibility cloak at optical wavelengths, Science 328 (2010) 337-339.

[113] W. Cai, U. K. Chettiar, A. V. Kildishev, and V. M. Shalaev, Optical cloaking with metamaterials, Nat. Photonics 1(4) (2007) 224-227.

[114] M. Born, and E. Wolf, Principles of optics: Electromagnetic Theory of Propagation, Interference and Diffraction of Light, 6th Ed. Elsevier (2013).

[115] H. Fujiwara, Spectroscopic Ellipsometry: Principles and Applications, John Wiley and Sons (2007).

[116] Y. Liu, and X. Zhang, Metamaterials: A new frontier of science and technology, Chem. Soc. Rev. 40 (2011) 2494-2507.

[117] D. R. Smith, J. B. Pendry and M. C. K. Wiltshire, Metamaterials and negative refractive index, Science 305 (2004) 788–792.

[118] V. G. Veselago, The electrodynamics of substances with simultaneously negative values of and μ, Sov. Phys. Uspekhi 10 (1968) 509.

[119] D. R. Smith and J. B. Pendry, Homogenation of metamaterials by field averaging, J. Opt. Soc. Am. B 23(3) (2006) 391-403.

[120] J. B. Pendry, D. Schurig, and D. R. Smith, Controlling electromagnetic fields, Science 312 (2006) 1780-1782.

[121] F. Yang, X. Chen, E. H. Cho, C. S. Lee, J. Peng, and L. J. Guo, Periodic reduction lithography in normal UV range with surface Plasmon polaritons interference and hyperbolic meta-material multilayer structure, Appl. Phys. Exp. 8 (2015) 62004-4.

[122] R. B. M. Schasfoort, Handbook of surface plasmon resonance, 2nd Ed. R. Soc. Chem. UK (2017).

[123] S. A. Maier, Plasmonics: Fundamentals and Applications, Springer Science & Business Media (2007).

[124] J. M. Pitarke, V. M. Silkin, E. V.Chulkov, and P. M. Echenique, Theory of surface plasmons and surface-plasmonpolaritons, Rep. Prog. Phys. 70 (2006) 1.

[125] L. Ferrari, C. Wu, D. Lepage, X. Zhang and Z. Liu, Hyperbolic material and their applications, Prog. Quantum. Electron 40 (2015) 1-40.

[126] D. R. Smith and D. Schurig, Electromagnetic wave propagation in media with indefinite permittivity and permeability tensors, Phys. Rev. Lett. 90 (2003) 077405-4.

[127] L. Novotny, and B. Hecht, Principles of nano-optics, Cambridge University Press, New York, 2012.

[128] S. Ishii, A.V. Kildishev, E. Narimanov, V. M. Saleav, and V. P. Drachev, Sub wavelength interference pattern from volume Plasmon polaritons in a hyperbolic medium, Laser Photonics Rev. 7 (2013) 265-271.

[129] C. L Cortes, W. Newman, S. Molesky, Z. Jacob, Quantum Nanophotonics using hyperbolic meta-materials, J. Optics 14 (2012) 063001.

[130] W. Shen, X. Sun, Y. Zhang, Z. Liu, X. Liu and P. Gu, Narrow band filters in both transmission and reflection with metal/dielectric thin films, Opt. Commun. 282(2) (2009) 242-246.

[131] A. Kumar, N. Kumar and K. B. Thapa, Tunable broadband reflector and tunable narrowband filter of a dielectric and magnetized cold plasma photonic crystal, Eur. Phys. J. Plus 133 (2018) 250-8.

[132] D. N. Chigrin, A. V. Lavrinenko, D. A. Yarotsky, S. V. Gaponenko, All-Dielectric One-Dimensional Periodic Structures for Total Omni directional Reflection and Partial Spontaneous Emission Control**,** J. Light wave Technol. 17 (1999) 2018.

[133] A. Kumar, K. B. Thapa and A. K. Yadav, Enhancement of absorption property of one-dimensional ternary periodic structure containing plasma based hyperbolic material for the application of microwave devices, J. Mag. Mag. Mater 93 (2019) 165371-9.

[134] A. Kumar, N. Kumar, G. N. Pandey, D. Singh and K. B. Thapa, Metamaterial-plasma based hyperbolic material for sensor, detector and switching application at microwave region, J. Phys. Cond. Matt. 32 (2020) 1-12.

[135] T. F. Cross and R. M. De La Rue, Photonic Crystals in the optical regime- past, present and future, Prog. Quantum. Electron. 23(2) (1999) 51-96. http://dx.doi.org/10.1016/S0079-6727(99)00004-X

[136] C. Lopez, A. Blanco, H. Mignez and F. Mesquer, Photonic Crystals for Laser Action, Opt. Mater. 13(1) (1999) 187-192. DOI: 10.1016/S0925-3467(99)00029-4

[137] S. V. Frolov, Z. V. Vardeny, A. A. Zakhidov and R. H. Baughman, Laser-like emissions in opal photonic crystals, Opt. Commun. 162 (1999) 241-246. DOI: 10.1016/S0030-4018(99)00089-9

[138] H. Kosaka, T. Kawashima, A. Tomita, M. Notomi, T. Tamamura, T. Sato, S. Kawakami, Self Collimating phenomenon in photonic crystals, Appl. Phys. Lett. 74 (1999) 1212-1214.

[139] M. Notomi, Negative refraction in photonic crystals, Opt. Quant. Electron. 34 (2002) 133-143.

[140] J. B. Pendry and A. MacKinnon, Calculation of photon dispersion relations, Phys. Rev. Lett. 69 (1992) 2772–2775.

[141] J. B. Pendry, Calculating photonic band structure, J. Phys. Cond. Mat. 8 (1996) 1085–1108.

[142] A. Taflove, Computational Electrodynamics,The Finite-Difference Time-Domain Method, Artech House, Boston, London (1995).

[143] G. Pelosi, R. Coccioli, and S. Selleri (Ed.), Quick Finite Elements for Electromagnetic Waves, 2nd Ed. Artech House Publications (2009).

[144] D. Felbacq, G. Tayeb, and D. Maystre, Scattering by a random set of parallel cylinders, J. Opt. Soc. America A11(9) (1994) 2526-2538.

[145] F. D. Daran, V. V. Lefebvre, and J. P. Parneix, T-matrix theory of electromagnetic scattering by particles and its applications: a comprehensive reference database, IEEE Trans. on Magnetics 31(3) (1995) 1598-1601.

[146] D. Maystre, Photonic crystal diffraction grating, Pure Appl. Opt. 3 (1994) 975-993.

[147] P. Yeh, Optics in Layered Media, John Willey and Sons, New York (1988).

[148] A. Sopaheluwakan, Thesis on Defect States and Defect modes in 1-D photonic crystals, Univ. of Twente, Nitherland, December, 2003; A. Rung, Thesis on Numerical studies of energy gaps in photonic crystals, Uppsala Univ. 2005.

[149] M. Born, Wave Propagation in periodic structures, Nature 158 (1946) 926.

[150] M. Tokushima, T. H. Kosaka, A. Tomita, and H. Yamada, Light wave propagation through a 120° sharply bent single-line-defect photonic crystal waveguide, Appl. Phys. Lett. 76 (2000) 952-954.

[151] A. B. Redondo, C. Husko, D. Eades, Y. Y. Zhang, J. Li, T. F. Krauss, B. J. Eggleton, Observation of Soliton compression in silicon photonics crystal, Nat. Comnun. 5 (2014) 3160.

[152] Y. A. Vlasov, X. Z. Bo, J. C. Sturm and D. J. Norris, On-chip natural assembly of silicon photonic bandgap crystals, Nature 414 (2001) 289-5.

[153] I. I. Tarhan and G. H. Watson, Photonic band structure of fcc colloidal crystals, Phys. Rev. Lett. 76 (1996) 315-4.

[154] M. Plihal, A. Shambrook and A. Maradudin, Two-Dimensional Photonic Band Structures, Opt. Comm. 80 (1991) 199-6.

[155] P. Villeneue and P. Michel, Photonic band gaps in two-dimensional square and hexagonal lattices, Phys. Rev. B 46 (1992) 4969-4.

[156] R. D. Meade, Karl D. Brommer, Andrew M. Rappe, and J. D. Joannopoulos, Existence of a photonic band gap in two dimensions, Appl. Phys. Lett. 61 (1992) 495-497.

[157] O. Painter, A. Husain, A. Scherer, P. T. Lee, I. Kim, J. D. O'Brien and P. D. Dakpus, Lithographic tuning of a two-dimensional photonic crystal laser array, IEEE Photon. Technol. Lett. 12 (2000) 1126-1128.

[158] P. Pottier, C. Seassal, X. Letartre, J. L. Leclercq, P. Viktorovitch, D. Cassagne, and C. Jouanin, Triangular and Hexagonal High Q-Factor 2-D Photonic Bandgap Cavities on III-V Suspended Membranes**,** IEEE J. Lightwave Technol. 17 (1999) 2058-2062.

[159] J. D. Joannopoulos, S. Fan, A. Mekis, and S. G. Johnson, Chapter 3: Novelties of light with photonic crystals, C. M Soukoulis Editor Book: Photonic Crystals and Light Localization in the 21st century; Dordrecht, Kluwer Academic, U. S. A. (2001) 1-24.

[160] S. Fan and J. D. Joannopoulos, Photonic crystals: towards large-scale integration of optical and optoelectronic circuits, Appl. Opt. and Photonics News 11 (2000) 28-33.

[161] R. Costa, A. Melloni, and M. Martinelli, Bandpass resonant filters in photonic-crystal waveguides, IEEE Photonic Technol. Lett. 15 (3) (2003) 401-403.

[162] L. Raffaele, R. M. De La Rue, J. S. Roberts, and T. F. Krauss**,** Edge-emitting semiconductor microlasers with ultrashort-cavity and dry-etched high-reflectivity photonic microstructure mirrors, IEEE Photon. Technol. Lett. 13 (2001) 176-178.

[163] W. Saj, FDTD simulations of 2D Plasmon waveguide on silver nanorods in hexagonal lattice, Opt. Exp. 13 (2005) 4818-4827.

[164] Y. A. Vlasov, X. Z. Bo, J. C. Sturm and D. J. Norris, On-chip Natural Assembly of Silicon Photonic Band Gap Crystals, Nature (London) 414 (2001) 289-293.

[165] S. H. Park and Y. Xia, Assembly of Mesoscale Particles over Large Areas and Its Application in Fabricating Tunable Optical Filters, Langmuir 15 (1999) 266-273.

[166] U. Mescheder, I. Khazi, A. Kovacs and A. Ivanov, Tunable optical filters with wide wavelength range based on porous multilayers, Nanoscale Res. Lett. 9(1) (2014) 427-6.

[167] J. C. Knight, T. A. Birks, P. St. J. Russell and D. M. Atkin, All-Silica Single-Mode Fiber with Photonic Crystal Cladding, Opt. Lett. 21 (1996) 1547-1549.

[168] D. Almalawi, K.A. Bosnick, A. Osika and M. Moskovits, Fabrication of Nanometer-Scale Patterns by Ion-Milling with Porous Anodic Alumina Masks, Adv. Mater.12 (2000) 1252-1257.

[169] H. Masuda, M. Ohya, K. Nishio, H. Asoh, M. Nakao, M. Nohtomi, A. Yokoo and T. Tamamura, Photonic Band Gap in Anodic Porous Alumina with Extremely High Aspect Ration Formed in Phosphoric Acid Solution, Jpn. J. Appl. Phys. 39(2) (2000) L 1039-L 1041. DOI: 10.1143/JJAP.39.L1039

[170] P. Hoyer, N. Baba and H. Masuda, Small Quantum-Sized CdS Particles Assembled to Form a Regularly Nanostructured Porous Film, Appl. Phys. Lett. 66 (1995) 2700-2702.

[171] S. Shoji, and S. Kawata, Photo fabrication of Three-Dimensional Photonic Crystals by Multi beam Laser Interference into a Photo polymerizable Resin, Appl. Phys. Lett. 76 (2000) 2668-2670.

[172] R. Jakubiak, T. J. Bunning, R. A. Vaia, L.V. Natarajan and V. P. Tondiglia, Electrically Switchable One-dimensional Polymeric Resonators from Holographic Photopolymerization: A New Approach for Active Photonic Bandgap Materials, Adv. Mater. 15 (2003) 241-4.

Chapter 2
Theory and mathematical formulation

Chapter -2

Theory and mathematical formulation

The optics of material is the interaction of light, with material, and the optical density or optical constant of the material is measured in the interaction of incident field waves with the materials. The interaction of incident field waves with the materials is related with the electric permittivity (ε) and the magnetic permeability (μ) of the optical materials, because these two parameters are pondered with the polarizations of materials. The square of optical density of material is the product of the relative permittivity (ε_r) to the relative permeability (μ_r) of the material, which is given as:

$$n^2 = \varepsilon_r \mu_r \tag{2.1}$$

This refractive index or optical density of material gives the wave propagation inside the material and given by:

$$\vec{k} = \frac{n\omega}{c}\hat{k} \tag{2.2}$$

where $n = \pm\sqrt{\varepsilon_r \mu_r}$, ω is angular frequency of incident wave and $c = \frac{1}{\sqrt{\varepsilon_0 \mu_0}}$, c is speed of light. The positive value of optical density of the material is called *Positive Index Material (PIM)* and the negative value of optical density of the material is called the *Negative Index Material (NIM).*

According to Snell's law, the refractive index (n) is defined as:

$$n = \frac{c}{v} \tag{2.3}$$

where c is the velocity of light in the free space and v is the velocity of light in medium. For two optical media of refractive indices n_1 and n_2 with the incident and refracted angles θ_1 and θ_2, the surface wave propagation condition is given by the Snell's law is:

$$n_1 \sin\theta_1 = n_2 \sin\theta_2 \tag{2.4}$$

It means the propagation of wave in the medium or material is depends on the optical density of the materials. In propagation point of view, the optical materials are

classified in to two types: (i) *isotropic material*; (ii) *anisotropic material*. In the next section, we will discuss about the isotropic and anisotropic materials in the details:

2.1 Isotropic and anisotropic medium

As discussed earlier that the optical density of the material is depends on two physical parameters of the materials; that is electric permittivity and magnetic permeability. These parameters are related with the polarizations of material, when EMWs are interacted with the materials. However, ε or μ is tensor quantity. Therefore, the materials are two types: (i) isotropic material when ε and μ are independent of direction whereas (ii) anisotropic material when ε and μ is direction dependent. The isotropic and anisotropic materials follow cubic symmetry mechanism and inhomogeneous medium follow composite asymmetry, respectively. It has been observed from the time of Maxwell that transport properties of randomly inhomogeneous materials have been of great intrigue to the researchers. The demand of high-speed information's in today's scientific and technological world is fulfilled with the practice of novel materials, which have unique optical properties that have not been witnessed in the already existing materials. There has always been exhausting the amount of researches on manufacturing or developing such unique materials or modifying the existing materials to exhibit special properties and the researchers have been fabricating the special materials by the available technique, for instance of the preparation of thin films in nanoscience and nanotechnology.

The several approaches are used to achieve the best optical properties of the materials, called composite materials, in which these properties of the composite thin films are modified generally in a more convenient way and so it is ease of implementation. The techniques involving the thin films modification or deposition techniques are namely, evaporation, sputtering and ion beams assisted depositions which have been proved to be quite successful for preparing composite or *inhomogeneous/anisotropic dielectric thin films*. The thin films manufacturing using the above mentioned techniques have been found to be useful in optical thin film devices. Cermets films have been developed by the co-deposition of dielectrics with different metals and have found applications in devices for solar energy conversion. Dielectric-dielectric and metal-dielectric composite thin films have been vastly researched with special emphasis on their optical properties in the near infrared and solar regions [1-4].

The most astonishing fact about the thin metallic films is that the metallic films show different optical properties from those of just the bulk metal. These films show very selective absorption, and the optical properties strongly depend on the film structure, for example their thicknesses. The electron-microscopic results suggested that actual thin films are not parallel-sided homogeneous slabs, but they are films having some in-homogeneity like unevenness or some cracks or particles isolated from each other. The experimental results have shown that when the very thin films of silver are heated they show resonance type absorption and whose peaks exist at around 435μm or at longer wavelength. These films are composed of a large number of small particles of silver [5]. Another results from experiments showed that thin metallic films could be regarded as a two dimensional aggregate of small rotational ellipsoids. The shape of the ellipsoids influences resonating of the free electron gas bounded within an ellipsoid at particular frequency [6].

These results reveal that the thin films of the materials have different optical properties or different optics of material due to thickness. The interaction of light or EMW with thin film material can be analyzed by studying the EMWs in thin film using Maxwell's equations.

2.2 Electromagnetic waves in isotropic medium

An isotropic material is that in which the optical properties are independent of the polarization state of an electromagnetic wave, when EMW passes through the material [7]. The some constitutional relations for isotropic media hold true and the Maxwell's equations can be solved easily.

2.2.1 Fields and waves in isotropic medium

When EMW is interacted with isotropic medium, the polarization is induced by the electric field of the wave and the induced polarization is directly proportional to the parallel electric field. The relation between the induced polarization and the electric field is given by [8]:

$$\vec{P} = \varepsilon_0 \chi \vec{E} \tag{2.5}$$

where- $\vec{P}$ = polarization , $\vec{E}$ =electric field of wave, χ =electric susceptibility and ε_0 =electric permittivity of free space.

As we know, the constitutional relation for displaced electric field and induced polarization, and the relation are given by:

$$\vec{D} = \varepsilon_0 \vec{E} + \vec{P} \tag{2.6}$$

where $\vec{D}$ =dielectric displacement vector, $\vec{P}$ =induced polarization, $\vec{E}$ =electric field of wave.

On substituting polarization form Eq. (2.5) in Eq. (2.6), we get,

$$\vec{D} = \varepsilon_0 (1+\chi)\vec{E} \tag{2.7}$$

$(1+\chi) = \varepsilon_r$, called relative permittivity of the material, then Eq. (2.7) becomes:

$$\vec{D} = \varepsilon_0 \varepsilon_r \vec{E} \tag{2.8}$$

Generally, optical constant of the material is given by:

$$\varepsilon_r = \varepsilon' - i\varepsilon'' \tag{2.9}$$

where ε' real electric permittivity and ε'' imaginary electric permittivity.

This relative electric permittivity is called the square optics of material or square of optical density or square refractive index. The optical density of the material is given by:

$$n = \sqrt{\varepsilon_r} = \sqrt{\varepsilon' - i\varepsilon''} \tag{2.10}$$

The dielectric constant of medium depends on the frequency of the wave, and hence, the refractive index is also related to the frequency of the wave. This phenomenon is well known as the *dispersion*. The dispersion phenomenon in the geometry optics is caused for the separation of the white light into its constituent colors of a prism.

We have discussed earlier the wave propagation vector $\vec{k}$ which depends on the optical density. For the EMW propagation in isotropic media, the wave propagation vector $\vec{k}$ is perpendicular to the phase front i.e. $\vec{k}$ is perpendicular to the vectors $\vec{D}$ and $\vec{B}$. The Poynting vector of the wave represents the magnitude and the direction of flow of energy. This pointing vector is parallel to the wave propagation vector $\vec{k}$. The Poynting vector is given by [8]:

$$\vec{S} = \vec{E} \times \vec{H} \tag{2.11}$$

where, $\vec{E}$ = electric field, and $\vec{H}$ = magnetic field intensity.

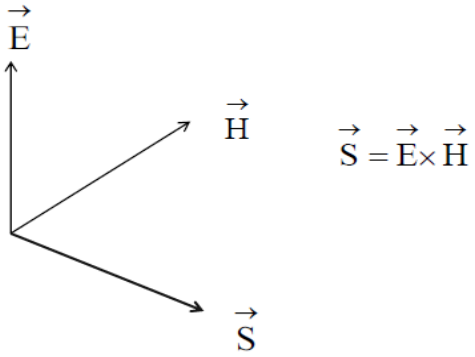

Figure 2.1: The electric field ($\vec{E}$), magnetic field intensity ($\vec{H}$) and Poynting vector ($\vec{S}$) in isotropic medium.

The Figure 2.1 explains the direction of energy propagation with the coupling field waves. The local direction of $\vec{S}$ is also called the ray direction. Only for the wave front is the ray direction which is the same at all points on the phase fronts. The best way to understand the properties of an optical system is to find out when a ray of light enters in the medium. It is necessary to understand the direction of light as it encounters medium as well as the intensity of light when it crosses an interface [8].

2.2.2 Maxwell's equations for material

The EMW propagation in a material medium is started by the four most fundamental equations of electrodynamics, which are known as the Maxwell's equations:

$$\vec{\nabla} \cdot \vec{D} = \rho \tag{2.12}$$

$$\vec{\nabla} \cdot \vec{B} = 0 \tag{2.13}$$

$$\vec{\nabla} \times \vec{E} = -\frac{\partial \vec{B}}{\partial t} \tag{2.14}$$

$$\vec{\nabla} \times \vec{H} = \vec{J} + \frac{\partial \vec{D}}{\partial t} \tag{2.15}$$

where, $\vec{E}$ and $\vec{H}$ denotes the electric field and the magnetic field, respectively. Electromagnetic wave field in the material is termed by these two fields $\vec{D}$ and $\vec{B}$; where $\vec{D}$ shows the dielectric displacement vector and $\vec{B}$ is the magnetic induction. These four field vectors are related with the constituent relations, which include the effect of the wave field on materials. The quantities ρ and $\vec{J}$ denotes the electric charge density and the current density that are related with the sources of the wave fields $\vec{E}$ and $\vec{H}$. Using these equations govern the electromagnetic wave field in the medium.

Maxwell's equations cannot be derived exclusively unless the connection between $\vec{B}$ & $\vec{H}$, and $\vec{E}$ & $\vec{D}$ are known to get a unique purpose of the wave field vectors because these variable contains the eight scalar equations which relates to the twelve variables, three for each four vectors $\vec{E}$, $\vec{H}$, $\vec{D}$ and $\vec{B}$.

The materials constituent equations are:

$$\vec{D} = \varepsilon_0 \vec{E} + \vec{P} = \varepsilon_0 (1 + \chi_e) \vec{E} = \varepsilon \vec{E} \tag{2.16}$$

$$\vec{B} = \mu \vec{H} = \mu_0 \left(\vec{H} + \vec{M}\right) = \mu_0 (1 + \chi_m) \vec{H} \tag{2.17}$$

where ε and μ are the tensors of rank two; $\vec{P}$ and $\vec{M}$ are electric and magnetic polarization, respectively. The electric wave field perturbs the movement of electron and produces an electric dipole polarization $\vec{P}$ per unit volume having permittivity different from ε_0. The magnetic field also induces a magnetization $\vec{M}$ per unit volume in materials having permeability different from μ_0. The permeability constant μ_0 is equal to $4\pi \times 10^{-7}$ H/m.

In the isotropic or linear medium, both ε and μ tensors diminish to scalar. The quantities ε and μ are presumed to be independent of the field forces. But for the adequately strong field, the dependence of quantities ε and μ on $\vec{E}$ and $\vec{H}$ must be incorporated for the anisotropic medium.

The Maxwell's equations have coupled field wave equations. The Eq. (2.14) in the Maxwell's equations for the isotropic medium is given below:

$$\vec{\nabla} \times \vec{E} = -\frac{\partial \vec{B}}{\partial t} = -\mu \frac{\partial \vec{H}}{\partial t} \tag{2.18}$$

Now, we have considered that a plane wave of $\vec{E}$ and $\vec{B}$ is incident on the isotropic medium. The $\vec{E}$ (electric field) and the $\vec{H}$ (magnetic field) composed of product of a function of wave vector position and a function of angular form time as:

$$\vec{E}(r,\ t) = \vec{E}_0 e^{-i\omega t + i\vec{k}\cdot\vec{r}} \text{ and } \vec{H}(r,t) = \vec{H}_0 e^{-i\omega t + i\vec{k}\cdot\vec{r}} \tag{2.19}$$

where $\vec{E}_0$ and $\vec{H}_0$ are the initial electric and magnetic fields.

Using Eq. (2.19), the derivatives of Maxwell's equations become:

$$\frac{\partial}{\partial t} \leftrightarrow -i\omega \tag{2.20}$$

$$\text{and } \frac{\partial}{\partial x} \leftrightarrow -ik \ \nabla \leftrightarrow -ik \tag{2.21}$$

Using Eq. (2.19), the Eq. (2.18) becomes:

$$\vec{\nabla} \times \vec{E} = -i\omega\vec{B} = -i\omega\mu\vec{H} \tag{2.22}$$

where μ = magnetic permeability, ω= frequency of time harmonic fields an $\mu = \mu_0(1+\chi_m)$.

Similarly, from the Maxwell's equations, the Eq. (2.15) takes the form:

$$\vec{\nabla} \times \vec{H} = \vec{J} + \frac{\partial \vec{D}}{\partial t} \tag{2.23}$$

Using Eq. (2.19), the Eq. (2.23) becomes:

$$\vec{\nabla} \times \vec{H} = \vec{J} - i\omega\varepsilon\vec{E} \tag{2.24}$$

where $\vec{J}$ = total current density and $\varepsilon = \varepsilon_0(1+\chi_e)$.

From Maxwell's equations, the Eq. (2.12) gives the electric permittivity:

$$\vec{\nabla}\cdot\vec{E} = \frac{\rho}{\varepsilon} \tag{2.25}$$

where, ρ = total charge density and $\varepsilon = \varepsilon_0(1+\chi_e)$

Similarly, from Maxwell's equation, Eq.(2.17), the equation can be simplified:

$$\vec{\nabla}\cdot\vec{B}=\vec{\nabla}\cdot\left(\mu\vec{H}\right)=0 \tag{2.26}$$

where $\mu=\mu_0(1+\chi_m)$ and $\vec{B}=\mu\vec{H}$

2.2.3 Master equation for photonic crystal

To develop the master equation for the periodic structure, we have started with Maxwell's equation, Eq. (2.12) to Eq. (2.17), where they are the coupled wave equation with constituent relation with the $\vec{E}$ and $\vec{H}$ fields. These waves are incident on the material having constant phase velocity. So, the $\vec{E}$ and $\vec{B}$ fields are considered plane waves as given in the Eq. (2.19), and they are used in the calculation of the Master's equation.

Throughout the thesis, we have considered two cases: (i) isotropic material that is linear or isotropic dielectric material considering the optics of material not dependent on $\vec{E}$ and non-magnetized material ($\vec{M}=0$); $\vec{J}$ and ρ is also zero for source free. The constituent relation of electric field, $\vec{D}=\varepsilon\vec{E}$ is more effective for linear medium. However, the magnetic field of the material is changed due to the effect of polarization. The magnetic permeability is near to be unity for the most interested dielectric materials, like set $\vec{B}=\vec{H}$. (ii) Anisotropic material i.e. inhomogeneous medium that is nonlinear dielectric material (permittivity is a tensor). The optics of anisotropic material is dependent on the direction of field $\vec{E}$ with displacement electric field ($\vec{D}=\overline{\overline{\varepsilon}}\vec{E}$) and for nonmagnetic field $\left(\vec{M}=0\right)$.

For isotropic medium $(\vec{J}=\rho=0)$ for some free, Eq. (2.24) and Eq. (2.22) reduce to:

$$\vec{\nabla}\times\vec{H}=-i\omega\varepsilon\vec{E} \tag{2.27}$$

$$\vec{\nabla}\times\vec{E}=+i\omega\mu\vec{H} \tag{2.28}$$

where $\varepsilon=\varepsilon_0\varepsilon_r$ and $\mu=\mu_0\mu_r$

The Eq. (2.12) becomes:

$$\vec{\nabla}\cdot\vec{D}=\left(\vec{\nabla}\varepsilon\cdot\vec{E}+\varepsilon\vec{\nabla}\cdot\vec{E}\right)e^{-i\omega t} \text{ or } \vec{\nabla}\cdot\vec{D}=\varepsilon\vec{\nabla}\cdot\vec{E}\ e^{-i\omega t}=0 \text{ or } \vec{\nabla}\cdot\vec{E}=0 \tag{2.29}$$

Hence, Eq. (2.29) and Eq. (2.26) have the form:

$$\vec{\nabla} \cdot \vec{E} = 0 \tag{2.30}$$

$$\vec{\nabla} \cdot \vec{H} = 0 \tag{2.31}$$

The decoupled wave equation for the electric field can be achieved by the cross product of Eq. (2.28) and combining with Eq. (2.27) that is given as:

$$\vec{\nabla} \times \vec{\nabla} \times \vec{E} = \omega^2 \mu \varepsilon E \tag{2.32}$$

Using the identity of the vector operation: $\vec{\nabla} \times \vec{\nabla} \times \vec{E} = \vec{\nabla} (\vec{\nabla} \cdot \vec{E}) - \vec{\nabla}^2 \vec{E}$, the Eq. (2.32) can be simplified for electric field (E).

$$\vec{\nabla}^2 E + \frac{\omega^2}{c^2} \varepsilon_r \mu_r \vec{E} = 0 \tag{2.33}$$

Similary, we can solve for other field wave that is the magnetic field wave which is given as:

$$\vec{\nabla}^2 \vec{H} + \frac{\omega^2}{c^2} \varepsilon_r \mu_r \vec{H} = 0 \tag{2.34}$$

where $c^2 = \frac{1}{\varepsilon_0 \mu_0}$, $\varepsilon_r = \frac{\varepsilon}{\varepsilon_0}$, $\mu_r = \frac{\mu}{\mu_0}$.

These two equations, Eq. (2.33) and Eq. (2.34), are called decoupled wave field equations for plane waves and are also called the *scalar Helmholtz's equations*. The Electromagnetic Wave (EMW) interacts at the interfaces of the dielectric materials and can be solved through these equations. Hence, we can say that the scalar forms of Helmholtz's equations can be used to study the behavior of photons in a photonic crystal, when light propagates in the periodic structure of the dielectric materials. For periodicity of the periodic structure, the waves at each interface used to calculate the reflected back wave by Bloch's wave functions, and the Bloch's wave function at the two different surfaces and produce phase difference and then the band gap structure of the blocks is formed, the lattice constant is equivalent to wavelength of light [9-11].

The Helmholtz equation, (2.33 or 2.34), are the principal equations for the phenomenon of electromagnetic wave in the periodic structure with different

dielectric material constituents. Using the continuity relationship of some components of field vectors at the boundary, the transmission and reflection coefficients of the EM wave at each interface can be calculated. This continuity relation can be derived by the Maxwell's equations.

For vector form of the wave equation with non-magnetic materials $\mu_r = 1$, the Eq. (2.27) and (2.28) can be simplified in terms of the relative permittivity $\varepsilon_r = n^2$ for isotropic medium.

$$\vec{\nabla} \times \vec{H} = -i\omega\varepsilon_r \varepsilon_0 \vec{E} \tag{2.35}$$

$$\vec{\nabla} \times \vec{E} = +i\omega\mu_0 \vec{H} \tag{2.36}$$

To solve the energy of the propagating wave in the materials, it must be in the vector form. Therefore, the coupled equation, Eq. (2.35), can be transformed into decoupled by dividing Eq. (2.35) by ε_r in the vector form, and then taking the curl both sides. After using Eq. (2.36), the obtained equation entirely in $\vec{H}$ is given as:

$$\vec{\nabla} \times \frac{1}{\varepsilon_r} \vec{\nabla} \times \vec{H} = \omega^2 \varepsilon_0 \mu_0 \vec{H} \tag{2.37(a)}$$

or we know that $\varepsilon_0 \mu_0 = \frac{1}{c^2}$, so above equation can be simplified into:

$$\vec{\nabla} \times \frac{1}{\varepsilon_r} \vec{\nabla} \times \vec{H} = \frac{\omega^2}{c^2} \vec{H} \tag{2.37(b)}$$

The Eq. (2.37) is well-known as the *Master Equation* as the vector form, and this equation is used to study the *Photonic Crystals or Periodic Structures of Dielectric Materials or Photonic Band Gap materials* [12, 13].

The Master's Equation can be used to determine the magnetic field modes $\vec{H}$. Using Eq. (2.36) $\vec{E}$ can be used to find $\vec{H}$.

$$\vec{H} = -\frac{i}{\omega\mu_0} \left(\vec{\nabla} \times \vec{E} \right) \tag{2.38}$$

Since the phenomenon of electromagnetic wave in a dielectric medium has no fundamental length, the coefficients of Helmholtz equations have no length as per

dimension. Hence, the electromagnetic problems differ only by considering an expansion or a contraction.

Generally, the Master's equation Eq. (2.37) and Eq. (2.38) are used in PWEM, FEM and FDTD method. But, we have used the simple optics method using Helmholtz equation that is called *transfer matrix method*.

2.2.4 Calculation of optical properties of photonic crystal

The Maxwell's equation can be solved by the two ways (i) scalar form and (ii) vector form. As per the review of journals and books for periodic structures/photonic crystals, there are main six numerical methods, which are used to study the optical properties of the periodic structures: (1) Plane Wave Expansion Method (PWEM) [14], (2) Finite Difference Time Domain (FDTD) method [15], (3) Finite Element method [16], (4) Transfer Matrix Method (TMM) [17], (5) Rigorous Theory of Scattering Method (RTSM) [18] or a set of considered spheres [19], and (6) Diffraction Grating Method (DGM) [20].

Above methods are used to calculate with maximum efficiency for the optical property of photonic crystal. These methods give results with full accuracy and the good agreement with practical results. The different methods for photonic crystals are chosen according to tackling of the problems. The above methods PWEM, FDTD, FEM, and TMM can simulate any doped or non-doped crystals [15-17] as they are extremely flexible. RTSM (5) is limited to the particular types of photonic crystals, which are parallel cylinders (for two-dimensional photonic crystals) and spheres (for three dimensional photonic crystals) [18, 19]. These methods (1), (4) and (6) can be used with infinite crystals [15, 16, 20] and (5) only with finite-sized structures [18, 19]. Finally, methods PWEM, FDTD, FEM, TMM, RTSM and DGM are used a super-cell to analyze the structures of defect. On the other hands, methods (2), (3) and (5) can be used with a finite structure containing a single defect. In the following section, we have given the brief outline of all methods, which are used to study the band structure, transmittance, reflectance etc.

2.2.4.1 Plane wave expansion method

Plane Wave Expansion Method (PWEM) is very easy method to calculate the band structure of the periodic structure. The infinite photonic crystal with a defect will be treated as a super-cell. Numerous results are calculated with this method for

evaluating the band structure of materials [21-23]. The limitation of this method is the memory storage which depends on the set of plane waves for the expansion of the field. This set escalates when the photonic crystal deviates from a periodic structure to another structure.

2.2.4.2 Finite difference time domain method

This method describes the Maxwell's equations in a time domain form. These results are gives excellent behavior with experiment [24-26]. However, the electromagnetic modes of a defect mode are calculated as the transmission ratio of the optical materials for the Finite Element Method (FEM). To calculate the transmittance of the periodic structure, an EMW pulse is incident on the material in which EMW signal is noted. The FDTD method permits the simulation of finite or infinite crystals with inner or outer EMW sources. This method allows the simulation of an entire practical setup with a periodic structure. This is most common method to simulate the optics of photonic crystals. The limitation of the FDTD is the size of the memory to calculate the large crystal and the lack of an accurate Electromagnetic (EM) model for some particular substances like thin wires. An excellent advantage of this method is the smart capability to simulate anisotropic or nonlinear materials [16].

2.2.4.3 Finite element method

This method is well defined in electrodynamics and it has an attractive advantage to be implemented for studying the optics of photonics. There is several commercial software available like COMSOL, MAFIA, HFSS etc. It can be simulated the infinite and finite un-doped or doped photonic crystals with inner or outer source.

2.2.4.4 Transfer matrix method

Transfer Matrix Method (TMM) is well-defined method to calculate the optical properties of the one-dimensional periodic structures [9]. The TMM govern the Maxwell's equations in the k-space. It is capable to manage the PBG materials of finite thickness with layer-by-layer calculations. Periodic structures with defects can be dealt with by taking a super-cell. The band structures, reflectance and transmission coefficients establish easily by this method. Therefore, this method is popular among many researchers in the field of the optics and photonics [27-30]. This method is also proved as a very useful and an accurate method with respect to experimental results

[29, 30]. The limitation of this method is also the memory storage but TMM is difficult to use in the different geometry structures.

2.2.4.5 Rigorous theory of scattering method

Many research groups implemented this method, which is based on the rigorous scattering of electromagnetic wave/light by a finite number cylinders/spheres for a three dimensional photonic crystal [18, 19]. The most advantage of the method is to locate the cylinders/spheres everyplace in space. Accordingly, a periodic arrangement is just a specific case and this method makes possible to deal with a single defect exclusive of the need of a super-cell. It is also very easiest method to change the geometry of the structure. Although, these limitations are connect to the memory size when one hundred cylinders are implemented in the calculation.

2.2.4.6 Diffraction grating method

Using the diffraction gratings theory [20], the computation of reflection and transmission coefficients of a photonic crystal is allowed where the stack of a set of infinite grating layers constitute the photonic crystal. This method can be used only with an infinitely extended cavity chosen as an imperfection for the periodic structure. But this method cannot be implemented to simulate photonic band gap materials having the sophisticated doped and active structures.

Throughout the thesis, we have adopted Helmholtz's equations to understand the basic optics behind photonics. The Helmholtz's equation is used to solve the optics of materials and optical property of periodic structure or optics behind photonics, because the dielectric layer in the photonic crystals for photons using scalar method is similar to the potential well in the semiconductors for electrons in the quantum mechanics. Now, we formulate the TMM for one-dimensional periodic structure.

2.2.4.7 TMM for one-dimensional photonic crystal

The TMM method is a powerful tool for PBG structures and optical properties of one-dimensional photonic crystals. The calculations of optical properties of photonic crystals (PCs) are similar to the electronic properties calculations of atomic crystals. For an atomic crystal, the atomic crystal is designated by periodicity of the atomic potentials and Schrödinger's equation solves the Eigen value of wave function. However, in the photonic crystals, the Eigen value of wave function is used to

calculate the master equation $\vec{\nabla}\times\frac{1}{\varepsilon_r}\vec{\nabla}\times\vec{H}=\frac{\omega^2}{c^2}\vec{H}$ where the photonic crystal lays the periodicity of dielectric materials.

The operator in the left part of Eq. (2.37), the master equation, is a Hermition for dielectric material (ε is simply real) and this gives a set of orthogonal Eigen states as the solution. For a periodicity in ε such that $\varepsilon(\vec{r}+\vec{R})=\varepsilon(\vec{r})$; where $\vec{R}$ is the lattice displacement which is the product of multiple number of layers, the Bloch's theorem is acceptable for the Eigen solution of $\vec{H}_{n,k}(\vec{r}+\vec{R},t)=e^{-i(\vec{k}\cdot\vec{r}+\omega t)}\vec{H}_{n,k}(\vec{r})$, where $\vec{H}_{n,k}(\vec{r})$ is field vector having a periodic envelope function satisfying, $\left(\vec{\nabla}+i\vec{k}\right)\times\left(\frac{1}{\varepsilon_r}\left(\vec{\nabla}+i\vec{k}\right)\times H_{n,k}(\vec{r})\right)=\left(\frac{\omega_n(k)}{c}\right)^2\vec{H}_{n,k}(\vec{r})$, which gives to different Hermitian Eigen problems for each Bloch wave vector $\vec{k}$. For the structure with periodicity in all directions, it leads to discrete Eigen values $\omega_n(\vec{k})$ for n=1, 2, 3..., which are continuous functions. Plotting the Eigen value versus $\vec{k}$, it gives a dispersion relation of the periodic structure, called photonic band gap (PBG) materials.

Now, this concept can be implemented in one-dimensional periodic structure where the propagation wave vector in the each layer of the one-dimensional periodic lattice can be formulated with the boundary conditions of each layer. By implementing the boundary conditions and considering the conservation of energies on the interfaces, we calculate the characteristics matrices for layers and are called Transfer Matrix Method (TMM) technique [9-11, 17]. We chose a periodic arrangement of a multilayer thin film i.e. binary periodic structure of dielectric materials with index of refraction n_1 and n_2 and thicknesses d_1 and d_2, respectively. The master equation has scalar form and the solution of the scalar wave equation is a plane field wave. The plane field waves are the superposition of first the right going and left going plane waves for layer with thickness d_1 and index n_i. If the amplitudes A_1 and B_1 are the forward and backward going waves in the layer of the refractive index n_1. Then, the field wave for the layer of the refractive index $n_1$as shown in Figure 2.2, using Eq. (2.19), is given as:

$$\vec{E}(x) = A_1 e^{ik_{1x}x} + B_1 e^{-ik_{1x}x} \tag{2.39}$$

Similarly, the solution of field waves is the superposition of the forward (right) going and backward (left) going plane waves having amplitudes C_1 and D_1 for the layer of the refractive index n_2. Hence, the solution of field waves can be represented for n_2, using Eq. (2.19), as:

$$\vec{E}(x) = C_1 e^{ik_{2x}(x-d_1)} + D_1 e^{-ik_{2x}(x-d_1)} \tag{2.40}$$

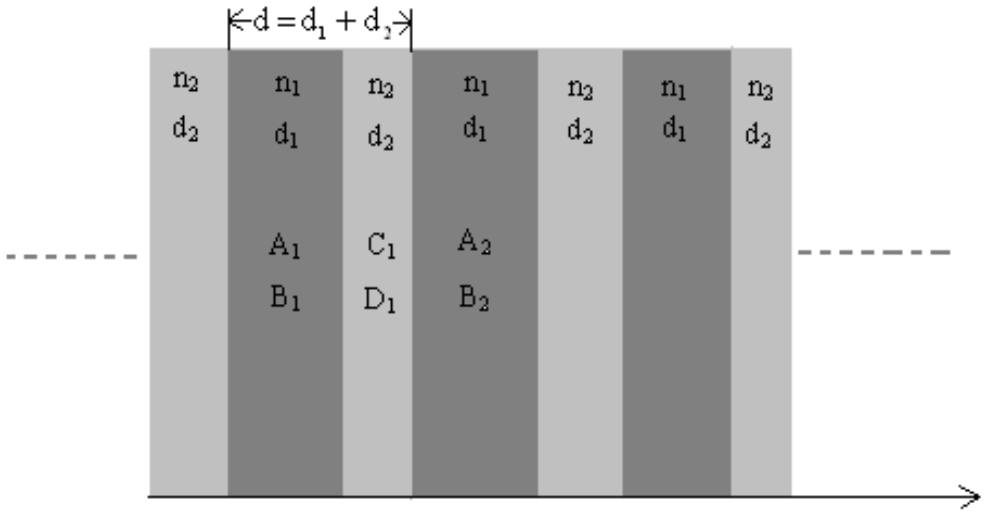

Figure 2.2: Schematic diagram of bilayers unit cell of refractive indices n_1 and n_2 with thicknesses d_1 and d_2, respectively.

The wave numbers k_{1x} and k_{2x}, Eq. (2.39) and Eq. (2.40) are defined as:

$$k_{1x} = \frac{\omega}{c} n_1 \cos\theta_1 \quad \text{and} \quad k_{2x} = \frac{\omega}{c} n_2 \cos\theta_2 \tag{2.41}$$

where θ_1 and θ_2 are the ray angles in the two layered media, respectively. At the interface between layers ($x = d_1$), the solution of Eq. (2.39) and Eq. (2.40) and its derivative should be continuous. The relation between plane wave amplitudes at the interface of n_1 and n_2 materials is analyzed. On applying the boundary conditions at $x=d_1$, we found a characteristic matrix equation for thickness d_1 of n_1 material.

$$\begin{pmatrix} C_1 \\ D_1 \end{pmatrix} = M_{12} \begin{pmatrix} A_1 \\ B_1 \end{pmatrix} \tag{2.42}$$

$$\text{with } M_{12} = \begin{pmatrix} \frac{1}{2}\left(1+\frac{k_{1x}}{k_{2x}}\right)e^{ik_{1x}d_1} & \frac{1}{2}\left(1-\frac{k_{1x}}{k_{2x}}\right)e^{-ik_{1x}d_1} \\ \frac{1}{2}\left(1-\frac{k_{1x}}{k_{2x}}\right)e^{ik_{1x}d_1} & \frac{1}{2}\left(1+\frac{k_{1x}}{k_{2x}}\right)e^{-ik_{1x}d_1} \end{pmatrix} \tag{2.43}$$

And likewise at x = d, the continuity of the plane waves at the periodic interface with index n_2 and n_1 and we get:

$$\begin{pmatrix} A_2 \\ B_2 \end{pmatrix} = M_{21}\begin{pmatrix} C_1 \\ D_1 \end{pmatrix} \tag{2.44}$$

where the matrix M_{21} is the identical as (2.43) with interchanging the indices for d_2 thickness.

For a period of two materials of refractive indices n_1, n_2 and thicknesses d_1 and d_2 respectively, we have the matrix for two materials with'd' as lattice parameter using matrices Eq. (2.43) and Eq. (2.44), and we have,

$$\begin{pmatrix} A_2 \\ B_2 \end{pmatrix} = M_{21}M_{12}\begin{pmatrix} A_1 \\ B_1 \end{pmatrix}$$

$$\text{or} \begin{pmatrix} A_2 \\ B_2 \end{pmatrix} = M_{i,j}\begin{pmatrix} A_1 \\ B_1 \end{pmatrix} \tag{2.45}$$

where $M_{i,j} = M_{21}M_{12}$.

The matrix component of the matrix $M_{i,j}$ for binary periodicity with d (=d1+d2) is given by

$$M_{1,1} = e^{ik_{1x}d_1}\left[\cos(k_{2x}d_2) + \frac{1}{2}i\left(\gamma + \frac{1}{\gamma}\right)\sin(k_{2x}d_2)\right] \tag{2.46}$$

$$M_{1,2} = e^{-ik_{1x}d_1}\left[1 + \frac{1}{2}i\left(\frac{1}{\gamma} - \gamma\right)\sin(k_{2x}d_2)\right] \quad M_2 = \overline{M}_{1,2}, \qquad M_{2,2} = \overline{M}_{1,1} \tag{2.46}$$

where $\vec{M}_{ij} = \text{transpose of matrix } M_{ij}$, $k_{jx} = \frac{\omega}{c}n_j\cos\theta_j$ and $\gamma = \frac{k_{1x}}{k_{2x}}$ for TE mode and $\gamma = \frac{k_{1x} \times n_2^2}{k_{2x} \times n_1^2}$ for TM mode..The matrix $M_{i,j}$ is called as the *transfer characteristic matrix for* the periodic lattice [9]. The square matrix $M_{i,j}$ depends on the frequency ω,

and it is called uni-modular viz. the determinant of the square matrix is equal to unity. Hence, the square matrix $M_{i,j}$ for each ω defines a unique mapping for the amplitudes of the plane waves in first mediumn$_1$ into the amplitude of the plane waves in second medium with index n_2.

For an infinite periodic lattice extending on the entire x-axis, the solution of the Helmholtz Eq. (2.46) can be written in terms of Bloch's waves [9-12, 30].

$$\vec{E}(x,K) = U_K(x)\, e^{i\,K(\omega)\,x} \tag{2.47}$$

where $U_K(x)$ is a periodic function with lattice ($d= d_1 +d_2$) with $U_K(x) = U_K(x+d)$ and its value is complex. They $K(\omega)$ are named as the Bloch wave number for a periodic lattice with thicknesses d_1 and d_2, with index of refraction n_1 and n_2, respectively.

The expression for $K(\omega)$ is given as:

$$K(\omega) = \frac{1}{d}\cos^{-1}\left(\frac{1}{2}\mathrm{Tr}\left[M_{i,j}\right]\right) \tag{2.48}$$

with $M_{i,j}$ is specified in Eq. (2.46).

After solving Eq. (2.48), we obtain the total dispersion relation for a unit cell of thickness d ($=d_1+d_2$), which is given as:

$$K(\omega) = \frac{1}{d}\cos^{-1}\left[\cos(k_{1x}d_1)\times\cos(k_{2x}d_2) - \frac{1}{2}\left(\gamma+\frac{1}{\gamma}\right)\times\sin(k_{1x}d_1)\times\sin(k_{2x}d_2)\right] \tag{2.49}$$

where $\gamma = \dfrac{k_{1x}}{k_{2x}}$ for TE mode and, $\gamma = \dfrac{k_{1x}\cdot n_2^2}{k_{2x}\cdot n_1^2}$ for the TM mode and $k_{jx} = \dfrac{\omega}{c} n_j \cos\theta_j$ with j=1,2.

The Eq. (2.49) is called photonic band gap of photonic crystal or *dispersion relation of the periodic lattice.*

The dispersion relation characterizes the behavior of Bloch's waves. The Bloch wave for the periodic lattice has three cases:

(i) Real K (ω) lies in the first Brillouin zone [0, π/d], the travelling field wave function, E(x, K), is in the periodic structure. The real $K(\omega)$ is said that ω is the allowed band gap.

(ii) Imaginary $K(\omega)$ is defined by $K(\omega) = \pi/d + i\rho(\omega)$. The standing wave function of the $E(x,K)$ is the product of two periodic functions increases and decreases exponentially which depend on the $\rho(\omega)$. The imaginary $K(\omega)$ for the value of ω is the forbidden band gap.

(iii) At the $K(\omega) = \pi/d$, the $E(x, K)$ is the d-shift skew symmetric due to the periodic function $E(x, K)$ as the 2nd period with special properties i.e. $E(x + d, K) = -E(x, K)$.

Besides this, the other optics of photonics can be calculated using Eq. (2.45) and the reflection and transmission coefficients, and Fresnel's coefficients, can be calculated from the amplitude of reflected wave and transmitted wave with respect to the amplitude of the incident wave. Now, we are going to discuss the formalism for the optics of anisotropic, second case, and optics of photonics of such material in next section.

2.3 Optics of anisotropic medium

In anisotropic medium, the electric vector of a propagating wave is not parallel to its direction of polarization and it is described by the direction of an electric displacement vector [7, 31, and 32]. There are two different possible polarization directions that exist for plane waves travelling in a specific direction through a non-linear or anisotropic medium, and the waves that have these different polarization directions, travel with different velocities. The most common and the most important anisotropic media are generally crystalline. These anisotropic mediums have their optical properties closely associated to the several symmetry properties influenced by crystals.

In an isotropic medium, the propagation characteristics of an electromagnetic wave are independent of their directions of propagation. This, therefore, means that there is no other direction possible in the medium, which is different than any other direction. It is obvious then that we cannot just simply categorize liquid crystals as isotropic media, as we can do for gases or liquids, where any external field is not implementing. Such a field means the presence of a unique direction in the medium. The case of a gas in a magnetic field is fine example to understand the circumstance of an isotropic medium being converted into an anisotropic medium when an external field is applied. This phenomenon occurs because the gas alters the characteristics of

polarization of a wave, which propagates in the direction of the field. This very well known phenomenon is known as the "Faraday electro-optics Effect".

2.3.1 Fields and waves in anisotropic medium

The constitutional equations in anisotropic media, which has the permittivity and permeability tensors and are given by:

$$\vec{D} = \varepsilon_0 \bar{\bar{\varepsilon}} \vec{E} \tag{2.50}$$

$$\vec{B} = \mu_0 \bar{\bar{\mu}} \vec{H} \tag{2.51}$$

where, $\bar{\bar{\varepsilon}}$ = tensor permittivity, $\bar{\bar{\mu}}$ = tensor permeability. The tensor permittivity and the tensor permeability are complex and dependent on the frequency for steady state sinusoidal time varying fields. This implies that all the components of the permittivity and permeability matrices are complex. It is possible for a medium to be both electric and magnetic anisotropic, but it is common for an anisotropic medium to be either just electric anisotropic or magnetic anisotropic.

If the medium is just electric anisotropic, it is known as $\bar{\bar{\varepsilon}}$ anisotropic medium. In such a medium, the permittivity $\bar{\bar{\varepsilon}}$ becomes a tensor and the permeability $\bar{\bar{\mu}}$ remains a scalar. Therefore, the governing relations for electric permittivity tensor are given as:

$$\bar{\bar{\varepsilon}} = \begin{pmatrix} \varepsilon_{xx} & \varepsilon_{xy} & \varepsilon_{xz} \\ \varepsilon_{yx} & \varepsilon_{yy} & \varepsilon_{yz} \\ \varepsilon_{zx} & \varepsilon_{zy} & \varepsilon_{zz} \end{pmatrix} \text{and } \bar{\bar{\mu}} = \mu \,(\text{scalar}) \tag{2.52}$$

Similarly, if the medium is just magnetic anisotropic, it is accepted as $\bar{\bar{\mu}}$ anisotropic medium. In such a medium the magnetic permeability $\bar{\bar{\mu}}$ becomes a tensor and the electric permittivity $\bar{\bar{\varepsilon}}$ remains a scalar. Therefore, the governing relations for such a medium become [33]:

$$\bar{\bar{\mu}} = \begin{pmatrix} \mu_{xx} & \mu_{xy} & \mu_{xz} \\ \mu_{yx} & \mu_{yy} & \mu_{yz} \\ \mu_{zx} & \mu_{zy} & \mu_{zz} \end{pmatrix} \text{ and } \bar{\bar{\varepsilon}} = \varepsilon \,(\text{scalar}) \tag{2.53}$$

Since the permittivity and permeability are tensors in their respective anisotropic mediums, their inverse has similar importance in calculations.

2.3.2 Dispersion relation for hyperbolic material

The dispersion relation with hyperbolic behavior comes from the optics of crystal structure. Such type of crystal materials has a constitutive relation between the dielectric displacement $\vec{D}$, and magnetic induction, $\vec{B}$, to the fields $\vec{E}$ and $\vec{H}$ respectively. The electric and magnetic fields also depend on the permittivity and the permeability of the material. Now, the dielectric displacement and magnetic induction are related in hyperbolic behavior due to crystal materials. And here,

$$\vec{D} = \varepsilon_0 \overline{\overline{\varepsilon}} \vec{E} \tag{2.54}$$

$$\vec{B} = \mu_0 \overline{\overline{\mu}} \vec{H} \tag{2.55}$$

where $\overline{\overline{\varepsilon}}$ and $\overline{\overline{\mu}}$ are shown as electric permittivity tensor and magnetic permeability tensor of the material. In our work, we have considered nonmagnetic media in which $\overline{\overline{\mu}}$ reduces like unit tensor. The permittivity tensor takes in the diagonalized form for real and symmetric nature in such a way that the off diagonal elements vanish, as:

$$\overline{\overline{\varepsilon}} = \begin{pmatrix} \varepsilon_{xx} & 0 & 0 \\ 0 & \varepsilon_{yy} & 0 \\ 0 & 0 & \varepsilon_{zz} \end{pmatrix} \tag{2.56}$$

This matrix is in Cartesian form, so it called principal axis of the crystal. In the matrix, three diagonal components of the matrix are positive, and generally all depend on the angular frequency ω; the crystal is termed in the following ways:

(i) Biaxial crystal material, $\varepsilon_{xx} \neq \varepsilon_{yy} \neq \varepsilon_{zz}$

(ii) Uniaxial crystal material, $\varepsilon_{xx} = \varepsilon_{yy} \neq \varepsilon_{zz}$

(iii) Isotropic crystal material, $\varepsilon_{xx} = \varepsilon_{yy} = \varepsilon_{zz}$

Hyperbolic meta-material is a uniaxial type of material. To define the dispersion relation of EMW, we have the Eq. (2.56). Now, we take the two equations of Maxwell's in the absence of any external sources $(\vec{J} = \rho = 0)$ in the following forms:

$$\vec{\nabla} \times \vec{E} = -\frac{\partial \vec{B}}{\partial t} \tag{2.57}$$

$$\vec{\nabla} \times \vec{H} = \vec{J} + \frac{\partial \vec{D}}{\partial t} \tag{2.58}$$

where $\vec{D}$ and $\vec{B}$ are as in Eq. (2.54) into Eq. (2.55), respectively. By inserting Eq. (2.57) and Eq. (2.58), the plane wave expressions are written as $E = E_0 e^{i(\omega t - k.r)}$ and $H = H_0 e^{i(\omega t - k.r)}$, where k is the wave propagation vector. Solving the above equations, we obtain:

$$k \times E = \omega \mu_0 H \tag{2.59}$$

$$k \times H = -\omega \varepsilon_0 \bar{\bar{\varepsilon}} E \tag{2.60}$$

By taking curl of the Eq. (2.59) and substituting the curl H from Eq. (2.60), the Eq. (2.59) produces the Eigen value problem for the field E as:

$$k \times (k \times E) + \omega^2 \mu_0 \varepsilon_0 \bar{\bar{\varepsilon}} E = 0 \tag{2.61}$$

This Eq. (2.61) can be established in the matrix form by using Eq. (2.56) and the obtained equation shows the dispersion relation for anisotropic material, which is given as;

$$\begin{pmatrix} k_0^2 \varepsilon_{xx} - k_y^2 - k_z^2 & k_x k_y & k_x k_z \\ k_x k_{yz} & k_0^2 \varepsilon_{yy} - k_x^2 - k_y^2 & k_y k_z \\ k_x k_z & k_y k_z & k_0^2 \varepsilon_{zz} - k_x^2 - k_y^2 \end{pmatrix} \begin{pmatrix} E_x \\ E_x \\ E_x \end{pmatrix} = 0 \tag{2.62}$$

where $k_0 = \frac{\omega}{c}$ are the magnitude of propagation wave vector, and $c = \frac{1}{\sqrt{\varepsilon_0 \mu_0}}$, the speed of light in vacuum. Now, we emphasis on the hyperbolic media for the uniaxial material having the optical axis, which is oriented along the z-direction, that is $\varepsilon_{xx} = \varepsilon_{yy} = \varepsilon_\perp$ and $k_\perp = \sqrt{k_x^2 + k_y^2}$. The nontrivial solution to Eq. (2.62) leads to the dispersion relation:

$$\left(k_\perp^2 + k_z^2 - \varepsilon_\perp k_0^2\right)\left(\frac{k_\perp^2}{\varepsilon_{zz}} + \frac{k_z^2}{\varepsilon_\perp} - k_0^2\right) = 0 \tag{2.63}$$

In the above equations, we have two terms in the k-space, which are equal to zero and these equations have been resembled to a spherical and an ellipsoidal iso-frequency surface: the term $(k_\perp^2 + k_z^2 - \varepsilon_\perp k_0^2)$ is described as the wave polarized in the xy-plane

(ordinary or TE wave), the terms $\left(\frac{k_{\perp}^2}{\varepsilon_{zz}}+\frac{k_z^2}{\varepsilon_{\perp}}-k_0^2\right)$ is resembled to the wave polarized in the plane containing the optical axis (TM wave or extraordinary wave).

The condition changes significantly if we have assumed an extreme anisotropy, viz. when either $\varepsilon_{\perp}$ or ε_{zz} is negative. Then the medium shows an optical signature is named as indefinite from the mathematical view [34]. For the extraordinary polarization, the components of permittivity with an opposite sign for the shape of hyperbolical iso-frequency surface. As consequences, waves with subjectively large wave vector retain a propagating nature while in isotropic materials they become evanescent due to the bounded iso-frequency contour [35]. The choice $\varepsilon_{\perp}>0$, $\varepsilon_{zz}<0$ are agreed to a two-fold hyperboloid, and such hyperbolic medium is termed dielectric (with reference its behavior in xy-plane) or Type-I hyperbolic material [36]; the choice $\varepsilon_{\perp}<0$ and $\varepsilon_{zz}>0$ is described a one-fold hyperboloid, and such hyperbolic medium is named a metallic or Type-II hyperbolic material [37]. The hyperbolic materials are composite materials. Therefore, the effective medium theory is very popular theory for study the optics of composite materials. In next section we discuss about the effective medium theory, which is used in Hyperbolic Meta-materials (HMMs).

2.3.3 Effective medium theory

The effective medium theory used to calculate the permittivity's for a non-linear or anisotropic composite material with the uniaxial symmetry. This method is based on the generalized Maxwell-Garnet approach and used to obtain the analytical expressions of the parallel and perpendicular effective permittivity. The permittivity of such material has a unique property of the materials that is called filling fraction (f). Let us suppose that a composite material is combined with two materials of metal and dielectric and the dielectric and metal permittivity's are $\varepsilon_d\ (=n_1^2)$ and $\varepsilon_m\ (=n_2^2)$, respectively. For two materials, the filling fraction (f) of the composite material may be defined in term of thickness as follows:

$$f=\frac{d_d}{d_d+d_m} \tag{2.64}$$

where d_{HM} is the total thickness of the metal and dielectric in the system i.e. $d_{HM} = d_d + d_m$ where d_d is the thickness of dielectric and d_m is the thickness of metal. In general approach, the electric field displacement (D) in the materials is proportional to the electric field (E) and expressed by the following expression:

$$\overline{D} = \varepsilon_0 \bar{\bar{\varepsilon}} E \tag{2.65}$$

where $\bar{\bar{\varepsilon}}$ is effective permittivity tensor of the uniaxial medium. In the electrostatics, the tangential electric field $(\vec{E})$ is continuous across the interface as move from one medium to another. The condition must be satisfied for the propagating wave as

$$E_d^{\parallel} = E_m^{\parallel} = E^{\parallel} \tag{2.66}$$

where E_d is the electric field for n_1 layer, E_m is the electric field in the n_2 layer and E is the electric field of composite material. From the condition of continuity, the overall parallel dielectric displacement is averaging in the displacement field contributions from n_1 dielectric layer and n_2 metallic layer, which is given as;

$$D^{\parallel} = fD_d^{\parallel} + (1-f)D_m \tag{2.67}$$

Using Eq. (2.65) for dielectric, metal and composite material, the Eq. (2.67) becomes:

$$\varepsilon_{eff} E^{\parallel} = f\varepsilon_d E^{\parallel} + (1-f)\varepsilon_m E^{\parallel} \tag{2.68}$$

After simplification; we obtain the relation between the filling fraction and permittivity of the metal and dielectric materials as:

$$\varepsilon_{\parallel} = f\varepsilon_d + (1-f)\varepsilon_m \tag{2.69}$$

Putting the value of filling fraction from Eq. (2.64), the relation is obtained for hyperbolic materials is

$$\varepsilon_{\parallel} = \frac{\varepsilon_d \varepsilon_m (d_d + d_m)}{\varepsilon_d d_m + \varepsilon_m d_d} \tag{2.70}$$

Moreover, the perpendicular permittivity is derived using Maxwell's equations and boundary conditions. Pacifically, the normal dielectric displacement vector at each interface must be continuous and the expression is given as;

$$D_d^{\perp} = D_m^{\perp} = D^{\perp} \tag{2.71}$$

We also recognize that the total electric field will be the superposition of the components of electric field from the dielectric layer (n_1) and the metallic layer (n_2). Thus, we have the electric components;

$$E^{\perp} = fE_d^{\perp} + (1-f)E_m^{\perp} \tag{2.72}$$

On solving the Eq. (2.71) and Eq. (2.72) by using Eq. (2.65) for dielectric, metal and composite material, we obtain the relation:

$$\varepsilon_{\perp} = \frac{\varepsilon_d \varepsilon_m}{f\varepsilon_d + (1-f)\varepsilon_m} \tag{2.73}$$

Putting the value of filling fraction from Eq. (2.64) in the above Eq. (2.73), we obtain the relation:

$$\varepsilon_{\perp} = \frac{(\varepsilon_d d_d + \varepsilon_m d_m)}{d_d + d_m} \tag{2.74}$$

The volume weights of the composite material purely depend on the thickness of whole materials in term of the filling fraction, which can be considered in the optical calculations of photonic crystals [38]. The volume weight of the electric permittivity of the constituent media is acceptable for high wavelength and low frequency but it fulfills the concept of sub-wavelength for meta-materials that follows the concept of effective medium theory [39].

2.4 Conclusion

In the theory and mathematical formulations, we have discussed the optics of materials in which the optical density of material is dependent on the physical parameters i.e. ε and μ. These two parameters of the materials are also verified with the Maxwell's equations. The $\overline{\overline{\varepsilon}}$ and $\overline{\overline{\mu}}$ are tensors quantities, therefore, the materials or media are classified into two types: (i) isotropic and (ii) anisotropic medium. We have discussed the scalar and vector forms of the electromagnetic wave equations, which have been derived from Maxwell's equations. The scalar form of wave equation is called Helmholtz's equations, which is used to formulate the TMM method, and the vector form of wave equation is generally used to formulate the other methods like FEM, FDTD, PWEM, etc. There are several methods available to study the optics of photonics, but we have adopted the Transfer Matrix Method (TMM) in whole thesis for both materials viz. isotropic and anisotropic material, because TMM is used to

solve the optics of the photonic crystals, which is analogous and used to solve the electronics in the semiconductors by the quantum mechanics.

Throughout the thesis, we have used the scalar form of wave equation and plane wave solutions to derive the dispersion relation, and formulated the matrices to study the optical properties of the photonic crystal containing isotropic and anisotropic materials. The Helmholtz's wave equations have been used to solve the field equations in each layer of the materials. The amplitudes of the waves have been formulated with a characteristics matrix and this total matrix for binary and ternary layers can be used to study the optical properties of multilayered structure. To study the optical property of photonic crystal, we have used is TMM method. The TMM is the best method to analyze the optical properties of one-dimensional photonic crystal, and the obtained results have been also experimentally verified in the thin film optics [40, 29]. Besides this, the optics of the composite materials is studied and discussed in detail by using the effective medium theory.

References

[1] D. Bexeaux and J. Vlieger, A statistical theory of the dielectric properties of thin islands films: The surface material coefficients, Physica 73(2) (1974) 287-311. https://doi.org/10.1016/0031-8914 (74)90002-0

[2] P. H. Lissberger, P. W. Saunders, Optical and magneto optical properties of thin film cermats, Thin Solid Films 34 (1976) 323-333.

[3] S. Norrman, T. Andersson, C. G. Granquist, O. Hunderi, Optical properties of discontinuous gold films, Phys. Rev. B 18 (1978) 674-695.

[4] C. G. Granquist, O. Hunderi, Optical properties of ultrafine gold particles, Phys. Rev. B 16 (1977) 3513-3534.

[5] S. Yamaguchi, The resonance type absorption of very thin silver and gold films, J. Phys. Soc. Jpn. 15 (1960) 1577-1585.

[6] B. R. Cooper, H. Ehrenreich, and H. R. Philipp, Optical properties of noble metals. II, Phys. Rev. 138(2A) (1965) A494-14.

[7] C. C. Davis, Lasers and Electro-Optics: Fundamentals and Engineering, Cambridge University Press, U. K. (1996).

[8] D. J. Griffiths, Introduction to Electrodynamics, Prentice Hall, Upper Saddle River New Zersey U.S. (1999).

[9] P. Yeh, Optics in Layered Media, John Willey and Sons, New York (1988).

[10] A. Sopaheluwakan, Thesis on Defect States and Defect modes in 1-D photonic crystals, Univ. of Twente, Nitherland (2003); A. Rung, Thesis on Numerical studies of energy gaps in photonic crystals, Uppsala Univ. Swedon (2005).

[11] M. Born and E. Wolf, Principle of Optics, 7th Ed. Pergmon Press, Oxford (1999).

[12] S. G. Johnson, Photonic Crystal: From Theory to Practice, Chapter 1, (2001) 1-65.

[13] K. Yasumoto, Electromagnetic theory and applications for photonic crystals, Taylor & Francis Press, Boca Raton, London, New York (2005).

[14] J. B. Pendry, Calculating band structure, J. Phys. Cond. Mat. 8 (1996) 1085–1108.

[15] A. Taflove, Computational electrodynamics: The Finite-Difference Time-Domain Method, Artech House, Boston, London (2005).

[16] G. Pelosi, R. Coccioli, and S. Selleri, Quick Finite Elements for Electromagnetic Waves 2nd Ed. Arteh House, Boston, London (2009).

[17] J. B. Pendry and A. MacKinnon, Calculation of photon dispersion relations, Phys. Rev. Lett. 69 (1992) 2772–2775.

[18] D. Felbacq, G. Tayeb, and D. Maystre, Scattering by a random set of parallel cylinders, J. Opt. Soc. Am. A, 11(9) (1994) 2526–2538.

[19] F. de Daran, V. Vigneras-Lefebvre, J. P. Parneix, Modelling of electromagnetic waves scattered by a system of spherical particles, IEEE T. Magn. 31(3) (1995) 1598-1601.

[20] D. Maystre, Electromagnetic study of photonic band gaps, Pure Appl. Opt. 3 (1994) 975-993.

[21] E. Yablonovitch, Photonic band gap structures, J. Opt. Soc. Am. B 10 (1993) 283-295.

[22] R. D. Meade, K. D. Brommer, A. M. Rappe, and J. D. Joannopoulos, Electromagnetic Bloch waves at the surface of a photonic crystal, Phys. Rev. B 44 (1991) 13772–13774.

[23] Z. Li, L. L. Lin, and Z. Q. Zhang, Spontaneous emission from photonic crystals: Full vectorial calculations, Phys. Rev. Lett. 84 (2000) 4341–4344.

[24] S. Fan, P. R. Villeneuve, J. D. Joannopoulos, and E. F. Schubert, High extraction efficiency of spontaneous emission from slabs from photonic crystals, Phys. Rev. Lett. 78 (1997) 3294-3297.

[25] C. T. Chan, Q. L. Yu, and K. M. Ho, Order N-spectral method for electromagnetic waves, Phys. Rev. B 51 (1995) 16635-16642.

[26] A. Taflove, S. C. Hagness, Advances in Computational Electrodynamics, 3rd Ed. Artech House, Boston London (2005) 1038.

[27] J. B. Pendry, and L. Martin-Moreno, Energy loss by charged particle in complex media, Phys. Rev. B 50 (1994) 5062-5073.

[28] D. R. Smith, S. Schultz, N. Kroll, M. Sigalas, K. M. Ho, and C. M. Soukoulis, Experimental and theoretical results for a two-dimensional metal photonic band-gap cavity, Appl. Phys. Lett. 65 (1994) 645-647.

[29] F. Gadot, A. Chelnokov, A. De Lustrac, P. Crozat, and J. M. Lourtioz, D. Cassagne and C. Jouanin, Experimental demonstration of complete photonic band gap in graphite structure, Appl. Phys. Lett. 71 (1997) 1780-1782.

[30] K. Sakoda, Optical Properties of Photonic Crystal, Springer Verlag Press, Germany (2001).

[31] K. Zhang, D. Li, Electromagnetic Theory for Microwaves and Optoelectronics, 2nd Ed. Springer, Berlin Heidelberg (2008). https://doi.org/10.1007/978-3-540-74296-8

[32] V. A. De Lorenci, J. M. Salim, Aspects of light propagation in anisotropic media, Phys. Letts. A 360 (2006) 10-13.

[33] P. H. Lissberger, P. W. Saunders, Optical and magneto optical properties of thin film cermets, Thin Solid Films 34 (1976) 323.

[34] D. R. Smith and D. Schurig, Electromagnetic wave propagation in media with indefinite permittivity and permeability tensors, Phys. Rev. Lett. 90 (2003) 077405.

[35] L. Novotny, B. Hecht, Principles of Nano-optics, Cambridge University Press, New York (2012).

[36] S. Ishii, A. V. Kildishev, E. Narimanov, V. M. Saleav, V. P. Drachev, Sub wavelength interference pattern from volume Plasmon polaritons in a hyperbolic medium, Laser Photonics Rev. 7 (2013) 265-271.

[37] C. L. Cortes, W. Newman, S. Molesky, Z. Jacob, Quantum nanophotonics using hyperbolic meta-materials, J. Opt. 14 (2012) 063001-063019.

[38] T. Koschny, P. Markos, E. N. Economou, D. R. Smith, D. C. Vier, and C. M. Soukoulis, Impact of inherent periodic structure on effective medium description of left-handed and related meta-materials, Phys. Rev. B 71 (2005) 245105.

[39] D. Rousselle, A. Berthault, O. Acher, J. P. Bouchaud, and P. G. Zérah, Effective medium at finite frequency: Theory and experiment, J. Appl. Phys. 74 (1993) 475.

[40] H. A. Macleod, Thin film optical filters 3rd Ed. Taylor & Francis Group, CRC Press, Boca Raton, London, New York (2001).

[41] G. Kedavat, P. Kumar, Y. K. Vijay and B. K. Gupta, Fabrication of highly-efficient resonant structure assisted ultrathin artificially stacked Ag/ZnS/Ag multilayers films for color filter applications, J. Mater. Chem. C 3(26) (2015) 6745-6754.

Chapter 3
Tunable broadband reflector and narrowband filter of dielectric and magnetized cold plasma photonic crystal

Chapter-3

Tunable broadband reflector and narrowband filter of dielectric and magnetized cold plasma photonic crystal

3.1 General introduction

In general physics, we know basic three state of matter and they are solid, liquid and gas. Any one of the states can be transformed into another state through the exchange of energy. In our day-to-day life, water (H_2O) is a remarkable example, which found in all the states: ice (solid), water (liquid) and steam (gas). Obviously, the solid phase can be converted into the liquid phase and the liquid phase into the gaseous phase by supplying energy into the matter, and the reverse process of the water (H_2O) by extracting out energy from the matter. In the few cases, it is possible to convert directly, solid phase into a gaseous phase e.g. NH_4Cl, Camphor etc. Additional amount of energy to the gaseous phase of matter, the molecule of the gaseous phase breaks into the constituent atoms. After the strips off their electrons and produces the positively charged ions and negatively charged electrons are found. The minimum amount of energy is required to liberate an electron from an atom is identified as the ionization potential. This provided energy may be in the heat and radiation. Ionization of charge due to heat energy ionization occurs at high temperature of the order of million Kelvin that state can be produced in the laboratories. The ionized state of matter where charged particles as well as neutral particles exist concurrently, generally known as *plasma*.

3.1.1 Plasma

Plasma is an extensive diversity of macroscopically impartial particles containing numerous interacting free electrons and ionized atoms or molecules that exhibit collective property owing to the distant columbic force is called *plasma*. For the collection of interacting charged particles and neutral particles to show plasma behavior, it must be satisfied certain condition for plasma existence. The word of the plasma comes from the Greek word that means of it “something molded”. In 1929, first time Tonks and Langmuir [1] described the glowing ionized gas, which was formed by electrical discharge in a tube of the ionized gas a whole remaining electrically neutral. We know that when a solid or liquid substance is heated the atoms or molecules of substance acquires more thermal kinetic energy to overcome the

binding potential energy. This leads to the phase transition, which exhibit the temperature constant for a specified pressure. The required amount of energy for phase transition is known as latent heat. If sufficient energy is provided to substances, a molecular gas can dissociates into an atomic gases as a result of collision between those particles whole thermal kinetic energy gives the molecular binding energy. However, this transition from a gas to plasma is not a phase transition in the sense of thermodynamics, it occurs gradually with increasing the value of temperature [2, 3].

3.1.1.1 Macroscopic neutrality

Plasma is macroscopically neutral in the absence of any external disturbances. This means that under certain equilibrium conditions, there are no external forces present in plasma and net electric charge is zero. A volume of the plasma has contained sufficiently huge amount of ionized particles and it is sufficiently small compared with the characteristics lengths. The characteristics length and number of ionized particles are dependent for the variations of macroscopic parameters like "density" and "temperature". The macroscopic electrical neutrality exist only for certain distances in which a balance is obtained between the thermal energy, which tends to disturb the electrical neutrality and the electrostatic potential energy resulting from some charge separation, which tends to restore the electrical neutrality. This distance is of the order of a characteristics length parameter of the plasma called "Debye length". The charged particles arrange themselves in such a way as to effectively shield any electrostatic fields within a distance of the order of Debye length. This shielding of electrostatic field is a consequence of the collective behavior of the plasma particles. Debye first performed the shielding distance calculation. The Debye length (λ_D), is directly proportional to the square root of the temperature (T) and inversely proportional to the square root of the plasma density (n_e) is given as;

$\lambda_D = \left[\frac{\varepsilon_0 K_B T}{n_e e}\right]^{1/2}$, where ε_0 = permittivity of free space, K_B = Boltzmann constant, n_e = plasma density , e = electronic charge and T = temperature [2, 3].

3.1.1.2 Plasma frequency

An important parameter of plasma property is the stability of its macroscopic charge neutrality. When plasma is instantly disturbed from the equilibrium condition, the resulting internal space charge field gives rise to collective particle motions. Now

question arises that which tends to restore the original charge neutrality. These collective motions are characterized by a natural frequency of oscillation known as *plasma frequency* [2, 3]. Since, these collective oscillations are high frequency oscillations, due to their heavy mass, are unable to follow the motion of the electrons to a certain extent. The electrons are oscillating collectively about the heavy ions; the necessary collective restoring force is being provided by the ion electron columbic attraction. The angular frequency of the collective electron oscillation, called plasma frequency ω_p, is given by: $\omega_p = \left[\frac{n_e e^2}{m\varepsilon_0}\right]^{1/2}$. The plasma frequency depends on the plasma density that is also fundamental parameter of the plasma. From the relation between plasma frequency and mass, the plasma frequency is very high since mass of electron is very low. Using the values of various parameters, $\nu_p = \frac{\omega_p}{2\pi} > \nu_n \approx 9\sqrt{n}$, where n is plasma density per m^3. For a plasma having electron density, $n = 10^{10} m^{-3}$, we have, $\nu_p = 9\times(10^{18})^{1/2} = 9\times10^9 \text{Hz} = 9\text{GHz}$. Hence, the plasma frequency lies in the microwave region. As we know that electromagnetic radiation of frequency smaller than the plasma frequency $(\omega < \omega_p)$ is reflected back the plasma, whereas the radiation of frequency is larger than the plasma frequency $(\omega > \omega_p)$ transmit through the plasma. This property of plasma in the ionosphere around the earth has been exploited for communication purposes [4].

3.2 Plasma Photonic Crystal (PPC)

As discussed earlier that the periodic structure is a cumbersome structure, which is different from the continuous medium. Because, the periodic structures have reveals the photonic band gap due to the resonance of the waves at the surface of periodic lattice. Hence, the spontaneous emission of an atom placed in a periodic structure has a huge number of properties. When the atom is excited, the development can be forwarded in two forms i.e., either emission of photons in the allowed band with low probability or transition of excited state with high probability, that state is relatively long-lived state [5]. For a considered system, the identical dielectrics are composed in three-dimensional lattices and the secular equation for the energy of photons and diffraction in ultraviolet and visible forms. Hence, the low frequency of the diffracted electromagnetic wave rises to the Bragg reflections having the order of magnitude

stronger in the X-ray diffraction. Some characteristic aspects anticipated in low energy photon that discussed in relation to the low energy electron diffraction [6].

The homogeneous and inhomogeneous artificial periodic structure is called Photonic Crystals (PCs) and these PCs have unique property i.e. photonic band gap that was proposed by Yablonovitch [7] and John [8] in 1987. The photonic band gap of the different material has many applications because the photonic band gap is used to control the propagation of light. As we know that the propagation of electromagnetic waves inside the photonic crystal depends on the refractive index contrast, the lattice parameter, the filling fraction, and dimensionality, etc. [8, 9]. The one-dimensional periodic multilayer structure is the simplest type of the photonic crystal because it is easily fabricated using the concept of thin film technology. These one-dimensional photonic crystals have huge applications for optical filter; laser application, high-reflecting, omnidirectional mirror, resonance cavity, and optoelectronic circuit in the fields of modern optics and optical engineering [9–18].

The above various studies on plasma and periodic structure give an idea, to consider the optical properties of periodic structure containing the plasma materials. The plasma materials can change the optical property of the considered plasma photonic crystals and the Photonic Band Gap (PBG) due to have variable parameters. PBG can be tuned with the variation of variable parameters of the plasma material. So, the optical behavior of periodic structure with plasma and different material, called plasma photonic crystal, is analyzed theoretically and tried to find out the possible applications of plasma photonic crystals. Generally, Plasma Photonic Crystal (PPC) is a periodic arrangement of thin plasma and dielectric material like vacuum or air. The plasma photonic band gap is also obtained due to periodicity of thin plasma and dielectric materials. The plasma photonic band gap can be tuned with the variation of various parameters of the plasma material like the plasma density, the effective collision frequency, the thickness of plasma layer, and the applied external magnetic field [19-21].

Recently, magnetized cold plasma has concerned too many researchers towards the periodicity of the magnetized cold plasma and dielectric material. The magnetized cold plasma has one extra parameter as comparable to the conventional plasma i.e. presence of external magnetic field and this is related with gyro-effective frequency or cyclotron frequency. The gyro-effective frequency purely depends on applied external

magnetic field of magnetized cold plasma. The Right Hand Polarization (RHP) and Left Hand Polarization (LHP) of magnetized cold plasma have the positive and negative behavior of the gyro-effective frequency, respectively. Thus, the nature of refractive index of the magnetized cold plasma shows abnormal characteristics due to the variation of the external magnetic field, the electron density, and the effective collision frequency. Due to abnormal property of the magnetized cold plasma, the magnetized cold plasma may replace the metals or dielectrics in periodic structure. The optical properties of the considered periodic structure containing magnetized cold plasma are studied by several researchers [22-24]. Kumar et al. [25] proposed the band gap structure, reflection spectra of one-dimensional dielectric/magnetized cold plasma periodic structure. Kong et al. [26] have suggested an idea for a narrow tunable filter with defect mode of the transverse electric (TE) wave from one-dimensional periodic structure doped with magnetized cold plasma. Aly and Mohamed [27] recommended the transmission spectra of the superconductor and dielectric material for the applications in reflector and band pass filter. The transmittance property of magnetized cold plasma-superconductor periodic multilayer structure has been proposed by Aghajamali [28] for the applications in high pass filters and reflectors. Aly et al. [29] investigated the tenability of two-dimensional metallic photonic crystals by an external magnetic field. The dispersion relation and electric permittivity of metals can be affected by an applied external magnetic field, and it used for many optical devices.

Recently, Aly et al. [30] theoretically examined the transmission properties of one-dimensional periodic structure at Terahertz (THz) frequency range with the applications in the cutoff frequency of material at THz region. Aly and Elsayed [31] theoretically analyzed the effect of applied magnetic field on permittivity and transmittance characteristic of the defective one-dimensional periodic structure in UV radiations. Aly et al. [32] suggested the effect of magnetic field on the transmittance of two-dimensional n-doped semiconductor photonic crystals by using the concept of plane wave expansion method. Aly [33] explored the optical properties of superconductor-dielectric photonic band gap in ultraviolet radiations. Aly et al. [34] investigated the bandwidth of dielectric and superconductor periodic structure. Aly and Sayed [35] designed the photonic crystal structure to improve the light absorption by increasing the optical path length of the incident light inside the absorbing

material, which enhances the efficiency of thin film silicon solar cell. Aly et al. [36] explored the optical properties of new type of superconductor/semiconductor meta-material photonic crystals. Dehnavi et al. [37] studied the investigation of tunable omnidirectional band gap in one dimensional (1-D) magnetized full plasma photonic crystals and found that as increase the thickness of layer and density of plasma the omnidirectional band gap is increased. Ma et al. [38] studied the properties of unidirectional absorption and polarization splitting in plasma based photonic crystal with ultra-wideband. These findings are very useful to achieving reconfigurable unidirectional applications. Recently, Solaimani et al. [39] studied the band gap engineering in constant total length non-magnetized cold plasma-dielectric multilayer's structure forms the new type of multichannel filter applications

In this chapter, we have studied the band structures and the transmission spectra of one-dimensional periodic structure composed by dielectric (air) and magnetized cold plasma layers with periodicity ten i.e. N=10. The band structure and transmittance response against frequency (GHz) of the right hand polarization and left hand polarization structure, with variation of the magnetic field, the electron density and the effective collision frequency of magnetized cold plasma, are studied using transfer matrix method. The tunable band structure of the right hand polarization and left hand polarization structures may be used as optical filter and resonance cavity in the photonic device applications. Now, we discuss the dielectric property of plasma and study the optical properties the plasma photonic crystals using Transfer Matrix Method (TMM).

3.3 Theoretical model

In this study, we have derived the electric permittivity for the plasma using the Maxwell's equations. The refractive index of the plasma is calculated with the help of the electric permittivity of the plasma. Using TMM, the optical properties of plasma photonic crystals containing plasma with varying the parameters of the plasma has been investigated.

3.3.1 The electric permittivity of magnetized cold plasma

3.3.1.1 Magnetized-plasma

The study of wave motion inside plasma in presense of external magnetic field is called magnetized plasma. Here, two cases occurfirst the EM wave inside the internal

wave, and second the external wave and electromagnetic (EM) wave incident from outside in the presense of external magnetic field [4]. **Case-1:**When plasma is mixture of two-fluid (electron plasma fluid+ion plasma fluid) then we solve interaction of wave with magnetic field inside plasma. Then such type of wave are called hydromagnetic waves. Hydromagnetic wave has two types-(i) **Alfven waves:** when direction of wave proapgation is parallel to the applied magnetic field. (ii) **Magnetosonic wave:** direction of wave proapgation is perpendicular to the applied magnetic field. **Case-2:** In this case, the large density of plasma, considered as electron plasma fluid and ignored the ion plasma fluid. In this also exist two cases which are given as:

(a) EM wave perpendicular to the magnetic field $\left(\vec{k} \perp \vec{B}\right)$. This case is also two subcases. These are (i). $\left(\vec{E} \parallel \vec{B}\right)$, when electric field is parallel to the magnetic field is called the *ordinary waves*, and (ii) $\left(\vec{E} \perp \vec{B}\right)$, when electric field is perpendicular to the magnetic field is called the *extraordinary wave*

(b) EM wave parallel to the magnetic field $\left(\vec{k} \parallel \vec{B}\right)$. This case is also two subcases. These are(i) Right hand circular wave (R-wave). (ii) Left handed circular wave (L-wave).

To determine the wave equation in electron plasma fluid, we consider the EM wave parallel to the magnetic field. We start the Maxwell's equations, these equations are:

$$\vec{\nabla} \times \vec{E} = -\frac{\partial \vec{B}}{\partial t} \tag{3.1}$$

$$\vec{\nabla} \times \vec{H} = \mu_0 \vec{J} + \mu_0 \varepsilon_0 \frac{\partial \vec{E}}{\partial t} \tag{3.2}$$

On solving Eq.(3.1) & Eq. (3.2), these equation using the conditions- $\vec{B} = B_0 \hat{z}$, $\vec{k} = k_0 \hat{z}$ and $\vec{E} = \vec{E}_x \hat{x} + \vec{E}_y \hat{y}$. On solving the above equations, we obtain the obtained dispersion relation-

$$\omega^2 - c^2k^2 = \frac{\omega_p^2}{\left(1-\frac{\omega_c^2}{\omega^2}\right)}\left(1 \pm \frac{\omega_c}{\omega}\right) \tag{3.3}$$

Where, ω=angular frequency, $\omega_p\left(=\left[\frac{n_e e^2}{m\varepsilon_0}\right]^{1/2}\right)$ = plasma frequency, $\omega_c\left(=\frac{eB}{m}\right)$ = cyclotron frequency or gyro-effective frequency, e=electronic charge, B=external magnetic field, m=mass of electron, and $\vec{k}$ direction of propagation.Now the above equation can be simplified into two parts. If we take the possitive sign of the Eq. (3.3), then we obtain the relation, which is given below;

$$\omega^2 - c^2k^2 = \frac{\omega_p^2}{\left(1-\frac{\omega_c}{\omega}\right)} \tag{3.4}$$

Taking negative sign of Eq. (3.3), the obtained relation is given by-

$$\omega^2 - c^2k^2 = \frac{\omega_p^2}{\left(1+\frac{\omega_c}{\omega}\right)} \tag{3.5}$$

On combining the Eq. (3.4) & Eq. (3.5), and we can write a general form of the dispersion relation which can be written as;

$$\omega^2 - c^2k^2 = \frac{\omega_p^2}{\left(1\mp\frac{\omega_c}{\omega}\right)} \tag{3.6}$$

The Eq. (3.6) shows the dispersion relation of EM waves which is parallel to magnetic field inside the fluid plasma [4].

3.3.1.2 Refractive index

As we know that refrcative index or opical density is the ratio of velocity of light in vacuum to the velocity of light in medium.

$$n = \frac{c}{v} \tag{3.7}$$

The propagation vector for the plasma fluid is-

$$\vec{k} = \frac{n\omega}{c} \tag{3.8}$$

$$n^2 = \frac{c^2 k^2}{\omega^2} \tag{3.9}$$

This wave propagation equation of the wave can be related with the phase velocity. The phase velocity is given by the relation.

$$v_p = \frac{\omega}{\vec{k}} \tag{3.10}$$

Now, we can use the dispersion relation, Eq. (3.6) and the refractive index of the materials, Eq. (3.9). On solving the equations, we obtain the relation;

$$1 - \frac{c^2 k^2}{\omega^2} = \frac{\omega_p^2 \big/ \omega^2}{\left(1 \mp \frac{\omega_c}{\omega}\right)} \text{ or } \frac{c^2 k^2}{\omega^2} = 1 - \frac{\omega_p^2 \big/ \omega^2}{\left(1 \mp \frac{\omega_c}{\omega}\right)} \tag{3.11}$$

On simlifying the Eq. (3.11), we get;

$$n^2 = 1 - \frac{\omega_p^2 \big/ \omega^2}{\left(1 \mp \frac{\omega_c}{\omega}\right)} \text{ or } n^2 = 1 - \frac{\omega_p^2 \big/ \omega^2}{\left(1 \mp \frac{eB}{m}\right)} \tag{3.12}$$

Eq. (3.12) are classified into two types refractive index for (i) Right handed wave and (ii) Left handed wave.

(a) Right handed wave:

$$n^2 = 1 - \frac{\omega_p^2 \big/ \omega^2}{\left(1 - \frac{\omega_c}{\omega}\right)} \tag{3.13}$$

(b) Left handed wave:

$$n^2 = 1 - \frac{\omega_p^2 \big/ \omega^2}{\left(1 + \frac{\omega_c}{\omega}\right)} \tag{3.14}$$

On the basis of above calculation, we found the refractive index of fluid plasma in the presense of applied external magnetic field. When we consider the the collision are accounted for the dieletric constant then the real and imaginary part of the fluid plasma are obtaine in the given below Eq. (3.15) [4].

The complex permittvity for the magnetized cold plasma layer (B) can be expressed as [22],

$$\varepsilon_B(\omega) = 1 - \frac{\omega_{pe}^2}{\omega^2\left(1 - i\frac{\gamma}{\omega} \mp \frac{\omega_{le}}{\omega}\right)} \tag{3.15}$$

with μ_B=1; where ω, γ and ω_{le} are the angular, effective and gyro-effective collision frequencies.

Here, ω_{pe} is the plasma frequency which is given as:

$$\omega_{pe} = \left(\frac{n_e e^2}{m\varepsilon_0}\right)^{1/2}, \text{ and } \omega_{le} = \frac{eB}{m}; \tag{3.16}$$

where n_e, m, ε_0, B are the electron density, mass of electron, permittivity in free-space, applied external magnetic field, and e is the charge of electron [15].

3.3.2 Optical properties of the considered periodic structure containing magnetized cold plasma

The band structure and the transmittance versus frequency (GHz) of the chosen periodic structure are calculated theoretically using transfer matrix method (TMM) [40]. One-dimensional periodic structure is composed by dielectric (air) and magnetized cold plasma (MCP). If A and B represents the dielectric and magnetized cold plasma layers, respectively, then the form of $(AB)^N$ is the plasma photonic crystal with dielectric and magnetized cold where N is the number of periodicity which shown in Figure 3.1.

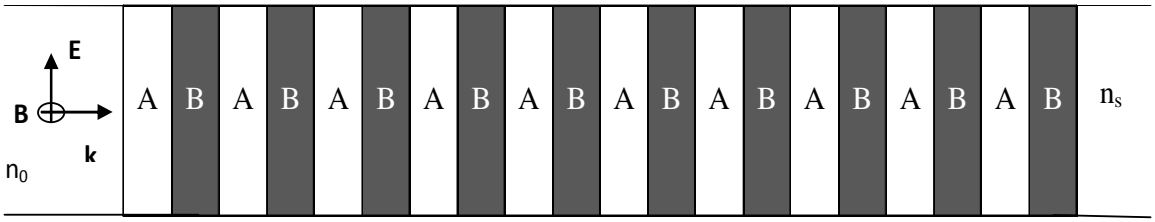

Figure 3.1: Schematic diagram of dielectric (air) and magnetized cold plasma (MCP) photonic crystal

The characteristic matrix for the periodic medium of the magnetic cold plasma can solve using characteristics method which was discussed in Chapter-2. Hence, the characteristic matrix for the i^{th} layer is given as;

$$M_i = \begin{bmatrix} \cos\gamma_i & -\frac{i}{p_i}\sin\gamma_i \\ -ip_i\sin\gamma_i & \cos\gamma_i \end{bmatrix}, \tag{3.17}$$

where $\gamma_i = \frac{\omega}{c} n_i d_i \cos\theta_i$, c is the speed of light in free space, θ_0 is the ray angle inside i^{th} layer (i=A and B material), the refractive index of the material $n_i = \sqrt{\mu_i \varepsilon_i}$, $p_i = \sqrt{\frac{\varepsilon_i}{\mu_i}}\cos\theta_i$ and $\cos\theta_i = \sqrt{1-\frac{n_0^2\sin^2\theta_0}{n_i^2}}$ in which n_0 is the refractive index of free space, where the incident wave interact to the considered structure with angle θ_0.

The characteristic matrix for the considered periodic structure $(AB)^N$ with the lattice thickness 'd' is given by:

$$M(d) = \begin{pmatrix} M_{1,1} & M_{1,2} \\ M_{2,1} & M_{2,2} \end{pmatrix}, \tag{3.18}$$

where $M(d) = (M_A M_B)^N$; M_A and M_B are the characteristics matrix for layers A and B, respectively. We have considered the M_A and M_B characteristic matrices for TE wave at the incident angle θ_0 [17].

The transmission coefficient of the multilayer structure is calculated by:

$$t = \frac{2p_0}{(m_{11}+m_{12}p_s)p_0 + (m_{21}+m_{22}p_s)}, \tag{3.19}$$

Where $p_0 = n_0\cos\theta_0$ and $p_s = n_s\cos\theta_s$; n_s is the refractive index of the substrate, whose ray angle is θ_s.

The transmittance of the multilayer is given by [40],

$$T = \left(\frac{p_s}{p_0} \right) |t|^2 . \tag{3.20}$$

3.4 Results and discussion

In this study, we have calculated theoretically the band structure and the transmittance of dielectric and magnetized cold plasma based periodic structure. The band structure and the transmittance of the considered periodic structure against frequency (GHz) are plotted with variation of varying the plasma parameters like applied external magnetic field (B), electron density (n_e) and effective collision frequency (γ), with lattice period i.e. N=10 and normal incident angle i.e. $\theta_0=0^0$. Each variable of the magnetized cold plasma has an important role, but the external magnetic field has excellent role in the magnetized cold plasma due to positive and negative values of external magnetic field when it acts as right hand and left hand polarizations, respectively. In addition to this, we have calculated all transmittances corresponds to the band structure for the dielectric having refractive index $n_A = 1 (\text{air})$ and thickness $d_A = 12\text{mm}$, and the refractive index of the magnetized cold plasma has been taken from Eq. (3.15), and thickness of magnetized cold plasma layer is chosen $d_B = 15\text{mm}$ [19]. The periodic structure of the air/right hand polarization and air/left hand polarization is called right hand polarization and left hand polarization structures, respectively.

In Figure 3.2, we have studied the transmittance corresponds to the band structure against frequency (GHz) for right hand polarization with variation of varying the magnetic field of magnetized cold plasma as B=0.4Tesla, 0.5Tesla, and 0.6Tesla with fixed electron density of magnetized cold plasma as $n_e=8 \times 10^{17}/m^3$; and the effective collision frequency, $\gamma=10^7$ Hz. The band structure versus frequency (GHz) response shows band gaps at the lower and higher frequency ranges for the different chosen values of the magnetic field. The band structure versus frequency (GHz) curves, with variation of varying the applied external magnetic field, we have found two band gaps for the different values of magnetic field. Here, the band edge at low frequency range doesn't shift much with the variation in the magnetic field, while the band edge at high frequency is much affected by the applied external magnetic field.

Transmittance characteristic corresponds to band gap of the chosen periodic structure also varies simultaneously with the shifting in the frequency region of the band gap

that appears due to the band edge effect. Transmittance versus frequency (GHz) response vary at lower as well as higher frequency ranges and obtained results acts as a narrow band tunable filter corresponding to the different values of the magnetic field, i.e. B=0.4Tesla, B=0.5Tesla, B=0.6Tesla, as shown in Figure 3.2(b).

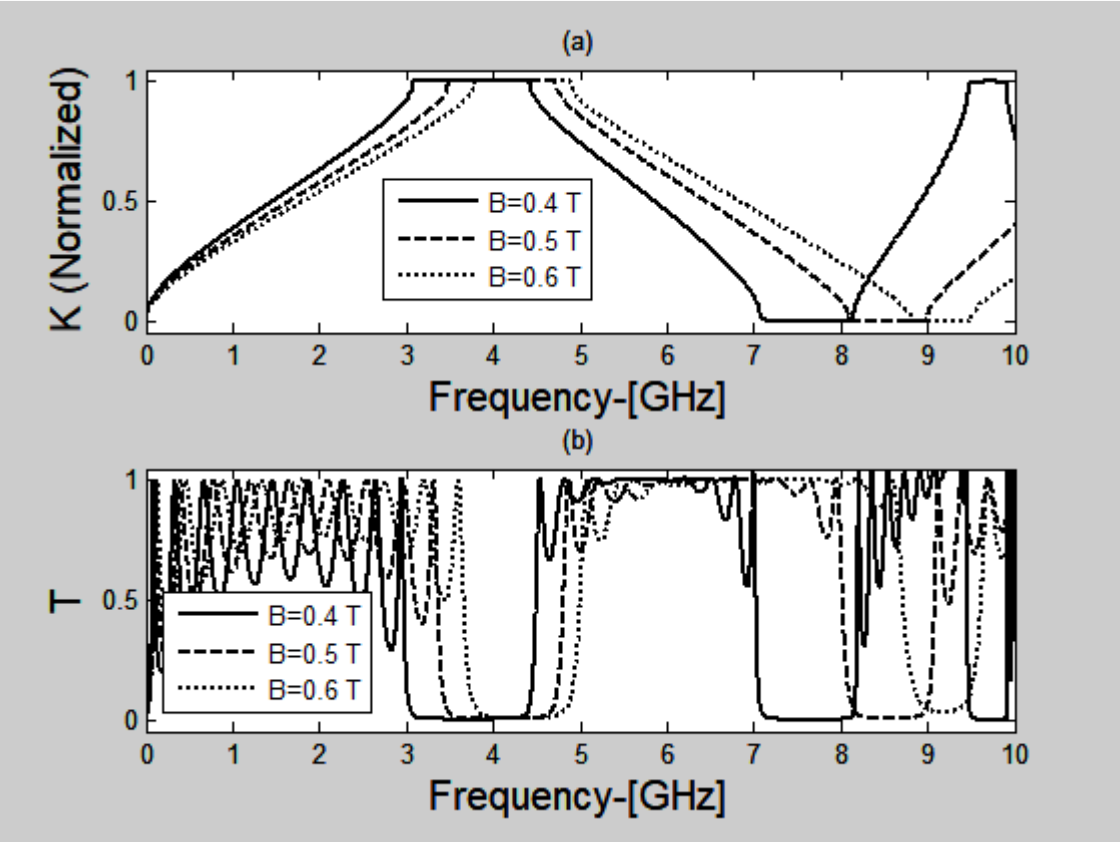

Figure 3.2: (a) Dispersion relation and (b) Transmittance versus frequency plots with varying the magnetic field of magnetized cold plasma for right hand polarization

The band structure and transmittance of the left hand polarization structure versus frequency (GHz) curves are drawn for different values of the magnetic field viz. B=0.4Tesla, 0.5Tesla, and 0.6Tesla for a fixed plasma density n_e=8 x $10^{17}/m^3$ and effective collision frequency $\gamma=10^7$ Hz as shown in Figure 3.2. The band gaps of the considered periodic structure shift at lower and higher frequency ranges. At low frequency range (0-2.5GHz), there exists a band gap that is shifted by change in the values of the magnetic field; and the structure also forms a band gap at higher frequency range (6-7.2GHz), which shifts with different values of the external magnetic field. The transmittance of the considered periodic structure corresponds to the value of band gap is calculated and we found that the structure acts as broadband reflector and narrow tunable filter at lower (0-2.5GHz) and higher frequency (6-

7.2GHz) ranges, respectively. Transmittance of the considered periodic structure, we found the left hand polarization structure as a better broadband reflector or high pass filter at low frequency with low value of magnetic field i.e. B=0.4Tesla. The photonic crystal of the left hand polarization structure acts as a narrow tunable filter for all values of magnetic field, i.e. B=0.4Tesla, 0.5Tesla,and 0.6Tesla at higher frequency ranges, which are shown in Figure 3.3(b).

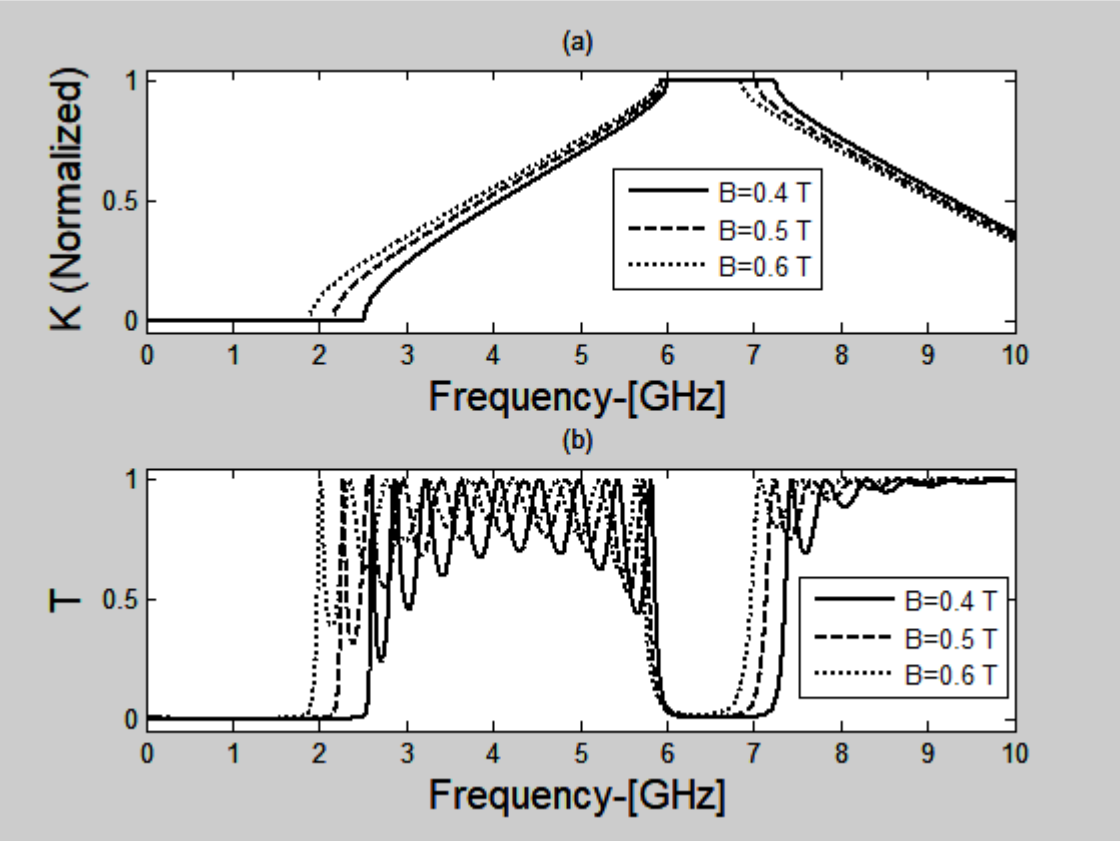

Figure 3.3: (a) Dispersion relation and (b) Transmittance versus frequency plots with varying magnetic field of the magnetized cold plasma for left hand polarization.

Similarly, we study the band gap structure and transmittance for the right hand polarization structure versus frequency curves for different values of plasma density viz. n_e=8 x $10^{17}/m^3$, 12 x $10^{17}/m^3$, 16 x $10^{17}/m^3$ at a fixed value of magnetic field B=0.6Tesla and effective collision frequency $\gamma=10^7$ Hz as shown in Figure 3.4(a). We found that band gap is shifted towards the lower and higher frequency ranges corresponding to these three values of plasma density for fixed value of magnetic field and effective collision frequency. We have calculated the transmittance of the right hand polarization structure corresponding to band gap structure for different chosen values of plasma density, i.e., n_e=8x $10^{17}/m^3$, 12 x $10^{17}/m^3$, 16 x $10^{17}/m^3$ at the

fixed magnetic field B=0.6Tesla and effective collision frequency $\gamma=10^7$Hz. The transmittance of the right hand polarization structure also varies for the different values of the plasma density and it forms a narrow tunable multichannel filter, which is shown in Figure 3.4(b). Further, the band gap structure and transmittance of the left hand polarization structure versus frequency curves are studied with different values of plasma density $n_e=8x10^{17}/m^3$, $12x10^{17}/m^3$, $16x10^{17}/m^3$ at a fixed magnetic field as B=-0.6Tesla and effective collision frequency $\gamma=10^7$Hz as shown in Figure 3.5. It is noticed that the band gap of the considered periodic structure is shifted for lower and higher frequency ranges as we increase the value of plasma density. The transmittance of left hand polarization structure exhibits unique result at the lower and higher frequency ranges. Transmittance of the considered periodic structure is zero at the lower frequency range for the different values of plasma density and it acts as a high band reflector or high pass filter, while it forms a tunable narrow band filter for higher frequency range.

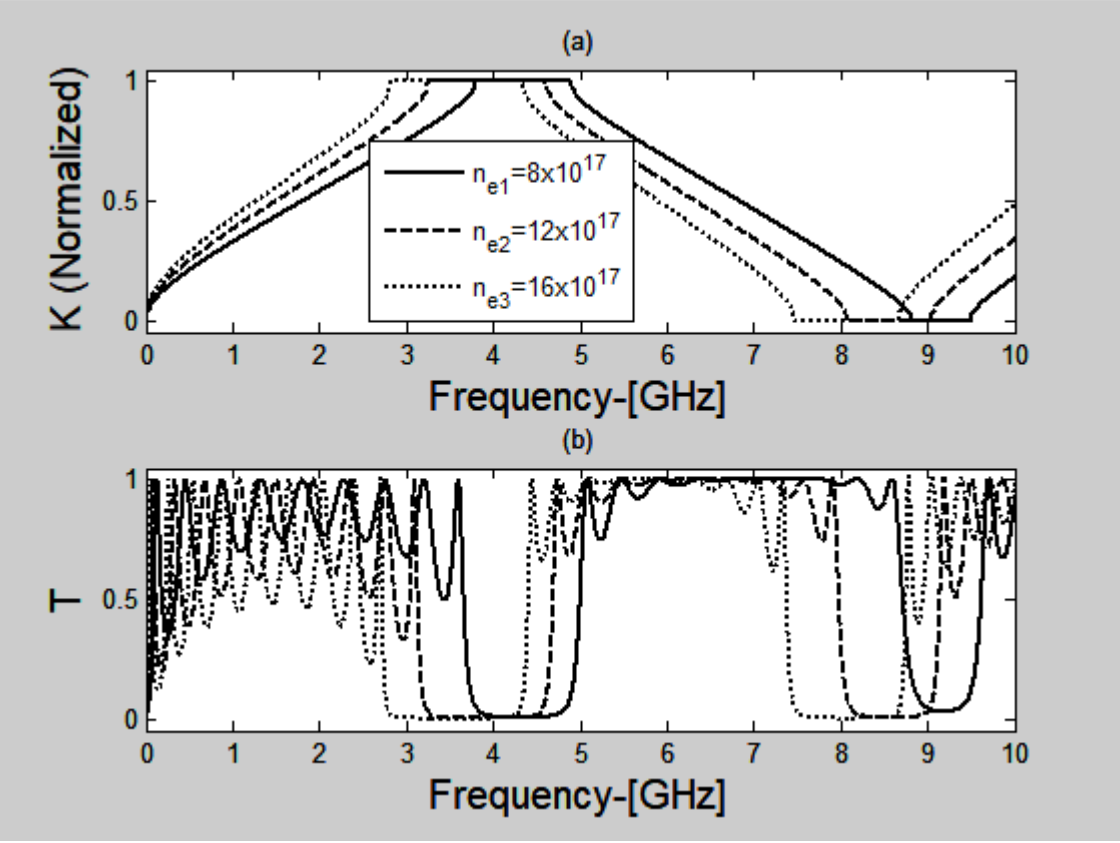

Figure 3.4: (a) Dispersion relation and (b) Transmittance versus frequency plots with varying plasma density of the magnetized cold plasma for right hand polarization

Now, we have focused on the band gap structure and transmittance versus frequency (GHz) curves with varying effective collision frequency, γ_1=1x10^{6}Hz, γ_2=5x10^{6}Hz, γ_3=1x10^{7}Hz at a fixed magnetic field B=0.6Tesla and electron density of magnetized cold plasma viz. n_e=8x10^{17} in both right hand polarization and left hand polarization structures as depicted in Figures 3.6 and 3.7. For the right hand polarization, it is observed that band structure and transmittance don't vary for the different values of the effective collision frequency with fixed magnetic field and electron density of magnetized cold plasma. The shifting in frequencies of band gaps and transmittances of the considered periodic structures are very small and the band gap and transmission spectra exist in frequency region (3.8-4.9 GHz), which shown is in Figure 3.6(a).

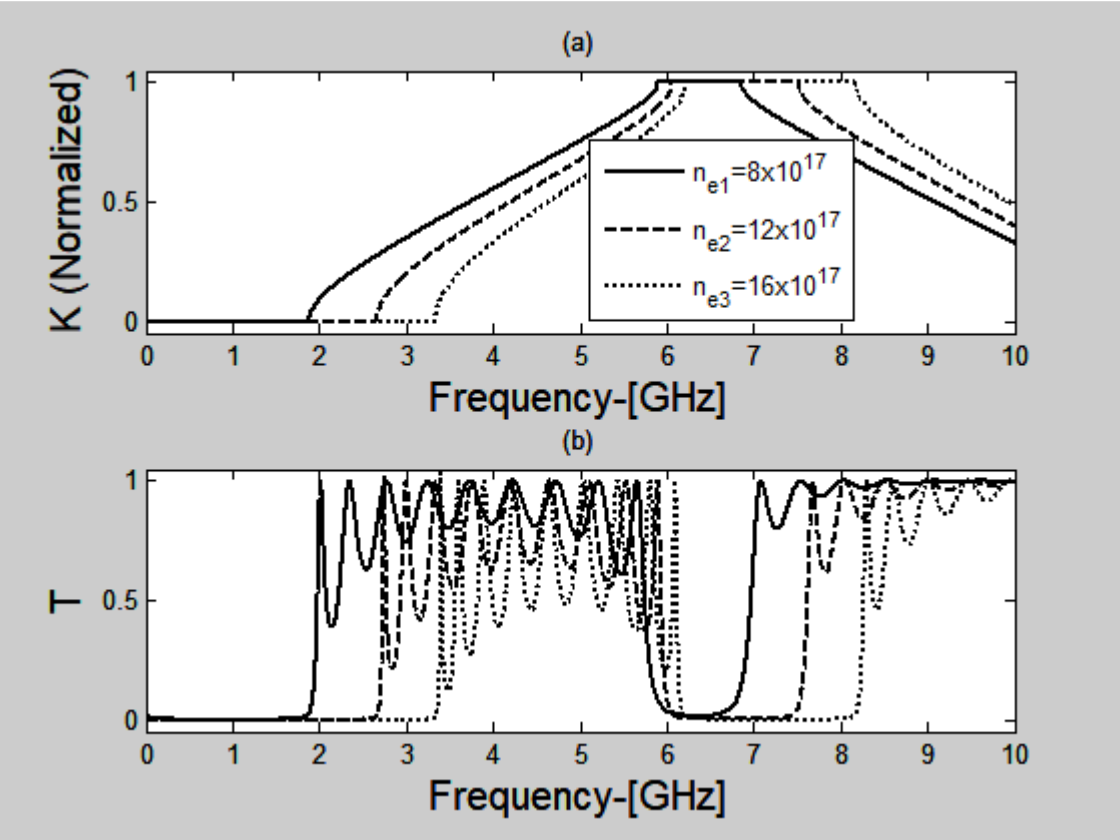

Figure 3.5: (a) Dispersion relation and (b) Transmittance versus frequency plots with varying plasma density of the magnetized cold plasma for left hand polarization

Likewise, we have analyzed the band gap structure and transmittance versus frequency (GHz) curves with varying the effective collision frequency for left hand polarization. Band gap and transmittance of considered periodic structure with different effective collision frequencies (γ_1=1x10^{6}Hz, γ_2=5x10^{6}Hz, γ_3=1x10^{7}Hz) for fixed magnetic field B=-0.6Tesla and electron density (n_e=8x10^{17}) of magnetized cold

plasma show very minor effect on band gap or transmittance at lower (0-1.9GHz) and higher (5.9-6.9GHz) frequency ranges for left hand polarization structure, as shown in Figures 3.7(a) and 3.7(b).

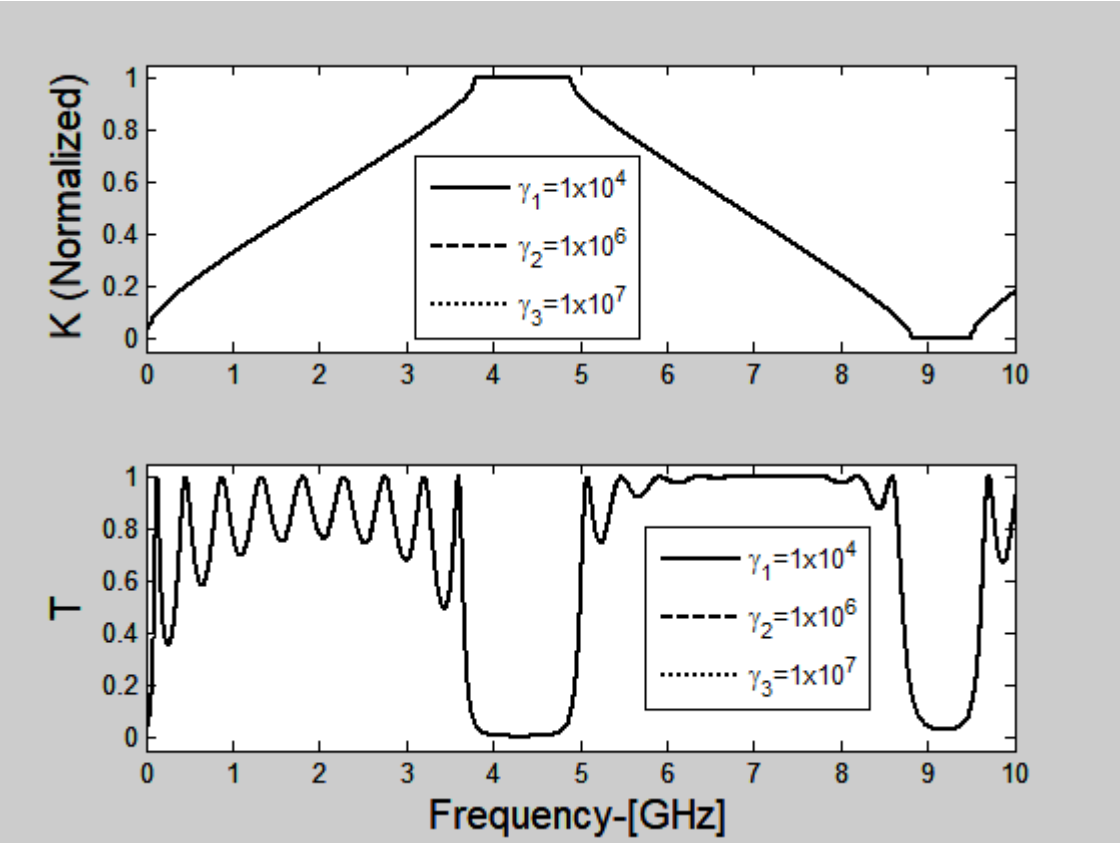

Figure 3.6: (a) Dispersion relation and (b) Transmittance versus frequency plots with varying effective collision frequency of the magnetized cold plasma for right hand polarization

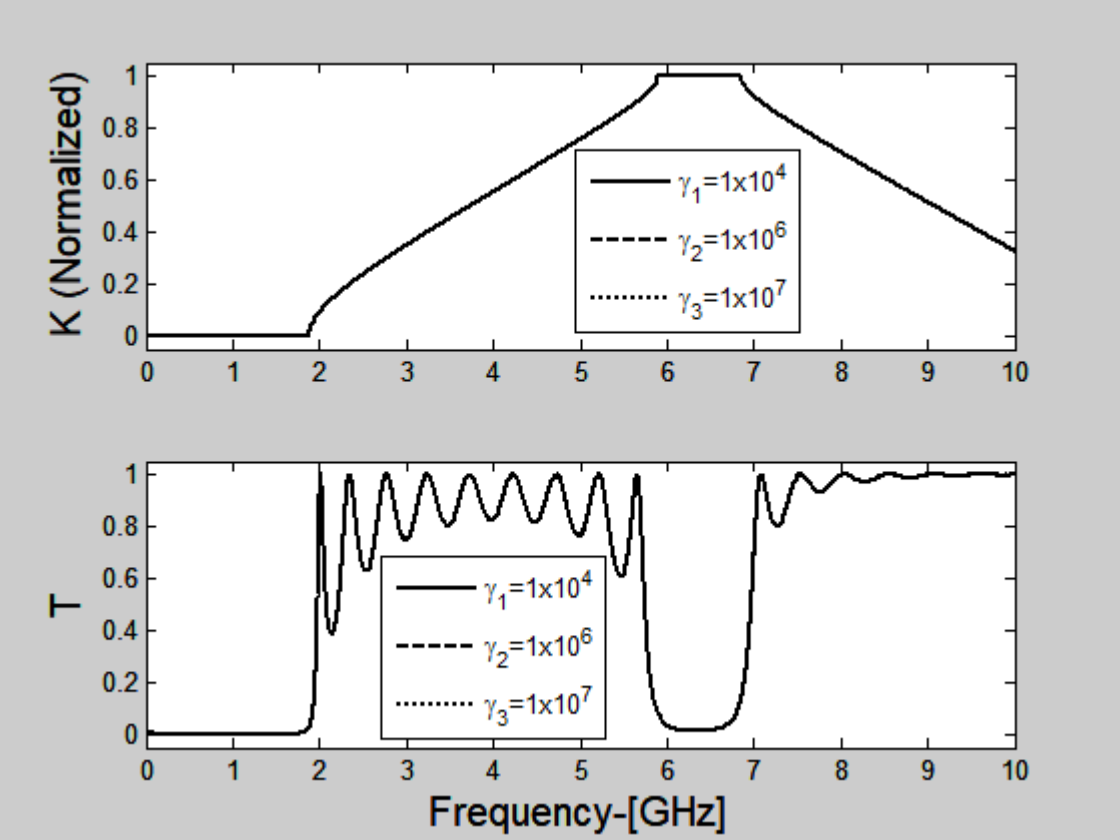

Figure 3.7: (a) Dispersion relation and (b) Transmittance versus frequency plots with varying effective collision frequency of the magnetized cold plasma for left hand polarization

3.5 Conclusion

Plasma is a hot ionized gas contains equal number of positively charged ions as well as negatively charged electrons. The featured properties of plasma are different from the ordinary neutral gases. A cold plasma or non-equilibrium plasma is that plasma which is not in thermodynamic equilibrium since temperature of electron is abundant hotter in comparison to the temperature of heavy species viz. ions and neutrals. Such type of material is called plasma. The study of wave motion inside plasma in presense of applied external magnetic field is called magnetized plasma and at lower temperature is called magnetized cold plasma. The cold plasma has the some variable parameters, which is affected the cold plasma refractive index. These variable parameters are used to study the optical property and band structure of the period structures containing cold plasma. The band structure and the transmittance versus frequency response were studied theoretically with varying magnetic field, plasma density and effective collision frequency of the magnetized cold plasma for RHP

(Right Hand Polarization) and LHP (Left Hand Polarization) structure. After the calculations, we found that the band gap structure of the RHP and LHP structures has the unique outcomes, where the broadband and tunable filter property may be obtained by changing the magnetized cold plasma parameters. We have proposed a tunable narrow band filter and multichannel filter for RHP structure for an increased value of the magnetic field, and broadband reflector or extraordinary pass filter for LHP structure at low value of the magnetic field. Besides this, a design of tunable narrow band filter for RHP structure were theoretically proposed where the transmittances of the structure is studied with different values of the electron density of magnetized cold plasma; and a broadband reflector and high pass filter for LHP structure was also proposed whose filter width increases with an increase in the value of the electron density of magnetized cold plasma. The band gap structure and transmittance were also calculated with varying the effective collision frequency for RHP and LHP structures where that no such effect is obtained in the variation on the band structure. These calculated results of the RHP and LHP structure; we investigated a novel idea for the broadband reflector and narrow tunable filter at the ranges of lower and higher frequency. Thus, this investigation may be useful in design of tunable one-dimensional photonic devices that can be used to control the propagation of electromagnetic wave by variation of varying the parameters of the magnetized cold plasma.

References:

[1] L. Tonks and I. Languimuir, Oscillations in ionized gases, Phys. Rev. 33 (1929) 195-210.

[2] J. A. Bittencourt, Fundamental of Plasma Physics, 3rd Ed. Springer Verlag, New York (2004).

[3] R. Fitzpartick, Introduction of Plasma Physics: A graduation level course (2005). http://dpbck.in/Ebooks/physics/18.pdf

[4] S. Chandra, Textbook of Plasma Physics, CBS Publishers & Distributors Pvt. Ltd., New Delhi (2012).

[5] V. P. Bykov, Spontaneous emission in a periodic structure, Soviet Physics J. Exp. Theor. Phys. 35(2) (1972) 269-273.

[6] K. Ohtaka, Energy band of photons and low energy photon diffraction, Phys. Rev. B 19 (1979) 5057-5067.

[7] E. Yablonovitch, Inhibited spontaneous emission in solid-state physics and electronics, Strong localization of photons in certain disordered dielectric super lattices, Phys. Rev. Lett. 58 (1987) 2059-2062.

[8] S. John, Strong localization of photons in certain disordered dielectric super lattices, Phys. Rev. Lett. 58 (1987) 2486-2489.

[9] J. D. Joannopoulos, S. G. Johnson, J. N. Winn and R. D. Meade, Photonic crystals: Molding the flow of light, Princeton Univ. Press, Princeton NJ, USA (2008).

[10] Y. Fink, J. N. Winn, S. Fan, C. Chen, J. Michel, J. D Joannopoulos, and E. L Thomas, A dielectric omni directional reflector, Science 282 (1998) 1679-1682.

[11] T. F. Krauss and R. M. De La Rue, Photonic crystals in the optical regime: past, present and future, Prog. Quant. Electron. 23 (1999) 51-96. https://doi.org/10.1016/S0079-6727(99)00004-X

[12] D. N. Chigrin, A. V. Lavrinenko, D. A. Yarotsky, and S. V. Gaponenko, Observation of total omni-directional reflection from a one-dimensional dielectric lattice, Appl. Phys. A 68 (1999) 25–28.

[13] K. Sakoda, Optical Properties of Photonic Crystals, Springer-Verlag Berlin Heidelberg (2005).

[14] Y. W. Lee, F. C. Fan, Y. C. Huang, B. Y. Gu, B. Z. Dong, and M. H. Chou, Nonlinear multi-wavelength conversion based on an aperiodic optical superlattice in lithium niobate, Opt. Lett. 27(24) (2002) 2191-2193. https://doi.org/10.1364/OL.27.002191

[15] S. Massaoudi, A. de Lustrac, and I. Huynen, Properties of metallic photonic band gap material with defect at microwave frequencies: calculation and experimental verification, J. Elec. Mag. Waves Appl. 20 (2006) 1967–1980.

[16] Q. R. Zheng, B. Q. Lin, Y. Q. Fu, and N. C. Yuan, Characteristics and applications of a novel compact spiral Electromagnetic Band Gap (EBG) structures, J. Elec. Mag. Waves Appl. 21 (2007) 199-213.

[17] K. Busch, G. von Freymann, S. Linden, S. F. Mingaleev, L. Tkeshelashvili, and M. Wegener, Periodic nanostructures for photonics, Phys. Rep. 444 (2007) 101-202.

[18] S. V. Gaponenko, Introduction to Nanophotonics, Cambridge University Press, Cambridge (2010).

[19] H. Hojo, K. Akimoto, and A. Mase, Conference Digest on 28th Int. Conf. Infrared and Millimeter Waves Otsu Japan (2003) 347-348.

[20] H. Hojo, and A. Mase, Dispersion relation of electromagnetic wave in one dimensional plasma photonic crystals, J. Plasma Fusion Res. Rapid Comm. 80 (2004) 89-90.

[21] R. Kumar, Plasma Photonic Crystal (Photonic Crystals - Innovative Systems, Lasers and Waveguides, Dr. Alessandro Massaro (Ed.), In Tech (2012). DOI: 10.5772/32106

[22] H. G. Booker, Cold Plasma Waves, Springer-Verlag, New York (1984).

[23] T. C. King; C. C. Yang, P. H. Hseih, T. W. Chang, and C. J. Wu, Analysis of tunable photonic band structure in an extrinsic plasma photonic crystal, Phys. E 67 (2015) 7-11.

[24] A. H. Aly, H. A. Elsayed, A. A. Ameen, and S. H. Mohamed, Tunable properties of one dimensional photonic crystal that incorporate a defect layer of magnetized cold plasma, Int. J. Mod. Phys. B 31 (2017) 1750239-9.

[25] V. Kumar, K. S. Singh, and S. P. Ojha, Band structure, reflection properties and abnormal behavior of one dimensional plasma photonic crystals, Prog. Electromagn Res. M 9 (2009) 227-241.

[26] X. K. Kong, S. B. Liu, H. F. Jhang, and C. Z. Li, A novel tunable filter featuring defect mode of the TE wave from one-dimensional photonic crystals doped by magnetized cold plasma, J. Appl. Phys. 17 (2010) 103506-5.

[27] A. H. Aly, and D. Mohamed, BSCCO/$SrTiO_3$ one dimensional superconducting photonic crystal for many applications, J. Supercond. Nov. Magn. 28 (2015) 1699-1703.

[28] A. Aghajamali, Transmittance properties in a magnetized cold plasma and superconductor periodic multilayer, Appl. Opt. 55 (2016) 6336-6340.

[29] A. H. Aly, H. A. Elsayed, and S. A. El-Naggar, Tuning the flow of light in two dimensional metallic photonic crystals based on Faraday Effect, J. Mod. Opt. 64(1) (2017) 74-80.

[30] A. H. Aly, W. Sabra, and H. A. Elsayed, Cutoff frequency in metamaterials photonic crystals within terahertz frequencies, Int. J. Mod. Phys. B 31(15) (2017) 1750123-8.

[31] A. H. Aly and H. A. Elsayed, Tunability of defective one dimensional photonic crystal based on Faraday Effect, J. Mod. Opt. 64(10) (2016) 871-877.

[32] A. H. Aly, S. A. El-Naggar and, H. A. Elsayed, Tunability of two dimensional n-doped semiconductor photonic crystal based on Faraday Effect, Opt. Express 23(11) (2015) 15038-15046.

[33] A. H. Aly, Superconductor dielectric photonic band gap in Ultraviolet region, Int. J. Adv. App. Phy. Res. Special issue (2016) 43-47.

[34] A. H. Aly, W. Sabra, and H. A. Elsayed, Dielectric and superconducting photonic crystals, J. Supercond. Nov. Magn. 26 (2013) 553-560.

[35] A. H. Aly, and H. Sayed, Enhancement of the solar cell based on the nanophotonic crystals, J. Nanophotonics, 11(4) (2017) 046020.

[36] A. H. Aly, D. Mohamed, H. A. Elsayed, and D. Vigneswaran, One dimensional metallo superconductor photonic crystals as a smart window, J. Supercond. Nov. Magn. 18 (2018) 4628-5.

[37] Z. N. Dehnavi, H. R. Askari, M. Malekshahi and D. Dorranian, Investigation of tunable omnidirectional band gap in 1-D magnetized full plasma photonic crystals, Phys. Plasmas 24 (2017) 093517.

[38] Y. Ma, H. Zhang, T. Liu, and Wenyu, Study on the properties of unidirectional absorption and polarization splitting in one dimensional plasma photonic crystals with ultra wideband, J. Opt. Soc. Am. B 36(8) (2019) 2250-9.

[39] M. Solaimani, M. Ghalandari, and A. Aghajamali, Band gap engineering in constant total length non-magnetized cold plasma-dielectric multilayer, Optik 207 (2020) 164476.

[40] P. Yeh, Optical Waves in Layered Media, John Wiley and Sons, New York (1988).

Chapter 4
A tunable broadband filter of ternary photonic crystal containing plasma and superconducting material

Chapter-4

A tunable broadband filter of ternary photonic crystal containing plasma and superconducting material

4.1 General introduction

The ternary photonic crystal with plasma and superconducting materials is considered to study the optical property. The ternary photonic crystal is the periodic structure of three materials. Such ternary structure has found the high tunability in the band in comparison to the binary structure. We discuss about the plasma and then the optics of the superconducting material briefly.

4.1.1 Plasma

As discussed earlier, the plasma is a hot ionized gas of charged ions and electrons where the positively ions and negatively electrons are in equal number. The features properties of plasma are diverse from those of normal neutral gases. A non-thermal plasma or cold plasma is that plasma which is not in thermodynamic equilibrium since temperature of electron is abundant hotter than the temperature of heavy classes like ions and neutrals. Introducing the plasma in the photonic crystals, plasma creates the tunable photonic band gap in microwave region [1]. After that the plasma photonic crystal becomes an active research area in the field of optics and photonics. The Plasma Photonic Crystal (PPC) is a one dimensional multilayer periodic structure of thin plasma and other dielectric materials. We have already discussed in detail the behavior and properties of plasma photonic crystal in the previous Chapter-3. Now, we will discuss the behavior of superconductor with plasma incoming section.

4.1.2 Superconductor

Basically, superconducting materials exist at very low temperature since Dutch physicist Onnes [2] discovered this theory in 1911. In a simple language, superconducting materials are those materials where electric resistance of the material becomes zero, also at which temperature the resistance becomes zero, that temperature is known as critical temperature of that material. In 1986, some cuprate-perovskite type ceramic material has a critical temperature above to 90 K. Such type of high transition temperature is theoretically impossible for a conventional superconductor, leading the material to be high temperature superconductor [3, 4]. Since, the discovery certain ceramic materials exist high temperature

superconductivity for the applications. These materials studied extensively for the design of practical devices. Though there has been much research done, but a lot of left is to be done in optics. Additionally, a large amount of research accomplished in the use of pulse laser to break quasi-particle bonds in High Temperature Superconductor (HTS), lowering the transition temperature and including the transition from the superconducting states to the ordinary state. The superconductor material exhibits markedly different optical properties in the superconducting state to the ordinary state. The infrared-pulsed laser (1.06μm wavelengths) is incident to illuminate a Yttrium Barium Copper Oxide (YBCO) thin films with an intensity above critical value, caused the thin film to switch from the superconductor to the normal state recover on the order of 1μs. Thus, when an HTS switches from superconducting to normal or ordinary its optical properties change, the degree to which they change depends on the frequency of incident light. If an HTS thin film was incorporated into a periodic structure (PBG materials), the transmittance characteristics of the resulting structure should reflect the optical properties of the HTS [5-9].

As we know that from the previous studies, photonic crystals are artificial dielectric, metallic nanostructures composed of two or more than two medium in which the dielectric constant varies periodically in the space. In 1987, the novel idea of the periodic structure of the dielectric materials was theoretically proposed by Yablonovitch and experimentally observed by John [10, 11]. This type of periodic structures affects the propagation of the electromagnetic wave and known as *Photonic Crystal* (PC).

Some previous years ago, the researchers focused on superconducting photonic crystal due to its unique behaviors like tenability and negligible loss in reflectance. The dielectric permittivity of a superconducting material can be tuned with the variation of critical and operating temperature and the thickness. So, the superconducting photonic crystals have enormous advantages over the metallic and dielectric photonic crystals due to the existence of the tenability parameters [12-33]. THz transmittance in one-dimensional superconducting nanomaterial and dielectric superlattice used in many optical applications was investigated by Aly et al. [34]. Wu et al. [35] studied the band gap extension in one-dimensional ternary metal-dielectric photonic crystal. Feng et al. [36] calculated the omnidirectional photonic band gap in

one-dimensional ternary superconductor dielectric based photonic crystal on a new Thue-Morse a periodic structure and demonstrated that the electromagnetic wave could not propagate through the periodic structure below a certain frequency that is known as cutoff frequency. Aly et al. [37] analyzed the properties of cutoff frequency in two-dimensional superconducting photonic crystals, and gave a detailed analysis of cutoff frequency where it is needed in the required frequency region for the proper implementation of numerical calculations in many optical applications. Aly and Mohamed [38] found an analysis of cutoff frequency in a one dimensional (1-D) binary superconductor and dielectric photonic crystal, and mentioned that it could be tuned effectively by using the various parameters of dielectric and superconductor. Suchtheoretical results could be forwarded to put into applications such as high pass filter and reflector. In addition to this, the theoretical investigations of cutoff frequency in 1-D binary structure of superconductor and meta-material [39], and superconductor magnetized cold plasma PCs explored in the microwave region [40]. The optical property of all 1-D superconducting photonic crystal in comprising pairs of high-high, high-low and low-low refractive indices of the superconductor materials in the visible region was investigated by Zamani [41]. Zamani shown in his study analyzed that the transmission and reflection spectra of different type of all superconducting photonic crystals are dependent on the temperature and the incident angle. Sreejith et al. [42] has discussed the cutoff frequency in the one-dimensional ternary superconducting photonic crystal. Recently, Aly and Sayed [43] proposed an efficient method to improve the optical property of the pin silicon solar cell by studying the absorption with an anti-reflecting layer. For the applications of optical devices, the optical properties of one-dimensional superconductor meta-material photonic crystals by adding two different layers of the semiconductor were investigated by Mohamed et al. [44]. Aly et al. [45] also proposed the novel type of smart window for house susing one-dimensional superconductor nano-metallic photonic crystal.

The theoretical investigation carried out in near and mid infrared band gaps for a periodic multilayer structure which is composed of superconductor, semiconductor and meta-material. It was found that two band gaps appeared with in the computational regions which were effectively optimized by manipulating the thickness of the superconductor film, filling fraction of semiconductor and meta-

material and the incident angle of the electromagnetic wave [46]. According to law of conservation of energy, the sum of the reflection and transmission of electromagnetic wave in this frequency band should be greater than one. This is to be anomalous phenomena [47]. The theoretical study investigated the symmetric defective annular photonic crystal containing semiconductor and high temperature superconductor with a radial defect layer. The obtained results led to gain valuable information for designing and fabrication of new types of annular Bragg resonators surrounding a radial defect and integrated like visible waveguide devices for optical switches and filters [48].

In this chapter, we report theoretically that the optical properties of considered ternary periodic structure depend on the parameters of magnetized cold plasma and the superconducting material. Basically, the magnetized cold plasmas form two types of polarization: (i) right-hand polarization having the positive value of the applied external magnetic field and (ii) left-hand polarization having the negative value of externalmagnetic field. Such type of right-hand polarization and the left-hand polarization ternary periodic structures are known as right-hand polarization and left-hand polarization structure. In our study, the transmittance characteristic of the ternary photonic crystal with variation of varying the incident angle, the magnetic field, the electron density, the temperature and the thicknesses of the magnetized cold plasma and superconducting material. The transmittance properties of considered ternary periodic structure examine by varying the parameters of the material and analyze the transmittance of the ternary periodic structure for a filter application. Now, we are going to discuss about the optics of the plasma and superconducting material, and the method of calculations for finding the optical properties of ternary structure.

4.2 Theoretical work and methodology

Transmittance characteristic of ternary photonic crystal containing dielectric, magnetized cold plasma, and high-temperature superconductor ($YBa_2Cu_2O_7$) material is calculated using transfer matrix method [50]. One-dimensional ternary photonic crystal is taken as $(ABC)^N$, where N is a number of the periodicity of the ternary materials; A, B and C are represented as dielectric, magnetized cold plasma, and high temperature superconducting material, respectively. Before going to discuss about the

optical properties of ternary photonic crystals containing dielectric, magnetic cold plasma and high temperature superconducting material, we discuss the optics of the magnetic cold plasma and high temperature superconducting material briefly.

The electric permittivity of the magnetized cold plasma i.e. layer (B), which is already discussed in Chapter-3, is given as [51];

$$\varepsilon_B(\omega) = 1 - \frac{\omega_{pe}^2}{\omega^2\left(\left(1 - \frac{i\gamma}{\omega}\right) \mp \frac{\omega_{le}}{\omega}\right)} \tag{4.1}$$

with the permeability, μ_B=1 for non-magnetic material; where ω ,γ and ω_{le} are the angular, effective and gyro-effective collision frequency or cyclotron frequency plasma, respectively. Here, ω_{pe} is the plasma frequency, which is known as:

$$\omega_{pe} = \left(\frac{n_e e^2}{m\varepsilon_0}\right)^{1/2}, \text{ and } \omega_{le} = \frac{eB}{m}; \tag{4.2}$$

where n_e, m, $\varepsilon_0$is the electron density, the mass of electron, the permittivity in free-space respectively, and e is the electronic charge [35].

The frequency gap of the dielectric permittivity of superconducting is close to the metallic material [41, 42 and 49]. The dielectric property of the superconductor is dependent on frequency, which can be described by the two-fluid model. According to this model, the relative permittivity of lossless superconducting material, layer C, can be expressed as the following relation [44],

$$\varepsilon_C = \left(1 - \left(\frac{\omega_{th}^2}{\omega^2}\right)\right) \tag{4.3}$$

where ω_{th} is called the threshold frequency and is given by,

$$\omega_{th} = \left(\frac{1}{\varepsilon_0 \mu_0 \lambda_L^2}\right) \tag{4.4}$$

Here λ_L is the London penetration depth. The temperature dependent of λ_L can be described by;

$$\lambda_L(T) = \left(\frac{\lambda_0}{\sqrt{1 - f(T)}}\right) \tag{4.5}$$

where λ_0 is the London penetration depth at T=0K. According to Groter-Casimir model, f(T) is suggested in the following form;

$$f(T)=\left(\frac{T}{T_c}\right)^p \tag{4.6}$$

where T_c is the critical temperature and T is the operating temperature, and p=2 for high-temperature superconductor and p=4 for low-temperature superconductor [46]. The electric permittivity of the superconductor layer, with no external source current and charge, Maxwell's equations becomes:

$$\vec{\nabla}.\vec{E}=0,\vec{\nabla}.\vec{B}=0,\ \vec{\nabla}\times\vec{E}=-\frac{\partial\vec{B}}{\partial t}\ \text{and}\ \vec{\nabla}\times\vec{B}=\mu_0\left(\sigma\vec{E}+\varepsilon_0\frac{\partial\vec{E}}{\partial t}\right) \tag{4.7}$$

Taking the curl of the last equation and using the convention $e^{-i\omega t+i\vec{k}\cdot\vec{r}}$, we have;

$$\vec{\nabla}\times\vec{\nabla}\times\vec{B}=\left(\frac{\omega^2}{c^2}-i\omega\mu_0\sigma(\omega)\right)\vec{B} \tag{4.8}$$

$$\vec{\nabla}^2\vec{B}+k_1^2\vec{B}=0$$

By substituting Eq. (4.8), we have;

$$k_1^2=\left(\frac{\omega^2}{c^2}-\frac{1}{\lambda_L^2}\right) \tag{4.9}$$

Using Snell's law, the length of the tangential wave vector k_{1x} (parallel to the dielectric superconductor interface) is conserved. That is $k_{1y}=\frac{\omega}{c}\sin\theta=\beta$, where θ is the incident angle (relative to normal of interface) of the electromagnetic wave as the vacuum. Then we have frequency dependent normal vector and the normal vector is $k_{1x}=\sqrt{\frac{\omega^2}{c^2}\cos^2\theta-\frac{1}{\lambda_L^2}}=\frac{\omega}{c}n_1(\omega)$, where $n_1(\omega)=\sqrt{\cos^2\theta-\frac{c^2}{\omega^2}\frac{1}{\lambda_L^2}}$. For dielectric layer with no external source current and charge, Maxwell's equation becomes;

$$\vec{\nabla}.\vec{E}=0,\vec{\nabla}.\vec{B}=0,\vec{\nabla}\times\vec{E}=-\frac{\partial\vec{B}}{\partial t}\ \text{and}\ \vec{\nabla}\times\vec{B}=\frac{\partial\vec{D}}{\partial t} \tag{4.10}$$

From Eq. (4.9) and Snell's law, we have;

$$k_2^2 = \varepsilon \frac{\omega^2}{c^2} \text{ or } k_{2x}^2 = \varepsilon \frac{\omega^2}{c^2} - \frac{\omega^2}{c^2} \sin^2\theta = \frac{\omega^2}{c^2}\left(\varepsilon - \sin^2\theta\right) \text{or } k_{2x} = \frac{\omega}{c} n_2 \tag{4.11}$$

where $n_2 = \sqrt{\varepsilon - \sin^2\theta}$.

The material with refractive index n_1, n_2 and n_3 are the dielectric (A), magnetized cold plasma (B) and superconductor (C) as shown in Figure 4.1.

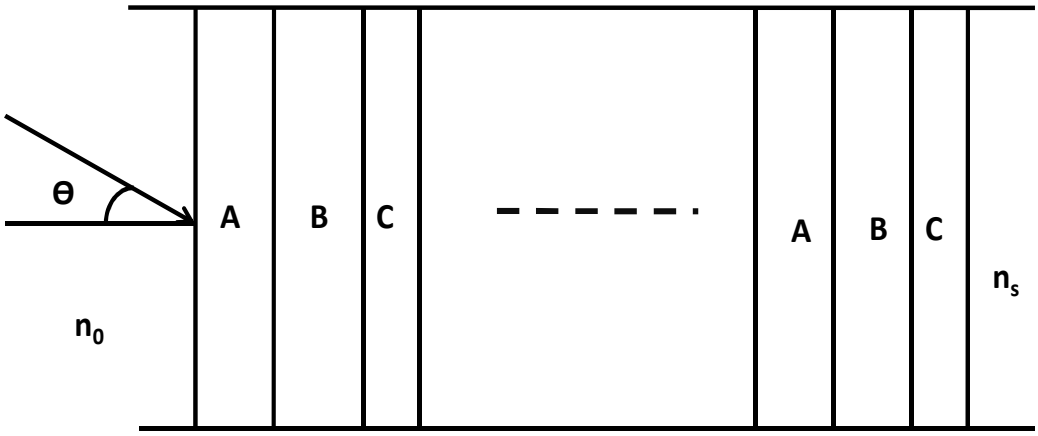

Figure 4.1: Schematic diagram of a ternary periodic structure with dielectric (A), magnetized cold plasma (B) and superconductor (C)

Now, the optical properties of the considered structure is calculated using the characteristic matrix method for considered ternary photonic crystal i.e. $(ABC)^N$ and the characteristic matrix for ternary layers can be expressed by [43]:

$$M(d) = \begin{pmatrix} m_{1,1} & m_{1,2} \\ m_{2,1} & m_{2,2} \end{pmatrix} \tag{4.12}$$

where $M(d) = (M_A M_B M_C)^N$; N is the periodicity of the photonic crystal, M_A, M_B and M_C are the characteristics matrices of layer A, B, and C, respectively.

The characteristics matrix of each layer can be derived by considering the electric field on each surface. For ternary periodic structure, we have considered three layers with boundary conditions in the x-direction. The electric field in each interface is given by:

$$\vec{E}=\begin{cases}(\overrightarrow{E_1}e^{i\vec{k_1}.\vec{r}}+\overrightarrow{E_1}'e^{-i\vec{k_1'}.\vec{r}})e^{i\omega t}, -d_A<x<0;\\ (\overrightarrow{E_2}e^{i\vec{k_2}.\vec{r}}+\overrightarrow{E_2}'e^{-i\vec{k_2'}.\vec{r}})e^{i\omega t},\ 0<x<d_B;\\ (\overrightarrow{E_3}e^{i\vec{k_3}.\vec{r}}+\overrightarrow{E_3}'e^{-i\vec{k_3'}.\vec{r}})e^{i\omega t},\ d_B<x<d_{B+C};\end{cases}$$

where k_1, k_2, and k_3 are the propagation vectors corresponding to the dielectric, the magnetized cold plasma and the superconducting material with the above boundary conditions. E_i and E_i' are the incident and the reflected waves where i=A, B and C layer. By using Maxwell's equations, we obtain the corresponding magnetic field of the incident electric field's equation. The electric and magnetic field can use for the formulation of the characteristics matrix of each layer.

The characteristic matrix for ternary structure is the product of the matrices of all three layers i.e. m=3. The characteristic matrix M_i for each layer where i=A, B &C is calculated for the TE wave at the angle of incidence θ_0 [39].

$$M_i=\begin{bmatrix}\cos\gamma_i & -\frac{i}{p_i}\sin\gamma_i\\ -ip_i\sin\gamma_i & \cos\gamma_i\end{bmatrix} \tag{4.13}$$

where $\gamma_i=\frac{\omega}{c}n_i d_i\cos\theta_i$, c is the speed of light in vacuum, θ_i is the ray angle inside i^{th} layer with a refractive index as, $n_i=\sqrt{\mu_i\varepsilon_i}$, $p_i=\sqrt{\frac{\varepsilon_i}{\mu_i}}\cos\theta_i$ and $\cos\theta_i=\sqrt{1-\frac{n_0^2\sin^2\theta_0}{n_i^2}}$ in which n_0 is the refractive index of air, where the incidence wave tends to enter the structure.

The transmission coefficient of the ternary photonic crystal is calculated by,

$$t=\frac{2p_0}{(m_{11}+m_{12}p_s)p_0+(m_{21}+m_{22}p_s)} \tag{4.14}$$

where $p_0=n_0\cos\theta_0$ and $p_s=n_s\cos\theta_s$, where n_s is the refractive index of the substrate, θ_s is the ray angle. The transmission spectra of the ternary photonic crystal are given by,

$$T=\left(\frac{p_s}{p_0}\right)\left|t^2\right| \tag{4.15}$$

4.3 Results and Discussion

In this chapter, we have theoretically studied the optical properties of one-dimensional ternary photonic crystal composed of alternating dielectric, magnetized cold plasma, and superconducting material using simple transfer matrix method for right-hand polarization and left-hand polarization [39]. As we know that, the magnetized cold plasma demonstrates the right-hand polarization and the left-hand polarization by changing the direction of the magnetic field only i.e. positive/negative values of the applied external magnetic field. The applied transverse magnetic field also changes the permittivity of the superconducting material and magnetized cold plasma. Due to simple fabrication of the one dimensional photonic crystal, transmittance of the right-hand polarization and the left-hand polarization 1-D ternary photonic crystal against frequency (GHz) are plotted by variation of most valuable parameters: the angle of incidence, the magnetic field, the electron density of magnetized cold plasma, the temperature of superconductor, and the thicknesses of magnetized cold plasma and superconducting materials. The transmittance study gives an informative idea for optical applications in filters.

As shown in the Figure 4.1, the ternary photonic crystal is $(ABC)^N$ where A, B, and C represent the air, the magnetized cold plasma and superconducting material ($YBa_2Cu_2O_7$) with critical temperature T_c=92K, and the operating temperature T=4.2K, respectively. The thickness of the A, B, and C materials are 18mm, 18mm, 80nm, respectively. The refractive indices of layer A, B, and C are n_A=1, $n_B=\sqrt{\varepsilon_B\mu_B}$, $n_C=\sqrt{\varepsilon_C\mu_C}$, respectively [40, 44, 45]. The periodicity of the lattice (N) is taken three periods i.e. N=3.

We calculate the transmittance of the one-dimensional ternary photonic crystal with varying most valuable parameters: the incident angle, the magnetic field, the electron density of the plasma, the temperature and the thickness of the magnetized cold plasma and superconducting material. Firstly, we calculate the transmittance characteristic of the considered structure with variation of the incident angle for the right-hand polarization and left-hand polarization structure. The transmittance of the considered ternary photonic crystal against frequency (GHz) with thickness d_A=18mm, refractive index n_A=1 (air), external magnetic field B=0.4T, plasma density $n_e=12\text{x}10^{17}/m^3$, effective collision frequency of magnetized cold plasma

$\gamma=1x10^7$ GHz, transition temperature of high temperature superconductor ($YBa_2Cu_2O_7$) T_C=92K and operating temperature T=4.2K with variation of incident angles $\theta= 0^0$, $\theta=30^0$ and $\theta=40^0$ are studied. The transmittance of the ternary photonic crystal with right-hand polarization material against frequency (GHz) with varying incident angles, $\theta=0^0$, 30^0 and 40^0, is shown in Figure4.2. The zero transmittance at the lower frequency range, 0-1.0 GHz, shows due to superconducting behavior inside the structure. The transmittance at the higher frequency range, 2.3-10.0 GHz, shows due to the effect of dielectric behavior of air and magnetized cold plasma material. Transmittance found a negligible shifting for all the incident angles at the lower frequency range i.e. $\theta= 0^0$, 30^0 and 40^0. This shows that the incident angles is independent on the angles at the low frequency because the refractive index of the superconductor does not vary with the angle of incidence. This region acts as a low cutoff frequency for the ternary photonic crystal and has a low pass filter characteristics and may use the low band reflector at the microwave frequency. On the other hand, the transmittance at the higher frequency range for the incident angles $\theta= 0^0$, 30^0 and 40^0 have shifted towards the higher frequency. Such band acts as a tunable narrowband filter and also use as a multichannel filter by varying the incident angle. As the angle of incidence increases, the band gap also increases at the higher frequency range due to the dielectric behavior of the material as shown in the Figure 4.2(a).

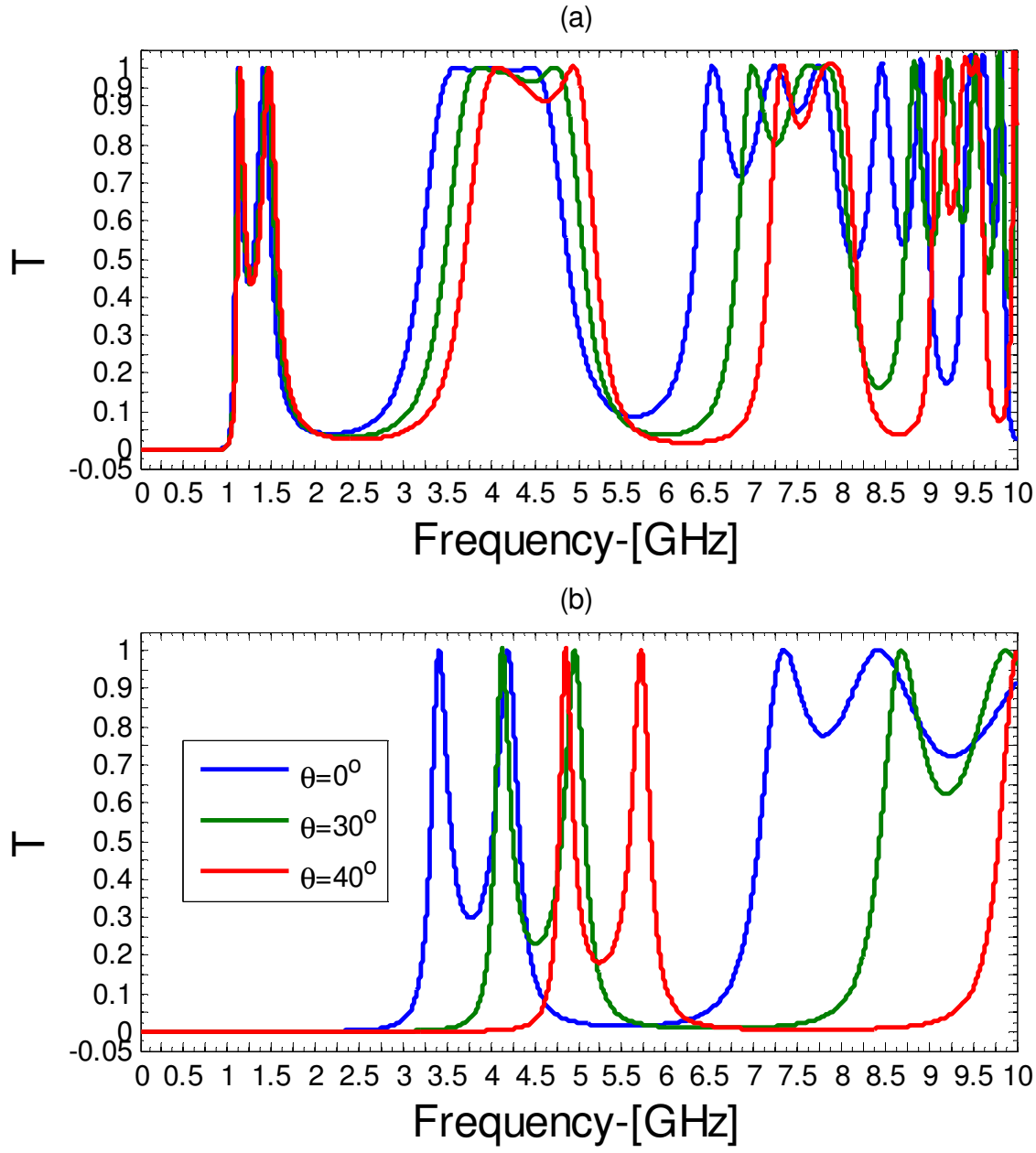

Figure 4.2: Shows the transmittance versus frequency with varying angle of incidence for (a) right hand polarization structure and (b) left hand polarization structure

Similarly, the transmittance of the considered ternary photonic crystal against frequency (GHz) with different values of angle of incidences $\theta = 0^0, 30^0, 40^0$ for left-hand polarization are studied. In this case, the cutoff frequency for the normal incidence i.e. $\theta=0^0$ is obtained at 3.2GHz due to the superconducting layer. The edge of the cutoff frequency shift towards the higher frequency when the value of incident angles increases due to the effective property of the dielectric material. In the

transmittance, the characteristics graph shows that the cutoff frequency becomes 4.5GHz when the angle of incidence maximum i.e. $\theta=40^0$. The transmittance of the considered structure at higher frequency range has a huge shifting i.e. 4.5-10 GHz, and obtain a large band gap as shown in Figure 4.2(b). The left-hand polarization ternary photonic crystal having the large band gap at the low frequency may be used as a broadband reflector or high pass filter application.

We have compared the transmittance of the right-hand polarization and the left-hand polarization ternary photonic crystal. The left-hand polarization ternary photonic crystal has the better results compared to the right-hand polarization ternary photonic crystal. The cutoff frequency of the left-hand polarization ternary photonic crystal is high in comparison to the right-hand polarization ternary photonic crystal. These studies carried out an informative idea to design a tunable filter which can be tuned by changing the angle of incidence. As we know that the magnetized cold plasma layer is externalmagnetic field dependent and the superconducting layer, ($YBa_2Cu_2O_7$), is also influenced by the operating temperature. Therefore, we have studied the transmittance of the right-hand polarization and the left-hand polarization ternary photonic crystal by varying the magnetic field. Thetransmittance of the considered ternary periodic structure against frequency (GHz) with the various values of the magnetic field of the magnetized cold plasma, B=0.4T, B=0.6T, and B=0.8T, for right-hand polarization, is studiedwhere the wave falls normally i.e. $\theta=0^0$. The transmittance behavior for the values of magnetic field B=0.4T, B=0.6T, B=0.8T are similar to the previous case when the angle of incidence is varied, but the cutoff band edge is distorted due to change of the gyro-effective frequency. We know that the transmittance is changed due to change in the refractive index. The refractive index of the magnetized cold plasma is dependent on the gyroeffective frequency. So, the refractive index of the right-hand polarization and left-hand polarization ternary photonic crystal is changed due to the applied externalmagnetic field of magnetized cold plasma. Therefore, the transmittance of the ternary photonic crystal with the right-hand polarization material is varied by changing the magnetic field. It means that the permittivity of the magnetized cold plasma is affected only with the applied magnetic field. The cutoff frequency of the right-hand polarization structure increases with increasing the value of magnetic fields shown in Figure 4.3(a).

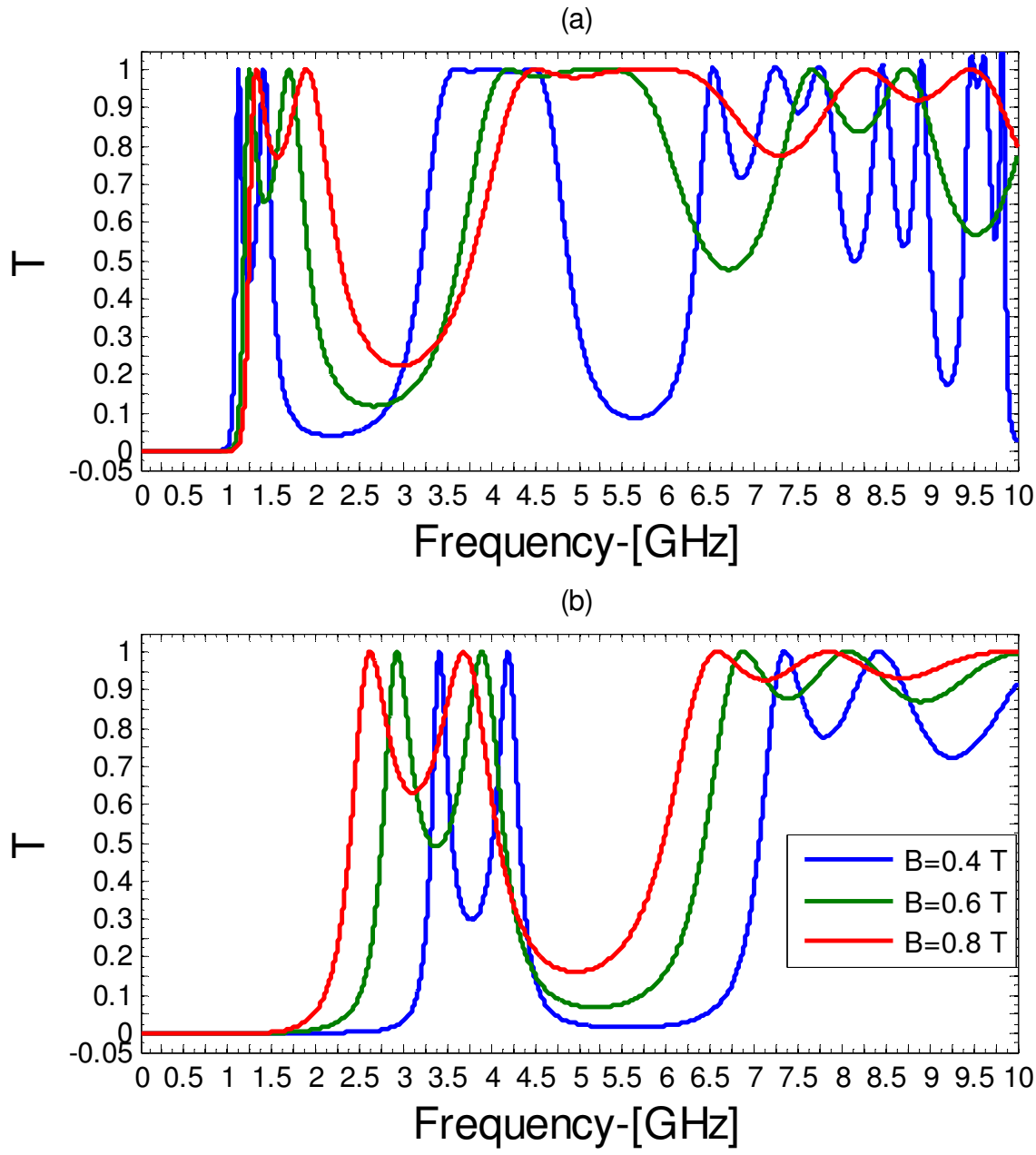

Figure 4.3: Shows the transmittance versus frequency with varying magnetic field for (a) right hand polarization structure and (b) left hand polartization structure

Similarly, now we havestudied the transmittance of considered ternary photonic crystal against frequency (GHz) with varying the magnetic field of magnetized cold plasma for the left-hand polarization i.e. B=-0.4T, B=-0.6T, B=-0.8T having $\theta=0^0$, $n_e=12x10^{17}/m^3$ and all parameters are same as the previous calculation. The changed refractive index of the left-hand polarization material is affected to the wave propagation. The transmittance behavior for the left-hand polarization ternary

photonic crystal has an opposite trend because the permittivity of the magnetized cold plasma is changed abnormally when the magnetic field applies in the negative direction. The zero transmittance is obtained the lowest value for B=-0.8T, but this is increased up to 3.2GHz when the value of the magnetic field decreases as shown in Figure 4.3(b). The tunable transmittance of the left-hand polarization ternary photonic crystal is obtained by varying the magnetic field. The band gaps at the low frequency, as well as the higher frequency region, are obtained. So, such transmittance behavior of the ternary photonic crystal may be used in the bandpass filter applications.

From Eq. (4.1), it has been shown that the plasma frequency of the magnetized cold plasma is dependent on the electron density which in next valuable parameter of the magnetized cold plasma and the refractive index of the magnetized cold plasma is dependent upon the plasma frequency. The transmittance of the right-hand polarization and the left-hand polarization ternary photonic crystal are studied by varying the electron density. Now, we focused our study on the transmittance of the considered ternary photonic crystal with right-hand polarization material against frequency (GHz) with varying the values of electron density, i.e. $n_e=12x10^{17}/m^3$, $16x10^{17}/m^3$ and $20x10^{17}/m^3$. All parameters of the considered structure are same taken as in the above section. The transmittance of the right-hand polarization ternary photonic crystal at the lower to higher frequency ranges is varied the electron density of the magnetized cold plasma i.e. $n_e=12x10^{17}/m^3$, $16x10^{17}/m^3$, $20x10^{17}/m^3$ having the positive magnetic field i.e. B=+0.4T as shown in Figure 4.4(a). Due to the presence of the superconductor layer, the zero transmittance at the lower frequency range, 0-1.0 GHz, is obtained which is the low cutoff frequency. Such ternary photonic crystal has a low pass filter characteristic. The cutoff frequency is decreased when the value of electron density of the magnetized cold plasma increases, because of the permittivity of the magnetized cold plasma decreases by increasing the plasma frequency of the magnetized cold plasma.

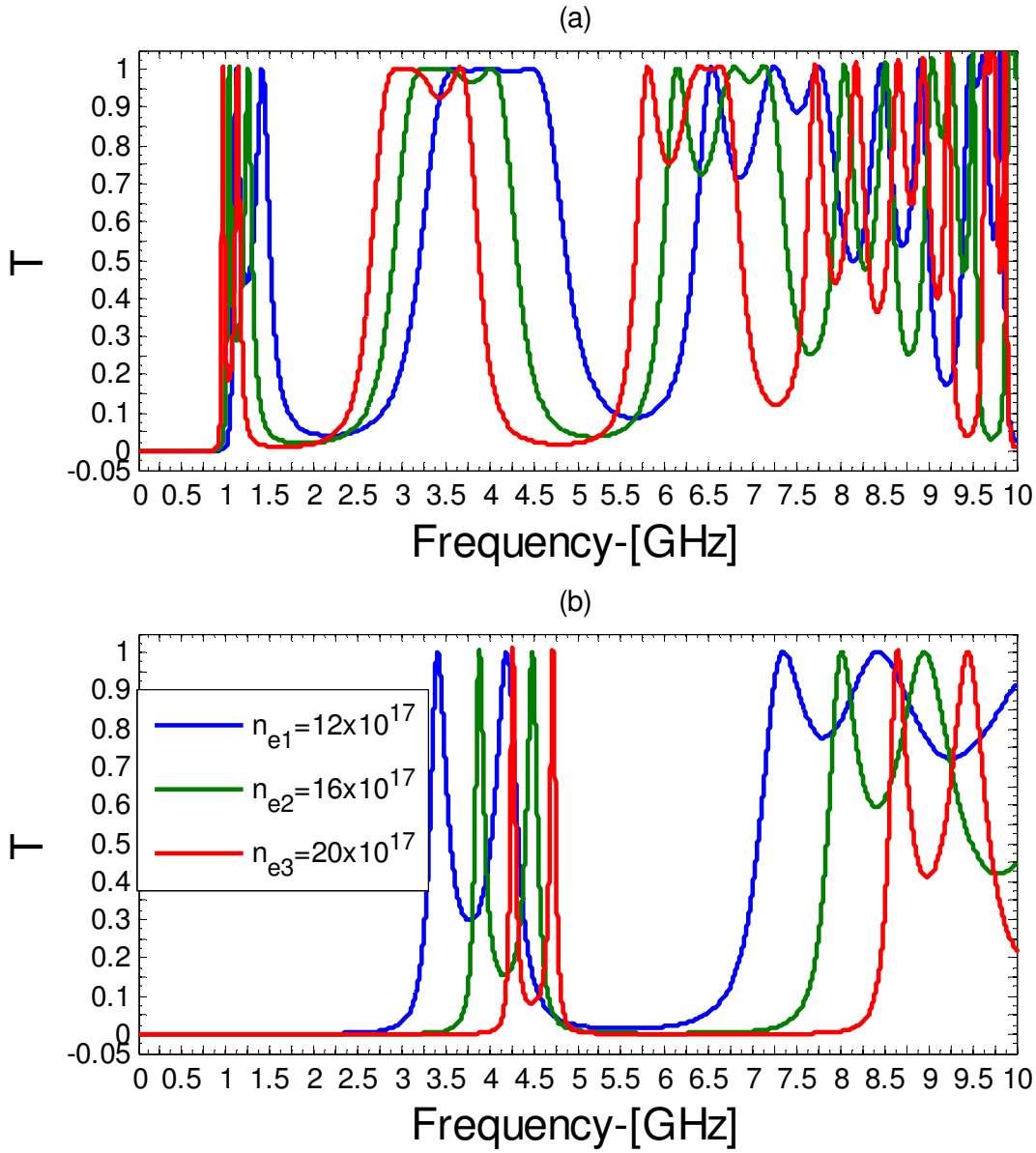

Figure 4.4: Shows the transmittance versus frequency with varying electron density of magnetized cold plasma for (a) right hand polarization structure and (b) left hand polarization structure

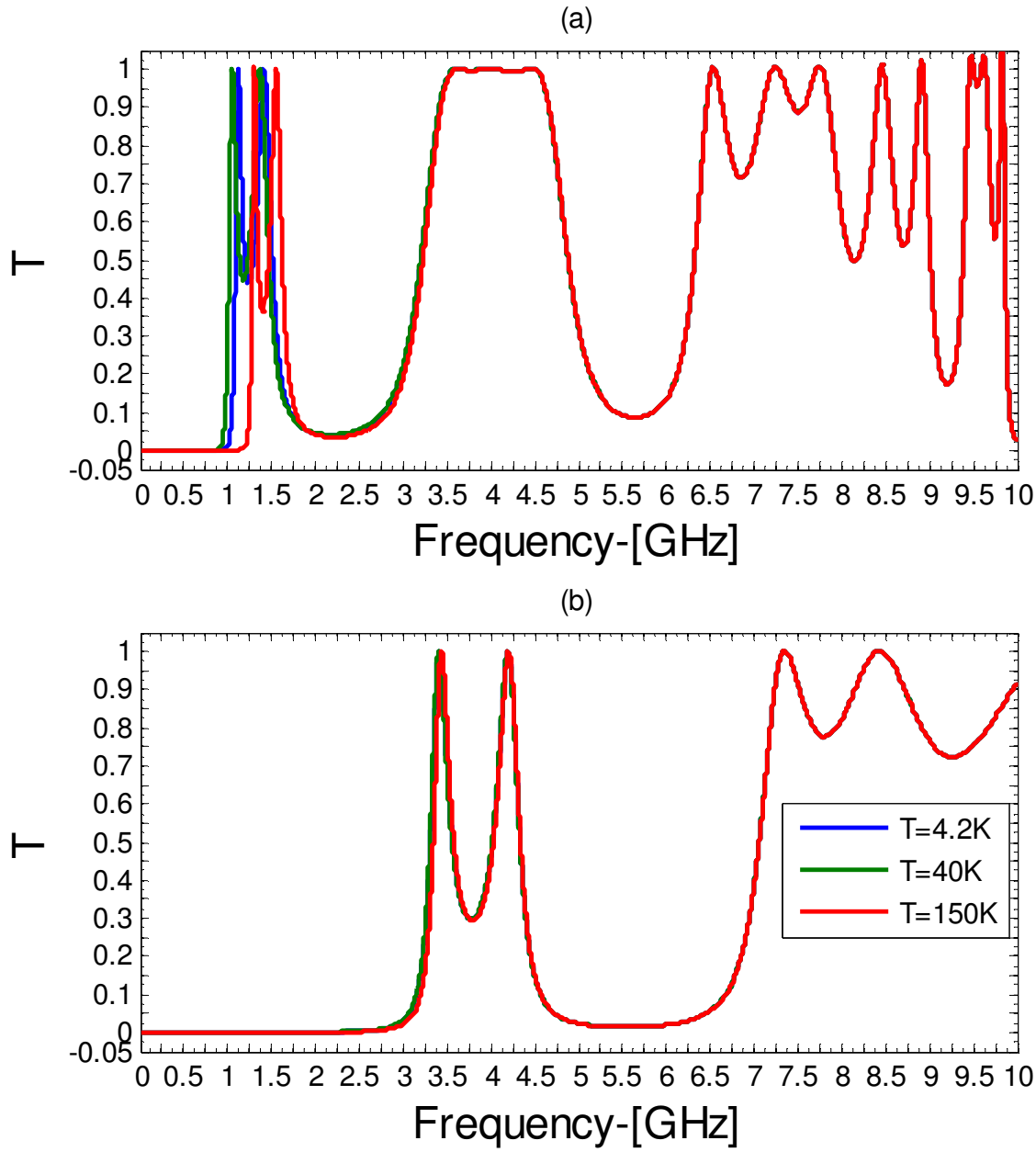

Figure 4.5: Shows the transmittance versus frequency with varying temperatue of superconductor for (a) right hand polarization structure and (b) left hand polarization structure

Similarly, we again studied the transmittance of the left-hand polarization ternary photonic crystal with varying the electron density of the magnetized cold plasma n_e=20x10^{17}/m^3, 16x10^{17}/m^3, 12x10^{17}/m^3 having negative magnetic field i.e. B=-0.4T. The transmittance at the lower and the higher frequency range is varied due to the effect of electron density of the magnetized cold plasma. The zero transmittance at the lower frequency range is enhanced up to 4.2GHz when the electron density of

magnetized cold plasma increases i.e. $12x10^{17}/m^3$, $16x10^{17}/m^3$, $20x10^{17}/m^3$ as shown in Figure 4.4(b). The maximum cutoff frequency is obtained at a maximum value of the electron density of magnetized cold plasma i.e. $n_e=20x10^{17}/m^3$for the left-hand polarization structure. From Eq. (4.1), the denominator of permittivity becomes positive when the left-hand polarization material has the negative magnetic field, and the plasma frequency increases with increasing the electron density. Therefore, the permittivity of the magnetized cold plasma is decreased when the value of electron density of the magnetized cold plasma increases. Such band gap of the left-hand polarization ternary photonic crystal region acts as a broadband reflector or a high pass filter.

The considered ternary photonic crystal has the superconducting material and this material is effected with different operating temperatures and applied magnetic fields.In this section, the transmittance against frequency (GHz) with varying operating temperature T_1=4.2K, 40K, 150K of the superconducting material is studied for the right-hand polarization and the left-hand polarization structure. We have taken $YBa_2Cu_2O_7$ material having T_c=92K, B=0.4T and same parameters as above calculations. The transmittance of the right-hand polarizationternary photonic crystal is varied at the lower frequency range due to the effect of superconducting material but it is not varied at the higher frequency range. So, the effective transmittance at the high frequency shows only due to the effect of dielectric behavior of the air and the magnetized cold plasma materials. The cutoff frequency of the ternary photonic crystal is very sensitive for the operating temperature. It shows that the cutoff frequency is decreased for the operating temperature below the critical temperature i.e. T=4.2K, 40K. But the transmittance is increased due to the effect of the magnetic field in the superconducting material when the operating temperature is larger than the critical temperature i.e. T=150K, Figure 4.5(a).

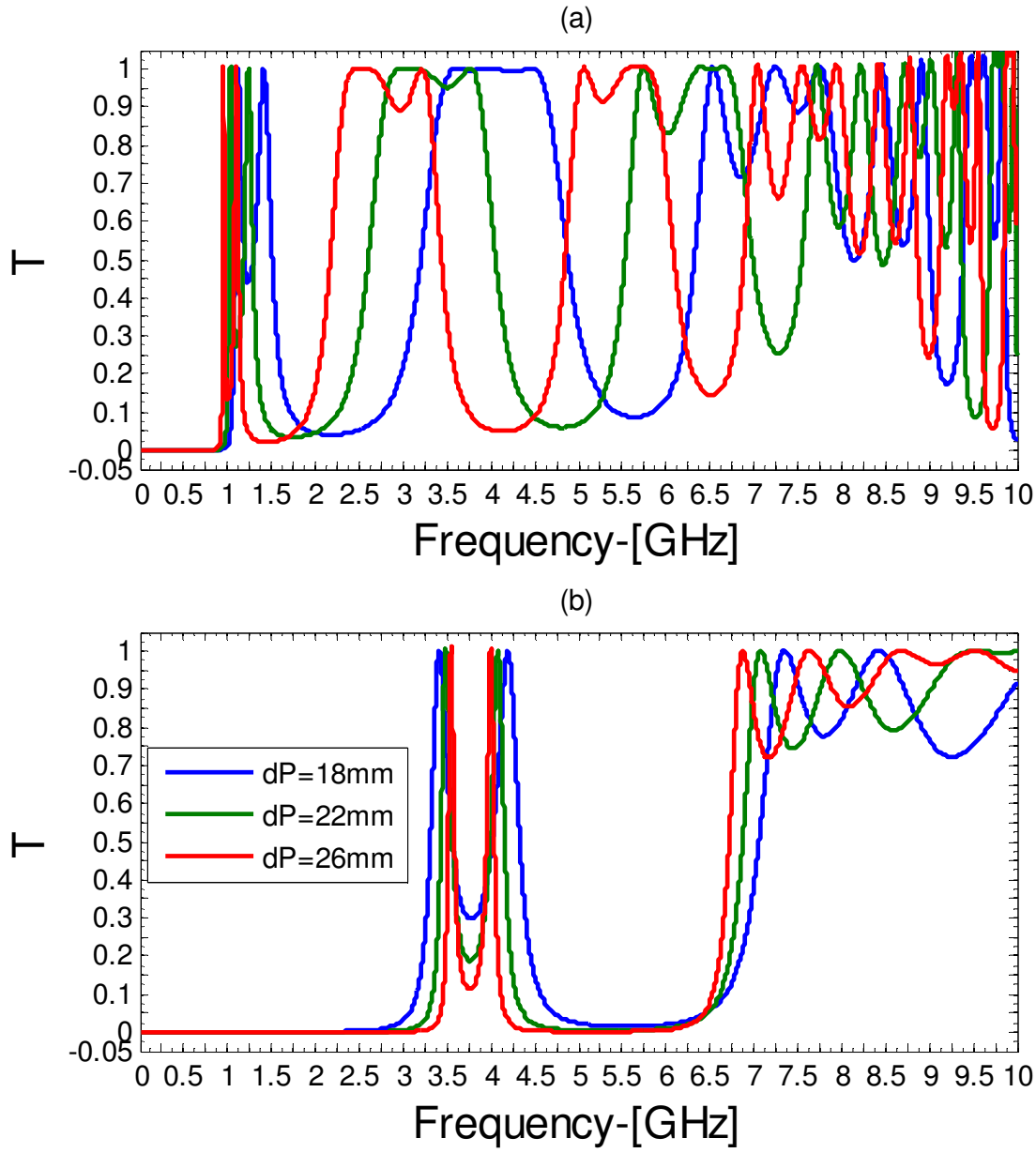

Figure 4.6: Shows the transmittance versus frequency with varying thickness of magnetized cold plasma for (a) right hand polarization structure and (b) left hand polarization structure.

Similarly, the transmittance of the left-hand polarizationternary photonic crystal against frequency (GHz) with varying operating temperature T=4.2K, 40K, 150K, magnetic field B=-0.4T is studied having the same parameters. The transmittance behavior of the left-hand polarization ternary photonic crystal is not found any change compare to the right-hand polarizationternary photonic crystal but the zero transmittance at the lower frequency range is found at 3.2 GHz frequency as shown in

Figure 4.5(b). It means that the transmittance of the considered left-hand polarizationternary photonic crystal does not affect with varying the temperatures. The left-hand polarization ternary photonic crystal may act as a broadband reflector having the cutoff frequency 3.2GHz.

In this section, we have studied the transmittance against frequency (GHz) with varying the thickness of the magnetized cold plasma for right-hand polarization and left-hand polarization as shown in Figure 4.6. The transmittance against frequency (GHz) with varying the thickness of the superconducting material for right-hand polarization/left-hand polarization as shown in Figure 7. The transmittance against frequency (GHz) for the right-hand polarization is studied with varying the thickness of the magnetized cold plasma i.e. 18 mm, 22 mm, and 26 mm having B=0.4T and $n_e=12x10^{17}$/m3, as shown in Figure4.6(a). The cutoff frequency for the right-hand polarizationternary photonic crystal with the superconducting material is decreased with increasing the thicknesses of the magnetized cold plasma material i.e. 0.0-1.0GHz. The transmittance at the higher frequency region has obtained large variation due to the effect of the thickness of the magnetized cold plasma layer.

Similarly, the transmittance of the considered ternary periodic the left-hand polarizationternary photonic crystal against frequency (GHz) is studied by varying the thickness of the magnetized cold plasma with the same parameters as earlier calculations. The cutoff frequency of the considered left-hand polarization ternary photonic crystal has an opposite trend for the lower frequency region to the higher frequency region i.e. the transmittance at the lower frequency range, 0-3.4GHz, is increased with increasing the thickness of the magnetized cold plasma material but the transmittance at the higher frequency range is decreased with increasing the thickness of the magnetized cold plasma material as shown in Figure 4.6(b). In between these frequencies, a low-value transmittance is obtained that is independent to the thicknesses of the magnetized cold plasma material. It may be used as a narrow band filter application.

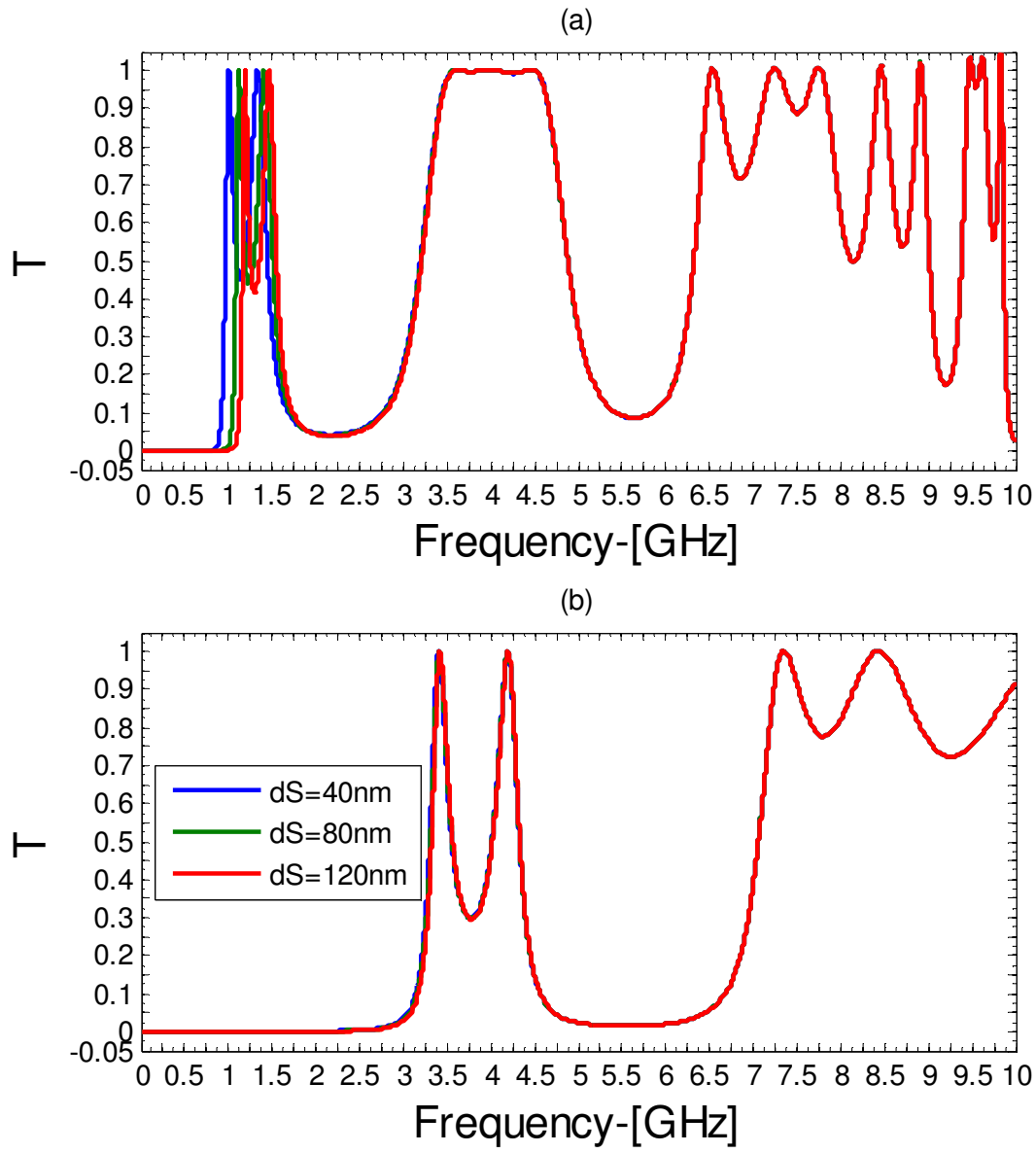

Figure 4.7: Shows the transmittance versus frequency with varying thickness of superconductor for (a) right hand polarization structure and (b) left hand polarization structure

Now, we studied the transmittance against frequency (GHz) with different values of the thickness of the superconducting layer i.e. 40 nm, 80 nm, and 120 nm and other parameters are same as previous calculation. The transmittance at the lower frequency range has varied only due to the effect of the thickness of the superconducting material as shown in Figure 4.7 (a). However, the transmittance at the higher frequency region is constant for all thicknesses. The cutoff frequency of the right-hand polarization ternary photonic crystal is slightly changed. The large cutoff frequency is found when the thickness of the superconducting material is 120nm. The

cutoff frequency of the superconducting material is increased with increasing the thickness of the superconducting material.

Similarly, the transmittance of the considered cutoff frequency for the left-hand polarization material is studied by varying thickness of the superconducting material i.e. 40nm, 80nm, and 120nm; as shown in Figure 4.7(b). The transmittance of the left-hand polarization ternary photonic crystal is independent of the thickness of the superconducting material. The study of transmittance of the left-hand polarization ternary photonic crystal reveals that the transmittance characteristics with varying thickness of the superconducting material have dielectric nature when the magnetic field is applied in reversed direction i.e. B=-4T. This result is similar to the right-hand polarization ternary photonic crystal having the same temperature as shown in Figure 4.5(b).

4.4 Conclusion

In this chapter, we have studied theoretically the transmittance characteristic of the considered ternary photonic crystal versus frequency (GHz) with variation of angle of incidence, magnetic field, electron density of the magnetized cold plasma, temperature and thickness of the magnetized cold plasma for right hand polarization (RHP)/left hand polarization (LHP) structure. The optical properties of the RHP and the LHP ternary photonic crystal are affected by the applicable parameters of the magnetized cold plasma and the superconductor. The optical property i.e. transmittance of the LHP ternary photonic crystal has established the better results compared to the transmittance of the RHP ternary photonic crystal due to the presence of the superconductor layer that is influenced by the operating temperature and the external magnetic field itself. The large band gap of the left-hand polarization ternary photonic crystal may be used as the broadband reflector or high pass filter applications. The superconducting layer is performed the important role to form the band gap of the ternary photonic crystal. However, the tunable transmittance of the RHP ternary photonic crystal has also achieved by varying parameters of the magnetized cold plasma (MCP). On the basis of our analyzed results, we have suggested an innovative idea to fabricate the broadband reflector or the high pass filter and the narrow tunable filter of the ternary photonic crystal having the MCP and the superconducting material under definite the transverse magnetic field and the working temperature.

References:

[1] S. Chandra, Textbook of Plasma Physics, CBS Publishers & Distributors Pvt. Ltd New Delhi (2010). ISBN: 9788123918518

[2] H. K. Onnes, The superconductivity of mercury, Com. Phys. Lab, Leiden (1911) 122-124.

[3] J. G. Bednorz and K. A. Muller, Possible high T_c superconductivity in the Ba-La-Cu-O system, Z. Phys. B Cond. Mat. 64 (1986) 189-193.

[4] F. Abbas, L. E. Davis and J. C. Gallop, Tunable microwave components based on dielectric nonlinearity by HTS/ferroelectric thin films, IEEE Trans. Appl. Super. 5 (1995) 3511-3517.

[5] C. Kittel, Introduction to solid state physics, 6^{th} Ed., Wiley, New York (1986).

[6] F. Abbas and L. E. Davis, Propagation coefficient in a superconducting asymmetrical transmission line with a buffer layer, J. Appl. Phys. 73 (1993) 4494-4499. https://doi.org/10.1063/1.352790

[7] C. J. Wu, Microwave propagation characteristics of a high temperature superconducting variable spacing parallel plate transmission line, J. Appl. Phys. 89 (2001) 3986-3992.

[8] J. E. Nestell, Jr. and R. W. Christy, Optical conductivity of bcc transition metals: V, Nb, Ta, Cr, Mo, W, Phys. Rev. B 21(8) (1980) 2173-7.

[9] W. R. Donaldson, A. M. Kadin, P. H. Ballentine, and R. Sobolewski, Interaction of picosecond optical pulses with high T_c superconducting films, Appl. Phys. Lett. 54 (1989) 2470-3.

[10] E. Yablonovitch, Inhibited spontaneous emission in solid-state physics and electronics, Strong localization of photons in certain disordered dielectric super lattices Phys. Rev. Lett. 58 (1987) 2059-2062.

[11] S. John, Strong localization of photons in certain disordered dielectric super lattices, Phys. Rev. Lett. 58 (1987) 2486-2489.

[12] J. D. Joannopoulos, S. G. Johnson, R. D. Meade and J. N. Winn, Photonic crystals: Molding the flow of light, Princeton Univ. Press Princeton NJ, USA (2007).

[13] E. Centeno, B. Guizal, and D. Felbacq, Multiplexing and demultiplexing of photonic crystals, J. Opt. A: Pure Appl. Opt. 1(5) (1999) L10.

[14] B. Temelkuran, M. Bayindir, E. Ozbay, R. Biswas, M. M. Sigalas, G. Tuttle, and K. M. Ho, Photonic crystal based resonant antenna with a very high directivity, J. Appl. Phys. 87(1) (2000) 603-605.

[15] Y. B. Chen, C. Zhang, Y. Y. Zhu, S. N. Zhu, and N. B. Ming, Tunable photonic crystals with superconductor constituents, Mater. Lett. 55 (2002) 12-16. https://doi.org/10.1016/S0167-577X(01)00610-3

[16] T. V. Murzina, F. Y. Sychev E. M. Kim, E. I. Rau, S. S. Obydena, O. A. Aktsipetrov M. A. Bader and G. Marowsky, One dimensional photonic crystal based on porous n-type silicon, J. Appl. Phys. 98(12) (2005) 123702-4. DOI: 10.1063/1.2142075

[17] P. St. J. Russell, Photonic crystal fibers, J. Light wave Technol. 24 (2006) 4729.

[18] Z. Qiang, W. Zhou and R. A. Soref, Optical add drop filters based on photonic crystals ring resonators, Opt. Exp. 15 (2007) 1823.

[19] B. Curtin, R. Biswas and V. Dalal, Photonic crystal based back reflectors for light management and enhanced absorption in amorphous silicon solar cells, Appl. Phys. Lett. 95 (2009) 231102-2.

[20] T. Ergin T. Benkert H. Giessen and M. Lippitz, Ultrafast time resolved spectroscopy of one dimensional metal-dielectric photonic crystals, Phys. Rev. B 79 (2009) 245134-6.

[21] P. Rani, Y. Kalra, R. K. Sinha, Realization of AND gate in Y shaped photonic crystal waveguide, Opt. Comm. 298 (2013) 227.

[22] C. Caër, S. Combrié, X. Le Roux, E. Cassan, and A. De Rossi, Extreme optical confinement in a slotted photonic crystal waveguide, Appl. Phys. Lett. 105 (2014) 121111.

[23] R. Kakimi, M. Fujita, M. Nagai, M. Ashida, and T. Nagatsuma, Capture of a terahertz of a photonic crystal slab, Nat. Photonics 8 (2014) 657-663.

[24] N. M. Dsouza and V. Mathew, Tunable filter using ferroelectric dielectric periodic multilayer, Appl. Opt. 54 (2015) 2187-2192.

[25] J. N. Dash, R. Jha, J. Villatoro, and S. Dass, Nano displacement sensor based on photonic crystal fiber model interferometer, Opt. Lett. 40 (2015) 467-470.

[26] X. Xiao, W. Wenjun, L. Shuhong, Z. Wanquan, Z. Dong, D. Qianqian, G. Xuexi, and Z. Bingyuan, Investigation of defect modes with Al_2O_3 and TiO_2 in one-dimensional photonic crystals, Optik- Int. J. Light Electron Opt. 127 (2016) 135-138.

[27] H. M. Lee, J. H. Shyu, L. Horng and J. C. Wu, Surface Plasmon polaritons assisted transmission in periodic superconducting grating, J. Vac. Sci. Technol. 29(4) (2011) 04D105.

[28] W. H. Lin, C. J. Wu, T. J. Yang and S. J. Chang, Terahertz multichanneled filter in superconducting photonic crystals, Opt. Express 18 (2010) 27155-27166.

[29] P. Athe, and S. Srivastava, Tunable fano resonance in one dimensional superconducting photonic crystal, J. Supercond. Nov. Magn. 28 (2015) 2331-2336.

[30] J. Wu and J. Gao, Analysis of temperature dependent optical properties in 1-D ternary superconducting photonic crystal with mirror symmetry, J. Supercond. Nov. Magn. 28 (2015) 1971-1976.

[31] M. Upadhyay, S. K. Awasthi, L. Shiveshwari, S. N. Shukla, and S. P. Ojha, Two channel thermally tunable band stop filter for wavelength selective by switching applications by using 1-D ternary superconducting photonic crystal, J. Supercond. Nov Magn. 28 (2015) 1937-1942.

[32] A. H. Aly, H. T. Hsu, T. J. Yang, C. J. Wu and C. K. Hwangbo, Extraordinary ordinary optical properties of a superconducting periodic multilayer in near zero permittivity operation range, J. Appl. Phys.105 (2009) 083917-8.

[33] A. H. Aly, A. Mehaney, and S. A. El-Naggar, Evaluation of photonic band gaps in one-dimensional photonic crystal that incorporate high T_c superconductor and magnetostrictive materials, J. Supercond. Nov Magn. 30 (2017) 2711-2716. https://doi.org/10.1007/s10948-017-4072-y

[34] A. H. Aly, S. W. Ryu, H. T. Hsu and C. J. Wu, THz transmittance in one dimensional superconducting nanomaterial dielectric superlattice, Mater. Chem. Phys. 113 (2009) 382-284.

[35] C. J. Wu Y. H. Chung, B. J. Syu, and T. J. Yang, Band gap extension in a one dimensional ternary metal dielectric photonic crystal, Prog. Electromagn. Res. 102 (2010) 81-93.

[36] Z. H. Feng, S. B. Lui and H. Yang, omnidirectional photonic band gap in one dimensional ternary superconductor dielectric ternary photonic crystals based on a Thue-Morse aperioodic structure, J. Supercond. Nov. Magn. 27 (2014) 41-52.

[37] A. H. Aly, H. A. Elsayed and S. A. El-Naggar, The properties of cutoff frequency in two dimensional superconductor photonic crystals, J. Mod. Opt. 61 (2014) 1064-1068.

[38] A. H. Aly and D. Mohamed, BSCCO/$SrTiO_3$ one-dimensional superconducting photonic crystal for many applications, J. Supercond. Nov. Magn. 28 (2015) 1699-1703.

[39] A. H. Aly, A. Aghajamali, H. A. Elsayed and M. Mobarak, Analysis of cutoff frequency in a one-dimensional superconductor meta-material photonic crystal, Physica C 528 (2016) 5-8.

[40] A. Aghajamali, Transmittance properties in a magnetized cold plasma superconductor periodic multilayer, Appl. Opt. 55 (2016) 6336-6340.

[41] M. Zamani, Spectral properties of all superconducting photonic crystals comprising pair of high-high, low-low, or high low temperature superconductors, Physica C 520 (2016) 42-46.

[42] K. P. Sreejith, D. M. Nirmala, and M. Vincent, Analysis of cutoff frequency in one dimensional ternary superconducting photonic crystal, Physica C 540 (2017) 44-47.

[43] A. H. Aly and H. Sayed, Photonic band gap materials and monolayer solar cell, Surf. Rev. Lett. 25(5) (2018) 1850103-6.

[44] D. Mohamed, H. A. Elsayed and D. Vigneshwaran, Optical properties of New type of superconductor semiconductor metamaterial photonic crystals, J. Supercond. Nov. Magn. 31(11) (2018) 3453-3457. https://doi.org/10.1007/s10948-018-4628-5

[45] A. H. Aly, A. A. Ameen, and D. Vigneshwaran, Superconductor nanometallic photonic crystal as a smart window as a low temperature applications, J. Supercond. Nov. Magn. 32(2) (2018) 191-197. https://doi.org/10.1007/s10948-018-4716-6

[46] C. Nayak, A. Aghajamali, A. Saha and N. Das, Near and mid infrared bandgaps in a 1-D photonic crystal containing superconductor and semiconductor meta-material, Int. J. Mod. Phys. B 33(20) (2019) 1950219-27.

[47] J. X. Liu, W. C. Tang, Y. Jiang, L. Ju, and H. W. Yang, A study of frequency selection characteristics of negative conductivity in high temperature plasma, Results Phys. 14 (2019) 102467-5.

[48] A. Aghajamali and T. Alamfard, Defective annular semiconductor superconductor photonic crystal, 2020. arXiv preprint arXiv:2004.08149.

[49] M. Tinkham, Introduction to Superconductivity, Courier Corporation, USA (1996).

[50] P. Yeh, Optical Waves in Layered Media, John Wiley & Sons, New York (1988).

[51] H. G. Booker, Cold Plasma Waves, Springer-Netherlands, New York (1984)

Chapter 5
Multichannel filter application of a magnetized cold plasma defect in periodic structure of ZnS/TiO_2 materials

Chapter-5

Multichannel filter application of a magnetized cold plasma defect in periodic structure of ZnS/TiO_2 materials

5.1 Introduction

In this chapter, we have analyzed the optical properties of photonic crystal containing ZnS/TiO_2 materials with defect Magnetized Cold Plasma (MCP). The defect photonic crystals have transmission peaks in the reflected band region due to the presence of resonance waves at the interfaces of defect MCP material. Hence, transmission peaks reveals that the defect MCP one-dimensional photonic crystal may be used as the multichannel filters or reflectors. Optics of photonics of defect and symmetric structure will discuss in detail in next section.

5.1.1 General introduction of photonic crystal

Photonic crystals (PCs) are periodic structure of microstructure to nanostructure in which the optical density of two or more than two medium that is varied in the space. First time, Yablonovitch and John analyzed the origin of photonic band gap in the same year 1987 [1, 2]. At present, photonic crystals are become more attractive materials in the field optics and photonics due to its abnormal optical properties. Photonic Band Gap (PBG) is the unique properties of periodic structure and this PBG of photonic crystal is also called photonic band gap material. The photonic band gap material has a great application in the optical science and technology because photonic band gap can be used to control and manipulate the flow of electromagnetic wave. The wave propagation inside the periodic structure depends on the unique property of material, which are refractive index, unit cell, the filling fraction, frequency and dimensionality, etc. [3]. There are three types of photonic crystals, but one-dimensional photonic crystal is the simplest one where the direction of the wave propagation is considered in one dimension, and it is easy to fabricate the one dimensional photonic crystals (1-DPCs) are used in many applications of optical engineered devices: optical filter; resonance cavity and high-reflecting omni-directional mirror etc. [4-12]. The materials considered for the periodic structure are studied in detail in the next section.

5.1.2 Plasma

The optical property and the nature of plasma material have been already discussed in the previous Chapters [13-15].

5.1.3 Semiconducting photonic crystal

The periodic structure of dielectric and semiconducting material is known as semiconducting photonic crystal. Dielectric and semiconducting coating of thin films of materials occur strong ionic or direct covalent bond. In most of the cases, they are transparent visible to infrared light. Applying Bloch's theorem and solving the Maxwell's equations at the boundary between different media, we have treated the interaction of the electromagnetic radiation with these films. In the optical coating process it is found that the wavelength of the electromagnetic wave is much larger than inter atomic dimensions. Thus, the optical properties within each layer, the interaction of light and matter, can be described macroscopically in terms of phenomenological parameters, which are called as optical density of the matter. The optical constant has real and imaginary parts of a complex refractive index. The real part of refractive index shows the ratio of the velocity of light in vacuum and light in medium, and the imaginary part is an attenuation coefficient or decaying wave, which measures the absorption of light or electromagnetic wave.

5.1.4 Plasma Photonic Crystal (PPC)

Plasma photonic crystal shows strong spatial dispersion resulting in the appearance of electromagnetic band gap structure [16-18]. In the same year, Sakai research group performed the experimental works on one-dimensional and two-dimensional plasma photonic crystals [19-21]. The plasma photonic crystal has also band gap, which is called plasma photonic band gap. The plasma photonic band gap can be also used to control the electromagnetic wave is similar fashion of the photonic crystals by the variable parameters of plasma material.

Some previous years, magnetized cold plasma has attracted to lot of researchers due to anomalous behavior of magnetized cold plasma where the electric permittivity or optics of magnetized cold plasma (MCP) is tuned with the external magnetic field. Researchers have introduced a new kind of photonic crystal containing magnetized cold plasma where the optics of plasma photonic crystal is controlled by externally applied magnetic field. MCP has also an extra variable in the presence of magnetic field, which is called gyro-effective frequency or cyclotron frequency. MCP has unique property of propagating wave along the positive and negative direction; this is decided by the direction of the applied externally magnetic field [22-24]. The extra controllable parameters are reasons where the magnetized plasma photonic crystals are more fascinating optical properties in comparison to the conventional plasma

photonic crystals [25]. The magnetized plasma materials exhibit tunable photonic band gap due to dependence of optics with main extra parameters like magnetic field and cyclotron frequency. On the basis of study of optical properties of the MCP materials, the adhesive materials with plasma are considered for possible fabrication of multilayer structure with magnetized cold plasma material. Kumar et al. [26] investigated the band structure, reflection spectra of the considered periodic structure of dielectric and magnetized cold plasma material and suggested the narrow and tunable filters in photonic crystal with defect of magnetized cold plasma. The considered structure of the plasma photonic crystals was similar to Zhang et al. [27]. Aly and Mohamed [28] recommended the transmission spectra of 1-DPC of the superconducting material and dielectric material for the applications of band pass filter. Aghajamali [29] proposed the transmittance property of magnetized cold plasma-superconductor periodic multilayer structure for the applications in reflectors. Aly and Sayad [30] designed the periodic structure to enhance the electromagnetic wave absorption by varying the optical length of the electromagnetic wave propagate inside the absorbing material which used to enhance the efficiency of silicon solar cell device. Aly group again [31] proposed an idea for the optical properties of a new type of superconductor and semiconductor meta-material photonic crystals. The transmittance property of one dimensional periodic structure of defective photonic crystal was done and analyzed by Aly and Elsayad [32] where the defect of photonic band gap at the central wavelength vary with variation angle of incidence in ultraviolet region. The transmittance of one dimensional defective photonic crystal structure was studied and the tunability of one-dimensional periodic structure based on Faraday Effect was analyzed [33]. Aly et al. [34] analyzed optical properties of one-dimensional defective photonic crystal containing nanocomposite material of silver (Ag) as a defect layer with varying other parameters in UV region [34]. Transmittance properties of two types of one dimensional periodic structure and the optical properties of meta-material superconductor photonic band gap with/without defect layer were analyzed by Aly group [35, 36]. Aly again [37] also analyzed the metal-dielectric periodic structure and defect mode characterizations. Kumar et al. [38, 39] recommended the optical property of one-dimensional photonic crystal of negative photonic crystal with the defect of plasma material and also analyzed for silicon and silicon dioxide periodic structure with defect of plasma material. Kumar et al. [40] also proposed the transmittance property of one-dimensional dielectric

magnetized cold plasma periodic structure for optical applications. Kumar et al. [41] also analyzed the transmittance of ternary periodic multilayer structure of dielectric, plasma and superconductor for the application tunable reflector applications.

Recently, several papers had been published on multichannel filter in one-dimensional photonic crystal. The tunable multichannel filter designed using one dimensional photonic crystal incorporating uniaxial meta-material in microwave region [42]. Jamshidi-Ghaleh et al. [43] studied the design of tunable narrow band filters using the plasma photonic crystal structure with sinusoidal plasma defect layer. Solaimani et al. [44] studied band gap engineering in constant total length non-magnetized dielectric plasma multilayer. Aghajamli and Alamfard studied defective annular semiconductor superconductor photonic crystal [45]. Wang et al. [46] studied tunable multichannel terahertz filtering properties of dielectric defect layer in one-dimensional magnetized plasma photonic crystal. Elsayed et al. [47] studied the transmission investigation of one-dimensional Fibonacci based quasi-periodic photonic crystals including nanocomposite material and plasma. On the basis of reviewing these research papers, we have found several ideas related to tunable narrowband filter applications in microwave region. On the other hand, we have chosen one-dimensional periodic structure for analyzing tunable narrowband filter due to cheap and easy to fabricate the devices.

Therefore, we have studied and analyzed the transmittance versus frequency (GHz) of one-dimensional periodic structure of ZnS and TiO_2 layers, called photonic crystal; and photonic crystal with defect magnetic cold plasma (MCP) for symmetric and asymmetric structures, called defect photonic crystal. The optical properties of considered structure have been calculated by Transfer Matrix Method (TMM) and Bloch's wave. The optical constant of MCP material is tuned with the plasma variables' parameters and the transmittance of the MCP defective photonic crystal is studied with variation of incident angle, electron density magnetic field and thicknesses of ZnS and TiO_2 material. Besides this, we have also calculated and compared the transmittance of the considered structures with the defect of one and two MCP layers. The transmittance versus frequency of considered periodic multilayer structures may be used as a tunable multichannel filter at microwave region.

5.2 Theory and methodology

The band gap, transmission spectra, reflection spectra and absorption spectra of One-Dimensional Photonic Crystal (1-D PC) are calculated using well known Transfer Matrix Method (TMM) and Bloch's wave [48]. We have considered structure in asymmetric and symmetric form: $(AB)^N$ as symmetric form, and $(AB)^{N/2}(BA)^{N/2}$ as an asymmetric form. We have chosen the symmetric structure with a two defects of magnetized cold plasmas in the form: $(AB)^{N/2}(CC)(BA)^{N/2}$, where A, B and C shows the zinc sulfide (ZnS) and titanium dioxide (TiO_2), and MCP layers [49-52] as depicted in the Figure 5.1.

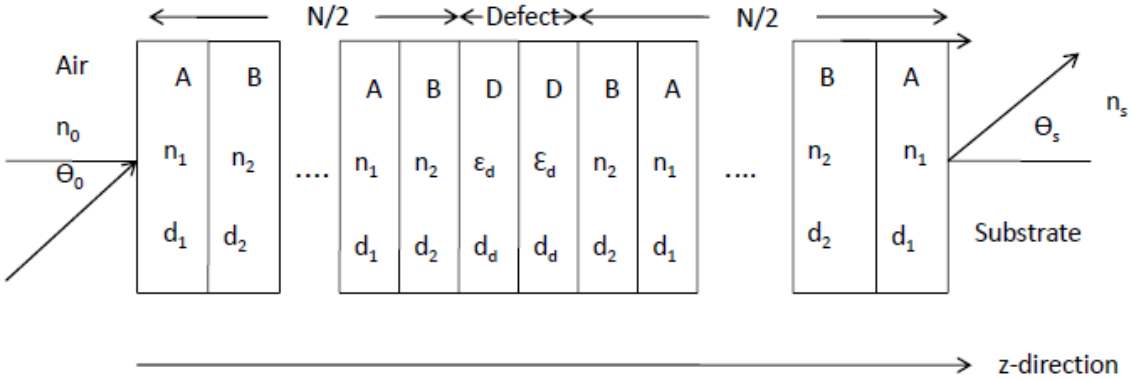

Figure 5.1: Schematic diagram of one-dimensional periodic structure with two defect of magnetized cold plasma

5.2.1 Electric permittivity for magnetized cold plasma

Now, the electric permittivity of magnetized plasma layer, C, has a complex permittvity as discussed in Chapter-3, which is followed as:

$$\varepsilon_c(\omega) = 1 - \frac{\omega_p^2}{\omega\left(\left(1 + \frac{i\gamma}{\omega}\right) \mp \frac{\omega_{le}}{\omega}\right)} \qquad \mu_c = 1 \tag{5.1}$$

where ω (angular frequency), γ (effective collision frequency) and ω_{le} (gyro-effective frequency) and ω_p (plasma frequency) and the plasma frequency is followed by:

$$\omega_p = \left(\frac{n_e e^2}{m\varepsilon_0}\right)^{1/2} \tag{5.2}$$

where n_e (electron density), m (mass of electron), ε_0 (permittivity in free space), e (electronic charge).

The gyro-effective frequency relation is given as:

$$\omega_{le} = \left(\frac{eB}{m}\right) \tag{5.3}$$

where e, B, and m are the electronic charge, applied external magnetic field and mass of electron, respectively [22].

Using transfer matrix method, the optical properties of the considered structure can be analyzed. For this, the characteristic matrix M_i is calculated for the transverse electric (TE) mode at the incident wave angle θ_0 from free space to a 1-D PC structure [48].The characteristic matrix M_i is given by;

$$M_i = \begin{bmatrix} \cos\gamma_i & -\frac{i}{p_i}\sin\gamma_i \\ -ip_i\sin\gamma_i & \cos\gamma_i \end{bmatrix} \tag{5.4}$$

where $\gamma_i = \left(\frac{\omega}{c}\right) n_i d_i \cos\theta_i$ c (speed of light in vacuum), θ_i (ray angle) inside layer i^{th} with refractive index $n_i = \sqrt{\mu_i \varepsilon_i}$, $p_i = \sqrt{\frac{\varepsilon_i}{\mu_i}}\cos\theta_i$ and $\cos\theta_i = \sqrt{1 - \frac{n_0^2 \sin^2\theta_0}{n_i^2}}$ in which n_0 is the optical constant of vacuum or free space. The total characteristic matrix for symmetric, asymmetric and defective symmetric structure can be calculated by multiplying the characteristic matrix of the each layer, which is given as:

$$M(d) = \begin{pmatrix} m_{1,1} & m_{1,2} \\ m_{2,1} & m_{2,2} \end{pmatrix} \tag{5.5}$$

where $M(d) = (M_A M_B)^N$ for symmetric, $M(d) = (M_A M_B)^{N/2}(M_B M_A)^{N/2}$ for asymmetric and $M(d) = (M_A M_B)^{N/2}(CC)(M_B M_A)^{N/2}$ for defective symmetric, where M_A, M_B and M_C are the characteristic matrix of the layer A, B and C, respectively.

The transmission coefficient of the considered defective periodic structure is calculated by [43]:

$$t = \left| \frac{2}{(m_{1,1} + \frac{m_{1,2}}{p_0}) + (m_{2,1}p_0 + m_{2,2})} \right| \tag{5.6}$$

where $p_0 = n_0 \cos\theta_0$ and $p_s = n_s \cos\theta_s$, n_s is the optical constant of substrate (air), whose incident angle is θ_s.

The transmission spectra of the periodic multilayer are followed by:

$$T = \left(\frac{p_s}{p_0}\right)|t|^2 \tag{5.7}$$

5.3 Results and discussion

In this chapter, we have analyzed the transmittance characteristics of symmetric and asymmetric 1-D periodic structures of zinc sulfide (ZnS) and titanium dioxide (TiO_2). Based on the transfer matrix method (TMM), the transmittance of considered periodic structure is analyzed by inserting the one and two plasma layers in symmetric and asymmetric structure. The parameters for ZnS material are $\varepsilon_A = 6.25$, $\mu_A = 1$, $d_A = 0.0188\,\text{mm}$; and TiO_2 material [49-52] are $\varepsilon_B = 5.05$, $\mu_B = 1$, $d_B = 0.0375\,\text{mm}$. The parameters for magnetized cold plasma material are considered from Ref. [22].

Transmittance of one-dimensional periodic structure of ZnS and TiO_2 is analyzed in asymmetric and symmetric structure as shown in Figure 5.2. The transmittance of the asymmetric structure shows a large bad gap due to symmetrical arrangement of the periodic structure in Figure 5.2 (a). Similarly, transmittance of the symmetric structure is analyzed which shows that the band gap divides into two bands due to symmetric arrangement as shown in Figure 5.2 (b). The bandwidth of the symmetric structure increases in comparison to the asymmetric structure due to exist the defect mode in a symmetric structure. The sharp defect transmission peak of the symmetric structure is used in many applications like filters and laser resonators etc. Further, we focus on the study of symmetric structure with defect of one or two defect layers of magnetized cold plasma with variation of incident angle and plasma parameters.

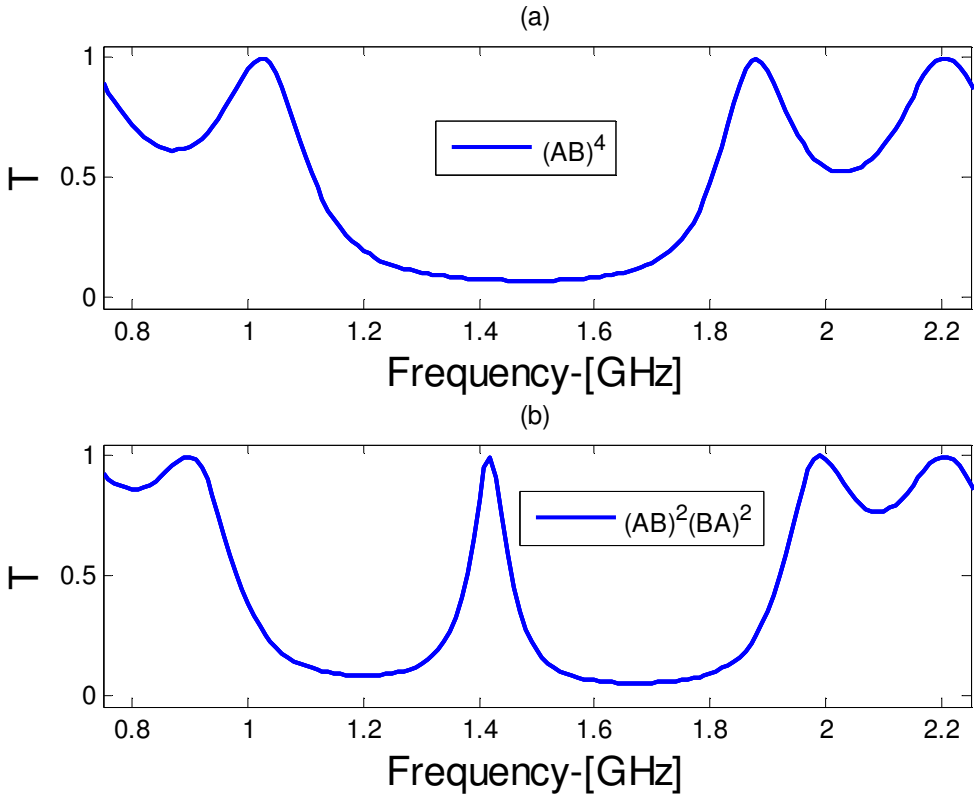

Figure 5.2: Transmission spectra versus frequency for: (a) asymmetric periodic structure, (b) symmetric periodic structure

As we know that optical properties of material changes due to changing the structure and the refractive index of material, and the incident angle plays an important role for such change. So, we have studied the optical properties of considered periodic structure with variation of wave angle or incident angle. Now, the transmittance of symmetric 1-DPS with zinc sulfide and titanium dioxide material with defect of MCP is analyzed on variation of incident angle $\theta = 0^o, \theta = 10^o, \theta = 20^o$ as shown in Figure 3. Figure 3(a) shows the transmittance of one dimensional periodic structure inserted one defect layer of magnetized cold plasma with variation of incident angle $\theta = 0^o, \theta = 10^o, \theta = 20^o$. The figure is depicted that defect transmission peaks and band gaps are shifted towards the higher frequency for increase the value of incident angles and also forms the multiband which can act as tunable multichannel filters.

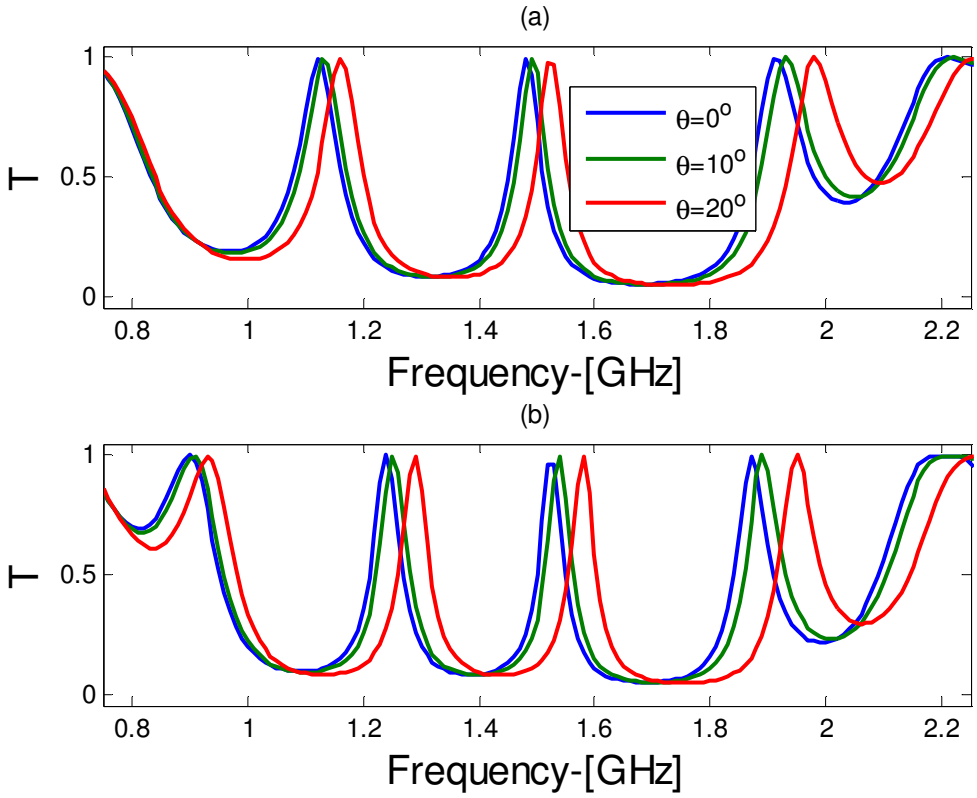

Figure 5.3: Transmission spectra versus normalized frequency of the 1-D PS of ZnS and TiO_2 with variation of incident angle $\theta = 0^o, \theta = 10^o, \theta = 20^o$ for (a) one defect layer of magnetized cold plasma, (b) two defect layers of magnetized cold plasma

Similarly, the transmittance of one-dimensional periodic structure with defect of two layers of magnetized cold plasma material with variation of incident angles is studied. The transmittance of considered periodic structure versus frequency is analyzed with variation of incident angle $\theta = 0^o, \theta = 10^o, \theta = 20^o$ as shown in Figure 5.3 (b). The figure is also depicted that the obtained transmittance is shifting towards the higher normalized frequency, which also forms multiband due to the defect of plasma material. The transmittance shows that the large shifting in transmittance obtains for corresponding to the large value of incident angle $\theta = 20^0$. These obtained results may act as tunable multichannel filters at microwave region as shown Figure 5.3 (b).

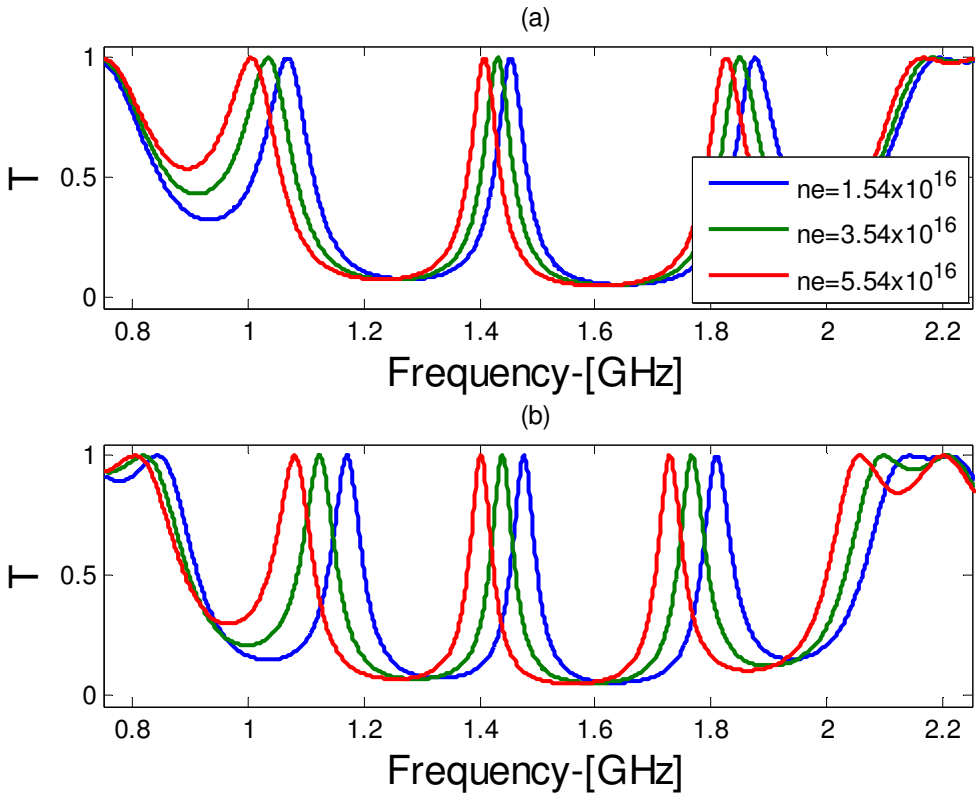

Figure 5.4: Transmission spectra versus normalized frequency of the one dimensional periodic structure of ZnS and TiO_2 with varying $n_e = 1.54\times10^{16}, n_e = 3.54\times10^{16}, n_e = 5.54\times10^{16}/m^3$ for (a) one defect layer of magnetized cold plasma, (b) two defect layers of magnetized cold plasma

Further, the magnetized cold plasma has an important parameter that is electron density, which plays a key role in changing the plasma frequency. The transmittance versus frequency (GHz) of periodic multilayer structure of zinc sulfide and titanium dioxide with defect of one and two layer of magnetized cold plasma as shown in Figure 5.4. The transmittance of the structure with defect of one layer of magnetized cold plasma versus frequency was analyzed on variation of varying electron density $n_e = 1.54\times10^{16}, n_e = 3.54\times10^{16}, n_e = 5.54\times10^{16}/m^3$ as shown in Figure 4(a). Transmittance versus frequency with varying electron density $n_e = 1.54\times10^{16}, n_e = 3.54\times10^{16}, n_e = 5.54\times10^{16}/m^3$ is shifted towards the lower frequency when the electron density increases. Similarly, the transmittance with defect of two magnetized cold plasma layer are analyzed on variation of different value of electron density $n_e = 1.54\times10^{16}, n_e = 3.54\times10^{16}, n_e = 5.54\times10^{16}/m^3$ and transmission peak shown slightly high and shifted towards the lower frequency when the electron density increases. The plasma frequency is dependent upon the electron

density. Therefore, the optics/electric permittivity of magnetized cold plasma material changes due to the electron density. The obtained results of transmittance defect peaks show as tunable multichannel filter at microwave region as shown in Figure 5.4 (b).

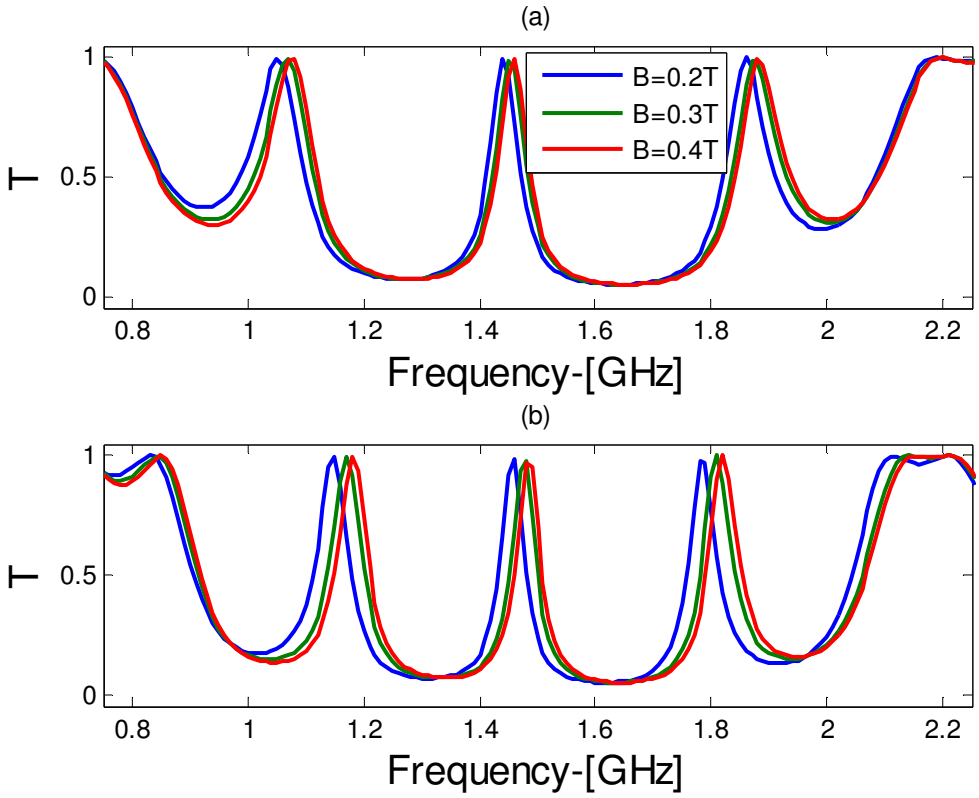

Figure 5.5: Transmission spectra versus normalized frequency of the one-dimensional periodic structure of ZnS and TiO_2 with varying $B=0.3T, B=0.4T, B=0.5T$ for (a) one defect layer of magnetized cold plasma, (b) two defect layers of magnetized cold plasma defect

In magnetized cold plasma, the applied external magnetic field has an important role to change the electric permittivity. The external magnetic field changes the variation of gyro effective frequency, as gyro effective frequency changes the electric permittivity of magnetic cold plasma material is also changed, and then the transmittance of periodic structure containing plasma is also varied. Therefore, we have studied the transmittance of periodic structure of zinc sulfide and titanium dioxide with inserted one and two defect layers of magnetized cold plasma on variation of the applied external magnetic field, $B=0.3T, B=0.4T, B=0.5T$, as shown in Figure 5.5(a) and Figure 5.5(b), respectively. Transmittance of one-dimensional periodic structure versus normalized frequency with variation of external magnetic field is analyzed that the transmission peak shifted towards the normalized frequency due to effect of magnetized cold plasma material. As the magnetic field increases, the

every band is shifted to the corresponding to the different values of magnetic field as shown in Figure 5.5(a).

Similarly, transmittance characteristic of one-dimensional periodic structure with inserted defect of two layer of magnetized cold plasma is studied and the abnormal behavior in transmittance of the structure is shown due to the large effect of plasma material. The shifted transmission peak have high wavelength range in comparison to the transmission peaks of the one defect layer of MCP due to thickness of plasma material becomes two times so the optical behavior of material changes corresponds to the plasma material as shown in Figure 5.5(b). The tunable multichannel filter is also obtained in the considered defect structure by external magnetic field for microwave devices.

As we have observed that the defect transmission peak is more variation for two defect layers of magnetic cold plasma. So, transmittances versus frequency (GHz) of one-dimensional periodic structure of ZnS and TiO2 materials have been analyzed with the variation of thickness of ZnS material with same data same as above. The transmittance property of the considered periodic structure is studied for one layer of MPC, which is inserted in the symmetric periodic structure with variation of different value of thicknesses of ZnS i.e. $dA = 0.0188\text{mm}, dA = 0.0208\text{mm}, dA = 0.0228\text{mm}$. The transmittance does not change but it is shifted towards lower frequency on increase the value of thickness of ZnS which shown in Figure 5.6 (a) and the corresponding 2D image, Figure 5.6 (b), is also verified the similar data.

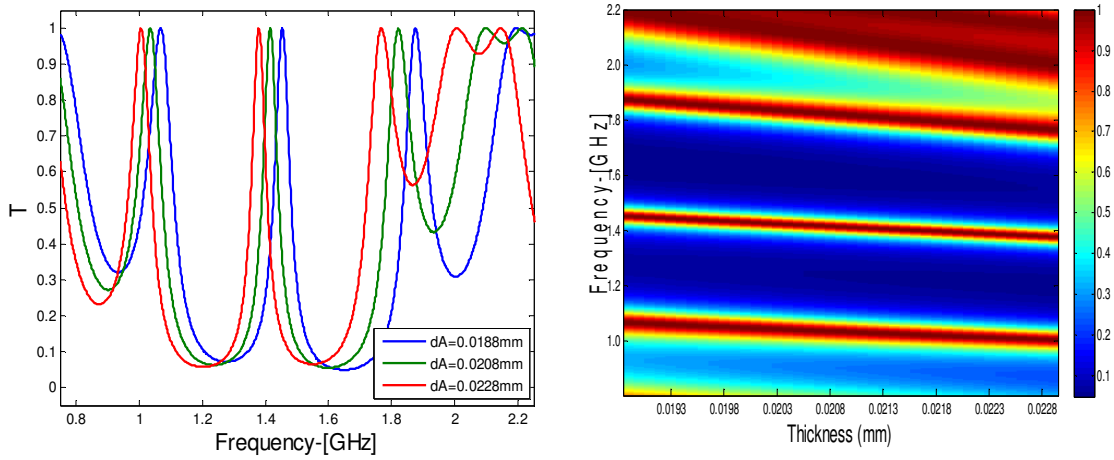

(a) (b)

Figure 5.6: (a) Transmittance versus frequency with variation of thickness of ZnS material and (b) 2D image plot of frequency versus variation of thickness of ZnS material

Similarly, transmittances of the considered symmetric structure with two defect layers of magnetized cold plasma versus frequency (GHz) have analyzed with the variation of thickness of ZnS material i.e. $dA = 0.0188\,\text{mm}, dA = 0.0208\,\text{mm}, dA = 0.0228\,\text{mm}$ Figure 5.7(a). The transmittance peak, photonic band gap, is tuned for corresponding thickness of ZnS material where it goes to the lower frequency on increase the value of thickness of material. The multiple bands of the structure is controlled by the thickness of the ZnS material and such defect structure may be used in multichannel tunable filter as predicted in Figure 5.7(b).

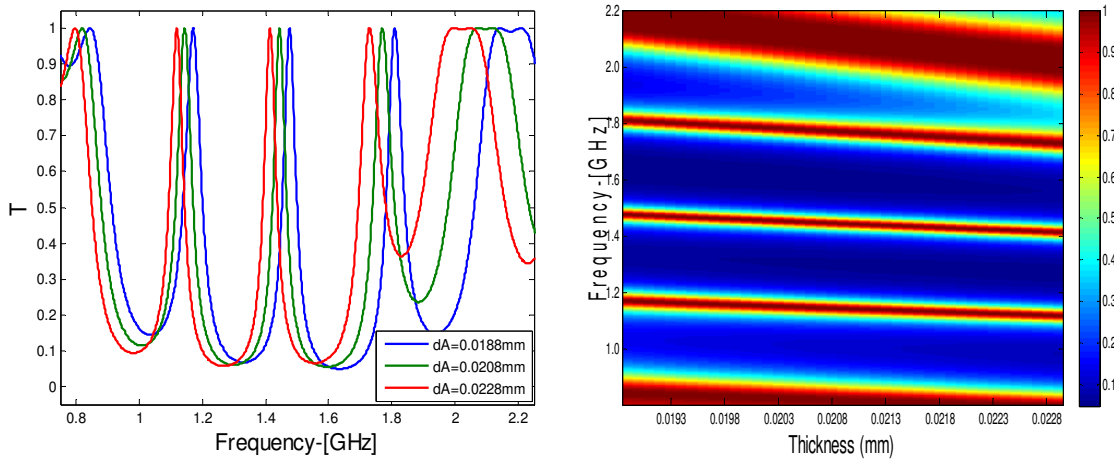

(a) (b)

Figure 5.7: (a) Transmittance versus frequency with variation of thickness of ZnS material (b) 2D image plot of frequency versus variation of thickness of ZnS material

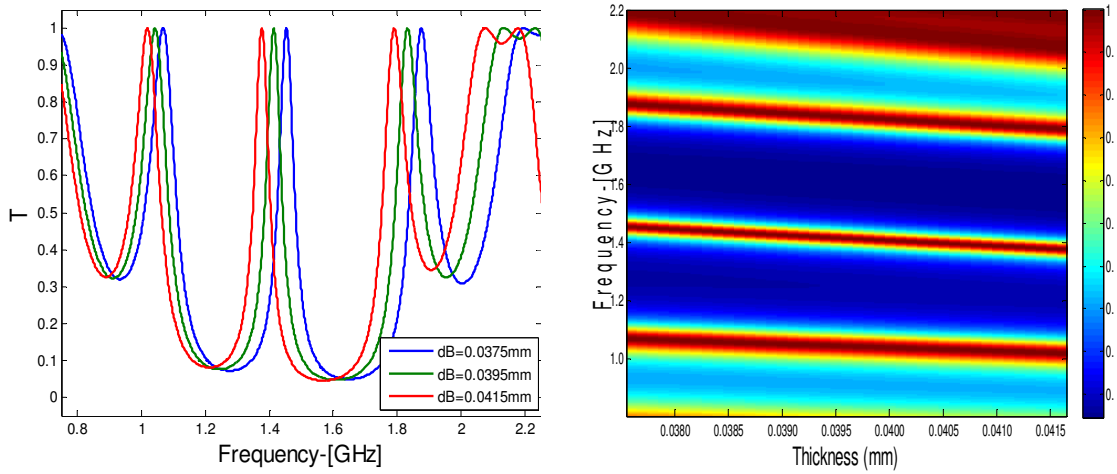

(a) (b)

Figure 5.8: (a) Transmittance versus frequency with variation of thickness of TiO_2 material (b) 2D image plot of frequency versus variation of thickness of TiO_2 material

Now, the transmittances of one-dimensional defective symmetric periodic structure of incorporated the one layer of magnetized cold plasma versus frequency (GHz) with varying the variation of thickness of titanium oxide material have been analyzed. The transmittance peaks varies with increase the value of thickness of titanium oxide material i.e. $dB = 0.0375\,mm, dB = 0.0395\,mm, dB = 0.0415\,mm$. The transmittance peaks is again shifted towards the lower value of frequency on increasing the value of thicknesses as shown in Figure 5.8 (a), and corresponding transmittance peaks results is plotted the 2D image plot for same data as shown Figure 5.8 (b).

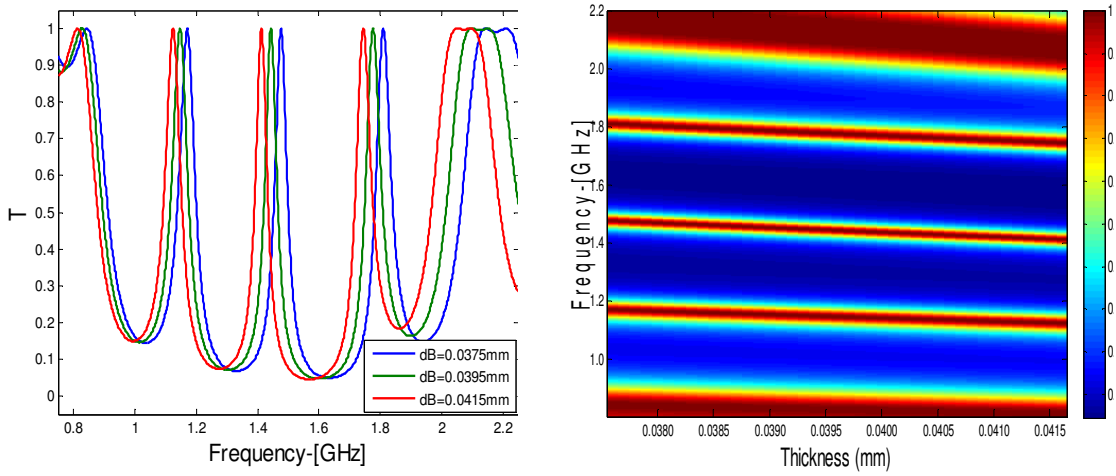

(a) (b)

Figure 5.9: (a) Transmittance versus frequency with variation of thickness of TiO_2 material (b) 2D image plot of frequency versus variation of thickness of TiO_2 material

On the similar way, the transmittance property of one-dimensional periodic structure with two layer of magnetized cold plasma in the symmetric periodic structure versus frequency has been analyzed. The transmittance has obtained same results with large number of multiple transmittance peaks which varies with the value of thickness of titanium oxide material i.e. $dB = 0.0375\,mm, dB = 0.0395\,mm, dB = 0.0415\,mm$ as shown in Figure 5.9 (a), and corresponding 2D image plot is shown in Figure 5.9 (b).

From the above calculations, the transmittances of the considered symmetric structures with defect MCP have predicted that such structures have multichannel transmission defect peaks. These defect transmission peaks are increased when the MCP defect is increased. Besides this, we have also predicted that these defect transmission peaks are also varied with the thickness of the ZnS and TiO_2 material.

5.4 Conclusion

We have discussed about the optics of magnetic cold plasma and also discussed about the optical properties of defect MCP periodic structure containing ZnS and TiO_2 materials. The defect photonic crystals have found transmission peaks inside the reflection band due to high resonance at the interfaces of the defect layers. The transmittance of symmetric and asymmetric one-dimensional photonic crystal containing zinc sulfide and titanium dioxide was studied. The symmetric one dimensional periodic structure containing ZnS and TiO_2 with one or two defect of magnetized cold plasma layer versus frequency (GHz) was analyzed. The defect MCP structure has found the transmittance defect peak. Hence, the transmittance of the symmetric one dimensional periodic structure containing zinc sulfide and titanium dioxide with inserted one or two layers of magnetized cold plasma was analyzed with variation of incident angles, electron densities, and applied external magnetic fields of the magnetized cold plasma material. The transmittance peaks of two MCP layer inserted in symmetric photonic crystal with varying the variation of electron density of plasma as well as thickness of ZnS and TiO_2 material have found better response as comparison to one defect layer in same periodic structure. These calculated results have suggested a simple and innovative idea to fabricate the tunable multichannel filter at microwave region.

References

[1] E. Yablonovitch, Inhibited spontaneous emission in solid-state physics and electronics, Phys. Rev. Lett. 58 (1987) 2059-2062.

[2] S. John, Strong localization of photons in certain disordered dielectric super lattices, Phys. Rev. Lett. 58 (1987) 2486-2489.

[3] J. D. Joannopoulos, S. G. Johnson, J. N. Winn and R. D. Meade, Photonic crystals: Molding the flow of light, Second Ed., Princeton Univ. Press, Princeton NJ, USA (2008). http://ab-initio.mit.edu/book/photonic-crystals-book.pdf

[4] Y. Fink, J. N. Winn, S. Fan, C. Chen, J. Michel and J. D. Joannopoulos and E. L. Thomas, A dielectric omnidirectional reflector, Science 282 (5394) (1998) 1679-1682.

[5] T. F. Krauss, and R. M. De La Rue, Photonic crystals in the optical regime: past, present and future, Progress. Quant. Electron. 23(2) (1999) 51-96. https://doi.org/10.1016/S0079-6727(99)00004-X

[6] D. N. Chigrin, A. V. Lavrinenko, D. A. Yarotsky and S. V. Gaponenko, Observation of total omni-directional reflection from a one-dimensional dielectric lattice, Appl. Phys. A 68 (1999) 25-28.

[7] K. Sakoda, Optical Properties of Photonic Crystals, Springer Berlin (2004).

[8] X. Gu, X. Chen, Y. Chen, X. Zheng, Y. Xia and Y. Chen, Narrowband multiple wavelengths filter in aperiodic optical superlattice, Opt. Comm. 237 (2004) 53-58. https://doi.org/10.1016/j.optcom.2004.03.058

[9] S. Massaoudi, A. de Lustrac, and I. Huynen, Properties of metallic photonic band gap material with defect at microwave frequencies: calculation and experimental verification, J. Electromagnet Wave 20(14) (2006) 1967-1980.

[10] Q. R. Zheng, B. Q. Lin, and N. C. Yuan, Characteristics and applications of a novel compact spiral electromagnetic band gap (EBG) structures, J. Elec. Mag. Waves Appl. 21 (2007) 199-213.

[11] K. Busch, G. von Freymann, S. Linden, S. F. Mingaleev, L. Tkeshelashvili, and M. Wegener, Periodic nanostructures for photonics, Phys. Rep. 444 (2007) 101-202.

[12] S. V. Gaponenko, Introduction to Nanophotonics, Cambridge University Press, Cambridge (2010).

[13] H. Hojo, K. Akimoto and A. Mase, Conference Digest on 28th Int. Conf. Infrared and Millimeter Waves Otsu, Japan (2003) 347-348. http://www.jspf.or.jp/RCPDF/RC66.pdf

[14] H. Hojo and A. Mase, Dispersion relation of electromagnetic wave in one-dimensional plasma photonic crystal, J. Plasma Fusion Res.: Rapid Comm. 80(2) (2004) 89-90.

[15] R. Kumar, Plasma Photonic Crystal (Photonic Crystals - Innovative Systems, Lasers and Waveguides) (2012). DOI:10.5772/32106

[16] X. K. Kong, H. W. Yang, and S. B. Liu, Anomalous dispersion in one-dimensional plasma photonic crystals, Optik 121(20) (2010) 1873-1876.https://doi.org/10.1016/j.ijleo.2009.05.010

[17] H. F. Zhang, S. B. Liu, and X. K. Kong, Photonic band gaps in one-dimensional magnetized photonic crystals with arbitrary magnetic declination, Phys. Plasmas 19 (2011) 122103-13.

[18] L. Qi, Z. Yang and T. Fu, Defect modes in one-dimensional magnetized plasma photonic crystals with a dielectric defect layer, Phys. Plasmas 19 (2012) 012509.

[19] O. Sakai, T. Sakaguchi and K. Tachibana, Photonic bands in two-dimensional micro plasma arrays. I. Theoretical derivation of band structure of electromagnetic waves, J. Appl. Phys. 101 (2007) 073304-9.

[20] O. Sakai, T. Sakaguchi, and K. Tachibana, Photonic bands in two dimensional micro plasma arrays, II. Band gaps observed in millimeter and sub terahertz ranges, J. Appl. Phys. 101 (2007) 073305-7.

[21] O. Sakai, Y. Kishimoto, and K. Yachibana, Integrated coaxial hollow micro dielectric-barrier-discharges for a large area plasma source operating at around atmospheric pressure, J. Phys. D: Appl. Phys. 38(3) (2005) 431-441. http://dx.doi.org/10.1088/0022-3727/38/3/012

[22] H. G. Booker, Chapt.-3: Isotropic Plasma, 23-38, Book: Cold Plasma Waves, H. G. Brooker (Edt.), Springer-Verlag, New York (1984).

[23] T. C. King, C. C. Yang, P. H. Hseih, T. W. Chang, and C. J. Wu, Analysis of tunable photonic band gap structure in an extrinsic plasma photonic crystal, Phys. E: Low Dimens. Syst. Nanostruct. 67 (2015) 7-11.

[24] A. H. Aly, H. A. Elsayed, A. A. Ameen and S. H. Mohamed, Tunable properties of one dimensional photonic crystal that incorporate a defect layer of magnetized cold plasma, Int. J. Mod. Phys. B 31(31) (2017) 1750239-9.

[25] H. F. Zhang, S. B. Liu and X. K. Kong, Photonic band gap in one-dimensional magnetized plasma photonic crystals with arbitrary magnetic declination, Phys. Plasmas 19 (2012) 122103-15.

[26] V. Kumar, K. S. Singh, and S. P. Ojha, Band structure, reflection properties and abnormal behavior of one dimensional plasma photonic crystals, Prog. Electromagn Res. M 9 (2009) 227-241.

[27] H. F. Zhang, S. B. Liu, X. K. Kong, B. R. Bian, and Y. Dai, Omnidirectional photonic band gap enlarged by one-dimensional ternary unmagnetized plasma photonic crystals based on a new Fibonacci quasiperiodic structure, Phys. Plasmas 19 (2012) 112102-9.

[28] A. H. Aly and D. Mohamed, BSCCO/$SrTiO_3$ one dimensional superconducting photonic crystal for many applications, J. Supercond. Nov. Magn. 28 (2015) 1699-1703.

[29] A. Aghajamali, Transmittance properties in a magnetized cold plasma and superconductor periodic multilayer, Appl. Opt. 55 (2016) 6336-6340.

[30] A. H. Aly and H. Sayed, Enhancement of the solar cell based on the nanophotonic crystals. J. Nanophotonics, 11(4) (2017) 046020. https://doi.org/10.1117/1.JNP.11.046020

[31] A. H. Aly, D. Mohamed, H. A. Elsayed and D. Vigneswaran, One dimensional metallo superconductor photonic crystals as a smart window, J. Supercond. Nov. Magn. 32 (2019) 2313-2318.

[32] A. H. Aly and H. A. Elsayad, Defect mode properties in a one-dimensional photonic crystal, Physica B: Cond. Matt. 407(1) (2012) 120-125. https://doi.org/10.1016/j.physb.2011.09.137

[33] A. H. Aly and H. A. ElSayad, Tunability of defective one dimensional photonic crystals based on Faraday Effect, J. Mod. Opt. 64(8) (2016). https://doi.org/10.1080/09500340.2016.1265676

[34] A. H. Aly, H. A. ElSayad, and C. Malek, Optical properties of one dimensional defective photonic crystal containing nanocomposite material, J. Nonlinear Opt. Phys. 26(1) (2017) 1750008-8.

[35] A. H. Aly, The transmittance of two types of one-dimensional periodic structures, Mater. Chem. Phys. 115(1) (2009) 391-394.

[36] A. H. Aly and D. Mohamed, The optical properties of meta-material superconductor photonic band gap with/without defect layer, J. Supercond. Nov. Magn. 32 (2019) 1897-1902.

[37] A. H. Aly, Metalllic-Dielectric Periodic Structure and Defect Mode Characterizations, J. Comput. Theor. Nanosci. 9 (12) (2012) 2045-2051.

[38] A. Kumar, and K. B. Thapa, Study of optical property of defect mode in one dimensional double negative photonic crystal with plasma, Adv. Sci. Eng. Med. 10(7-8) (2018) 837-841.

[39] A. Kumar, P. P. Singh, and K. B. Thapa, A new idea for broadband reflector and tunable multi-channel filter of one dimensional symmetric photonic crystal with magnetized cold plasma defects, AIP Conf. Proc. 1953(1) (2018) 060043-4.

[40] A. Kumar, N. Kumar, and K. B. Thapa, Tunable broadband reflector and tunable narrowband filter of a dielectric and magnetized cold plasma photonic crystal, Eur. Phys. J. Plus 133 (2018) 250-8.

[41] A. Kumar, K. B. Thapa and S. P. Ojha, A tunable broadband filter of ternary photonic crystal containing plasma and superconducting material, Ind. J. Phys. 93(6) (2019) 791-798.

[42] B. Kazempour, Design of tunable multichannel filter in a one dimensional photonic crystal incorporating uniaxial meta-material at microwave frequency, Optica Applicata XLIX (1) (2019) 13-25. DOI: 10.5277/oa190102

[43] K. Jamshidi-Ghaleh, F. Karami-Garehgeshlagi and F. Bayat, Designing tunable narrowband filters using a plasma photonic crystal structures with sinusoidal modulated plasma defect layer, Opt. Quant. Electron 52 (2020) 205. https://doi.org/10.1007/s11082-020-02325-5

[44] M. Solaimani, M. Ghalandari and A. Aghajamali, Band gap engineering in constant total length nonmagnetized plasma dielectric multilayers, Optik 207 (2020) 164476. DOI: 10.1016/j.ijleo.2020.164476

[45] A. Aghajamali and T. Alamfard, Defective annular semiconductor superconductor photonic crystal, Opt.arXiv:2004.08149 (2020). https://arxiv.org/pdf/2004.08149.pdf

[46] Y. Wang, S. Liu and S. Zhong, Tunable multichannel terahertz filtering properties of dielectric defect layer in one-dimensional magnetized cold plasma

photonic crystal, Opt. Comm. 473 (2020) 125985. DOI: 10.1016/j.optcom.2020.125985

[47] H. A. Elsayed and M. M. Abadla, Transmission investigation of one dimensional Fibbonacci based quasi periodic photonic crystals including nanocomposite material and plasma, Phys. Scr. 95(3) (2020) 0355504. https://iopscience.iop.org/article/10.1088/1402-4896/ab4c68/meta

[48] P. Yeh, Optical Waves in Layered Media, John Wiley & Sons, New York (1988).

[49] H. Y. Lee and T. Yao, Design and evaluation of omni-directional one dimensional photonic crystals, J. Appl. Phys. 93 (2003) 819-830.

[50] E. D. Palik, Handbook of optical constants of solids, Academic Press Ltd., London (1998).

[51] W. Cai and W. Shalaev, Optical metamaterials: Fundamental and applications, Springer Verlag, New York (2010).

Chapter 6
Enhancement of absorption property of one dimensional ternary periodic structure containing plasma based hyperbolic material for the application of microwave devices

Chapter-6

Enhancement of absorption property of one-dimensional ternary periodic structure containing plasma based hyperbolic material for the application of microwave devices

6.1 General introduction

In this chapter, we have analyzed theoretically the optical properties of the one-dimensional ternary periodic structure containing plasma based hyperbolic material. Generally hyperbolic materials are the composite materials of metal and dielectric. Similarly, plasma based hyperbolic materials are the composite materials of plasma and dielectric. The optics of such composite materials is calculated by Maxwell-Garnet equation.

6.1.1 Photonic crystals

From the previous Chapter, photonic crystals are an artificial periodic structure of different materials like dielectric, metallic or plasma nanostructures composed of two or more than two medium where the optical density of the material varies in the space. The novel characteristic of the periodic structure of materials is photonic band gap (PBG), which was observed experimentally by Yablonovitch, and proposed theoretically by John [1, 2]. Such periodic structure has unique features where electromagnetic wave is forbidden to propagate through the structure, which is similar to the electron propagation inside the periodic potential [3-5]. Such photonic band gaps play an excellent role in the several optical applications [6-9]. The analysis of periodic structure containing different materials has opened a new roadmap for optical meta-materials. The optical meta-materials are artificial materials or human made materials, and the study of optical meta-material has opened a very informative concept for beyond the materials due to unusual behavior of its optics. Therefore, meta-materials have already opened the magical applications in field of the science [10]. Among the various meta-material proposed in the past decades, the hyperbolic meta-materials were significant noticed due to their ability of presenting sub-wavelength condition. Now, we will discuss the concept of hyperbolic meta-material and plasma based hyperbolic meta-material, which will use to study the optical properties of the periodic structure of plasma based hyperbolic meta-material.

6.1.2 Hyperbolic meta-materials

Hyperbolic Meta-materials (HMMs) are an anisotropic medium, which shows the hyperbolic shape in the dispersion relation at terahertz (THz), optical and near-infrared frequency regions. Basically, the hyperbolic meta-materials are the composite material of metal and dielectric. The hyperbolic material has a lots of potential applications including absorption based devices, negative refraction, optical switch, optical waveguide, and imaging hyper lens [11-15]. Recently, a novel implementation of HMMs at the far-infrared frequency wasproposed with the compositions of the stacked graphene sheets separated by thin dielectric layer and had a super absorber for near fields. Such HMMswerealso used to enhance the decay rate of emitters near its surface for designing efficient and innovative absorbers [16-17].

Hyperbolic meta-material shows dual behavior like metallic and dielectric. In metallic behavior, the large number of free electrons is parallel to the direction of propagation so it shows high reflectance and absorption. Onthe other hand, the dielectric behavior of HMMs has less number of electrons which propagate in the direction of propagation so it behaves like dielectric and also has high transmission. Therefore, these hyperbolic material are also known as type I (metallic) and type II (dielectric) material. In theoretical characterization of the epsilon near zero, epsilon near pole plays an important role in the propagation wave spectrum. Epsilon near zero always occurs in the direction of wave propagation and epsilon near pole always occurs in that region in which no free electron motion [18-23].

Recently, the absorption based optical devices have been paid attention to the scientists and the researchers in the field of optical science and nanotechnology. The absorption property of hyperbolic material is very high and changed with the variation of variable parameters of the material. So, there are several researchers who have contributed their research works to develop the innovative ideas in the field of hyperbolic meta-materials. The tunable absorption properties of composed graphene sheets were studied at near infrared frequency where the graphene sheets were separated by thin dielectric layer. Using the concept of surface conductivity theory, a homogenization formula exists for the multilayer structure, which was proposed by Oatham et al. [24]. A novel implementation of the dual-gated tunable absorption of the graphene-based hyperbolic material for optical gate applications was investigated by Ning et al. [25]. The spectral characteristic of nanostructure hyperbolic material

based UV-absorber in the ultraviolet region of electromagnetic spectrum was investigated. The hyperbolic meta-material structure of the periodically assemble of gold nanostrips was studied by Baqir et al. [26].

The new research based on the concept of grating coupled hyperbolic meta-materials as multiband perfect absorber at spanning frequencies from microwave to visible frequencies was investigated by Sreekanth et al. [27]. A new structure of N-doped Si/Si hyperbolic meta-material integrated with sub-hole Si grating was investigated and the absorption of the structure was worked as Si based HMM for mid IR super absorber. The absorption spectra of proposed structure can have tuned with the grating parameter [28]. The dielectric singularity in the anisotropic permittivity response of the possibility of HMM was presented where a transition point of inverted but coexisting anisotropies was obtained at a specified wavelength due to the particular design of the multilayer structure and possessing different optical properties, which was depending on the investigated frequency [29]. A hyperbolic dispersion of the photonic multilayer waveguide with the layers of dielectric and meta-materials had different geometric waveguides when a long-range propagation of plasmon and phonon polariton at the dielectric HMM interfaces. The absorption of the waveguides with natural hyperbolic properties had the higher lengths compare to metal based HMM waveguides which was proposed by Babicheva et al. [30]. The optical properties of quantum dipole emitters coupled to hyperbolic meta-material nano resonators had proposed using semi analytical quasi-normal mode.

An informative idea about the hyperbolic meta-material nano-resonators for developing the poor single photon was investigated by Axelrod et al. [31]. The measurement and simulation of the polarization dependent Purcell factor for the microwave fishnet material was investigated by Rustomji et al. [32]. The low threshold spaser based on deep sub-wavelength spherical hyperbolic material cavities was investigated by Wan et al. [33]. The tunable mid-IR focusing of Indium Arsenide (InAs) based semiconductor hyperbolic material was analyzed by Desouky et al. [34]. The experimentally demonstration of angle-independent gap in the one-dimensional photonic crystal containing layered hyperbolic materials and dielectrics at visible wavelengths was investigated by Wu et al. [35]. The nearly perfect broadband absorption property of hyperbolic meta-materials was investigated by Riley et al. [36].

The controlled near-infrared surface Plasmon polariton dispersion of the hyperbolic material was investigated by Luk et al. [37].

The optical meta-materials are gradually changed from positive to negative value with varying the parameters of electromagnetic material, which is called transition materials. They are predicted to induce a strong enhancement of the local electric or magnetic field in the vicinity of zero index point. This study had opened the new opportunity for sensing and low intensity nonlinear optical applications [38]. Basically, HMM were originally introduced to overcome the diffraction limit of optical imaging. Recent imaging experiments with plasmonic meta-materials and novel VCSEL geometries was performed in which the Bragg mirrors was engineered in such a way that plasmonic meta-materials and novel VCSEL geometries was exhibited hyperbolic meta-material properties in the long wavelength infrared range. So that plasmonic meta-materials and novel VCSEL geometries could be used to efficiently remove excess heat from the laser cavity [39]. The investigations of hyperbolic meta-materials were reviewed in detail [40]. Hyperbolic meta-material is the composite material of stacked layer and pairs of epitaxial growth ZnO/ZnO:Ga in a monolithic optical micro cavity. These experimentally and theoretically results arising unique resonant effects. Unlike traditional metal, the semiconductor based approach allowed to utilize all three permittivity region of the HMM in the near-infrared spectral range. This configuration gave rise to the modes of identical orders appearing at different frequencies, a zero-order resonance in all positive permittivity regions, and a continuum of the high order modes [41]. Generally, photonic gaps in all dielectric One-Dimensional Photonic Crystals (1-D PCs) shifted towards short wavelengths (blue shift) as the incident angle increased for both Transverse Electric (TE) and Transverse Magnetic (TM) modes. Wu et al. theoretically studied and experimentally the red shift gaps in 1-D PCs composed of alternative hyperbolic meta-material and dielectric for TM polarization.

HMM is the composite material of titanium dioxide and silver material. At operating wavelength 365 nm, an efficient polarization was achieved for the different value of incident angle, which is ranging from 50^0 to 80^0 [42]. HMMs with bi-layer support the transverse electric and transverse magnetic polarized surface waves beyond the Maxwell's Garnett approximation due to the spatial dispersion and interpreted as effective magneto electric coupling, which was studied by Papov et al. [43]. The study

and the effect of resonance on the ability of prisms made of hyperbolic meta-materials in the canalization region. To couple the evanescent wave high spatial frequencies (or high k-modes) to low spatial frequencies that propagate in the far-field zone had been analyzed [44]. The non-locality results for the formation of a hyperbolic layer near the metal dielectric interface with a strong anisotropy of its electromagnetic response. The hyperbolic layer also supports a different class of surface waves, which offer longer propagation distance and strong field confinement, simultaneously. Furthermore, this hyper Plasmon's are not limited to the proximity of the Plasmon resonance, which extends the operational bandwidth of plasmonic devices [45]. Unexpected light propagation effects, like negative refraction have been reported in artificial media. Leveraging on the inter sub band resonance in hetero-structured semiconductor materials. We have showed that all possible optical regions, ranging from classical dielectric and metal to hyperbolic meta-materials, these are type 1 and type 2 was achieved. The negative refraction effect can occur at a designed frequency by controlling the electronic quantum confinement [46]. Optical resonant cavities play an important role in electromagnetic wave control; they confine electromagnetic wave and improve the interaction between light and matter [47]. Nanostructures with one-dimensional periodicity, such as multilayered structures, are currently in the focus of active research in the field of hyperbolic meta-materials and photonic topological structures. An efficient way to describe the material with sub wavelength periodicity is based on the concept of effective material parameters, which can be rigorously derived incorporating both local and non-local responses [48]. HMMs an unusual class of EM meta-materials has found important applications in various field of due to their distinctive properties. A surprising feature of HMMs was that even continuous HMMs can posses' topological edge modes [49].

Using finite length electric dipole, the far-field radiation was analyzed in the hyperbolic medium. To description for the arbitrary orientation of the dipole, the results were presented when the electric dipole and the optic axis are parallel to each other or when they are perpendicular to each other. Analytical as well as numerical results for both the ordinary and extra ordinary waves were presented [50]. The interface states with a high reflectance in photonic hetero structures composed of two kinds of all dielectric 1-D PCs with symmetric unit cells were achieved. The reflectance of interface states can be controlled flexibly by using the tuning the

mismatch degree between the imaginary phases of two types of 1-D PCs. The interface state of a high reflectance as well as a high Q-factor and the shifting Goos-Hanchen (GH) greatly enhanced to larger than three orders of wavelength [51]. The ability to control the directional and spectral properties of thermal emission has the fundamental importance for many applications. Here, a method to design the Directional and Broadband Thermal Emitters (DBTEs) and Directional and Narrowband Thermal Emitters (DNTEs) based on classic thermal emitters and angular selectors. DBTEs exhibited thermal emission at a specific angle and analyzed a broadband wavelength range [52].

After reviewing these research papers, we have proposed a new type of hyperbolic meta-material (HMM) composed with dielectric and plasma material. In this Chapter, we have analyzed the perpendicular and parallel permittivity of the considered hyperbolic meta-material with variation of filling fraction and electron collision frequency. Based on simple transfer matrix method, the absorption properties of ternary periodic structure are studied with the variation of incident angle, electron collision frequency of plasma, filling fraction and thickness of the dielectric material. Firstly, the absorption of ternary periodic structure against normalized frequency has been studied with variation of incident angles i.e. $\theta=0^0,\theta=20^0,\theta=40^0,\theta=60^0,\theta=80^0$. Then, the optical properties of the ternary periodic structure, especially absorption, have been studied by choosing other parameters filling fraction, electron collision frequency and thickness of dielectric of A material with keeping fixed incident angle $\theta = 80^0$. Such absorption property of the periodic structure is very important for designing the absorption-based devices like logic gate, electromagnetic switch, sensor, photodetector, and microwave absorber. We have also proposed to design the tunable absorber for microwave devices composed of the hyperbolic material at higher frequency range.

6.2 Theoretical model

The absorption spectra of one-dimensional ternary photonic crystal of dielectric, SiO_2 (Silicon dioxide), and hyperbolic metamaterials are calculated using a simple transfer matrix method and Bloch' function [53]. The hyperbolic material is the composite material of dielectric and metal. In this case, we consider the plasma based HMM, also the composite material of dielectric (air) and plasma-material [54]. One-

dimensional ternary periodic structure is taken as $(ABC)^N$, where N is the number of the periodicity; and A, B and C are the layer of dielectric (air), SiO_2 and hyperbolic material, respectively, as shown in Figure 6.1.

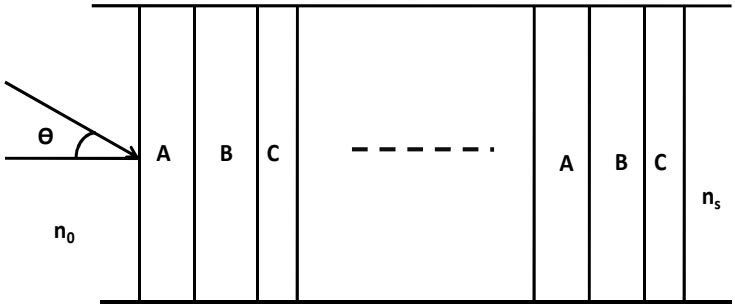

Figure 6.1: Schematic diagram of one-dimensional dielectric, silicon dioxide, and hyperbolic material ternary periodic structure

The dielectric permittivity and magnetic permeability of dielectric (air) and silicon dioxide material are taken as; $\varepsilon_{die} = \mu_{die} = 1$, and $\varepsilon_{SiO_2} = 2.2, \mu_{SiO_2} = 1$. However, the hyperbolic material is a composite of dielectric and plasma material and the complex permittivity of plasma is taken from Ref. [39];

6.2.1 Optics of metals and dielectrics

The interactions between metals and electromagnetic wave are firstly determined by the collective movements of free electrons. The electrons are not found in any particular nucleus, which are considered to move about freely around the metal lattice in the absense of a restoring force. Using Drude and Lorentz model for free electron motion, the equation of motion for a free electron in an alternating electric field is described by;

$$m_e \frac{d^2 r}{dt^2} + m_e \gamma \frac{dr}{dt} = -q_e E_0 e^{-i\omega t} \tag{6.1}$$

where q_e, is the electric charge of free electron, the damping coefficient γ is proportional to the Fermi velocity $\gamma = \frac{v}{l} = \frac{1}{\tau}$, where v denotes the Fermi velocity and l is the mean free path of an electron of successive collisions. The relaxation time τ is the averaged interval time subsequent collision of an electron. In general, the relaxation time is about 10^{-14} second.

The solution of instantaneous in Eq. (6.1) for a monochromatic electric field is solved to be-

$$r(\omega)=\frac{N_e q_e^2}{m_e\left(\omega^2+i\gamma\omega\right)}E(\omega) \tag{6.2}$$

The polarization density is the total dipole moment per unit volume. The gross polarization of all of the elctrons in the unit volume is-

$$P=N\times q_e\times r(\omega)=\frac{N_e q_e^2}{m_e\left(\omega^2+i\gamma\omega\right)}E(\omega) \tag{6.3}$$

The polarization of a dipole moment cause the electric charge timing distance to deviate from its balanced position. The gross polarization of the whole elctrons in unit volume is-

$$P=N\times q_e\times r(\omega)=\frac{N_e q_e^2}{m_e\left(\omega_0^2-\omega^2-i\gamma\omega\right)}E(\omega) \tag{6.4}$$

where N_e is the electron density per unit volume. The induced dielectric polarization density is proportional to an electric field by the constant electric susceptibility is-

$$P=\varepsilon_0\chi_e E(\omega)=\varepsilon_0(\varepsilon_r-1)E(\omega) \tag{6.5}$$

Comparing Eq. (6.3) & Eq. (6.5)

$$\varepsilon_0(\varepsilon_r-1)=\frac{N_e q_e^2}{m_e\left(\omega^2+i\gamma\omega\right)} \quad \approx \quad (\varepsilon_r-1)=\frac{N_e q_e^2}{m_e\varepsilon_0\left(\omega^2+i\gamma\omega\right)}\approx\varepsilon(\omega)=1-\frac{\omega_p^2}{\left(\omega^2+i\gamma\omega\right)}.$$ On simplification, we get;

$$\varepsilon_{plasma}(\omega)=1-\frac{\omega_p^2}{\omega\left(\left(\omega+\frac{i\gamma}{\omega}\right)\right)} \tag{6.6}$$

where ω and γ is the angular frequency and effective collision frequency, respectively. For non-magnetic material, the magnetic permeabilityis one i.e. μ_{plasma}=1. Here, ω_p is the plasma frequency of bulk media, which is given as [55, 56];

$$\omega_p=\left(\frac{n_e e^2}{m\varepsilon_0}\right)^{1/2} \tag{6.7}$$

The optics of the metals is dependent on three frequencies: collision frequency, plasma frequency and incident frequency. If the collision frequency is zero then optics of metals are dependent on plasma frequency and incident frequency only. At the plasma frequency is equal to incident frequency, the optics of electromagnetic response of a material changes from the metallic behavior to those of dielectric material. At the below plasma frequency, the optics of a medium exhibits a metal like behavior. However, operating frequency is greater than plasma frequency, the optics of medium looks more like the dielectric media.

Now, we will discuss about the optics of the hyperbolic materials. The concept of hyperbolic behavior in the material originates from the optics of crystals. In such media, the constitutive relations of the electric displacement, **D,** and the magnetic induction, **B,** to the electric and the magnetic fields **E** and **H** can be written as;

$$\overline{D} = \varepsilon_0 \overline{\overline{\varepsilon}} \overline{E} \tag{6.8}$$

$$\overline{B} = \mu_0 \overline{\overline{\mu}} \overline{H} \tag{6.9}$$

where ε_0, μ_0 are the electric permittivity and magnetic permeability in vacuum and $\overline{\overline{\varepsilon}}$, $\overline{\overline{\mu}}$ are relative permittivity and relative permeability tensors. For non magnetic media, $\overline{\overline{\mu}}$ simply reduces to the unit tensor. Upon diagonalization of the electric permittivity, $\overline{\overline{\varepsilon}}$ assumes the form of dielectric tensor. The hyperbolic material is an anisotropic medium with uniaxial dielectric tensor components that are approximated as follows [18];

$$\overline{\overline{\varepsilon}} = \begin{bmatrix} \varepsilon_{xx} & 0 & 0 \\ 0 & \varepsilon_{yy} & 0 \\ 0 & 0 & \varepsilon_{zz} \end{bmatrix} \tag{6.10}$$

In a Cartesian frame of reference, the orientation direction along to the axis of crystal, so it is called principal axes of the crystal. The three diagonal components are all positive and in general it depend on the angular frequency ω; they are the termed as (i) Biaxial, when $\varepsilon_{xx} \neq \varepsilon_{yy} \neq \varepsilon_{zz}$, (ii) Uniaxial, when $\varepsilon_{xx} = \varepsilon_{yy} \neq \varepsilon_{zz}$ and (iii) Isotropic, when $\varepsilon_{xx} = \varepsilon_{yy} = \varepsilon_{zz}$.

To determine the dispersion relation of light in a medium described by Eq. (6.10), we consider the following two Maxwell's equations in the absence of source:

$$\nabla \times \mathrm{E} = -\frac{\partial \mathrm{B}}{\partial \mathrm{t}} \tag{6.11}$$

$$\nabla \times \mathrm{H} = \frac{\partial \mathrm{D}}{\partial \mathrm{t}} \tag{6.12}$$

where **D** and **B** are as in the Eq. (6.8) and Eq. (6.9), respectively. The plane wave expressions for both fields can be given by $\mathrm{E} = \mathrm{E}_0 \mathrm{e}^{\mathrm{i}(\omega t - \mathrm{k}.\mathrm{r})}$ and $\mathrm{H} = \mathrm{H}_0 \mathrm{e}^{\mathrm{i}(\omega t - \mathrm{k}.\mathrm{r})}$, where k is wave vector. By inserting the **D** and **B** in the Eq. (6.11) & Eq. (6.12), we obtain;

$$\mathrm{k} \times \mathrm{E} = \omega \mu_0 \mathrm{H} \tag{6.13}$$

$$\mathrm{k} \times \mathrm{H} = -\omega \varepsilon_0 \overline{\overline{\varepsilon}} \mathrm{E} \tag{6.14}$$

By taking curl of the k and substitution of Eq. (6.13) into Eq. (6.14), the Eigen value problem of electric field;

$$\vec{\mathrm{k}} \times \left(\vec{\mathrm{k}} \times \vec{\mathrm{E}} \right) + \omega^2 \mu_0 \varepsilon_0 \overline{\overline{\varepsilon}} \vec{\mathrm{E}} = 0 \tag{6.15}$$

This can be simplified in the matrix form; and it is also called the dispersion relation;

$$\begin{pmatrix} \mathrm{k}_0^2 \varepsilon_{xx} - \mathrm{k}_y^2 - \mathrm{k}_z^2 & \mathrm{k}_x \mathrm{k}_y & \mathrm{k}_x \mathrm{k}_z \\ \mathrm{k}_x \mathrm{k}_{yz} & \mathrm{k}_0^2 \varepsilon_{yy} - \mathrm{k}_x^2 - \mathrm{k}_y^2 & \mathrm{k}_y \mathrm{k}_z \\ \mathrm{k}_x \mathrm{k}_z & \mathrm{k}_y \mathrm{k}_z & \mathrm{k}_0^2 \varepsilon_{zz} - \mathrm{k}_x^2 - \mathrm{k}_y^2 \end{pmatrix} \begin{pmatrix} \mathrm{E}_x \\ \mathrm{E}_x \\ \mathrm{E}_x \end{pmatrix} = 0 \tag{6.16}$$

where $\mathrm{k} = \frac{\omega}{\mathrm{c}}$ are the magnitude of wave vector and $c = \frac{1}{\sqrt[2]{\varepsilon_0 \mu_0}}$ the speed of light in vacuum. We now focus on the hyperbolic media with optical axis oriented along the z direction, $\varepsilon_{xx} = \varepsilon_{yy} = \varepsilon_\perp$ and $\mathrm{k}_\perp = \sqrt{\mathrm{k}_x^2 + \mathrm{k}_y^2}$. The imposition of non-trivial solution to Eq. (6.16) leads to the dispersion relation for the hyperbolic media [18]:

$$\left(\mathrm{k}_\perp^2 + \mathrm{k}_z^2 - \varepsilon_\perp \mathrm{k}_0^2 \right) \left(\frac{\mathrm{k}_\perp^2}{\varepsilon_{zz}} + \frac{\mathrm{k}_z^2}{\varepsilon_\perp} - \mathrm{k}_0^2 \right) = 0 \tag{6.17}$$

In the above Eq. (6.17) have two terms, one of them equal to zero and correspond to spherical behavior and an ellipsoidal iso-frequency surface in the k-space, the first term describes the wave polarized the xy-plane (ordinary or TE waves); second terms

correspond to the wave polarized in the plane containing the optical axis (extraordinary waves or TM waves).

The condition changes substantially if we assume an extreme anisotropy, namely when one between $\varepsilon_{\perp}$ and ε_{zz} is negative. Media with such an optical signature are termed an indefinite from the point of view of mathematics [57], since their permittivity tensor represents an indefinite non-degenerate quadratic form, and exhibits a number of unconventional properties. Permittivity components with an opposite sign result in hyperbolical iso-frequency surface for the extraordinary polarization and hence the physical denomination hyperbolic material. As consequences, waves with arbitrarily large wave vector retain a propagating nature while in isotropic materials they become evanescent due to the bounded iso-frequency contour [58]. The choice $\varepsilon_{\perp}>0$, $\varepsilon_{zz}<0$ correspond to a twofold hyperboloid, and the hyperbolic medium is called dielectric (with reference its behavior in xy-plane) [59] or Type I(metallic); [60] the choice $\varepsilon_{\perp}<0$ and $\varepsilon_{zz}>0$ describes a one fold hyperboloid, namely a metallic or Type II (dielectric)medium.

In our calculation, we have considered $\varepsilon_{xx}=\varepsilon_{\perp}$, $\varepsilon_{yy}=\varepsilon_{zz}=\varepsilon_{\parallel}$, $\varepsilon_{\parallel}$ and $\varepsilon_{\perp}$ are the parallel and perpendicular component of relative permittivity, respectively, which can be calculated by effective medium theory. So, $\varepsilon_{\parallel}$ and $\varepsilon_{\perp}$ can be approximated as [61];

$$\varepsilon_{\parallel}=\frac{\varepsilon_{die}\varepsilon_{plasma}\left(d_{die}+d_{plasma}\right)}{\varepsilon_{die}d_{plasma}+\varepsilon_{plasma}d_{die}} \tag{6.18}$$

$$\varepsilon_{\perp}=\frac{d_{die}\varepsilon_{die}+d_{plasma}\varepsilon_{plasma}}{d_{die}+d_{plasma}} \tag{6.19}$$

where d_{die}, d_{plasma} are the thicknesses of considered dielectric and plasma material, respectively and ε_{die} and ε_{plasma} are the electric permittivity of considered dielectric material and plasma material, respectively. The filling fraction $f=\frac{d_{plasma}}{d_{HM}}$ is the volume percentage of plasma in a unit cell or period, dielectric layer and a plasma layer with thickness d_{die} and d_{plasma} and permittivity's ε_{die} and ε_{plasma}.

For the Transverse Magnetic (TM) wave propagation in the periodic structure, the spatial dispersive curve can be performed as;

$$\frac{k_{zz}^2}{\varepsilon_{xx}} + \frac{k_{xx}^2}{\varepsilon_{zz}} = k_0^2 \tag{6.20}$$

The product of perpendicular and parallel permittivity is less than zero it always shows the dispersive curve is hyperbolic behavior $(\varepsilon_\perp \varepsilon_\parallel < 0)$,and the product of perpendicular and parallel permittivity is greater than zero, the dispersive curve is shown elliptical $(\varepsilon_\perp \varepsilon_\parallel > 0)$ [62, 63].

The characteristic matrix of then one-dimensional ternary periodic structure i.e. $(ABC)^N$ is expressed as [53]

$$M(d) = \begin{pmatrix} m_{11} & m_{12} \\ m_{21} & m_{22} \end{pmatrix} \tag{6.21}$$

where $M(d) = (M_A M_B M_C)^N$; N is the number of unit cell, M_A, M_B, and M_C are the characteristics matrices of layers dielectric (A), silicon dioxide (B), and hyperbolic material (C), respectively.

The characteristic matrix M_i for each layer of the periodicity of the ternary structure is calculated for the Transverse Magnetic (TM) wave at the angle of incidence (θ_0) from vacuum to a one-dimensional Photonic Crystal (PC) structure [53].

$$M_i = \begin{bmatrix} \cos\gamma_i & -\frac{i}{p_i}\sin\gamma_i \\ -ip_i \sin\gamma_i & \cos\gamma_i \end{bmatrix} \tag{6.22}$$

where $\gamma_i = \left(\frac{\omega}{c}\right) n_i d_i \cos\theta_i$, c are the speed of light in vacuum, θ_i is the ray angle inside i^{th} layer with the refractive index as, $n_i = \sqrt{\mu_i \varepsilon_i}$, $p_i = \sqrt{\frac{\mu_i}{\varepsilon_i}}\cos\theta_i$ and $\cos\theta_i = \sqrt{1 - \frac{n_0^2 \sin^2\theta_0}{n_i^2}}$ in which n_0 is the refractive index of air, where the incidence wave tends to enter the structure.

The characteristic matrix of each layer can be obtained by considering the electric field on each surface. For ternary periodic structure, we have considered three layers in the x-direction. The electric field distribution in each interface is given by;

$$\vec{E} = \begin{cases} (\overrightarrow{E_1} e^{i\overrightarrow{k_1}.\vec{r}} + \overrightarrow{E_1}' e^{-i\overrightarrow{k_1}'.\vec{r}}) e^{i\omega t}, -d_A < x < 0; \\ (\overrightarrow{E_2} e^{i\overrightarrow{k_2}.\vec{r}} + \overrightarrow{E_2}' e^{-i\overrightarrow{k_2}'.\vec{r}}) e^{i\omega t}, \ 0 < x < d_B; \\ (\overrightarrow{E_3} e^{i\overrightarrow{k_3}.\vec{r}} + \overrightarrow{E_3}' e^{-i\overrightarrow{k_3}'.\vec{r}}) e^{i\omega t}, \ d_B < x < d_{B+C}; \end{cases} \tag{6.23}$$

where k_1, k_2, and k_3 are the propagation wave vector corresponding to the dielectric, silicon dioxide and hyperbolic material respectively with the above boundary conditions. By using Maxwell's equations, we obtain the corresponding magnetic field. The electric and magnetic field may use to the formulation of the Eq. (18) at each interface.

The transmission coefficient of the ternary photonic crystal is calculated by,

$$t = \left| \frac{2}{(m_{11} + \frac{m_{12}}{p_0}) + (m_{21} p_0 + m_{22})} \right| \tag{6.24}$$

where $p_0 = n_0 \cos\theta_0$ and $p_s = n_s \cos\theta_s$, n_s is the refractive index of the substrate, θ_0 is the ray angle.

The transmission spectra of the ternary photonic crystal are given by [53],

$$T = \left(\frac{p_s}{p_0} \right) |t|^2 \tag{6.25}$$

The reflection coefficient of the one-dimensional ternary periodic structure containing dielectric, silicon dioxide, and hyperbolic material is calculated by:

$$r = \left| \frac{m_{11} + \frac{m_{12}}{p_0} - m_{21} p_0 - m_{22}}{(m_{11} + \frac{m_{12}}{p_0}) + (m_{21} p_0 + m_{22})} \right| \tag{6.26}$$

where $p_0 = n_0 \cos\theta_0$ and $p_s = n_s \cos\theta_s$, n_s is the refractive index of the air, whose ray angle is θ_i. The reflection spectra or reflectance of the one-dimensional photonic crystal containing dielectric, silicon dioxide, and hyperbolic material is given by:

$$R = |r|^2 \tag{6.27}$$

The absorption spectra of the one-dimensional ternary periodic structure of dielectric, silicon dioxide, and hyperbolic material are calculated by the equation:

$$A = 1 - R - T \tag{6.28}$$

6.3 Results and discussion

In this Chapter, we first discuss about the optical constant of the hyperbolic meta-material, and then optical property of the ternary periodic structure. The perpendicular and parallel permittivity of hyperbolic meta-material against normalized frequency $\left(\frac{\omega}{\omega_p}\right)$ is theoretically analyzed by varying filling fraction, electron collision frequency using Eq. (6.18) & Eq. (6.19). As we discussed earlier that hyperbolic material has specific property like filling fraction $\left(f = \frac{d_{plasma}}{d_{HM}}\right)$ due to the property of composite materials of dielectric and plasma and the electric permittivity of the HMM is an anisotropic property.

The material C is a hyperbolic meta-material (HMM) in our ternary periodic structure which is composed with two materials of plasma and air dielectric [64, 65]. The HMM has $d_{HM} = d_{plasma} + d_{die(air)} = 2mm$ and $f = \frac{d_{plasma}}{d_{HM}}$ with a thickness of the plasma material $d_{plasma} = 0.2mm$, plasma frequency $\omega_p = 28.4 \times 10^9$. The dielectric of the air is $\varepsilon_{die(air)} = \mu_{die(air)} = 1$. The permittivity of hyperbolic material varies along perpendicular and parallel directions, studied using Eq. (6.18) & Eq. (6.19). As we know that the hyperbolic material property is purely depending upon the dispersion relation of relative permittivity. By study the dispersion relation shows that the product of perpendicular and parallel permittivity is less than zero then the dispersive curve shows the hyperbolic behavior having the metallic behavior $(\varepsilon_\perp \varepsilon_\parallel < 0)$. On the other hand, the dispersion relation shows that the product of perpendicular and parallel permittivity obtains greater than zero; the dispersive curve shows dielectric behavior $(\varepsilon_\perp \varepsilon_\parallel > 0)$. We plot the relative permittivity against normalized frequency that shows hyperbolic behavior for parallel and perpendicular permittivity in a particular range of the frequency.

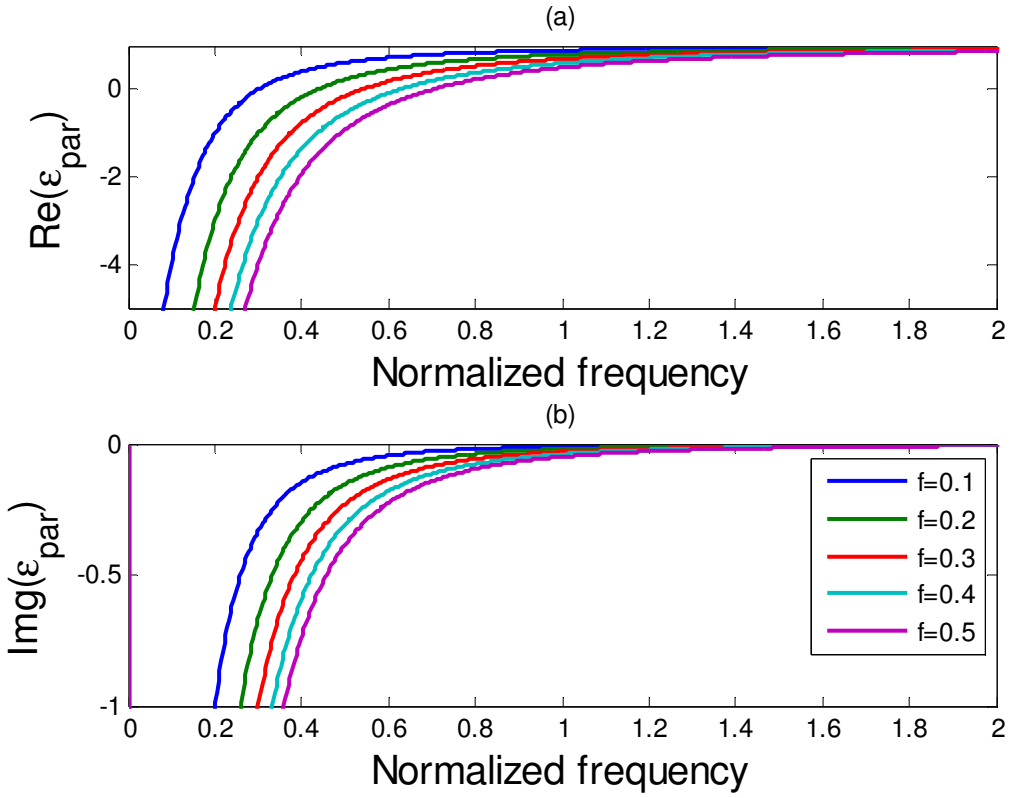

Figure 6.2: (a) Real part of $\varepsilon_{\parallel}$ for different value of filling fraction against normalized frequency, (b) Imaginary part of $\varepsilon_{\parallel}$ for different value of filling fraction versus normalized frequency

The real and the imaginary part of parallel permittivity of hyperbolic material are plotted using Eq. (6.18), which are shown in Figure 6.2 and analyzed. The real part of parallel permittivity against normalized frequency increases on increasing the value of filling fraction. The value of permittivity is negative at a certain range of frequency after that it is positive corresponding to the value of filling fraction. The real part of parallel permittivity is obtained the negative at a certain normalized frequency 0.30, 0.43, 0.55, 0.63, 0.71 for corresponding to the value of filling fraction $f = 0.1, f = 0.2, f = 0.3, f = 0.4, f = 0.5$ respectively, as shown in Figure 6.2 (a). Similarly, the imaginary part of parallel permittivity has found the same behavior but it has purely negative value and is also shifted towards the higher frequency on increase the value of filling fraction comparison to real permittivity. The imaginary part of parallel permittivity is negative at a certain normalized frequency 0.51, 0.63, 0.72, 0.82, 0.88 for corresponding to the value of filling fraction $f = 0.1, f = 0.2, f = 0.3, f = 0.4, f = 0.5$ respectively, as shown in Figure 6.2 (b). The real and the imaginary part of

perpendicular permittivity of hyperbolic material have plotted using Eq. (6.19), which is shown in Figure 3 and analyzed. The real part of perpendicular permittivity decreases on increase the value of filling fraction, and finds the blue shift. The real part of perpendicular permittivity is negative at a certain normalized frequency range 0.26-1.00, 0.43-1.00, 0.48-1.00, 0.62-1.00, 0.66-1.00 for the value of filling fraction $f = 0.1, f = 0.2, f = 0.3, f = 0.4, f = 0.5$ respectively, as shown in Figure 6.3 (a). Moreover, the imaginary part of the perpendicular permittivity shifts towards higher frequency on increases the value of filling fraction. The imaginary part of perpendicular permittivity is negative at a certain normalized frequency range 0.00-1.00, 0.02-1.00, 0.04-1.00, 0.06-1.00, 0.07-1.00 for the value of filling fraction $f = 0.1, f = 0.2, f = 0.3, f = 0.4, f = 0.5$ respectively, as shown in Figure 6.3 (b).

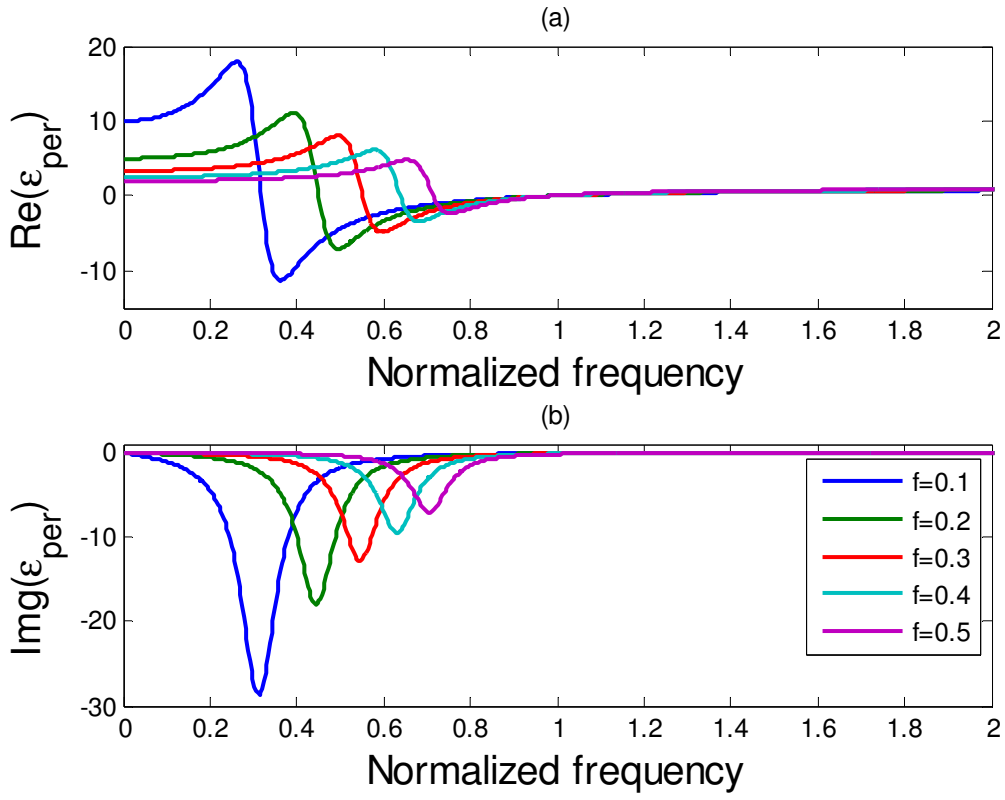

Figure 6.3: (a) Real part of $\varepsilon_{\perp}$ for different value of filling fraction against normalized frequency, (b) Imaginary part of $\varepsilon_{\perp}$ for different value of filling fraction against normalized frequency

Further, we have analyzed the real and the imaginary part of parallel permittivity against normalized frequency with the variation of electron collision frequency. The real part of parallel permittivity is decreased on increasing normalized frequency; it is

also found the blue shift. The real part of parallel permittivity is negative at a certain normalized frequency 0.30, 0.24, 0.10 for corresponding to the value of electron collision frequency $\gamma=0.1\omega_p, \gamma=0.2\omega_p, \gamma=0.3\omega_p$ as shown in Figure 6.4 (a). The imaginary part of parallel permittivity is decreased on increasing the value of electron collision frequency and is shown blue shift. The imaginary part of parallel permittivity is negative at a certain normalized frequency 0.75, 0.95, 1.05 for different electron collision frequency $\gamma=0.1\omega_p, \gamma=0.2\omega_p, \gamma=0.3\omega_p$ respectively, as shown in Figure 6.4 (b).

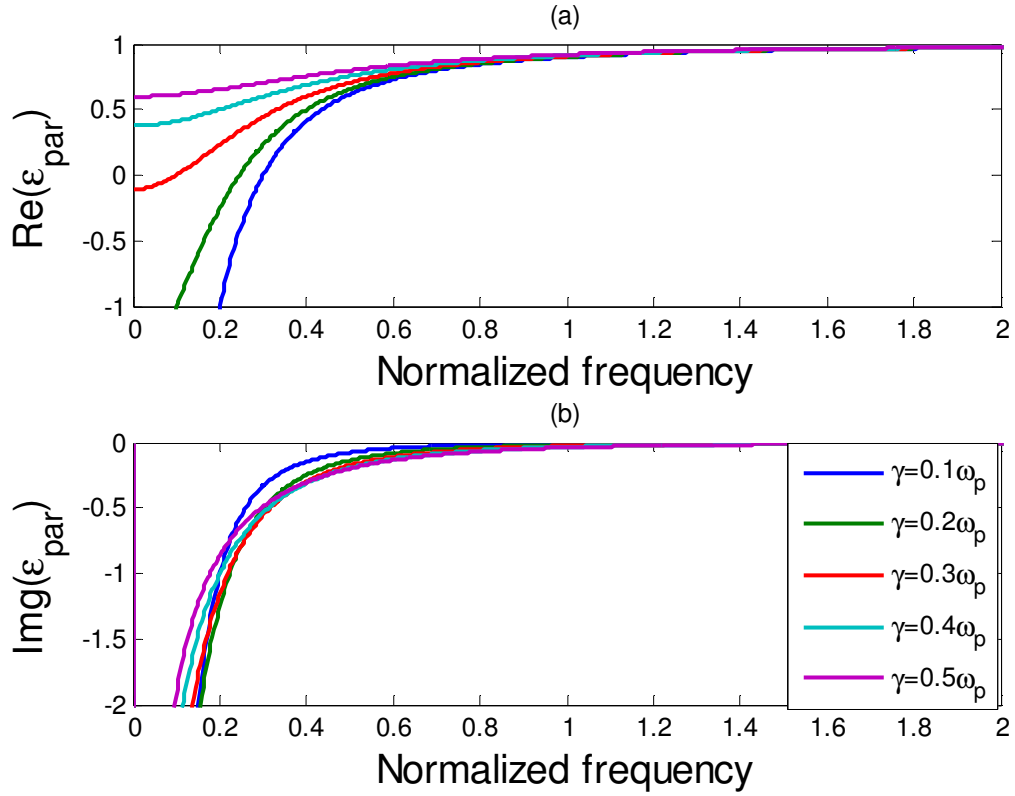

Figure 6.4: (a) Real part of $\varepsilon_{\parallel}$ for different value of electron collision frequency, γ against normalized frequency**,** (b) Imaginary part of $\varepsilon_{\parallel}$ for different value of electron collision frequency, γ against normalized frequency

In last calculation, the real and the imaginary part of perpendicular permittivity with variation of electron collision frequency are analyzed as shown in Figure 6.5. The real part of perpendicular permittivity decreases on increase electron collision frequency; it also behaves as a blue shift. The real part of perpendicular permittivity is negative at a certain normalized frequency 1.10, 0.99, 0.96, 0.91, 0.85 for the value of electron

collision frequency $\gamma = 0.1\omega_p, \gamma = 0.2\omega_p, \gamma = 0.3\omega_p, \gamma = 0.4\omega_p, \gamma = 0.5\omega_p$, respectively, as shown in Figure 6.5(a). The imaginary part of the permittivity increases on increasing the value of electron collision frequency it shows the red shift. The imaginary part of perpendicular permittivity is negative at a certain normalized frequency 0.99, 1.21, 1.35, 1.50, 1.60 for corresponding to the value of electron collision frequency $\gamma = 0.1\omega_p, \gamma = 0.2\omega_p, \gamma = 0.3\omega_p, \gamma = 0.4\omega_p, \gamma = 0.5\omega_p$, respectively, as shown in Figure 6.5 (b). These studies show that the perpendicular and the parallel permittivity of the considered material play the main role for the hyperbolic behavior because the permittivity affects the dispersion relation of the material.

Therefore, the absorption property of the ternary periodic structure containing HMMs against normalized frequency is studied for TM mode for corresponds to the parallel permittivity. The absorption property of the ternary periodic structure is calculated using simple transfer matrix method with variation of incident angle, filling fraction, electron collision frequency as well as the thicknesses of dielectric (A) material. The ternary periodic structure is the composite material of the three materials ABC, where A=air, $B = SiO_2$ and C=Hyperbolic Meta-material (HMM). The parameters for dielectric (A) and SiO_2 (B) materials are taken as $\varepsilon_{die} = 1, d_{die} = 2.8\text{mm}$, $\varepsilon_{SiO_2} = 2.2$, $d_{SiO_2} = 3\text{mm}, \mu_{die} = \mu_{SiO_2} = 1, \theta_0 = 0^o$, and number of unit cell i.e. N=10.

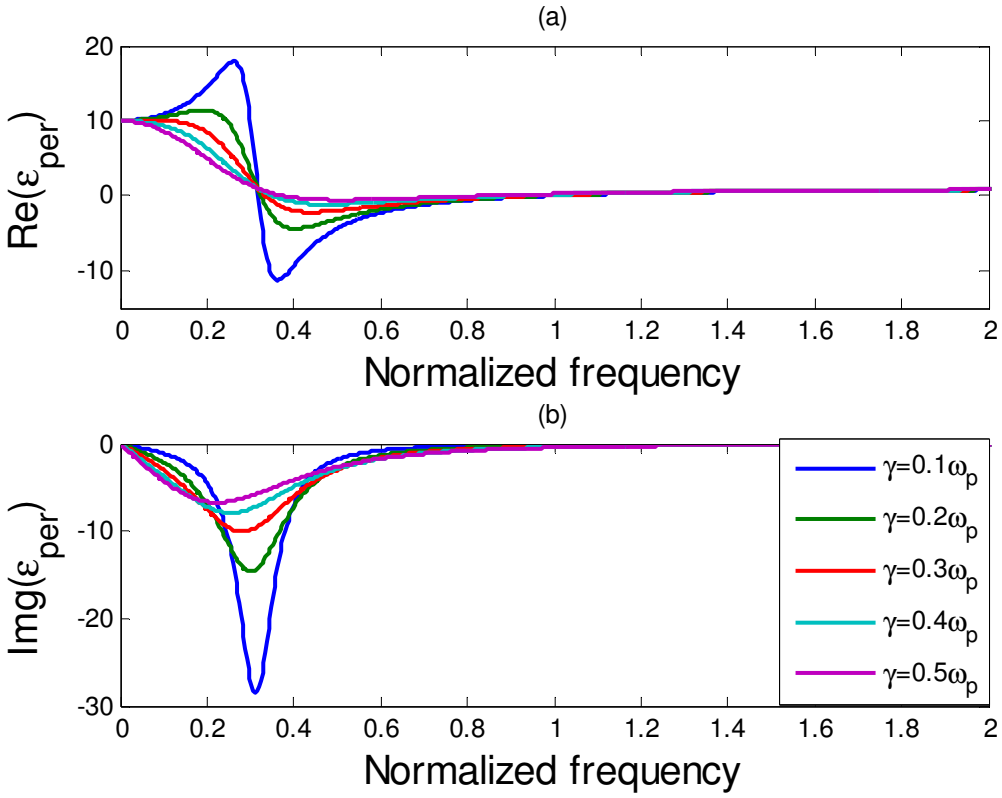

Figure 6.5: (a) Real part of $\varepsilon_{\perp}$ for different value of electron collision frequency, γ against normalized frequency, (b) Imaginary part of $\varepsilon_{\perp}$ for different value of electron collision frequency, γ against normalized frequency

First of all, we have calculated the absorption of the ternary periodic structure against normalized frequency with varying the incident angles $\theta=0^0,\theta=20^0,\theta=40^0,\theta=60^0,\theta=80^0$ having electron collision frequency $\gamma=0.1\omega_p$ and filling fraction (f=0.1) where normalized frequency is $\left(\frac{\omega}{\omega_p}\right)$. The wave incident on the multilayer structure is originated the band structure due to the fundamental property of the interfaces. So, we have obtained the increase absorptionspectra against normalized frequencywhen the incident angle increases, and it is achieved the maximum absorption at 0.14 normalized frequencies due to effective behavior of relative permittivity. The absorption spectra continuously decrease above the 0.15 normalized frequencies due to the multi-reflection inside the interfaces. Above this frequency, the absorption band gaps are formed between 1.0-1.5 normalized frequency ranges. The study shows that the absorption of the considered structure has obtained the better absorption for $\theta = 80^0$ as shown in Figure 6.6.

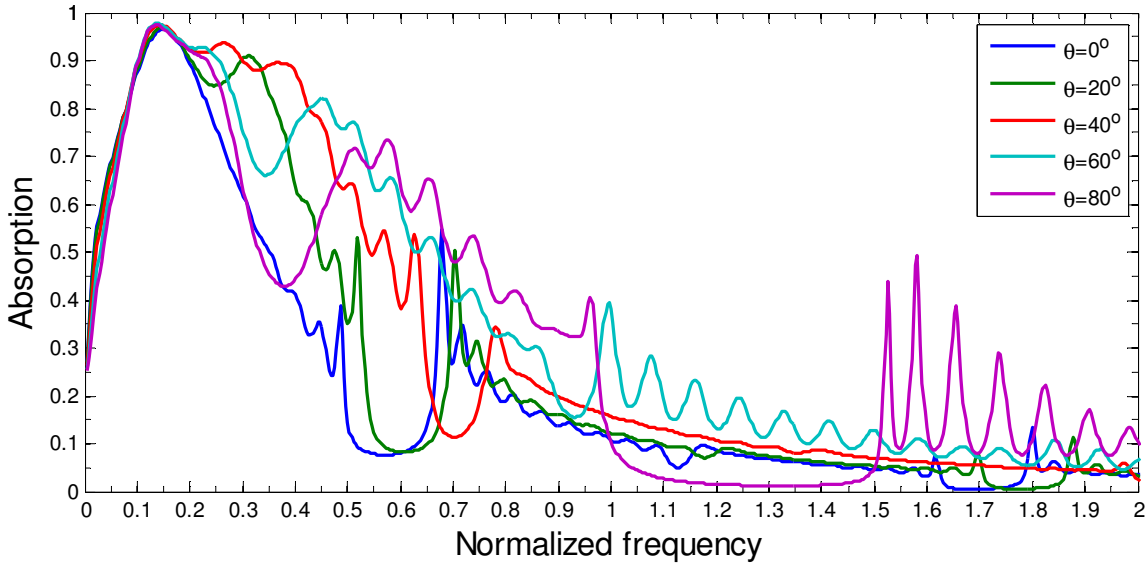

Figure 6.6: Absorption of multilayer structure at different value of incident angle against normalized frequency

Now we have focused our study on the absorption of the ternary periodic structure at the angle of incidence $\theta = 80^0$ by varying the most valuable parameters: filling fraction, electron collision frequency and thickness of dielectric material. The filling fraction (f) is an important parameter which defines how much volume of the material occupied in the hyperbolic meta-material. So, we have analyzed the absorption of the ternary periodic structure against normalized frequency at $\theta = 80^0$ with variation of filling fraction $f = 0.1, f = 0.2, f = 0.3, f = 0.4, f = 0.5$ with constant parameters: collision frequency $\gamma = 0.1\omega_p$ and thickness of the dielectric $d_{die} = 2.8\text{mm}$, and silicon dioxide $d_{SiO_2} = 3\text{mm}$, and hyperbolic meta-material $d_{HM} = d_{plasma} + d_{die(air)} = 2\text{mm}$, respectively. The absorption spectra shifts from lower to higher frequency, and obtain the maximum absorption on increase the value of filling fraction. The 100% absorption is found at 0.19 normalized frequencies for $f = 0.2$ has metallic behavior, and also shows red shift. After that the absorption spectra for the normalized frequency continuously decrease for the different values of filling fraction. The absorption spectra again shift toward lower to the higher frequency as the filling fraction increases. The 90% absorption is found for $f = 0.5$ due to highly metallic behavior and also obtained an absorption band in 1.00-1.50 range as shown in Figure 6.7. The study shows that the absorption of the structure containing HMMs has very informative results for designing the absorption-based devices in microwave region.

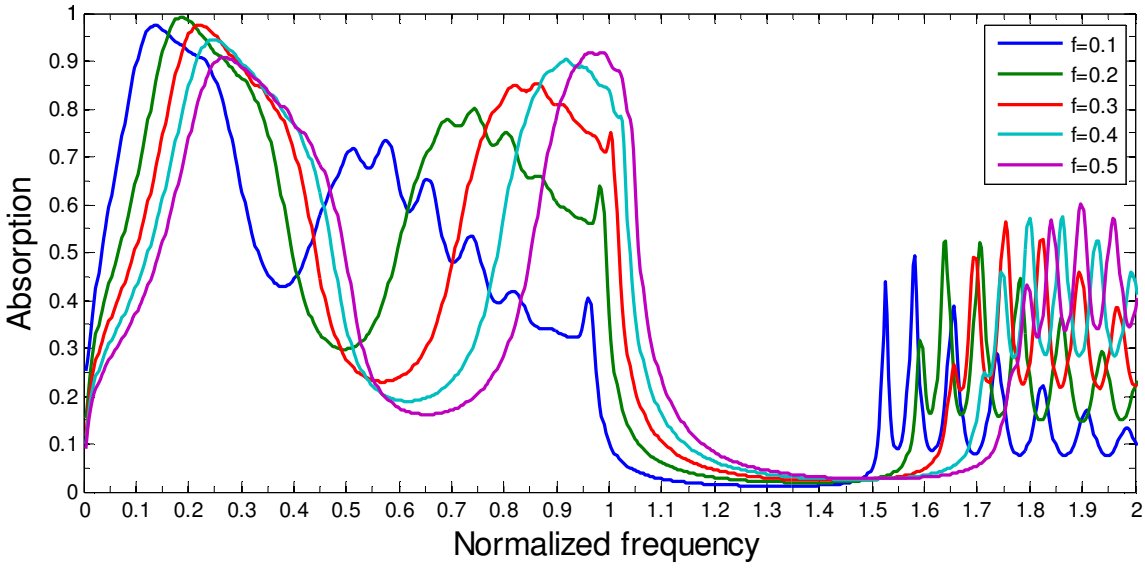

Figure 6.7: Absorption of multilayer structure at different value of filling fraction against normalized frequency

Similarly, we have also studied the absorption of the structure by variation of the electron collision frequency $\gamma = 0.1\omega_p, \gamma = 0.2\omega_p, \gamma = 0.3\omega_p, \gamma = 0.4\omega_p, \gamma = 0.5\omega_p$, with $f = 0.1$ and $\theta = 80^0$ having other parameters constant as in the above section. The absorption spectra against normalized frequency shift towards the higher normalized frequency for increase the value of electron collision frequency, but the 98% absorption found at 0.13 normalized frequencies for $\gamma = 0.1\omega_p$. The 80% absorption is achieved for $\gamma = 0.5\omega_p$ due to high absorption of the plasma that shows the metallic behavior of the HMMs. Further, the absorption spectra have found nearly zero absorption at 1.0-1.5 normalized frequency and formed an absorption band with large variation of band edges.

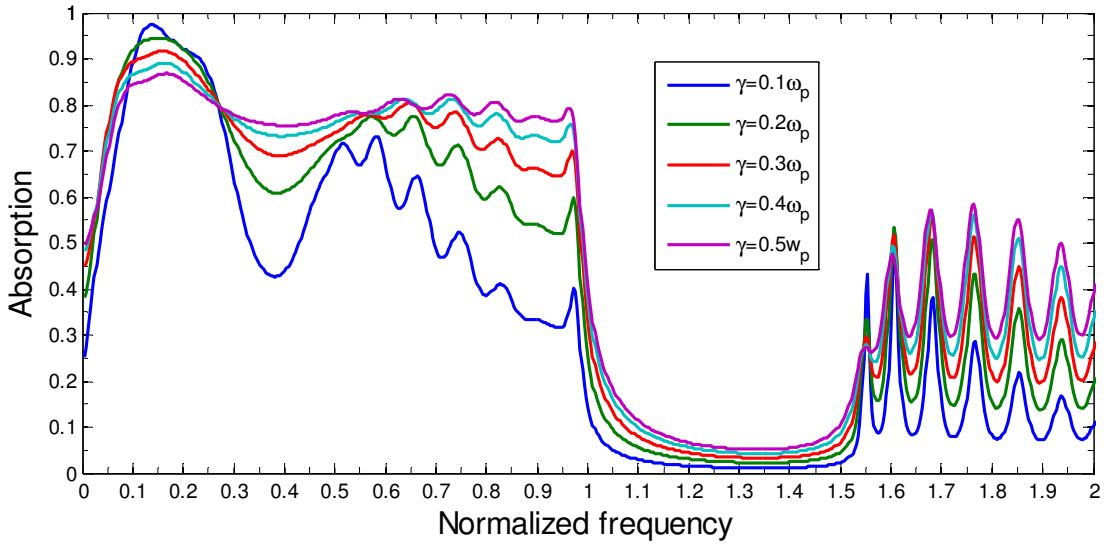

Figure 6.8: Absorption of multilayer structure at a different value of collision frequency against normalized frequency

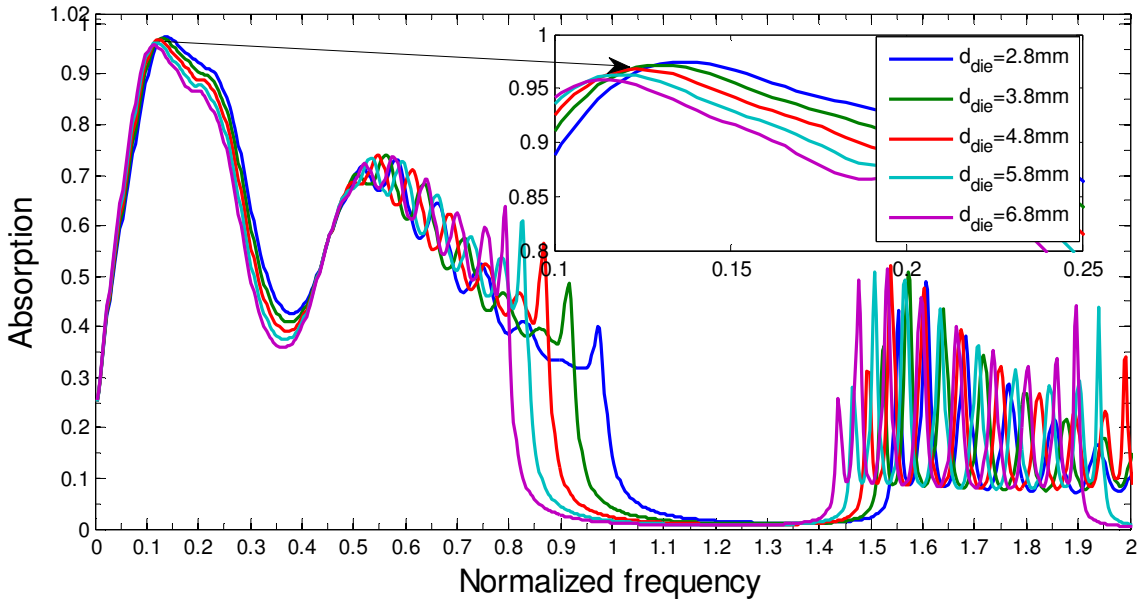

Figure 6.9: Absorption of multilayer structure at different value of the thickness of the dielectric material against normalized frequency

After this band range, the absorption is slightly increased as the value of electron collision frequency increases. The absolutely zero absorption band gaps are formed for $\gamma = 0.1\omega_p$ having maximum absorption at 1.40 as shown in Figure 6.8. We conclude that the absorption of the structure may be used to design the sensor as well as detector at low frequency range, and tunable absorber at band edges at high frequency range.

Again we have focused on another parameter that is thickness of A material. As we know that thickness of the dielectric (A) material of the periodic material affects the band gap structure. The absorption of the ternary periodic structure against normalized frequency is studied with variation of thickness of dielectric material $d_{die} = 2.8mm$ $d_{die} = 3.8mm$ $d_{die} = 4.8mm$ $d_{die} = 5.8mm$ $d_{die} = 6.8mm$ with fixed $\theta = 80^0$, $\gamma = 0.1\omega_p$ and $f = 0.1$. The absorption spectra of ternary periodic structure against normalized frequency shift from higher to lower normalized frequency as thickness increases and acts as the blue shift. The 98% absorption is achieved at 0.13 normalized frequencies for lowest value of dielectric thickness, which is predicted from Figure 6.9. The maximum absorption shifts from higher frequency to lower frequency on increase the thickness of dielectric material which clearly shown in the inset plot corresponding to the value of dielectric thickness $d_{die} = 2.8mm$ $d_{die} = 3.8mm$ $d_{die} = 4.8mm$ $d_{die} = 5.8mm$ $d_{die} = 6.8mm$. The absorption decreases continuously and become 40% absorption for $d_{die} = 6.8mm$. The absorption spectra for above 0.4 normalized frequencies increases and absorption becomes 0.75%. The absorption spectra continuously decrease above 0.5 frequencies, and form a band gap in between the frequency range of 0.85-1.55 as shown in Figure 6.9. Such absorption with variation of the thickness of dielectric may be applicable for absorption-based devices at microwave region.

In the last calculations, we have compared our calculated results of absorption of ternary periodic structure with binary periodic structure containing HMMs for $\theta = 80^0$ $\gamma = 0.1\omega_p$ and $f = 0.1$, having other parameters are same as previous calculations, which is shown in Figure 6.10. The binary structure is $(BC)^N$ where, $B = SiO_2$, $C = HMM$ and the ternary structure is $(ABC)^N$ where $A = Dielectric\,(air)$ $B = SiO_2$ and $C = HMM$. We have analyzed that the absorption for both structures, and obtained the same absorption at low frequency range and a band gap is obtained only for ternary periodic structure at higher frequency range. So our calculated results reveal that the absorption of ternary periodic structure is found better result than the absorption of binary periodic structure for low to high frequency ranges.

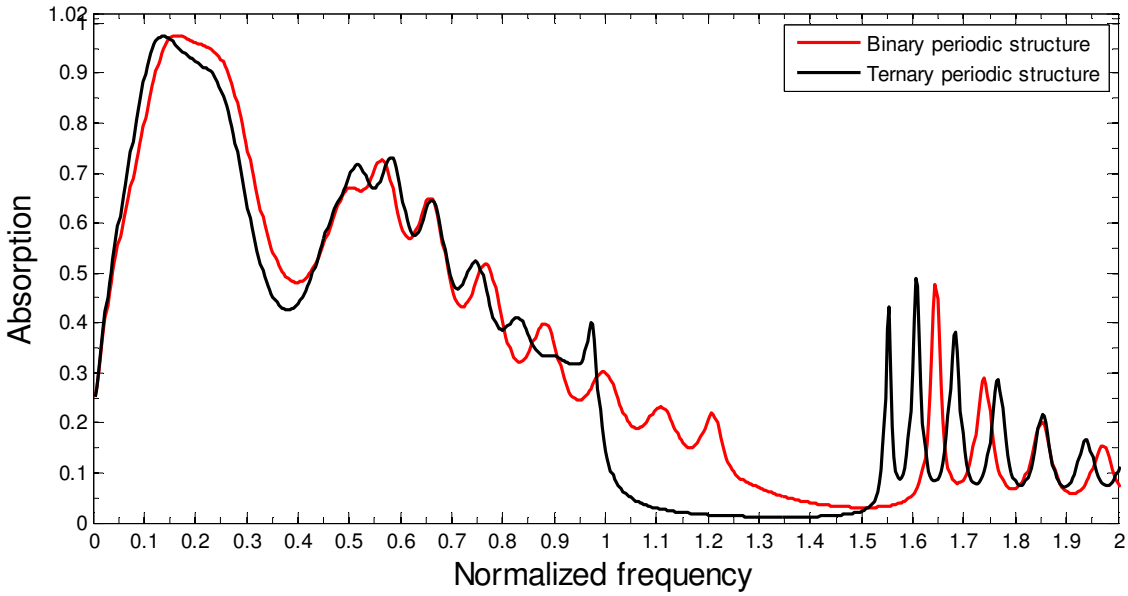

Figure 6.10: Comparison of absorption of multilayer structure for binary structure $(BC)^N$ (red) and ternary structure $(ABC)^N$ (black)

6.4 Conclusion

In this Chapter, the optics of metals and hyperbolic materials were explained briefly and derived theoretically. The optics of the metal was described using Drude and Lorentz model for free electron motion and also tried to differenciate the optics of metal in respect with plasma frequency and wave frequency. Using the dispersion relation, the parallel and the perpendicular permittivity of hyperbolic meta-material were analyzed theoretically with the variation of filling fraction and effective collision frequency. The study shows that the real part of the parallel and the perpendicular permittivity of hyperbolic meta-material have the metallic and dielectric behaviors at certain frequency range. Using these concepts of the HHMs, the absorption of one-dimensional ternary periodic structure containing dielectric, silicon dioxide and hyperbolic material were studied with varying incident angle, filling fraction, electron collision frequency as well as the thicknesses of dielectric (A) material. All absorption properties were calculated by using the well-known simple transfer matrix method. First, we calculated the absorption of the considered structure with varying the angles of incidence (θ). The calculated absorption was shown the maximum value at $\theta = 80^0$. In this continuation, we were also studied the absorption of considered ternary periodic structure with varying the other parameters like filling fraction, electron collision frequencies and thicknesses of dielectric material while the incident angle is

$\theta = 80^0$. The study shows that the 100% tunable absorption was found due to the filling fraction of the hyperbolic meta-material and the metallic nature of effective permittivity of the hyperbolic material. The study of the absorption property of the ternary periodic structure containing hyperbolic materials are very innovative results to design the optical switch, logic gate, sensor as well as the absorber at microwave region. In addition to this, the study of optical property of the ternary periodic structure containing HMMs has investigated the highest absorption property for application of the microwave devices. In our best knowledge our group has performed such calculations first time, and carried out the interesting result of the absorption of one-dimensional ternary periodic structure with a composite of dielectric, silicon dioxide and hyperbolic material.

References

[1] E. Yablonovitch, Inhibited spontaneous emission in solid-state physics and electronics, Phys. Rev. Lett. 58 (1987) 2059-2062.

[2] S. John, Strong localization of photons in certain disordered dielectric super lattices, Phys. Rev. Lett. 58 (1987) 2486-2489.

[3] J. D. Joannopoulos, S. G. Johnson, J. N. Winn and R. D. Meade, Photonic crystals: Molding the flow of light, Second Ed., Princeton Univ. Press Princeton, NJ, USA (2007).

[4] E. Centeno, B.Guizal, and D.Felbacq, Multiplexing and de-multiplexing with photonic crystals, J. Opt. A: Pure Appl. Opt. 1 (5) (1999) L10.

[5] B. Temelkuran, M. Bayindir, E. Ozbay, R. Biswas, M. M. Sigalas, G. K. Tuttle, M. Ho, Photonic crystal based resonant antenna with a high directivity, J. Appl. Phys. 87 (2000) 603-605.

[6] A. Kumar and K. B. Thapa, Study of optical property of defect mode in one dimensional double negative photonic crystal with plasma, Adv. Sci. Eng. Med. 10(7-8) (2018) 837-841.

[7] A. Kumar, P. P. Singh and K. B. Thapa, A new idea for broadband reflector and tunable multi-channel filter of one dimensional symmetric photonic crystal with magnetized cold plasma defects, AIP Conf. Proc. 1953 (2018) 060043-4.

[8] A. Kumar, N. Kumar and K. B. Thapa, Tunable broadband reflector and tunable narrowband filter of a dielectric and magnetized cold plasma photonic crystal, Eur. Phys. J. Plus 133 (2018) 250-8.

[9] A. Kumar, K. B. Thapa and S. P. Ojha, A tunable broadband filter of ternary photonic crystal containing plasma and superconducting material, Ind. J. Phys. 93(6) (2018) 791-798.

[10] A. M. Urbas, Z. Jacob, L. D. Negro, N. Engheta, A. D. Broadman, P. Egan, A. Khanikaev, V. Menon, M. Ferrera, N. Kinsey, C. Devault, J. Kim, V. Shalaev, A. Boltasseva, J. Valentine, C. Pfeiffer, A. Grbic, E. Narrimanov, L. Zhu, S. Fan, A. Alu, E. Poutrina, N. Litchnitser, M. A. Noginov, K. F. MacDonald, E. Plum, X. Liu, P. F. Nealey, C. R. Kagan, C. B. Murray, D. A. Pawlak, I. I. Smolyaninov, V. N. Smolyaninova, and D. Chanda, Roadmap on optical meta-materials, J. Opt. 18 (2016) 093005.

[11] D. R. Smith and D. Schuring, Electromagnetic wave propagation in media with indefinite permittivity and permeability tensors, Phy. Rev. Lett. 90 (2003) 077405-4.

[12] I. V. Iorsh, I. S Mukhin, I.V. Shadrivov, P.A. Belov, and Y.S. Kivshar, Hyperbolic metamaterials based on multilayer graphene structures, Phys. Rev. B 87 (2013) 075416-6.

[13] N. Engheta and R. W. Ziolkowski, A positive future for double-negative metamaterials, IEEE Trans. Microwave Theory Tech. 53 (2005) 1535-1556.

[14] K. V. Sreekanth, A. De Luca and G. Strangi, Negative refraction in graphene-based hyperbolic meta-materials, Appl. Phys. Lett. 103 (2013) 023107-4.

[15] Y. He, S. He and X. Yang, Optical field enhancement in nanoscale slot waveguides of hyperbolic metamaterials, Opt. Lett. 37 (2012) 2907–2909.

[16] T. Zhang, L. Chen, and X. Li, Graphene-based tunable broadband hyper lens for far-field sub diffraction imaging at mid-infrared frequencies, Opt. Exp. 21 (2013) 20888-20899.

[17] C. Guclu, S. Campionee, and F. Capolino, Hyperbolic metamaterial as super absorber for scattered fields generated at its surface, Phys. Rev. B 86 (2012) 205130-7.

[18] L. Ferrari, C. Wu, D. Lepage, X. Zhang and Z. Liu, Hyperbolic material and their applications, Prog. Quantum. Electron 40 (2015) 1-40.

[19] P. Shekhar, J. Atkinson, and Z. Jacob, Hyperbolic metamaterials: fundamentals and applications, Nano Converg. 1:14 (2014) 1-17.

[20] D. Korobekin, B. Neuner III, C. Fietz, N. Jegeneyes, G. Ferro, and G. Shvets, Measurement of the negative refractive index of sub diffraction waves propagating in a indefinite permittivity medium, Opt. Exp. 18(22) (2010) 22734-22746.

[21] S. Molesky, C. J. Dewalt, and Z. Jacob, High temperature epsilon near zero and epsilon near pole meta-material emitters for thermo photovaltaics, Opt. Exp. 21(S1) (2013) A96-A110.

[22] A. Alu, M. G. Silverinha, A. Salendrino, and N. Engheta, Epsilon near zero metamaterials and electromagnetic sources: tailoring the radiation phase pattern, Phys. Rev. B 75(15) (2007) 155410-13.

[23] M. Silverinha, and N. Engheta, Tunneling of electromagnetic energy through sub-wavelength channels and bends using epsilon near zero metamaterials, Phys. Rev. Lett. 97(15) (2007) 157403-4.

[24] M. A. K. Othman, C. Guclu, and F. Capolino, Graphene-based tunable hyperbolic metamaterials and enhanced near-field absorption, Opt. Exp. 21(6) (2014) 7614-7632.

[25] R. Ning, S. Liu, H. F. Zhang, and Z. Jiao, Dual-gated tunable absorption in graphene-based hyperbolic metamaterial, AIP Adv. 5 (2015) 067106-8.

[26] M. A. Baqir, and P. K. Chaudhary, Hyperbolic meta-material based UV absorber, IEEE Photon. Technol. Lett. 29(18) (2017) 1041-1135.

[27] K. V. Sreekanth, M. Elkabbash, Y. Alapan, A. R. Rashed, U. A. Gurkan, and G. Strangi, A multiband perfect absorber based on hyperbolic meta-material, Sci. Rep. 6 (2016) 26272-8.

[28] M. Desouky, A. M. Mahmoud, and M. A. Swillam, Silicon based mid-IR super absorber using hyperbolic metamaterial, Sci. Rep. 8 (2018) 2036-8.

[29] V. Caliguiri and A.D. Luca, Metal-semiconductor oxide extreme hyperbolic meta-material for selectable canalization of wavelength, J. Phys. D: Appl. Phys. 49 (2016) 08LT01-5.

[30] V. E. Babicheva, Long range propagation of Plasmon and phonon polaritons in hyperbolic meta-material waveguides, J. Opt. 19 (2017) 124013-15.

[31] S. Axelrod, M. K. Dezfouli, H. M. K. Wong, A. S. Helmy, and S. Hughes, Hyperbolic meta-material nanoresonator make a poor single photons, Phys. Rev. B. 95 (2017) 155424-7.

[32] K. Rustomji, R. Abdeddaim, C. M de Streke, B. Kuhulmey, and S. Enouch, Measurement and simulation of the polarization dependent Purcell factor in a microwave fishnet meta-material, Phys. Rev. B 95 (2017) 035156-9.

[33] M. Wan, P. Gu, W. Liu, Z. Chen and Z. Wang, Low threshold spaser based on deep sub-wavelength spherical hyperbolic meta-material cavities, Appl. Phys. Lett. 110 (2017) 031103-5.

[34] M. Desouky, A. M. Mahmoud, and M. A. Swillam, Tunable mid-IR focusing in InAs based semiconductor based hyperbolic metamaterials, Sci. Rep. 7 (2017) 15312-7.

[35] F. Wu, G. Lu, C. Xue, H. Jiang, Z. Guo, M. Zheng, C. Chen, G. Du, and H. Chen, Experimental demonstration of angle independent gaps in one dimensional photonic crystal containing layered hyperbolic meta-materials and dielectric at visible wavelengths, Appl. Phys. Lett. 112 (2018) 041902-5.

[36] C. T. Riley, Joseph S. T. Smalley, Jeffrey R. J. Brodie, Y. Fainman, D. J. Sirbuly and Z. Liu, Near perfect broadband absorption from hyperbolic metamaterial nanoparticles, Proc. Natl. Acad. Sci. 7(2017) 114-5.

[37] T. S. Luk, I. Kim, S. Campione, S. W. Howell, G. S. Subramania, R. K. Grubbs, I. Brener, H. T. Chen, S. Fan and M.B. Sinclair, Near infrared surface Plasmon polariton dispersion control with hyperbolic metamaterials, Opt. Exp. 21(9) (2013) 11107-11114.

[38] B. Wells, Zh. A. Kudyshev, N. Litchinister, and V. A. Podolskiy, Nonlocal effects in transition hyperbolic meta-materials, ACS Photonics 4 (2017) 2470-2478.

[39] I. I. Smolynoniv and V. N. Smolynaniv, Hyperbolic metamaterials: Novel Physics and Applications, Solid State Electron. Lett. 136 (2017) 102-112.

[40] T. Gric and O. Hess, Investigations of Hyperbolic metamaterials, Appl. Sci. 8 (2018) 1222-16.

[41] E. Travkin, T. Kiel, S. Sadofev, K. Busch, Oliver Benson, and S. Kalusniak, Anomalous resonances of an optical microcavity with a hyperbolic metamaterial core, Phys. Rev. B 97 (2018) 195133-5.

[42] F. Wu, G. Lu, Z. Guo, H. Jiang, C. Xue, M. Zheng, C. Chen, G. Du, and H. Chen, Red shift gaps in one-dimensional photonic crystals containing hyperbolic metamaterials, Phys. Rev. Appl. 10 (2018) 064022-7.

[43] V. Popov, A. V. Lavrinenko, and A. Novitsky, Surface waves on multilayer hyperbolic metamaterials: Operator approach to effective medium approximation, Phys. Rev. B 97 (2018) 125428-10.

[44] M. S. Habib, A. Stefani, S. Atakaramians, S. C. Fleming, and B. T. Kuhlmey, Analysis of a hyper prism for exciting high-k modes and sub-diffraction imaging, Phys. Rev. B 100 (2019) 115146-9.

[45] E. E. Narimanov, Hyperbolic modes of a conductor-dielectric interface, Phys. Rev. A 99 (2019) 023827-14.

[46] A. Hierro, M. M. Bajo, M. Ferraro, J. T. Arriola, N. Le Biavan, M. Hugues, J. M. Ulloa, M. Giudici, J. M. Chauveau, and P. Genevet, Optical Phase Transition in Semiconductor Quantum Metamaterials, Phys. Rev. Lett. 123 (2019) 117401-5.

[47] Y. Wang, Z. Guo ,Y. Chen, X. Chen, H. Jiang , and H. Chen, Circuit-Based Magnetic Hyperbolic Cavities, Phys. Rev. Appl. 13(2020) 044024-12.

[48] M. A. Gorlach, and M. Lapine, Boundary conditions for the effective-medium description of subwavelength multilayered structures, Phys. Rev. B. 101 (2020) 075127-12.

[49] J. Hou, Z. Li, X. W. Luo, Q. Gu, and C. Zhang, Topological Bands and Triply Degenerate Points in Non-Hermitian Hyperbolic Metamaterials, Phys. Rev. Lett. 124 (2020) 073603-6.

[50] A. Hayat and M. Faryad, Radiation by a finite-length electric dipole in the hyperbolic media, Phys. Rev. A 101 (2020) 013832-6.

[51] J. Wu, F. Wu, K. Lv, Z. Guo, H. Jiang, Y. Sun, Y. Li, and H. Chen, Giant Goos-Hänchen shift with a high reflectance assisted by interface states in photonic hetero structures, Phys. Rev. A 101 (2020) 053838-8.

[52] Y. Qu, M. Pan, and M. Qiu, Directional and Spectral Control of Thermal Emission and Its Application in Radiative Cooling and Infrared Light Sources, Phys. Rev. Appl. 13 (2020) 064052-12.

[53] P. Yeh, Optical Waves in Layered Media, John Wiley & Sons, New York (1988).

[54] Z. Jiao, R. Ning, Y. Xu, and J. Bao, Tunable angle absorption of hyperbolic metamaterials based on plasma photonic crystals, Phys. Plasmas 23 (2016) 063301-6.

[55] C.Y. Li, Plasmonic Optics: Theory and Applications, SPIE Bellingham, USA TT110 (2017) 250.

[56] H. G. Booker Cold Plasma Waves, Springer-Verlag, New York, 23 (1984).

[57] D. R. Smith and D. Schurig, Electromagnetic Wave Propagation in Media with Indefinite Permittivity and Permeability Tensors, Phy. Rev. Lett. 90(2003) 077405.

[58] L. Novotny, and B. Hecht, Principles of nano-optics, Cambridge University Press, New York (2012).

[59] S. Ishii, A. V. Kildishev, E. Narimanov, V. M. Shaleav, and V. P. Drachev, Sub-wavelength interference pattern from volume Plasmon polaritons in a hyperbolic medium, Laser Photonics Rev. 7(2013) 265-271.

[60] C. L Cortes, W. Newman, S. Molesky, and Z. Jacob, Quantum nanophotonics using hyperbolic meta-materials, J. Opt. 14(2012) 063001-15.

[61] W. Zhu, F. Xiao, M. Kang, D. Sikdar and M. Premaratne, Tunable terahertz left-handed metamaterial based on multilayer graphene dielectric composite, Appl. Phys. Lett. 104 (2014) 051902-4.

[62] C. Guclu, S. Campione and F. Capolino, Hyperbolic meta-material as super absorber for scattered fields generated at its surface, Phys. Rev. B 86 (2012) 205130-7.

[63] E. E. Narimanov, Photonic Hypercrystals, Phys. Rev. X 4 (2014) 041014-13.

[64] Y. Xiang, X. Dai, J. Guo, H. Jhang, S. Wen, and D. Tang, Critical coupling with graphene based hyperbolic meta-material, Sci. Rep. 4 (2014) 5483-7.

[65] O. Kidwai, S. V. Zhukovosky, and J. E. Sipe, Effective medium approach to planer multilayer hyperbolic meta-materials: Strengths and limitations, Phys. Rev. A 85 (2012) 053842-12.

Chapter 7
Conclusion and Future Prospects

Chapter -7

Conclusion and Future Prospects

Photonic crystals (PCs) is a cumbersome periodic pattern of the dielectric constants with thicknesses from micro to nanometer; where metals, dielectrics, semiconductors; plasma, magnetized cold plasma, superconductor materials etc. are considered as the constituents of photonic crystal. If the periodic arrangement is the scale of the wavelength of light wave, that is, Electromagnetic Wave (EMW), then light or EMW cannot pass through the periodic structure for some range of wavelengths called *Photonic Band Gap* (PBG). The PBG materials have the huge applications in research of the optical engineered materials because photonic band gap used to control the flow of light or EMW. Therefore, PBG is an unique property of photonic crystals, which is used to control the flow of light by adjusting the optical and the related parameters, i.e. refractive index contrast, scalability, periodicity, symmetry and unit cell of internal structure of the binary or ternary periodicity of the materials made of materials like metals, dielectrics, semiconductors; plasma, magnetized cold plasma, superconductor materials, etc.

However, the PBG of the photonic crystal occurs due to interference at the surface of interface and the localization of light occurs due to existence of the resonance. The position, width and shape of PBG strongly depend on the periodic structure, symmetry, dielectric contrast, and unit cell of internal structure. These will be also variable with variation of variable parameters of different materials. Originally photonic band gap material shows the dispersion relation for the periodic structure. The dispersion relation of the photonic crystals is equivalent to the Fresnel's reflection coefficients. Therefore, the optical properties of the periodic structured materials or PBG materials belong to the optics of photonics where reflectance, transmittance and absorption of the PBG materials are studied for their applications in designing the optical devices.

One-Dimensional Photonic Crystals (1-D PCs) offer the very interesting applications in the direction of photonics and optical engineering. The one-dimensional photonic crystals are used to fabricate in many photonic device like optical filters, optical switches, optical logic gates, optical storage devices, microwave absorber, sensor, resonance cavities, detectors, high-reflecting devices, laser applications, omni-

directional mirrors, optoelectronic circuits, etc. Due to advancement of the thin film technology as well as the concept of quantum dot, the study of the 1-D PCs has become more interesting among the researchers as well as industries.

The optics of periodic structures containing dielectric, plasma; superconductor and semiconducting material etc. have been reviewed. The literature survey of one-dimensional periodic structures has been found for many useful applications for making optical devices. Therefore, we targeted the possible and the better materials: dielectric, plasma, superconductor, semiconducting material, etc. in literature review; and studied the optics of these materials thoroughly with the help of Maxwell's equations. These materials have unique properties of the *optical density or refractive index*. Then, we have decided to consider these excellent materials for the study of optical properties of periodic structures. In this study, the development of optics of photonic crystal, especially one-dimensional periodic structure containing these materials, has been analyzed for the applications in science community.

Keeping in mind the availability of easy fabrication techniques and reviewing several applications of 1-D PCs, it has been investigated the optics of the metals, dielectric, plasma, superconductor and semiconducting materials using Maxwell's equations and studied the optical properties of one-dimensional photonic crystals containing the different materials by calculating the optics of materials/refractive index for metals, dielectric, plasma, superconductor and semiconducting materials. It has been studied, in details, the optics of the *Magnetized Cold Plasma (MCP)* with applying Maxwell's equation and found this material to be useful as a magic material for periodic structure, because this material has many variable parameters, which affect the optics of the magnetized cold plasma. In the present thesis, it has been studied the photonics of one-dimensional periodic structure containing MCP and other materials. The theory and methodology of 1-D periodic structure, namely One-Dimensional Photonic Crystal (1-D PC), were used to analyze the optical properties and dispersion relations of periodic structure with the help of the boundary conditions and Maxwell's equations, where the electromagnetic wave interaction with materials was analyzed and the optical constant of the materials was obtained. The concept of the wave propagation in each layer and applying boundary conditions, we have formulated the characteristics matrix for each layer, which is known as *Translational Matrix or Transfer Matrix Method* (TMM). This method is used to analyze the dispersion

relation, transmission, reflection and absorption spectra of the periodic structure. For calculation of the optical properties of periodic structure, we have chosen the appropriate theoretical values analogous to the experimental observations.

Initially, we have started the theoretical study of band structure and transmittance versus frequency (GHz) response of dielectric/Magnetized Cold Plasma (MCP) based periodic structure with the variation of varying parameters of the magnetized cold plasma for Right Hand Polarization (RHP) and Left Hand Polarization (LHP) using the transverse TMM. The MCP has unique property that offers right handed and left handed polarization in the presence of magnetic field. The dielectric and plasma are very important materials to investigate for better optical properties of this periodic structure. Plasma physicist Gallagher from NASA stated that 99.9% of the universe is made of the plasma. So, plasma material is very exciting material. Very shortly, the many researchers focused on the magnetized cold plasma. The plasma shows optical behavior in presence of external magnetic field at low temperature; called magnetized cold plasma. The right hand and left hand polarizations occur due to unique behaviors of external magnetic field in positive and negative directions. This also showed the forward and backward behaviors due to positive and negative directions. So, we have studied the band structure and transmittance of chosen periodic structure versus frequency with changing the value of incident angle, magnetic field and effective collision frequency of the MCP, and found the innovative results. These calculated results for the RHP and LHP structures, we have obtained an excellent thought for the design of the broadband reflector and narrow tunable filter at lower and higher frequency ranges. Thus, this analysis may be very useful to the design of tunable photonic devices which control the wave features by changing the parameters of the magnetized cold plasma. Lots of filters have already been developed by the researchers in this field but tunable and narrowband filters are new type of filter for photonic crystal containing MCP, which may be used either to pass or block the certain frequency of light or electromagnetic spectrum due to periodicity of the materials.

We have also theoretically analyzed the transmittance against frequency (GHz) of ternary photonic crystal with variation of the incident angle, the magnetic field, the electron density of the magnetized cold plasma, the temperature and the thickness of the superconducting material for the right hand polarization/left hand polarization

structure using the TMM. The transmittance of the left-hand polarization ternary photonic crystal has been found to offer superior results comparable to the transmittance of the right-hand polarization in ternary photonic crystal in the presence of the superconducting layer which is influenced by the temperature and the magnetic field. Superconducting materials are very exciting materials due to existence of zero resistivity at certain temperature. We have investigated the optical properties of a ternary periodic structure including dielectric, MCP and high temperature superconductor with variations of possible parameters, and found some possible outcome. Owing to the large band gap of the left-hand polarized ternary photonic crystal, it may be used as the broadband reflector or high pass filter applications at lower frequency region. However, the tunable transmittance of the right-hand polarized ternary photonic crystal has also been obtained by varying parameters of the magnetized cold plasma. Such a ternary structure may be used as a tunable filter.

Besides this, we have also wished-for an pioneering thought to design the broadband reflector or the high pass filter and the narrow tunable filter using the ternary photonic crystal containing the magnetized cold plasma and the superconducting material in presence of transverse magnetic field and operating temperature, because the magnetic field and operating temperature are the fundamental properties of any superconductor was studied in our work. In this work, high temperature superconductors have been considered in periodic structure to study the optical properties but till today any researcher have not found the same structure at room temperature with superconductor. Many researchers have worked out on the development of room temperature superconductor but till now no one has successfully developed the room temperature superconducting photonic crystal.

In one-dimensional periodic structure, the arrangements of different materials are very important to study the optical property of considered periodic structure. Here, we study the behavior of symmetric and asymmetric periodic structures with defect of one and two layer of different materials inserted in the middle of structure. Here, we have analyzed the transmittance of symmetric and asymmetric one-dimensional periodic structure containing zinc sulfide (ZnS) and titanium dioxide (TiO_2) with one or two defect layer of magnetized cold plasma using TMM. We have compared the optical properties of symmetric and asymmetric structure, and analyzed the better optical property for asymmetric structure for further studies. Now, considering the

asymmetric structure, the transmittance of one-dimensional periodic structure considering ZnS and TiO_2 with one or two defect layer of magnetized cold plasma was analyzed with variation of incident angles, electron densities, magnetic fields of the magnetized cold plasma material and thickness of ZnS and TiO_2. The transmittance of two MCP layer inserted in symmetric periodic structure with variation of variable parameters and found better response as comparison to one defect layer in same periodic structure. These calculated results recommended a novel proposal to fabricate the tunable multichannel filter at microwave region. Multichannel filter applications are very important for the development of pass and block certain frequency of light in the small band of the electromagnetic spectrum.

Today, the concept of plasmonics in *meta-materials* is used to fabricate the metatronic devices. The *metatronic* devices are based on the variable refractive index of the material, which is fulfilled with the variable refractive index offered by the hyperbolic materials. The hyperbolic material is the most popular topic for the researchers in the direction of optical science and nanotechnology. We have focused our theoretical study for the fabrication of devices having negative, zero and positive index material at nanoscale; and the optical devices at nanoscale having positive, zero and negative index material can be used as capacitor, inductor and resistance, respectively. In general the metatronic device has the real part of permittivity greater than zero and hence it acts as capacitor; when the real permittivity is less than zero acts as an inductor; and also when the imaginary parts of permittivity is not equal to zero it acts as resistance. These devices contained negligible loss and high gain and may purely work as the LCR circuit at nanoscale. In our research work, we have investigated the plasma based hyperbolic materials, which may be the most applicable in the metatronic devices. The researchers are working on the development the metatronic devices using the nanofabrication technique. For the nanofabrication technique, the several composite anisotropic materials are being developed. In this direction, we have also proposed a new composite anisotropic material which is the plasma based hyperbolic meta-material and applicable for the metatronic devices. Hence, the proposed composite anisotropic material may be developed with help of nanofabrication technique. The optics of the plasma based composite material has been studied using Maxwell-Garnet equations and such composite has the nature of hyperbolic meta-material (HMM). The composite material has perpendicular and

parallel permittivity for relative permittivity. The component of parallel and the perpendicular permittivity of hyperbolic meta-material were theoretically calculated with the variation of filling fraction and effective collision frequency. The calculated study shows that the real part of the parallel and the perpendicular permittivity of hyperbolic meta-material have the metallic and dielectric behaviors at certain frequency range. To understand the optics of the plasma based HMMs, we have considered the one dimensional ternary periodic structure containing dielectric, silicon dioxide and hyperbolic material and called one dimensional ternary photonic crystal. The optics of the plasma based HMMs can vary with filling fraction, electron collision frequency and magnetic field. Hence, the absorptions of 1-D TPC were studied with varying incident angle, filling fraction, electron collision frequency as well as the thicknesses of dielectric material. All absorption spectra were analyzed using transfer matrix method. Firstly, we have analyzed the absorption of the chosen structure with varying the incident angles (θ) and found the maximum absorption at $\theta = 80^0$. Further, we have also analyzed the absorption of chosen ternary periodic structure with variation of filling fraction, electron collision frequencies and thicknesses of dielectric material while fixing the incident angle is $\theta = 80^0$. The calculated results show the 100% tunable absorption was found owing to the filling fraction of the composite material and the metallic nature of effective permittivity of the hyperbolic material. The calculated absorption spectra of ternary periodic structure containing hyperbolic materials offers an innovative results to design the optical switch, logic gate, sensor as well as the absorber at microwave region.

These studies of optics of photonics containing magnetic cold plasma have been done with the help of simple theoretically method in one-dimensional space, i.e., TMM. Such studies for magnetic cold plasma might be continued with the methods like Finite Difference Time Domain (FDTD) method, Finite Element Method (FEM) and Plane Wave Expansion Method (PWEM) for higher dimensions. The several one-dimensional photonic crystals have been developed by thin film technology. But for higher dimensions, there are physical and chemical techniques for fabrications of devices experimentally. Generally, researchers are developing the multilayer structure with the help of physical methods like Laser interference lithography, physical vapor deposition technique, DC and RF sputtering methods, etc. The multilayer structures are also developed with the help of chemical techniques like Sol-Gel method, Spin-

Coating method, Chemical vaporization technique, Self-assembly method, Spray Pyrolysis, Green synthesis method, etc.

The photonic crystals, especially one-dimensional photonic crystals, are used in many useful applications. By varying the *refractive index or optics* of the material, the optical devices can be developed for the useful applications. Therefore, researchers have been studying the optics of photonics with varying the refractive index using metal, plasma and superconducting materials. Hence, we have been considered one-dimensional photonic crystals containing magnetic cold plasma and other materials like meta-material, superconductor, etc. The magnetic cold plasma is a magic material, because it has several parameters that affect the optics of the magnetic cold plasma (MCP). Recently, the multilayer structure containing Ag/ZnS/Ag materials has been fabricated for filter application with the help of physical vapor deposition technique. Our investigated results are useful to fabricate the optical devices like filters, multichannel filters etc. These studies open the application of MCP in different filter fabrications. The concept of plasmonics of metals in nano scale has the abnormal behavior of the optics of the materials like metal or plasma; and the photonic crystals of metal/MCP will open new dimension in direction of the nanofabrication for development of the optical devices. We have also investigated the optics of plasma based hyperbolic meta-material, where the optics of the hyperbolic materials is changed by varying the parameters of plasma as well as filling fraction. The permittivities or optics of the hyperbolic materials are found with zero, positive and negative value, when the parameters of the plasma materials are being changed. Such hyperbolic material is used in periodic structure to study the optical properties. The optics of photonics containing plasma based hyperbolic materials has shown the highest absorption behavior, which is useful in metatronic devices. This study open a new way to solve the dispersion relation as well as the optical property for other hyperbolic materials using Maxwell's equations, and the investigated dispersion relation of the new materials will be used to develop a new type of hyperbolic materials for the metatronic device.

Eur. Phys. J. Plus (2018) **133**: 250
DOI 10.1140/epjp/i2018-12073-3

THE EUROPEAN PHYSICAL JOURNAL PLUS

Regular Article

Tunable broadband reflector and narrowband filter of a dielectric and magnetized cold plasma photonic crystal

Asish Kumar[1], Narendra Kumar[2], and Khem B. Thapa[1,a]

[1] Department of Physics, School of Physical and Decision Sciences, Babasaheb Bhimrao Ambedkar University, Vidya Vihar, Raebareli Road, Lucknow - 226025 (UP), India
[2] Department of Physics, Mody University of Science and Technology, Lakshmangarh 332311, Sikar, Rajasthan, India

Received: 1 March 2018 / Revised: 22 May 2018
Published online: 6 July 2018

Abstract. The tunable broadband reflector and the narrowband filter of a periodic structure composed of dielectric and magnetized cold plasma materials have been studied. The optical properties are calculated theoretically using the well-known simple transfer matrix method (TMM). Dispersion relation and transmission spectra of the considered structure with right-hand polarization and left-hand polarization of the magnetized cold plasma materials are studied. The right-hand polarization and the left-hand polarization of the magnetized cold plasma are exhibited due to positive and negative values of the external magnetic field, respectively. The dispersion relation and transmission spectra of the considered periodic structure with the most valuable parameters, like external magnetic field, electron density, and effective collision frequency of the magnetized cold plasma, have been analyzed. The tunable narrow filter for right-hand polarization is obtained with a high value of the external magnetic field and a low value of the electron density. The broadband filter for the left-hand polarization is investigated with a low value of the external magnetic field and a high value of the electron density of the magnetized cold plasma. It is also noted that the impact of variation of effective collision frequency of the magnetized cold plasma is minute in both cases. These calculated results reveal an innovative idea for designing the tunable broadband reflector and narrowband filter.

1 Introduction

The spontaneous emission of an atom located in a periodic structure has a number of unique properties. When the atom is excited, the process can proceed in two ways: *i.e.*, either as emission of photons in the allowed band with low probability or as transition of the excited state with high probability, which is a relatively long-lived state [1]. For the system, identical dielectrics are composed of three-dimensional lattices and the secular equation of the energy of photons and diffraction of ultraviolet and visible light forms. This theory simulates void lattices in irradiated metals or ordered lattices with large lattice constants and hence the low frequency of the diffracted electromagnetic wave rises to the Bragg reflections having order of magnitude stronger in X-ray diffraction. Some characteristic aspects anticipated in low-energy photons, is discussed in relation to low-energy electron diffraction [2]. Photonic crystals (PCs) are homogeneous and inhomogeneous artificial, dielectric, periodic structures, in which the refractive index of the material changes periodically in space. In 1987, the photonic band gap was experimentally observed for the first time by Yablonovitch [3] and theoretically proposed by John [4]. Presently, photonic crystals attract interest due to various applications of the photonic bands of the materials. The photonic band gap has great applications in the search of engineered materials because it can be used to manipulate and control the flow of light. The photonic band gap is produced when an electromagnetic wave propagates through a periodic structure made of dielectric materials called photonic crystal. The propagation of electromagnetic waves inside the photonic crystal depends on the refractive index contrast, the refractive index of the material, the lattice parameter, the filling factor, the dimensionality of the material, etc. [4,5]. The simplest photonic crystal has a one-dimensional periodic multilayer structure, *i.e.*, a one-dimensional

[a] e-mail: khem.bhu@gmail.com

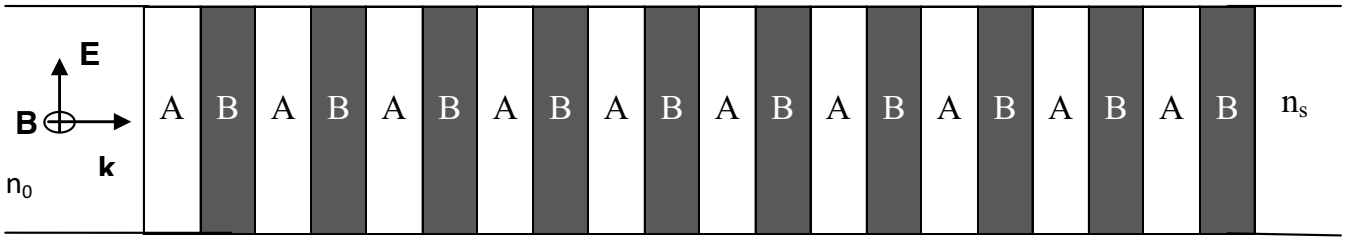

Fig. 1. Schematic diagram of dielectric (air) and magnetized cold plasma (MCP) symmetric photonic crystal.

photonic crystal, which is popular in the photonic field and it can be easily fabricated using thin film technology. In modern optics, one-dimensional photonic crystals have interesting applications in the fields of photonic and optical engineering, photonic devices, optical filters, resonance cavities, laser applications, high-reflecting omnidirectional mirrors, and optoelectronic circuits [5–14]. A plasma photonic crystal (PPC) is a periodic arrangement of thin plasma and dielectric material like vacuum. The plasma photonic band gap is also obtained owing to the periodicity of thin plasma and dielectric materials. The plasma photonic band gap can be tuned by changing various parameters of the plasma material, like plasma density, effective collision frequency, thickness of the plasma layer, and external magnetic field [15–17].

Recently, magnetized cold plasma has attracted the interest of many researchers towards the periodicity of magnetized cold plasma and dielectric materials. Magnetized cold plasma has one extra parameter, due to presence of the external magnetic field, which is called gyro-effective frequency. This gyro-effective frequency depends upon the external magnetic field of the magnetized cold plasma. The right-hand polarization and the left-hand polarization of magnetized cold plasma have the positive and negative values of the gyro-effective frequency, respectively. Thus, the behavior of the refractive index of the magnetized cold plasma shows unusual characteristics due to the variation in external magnetic field, electron density, and effective collision frequency. Due to the unusual property of the magnetized cold plasma with varying the parameters, the metals or dielectrics may be replaced by the magnetized cold plasma in fabrication of photonic crystal for a better control on the optical properties of the considered periodic structure containing magnetized cold plasma [18–20]. Kumar *et al.* [21] proposed band gap structure, reflection properties and abnormal behavior of one-dimensional dielectric/magnetized cold plasma photonic crystal. Kong *et al.* [22] suggested the idea of a narrow tunable filter with defect mode of the transverse electric (TE) wave from one-dimensional photonic crystals doped with magnetized cold plasma. Aly and Mohamed [23] recommended the transmission spectra of a one-dimensional photonic crystal of the superconductor and dielectric materials for applications in reflector and band pass filters. The transmittance properties of a one-dimensional photonic crystal with magnetized cold plasma and high-temperature superconductor materials in a periodic multilayer structure was proposed by Aghajamali [24], for applications in high pass filters and reflectors. Aly *et al.* [25] investigated the tunability of two-dimensional metallic photonic crystals by an external magnetic field. The band structure and permittivity of metals are also affected by an external magnetic field, and it is used for many optical devices. Recently, Aly *et al.* [26] theoretically investigated the transmission properties of a one-dimensional photonic crystal at the terahertz (THz) frequency range with applications in the cutoff frequency of the material in the THz region. Aly and Elsayed [27] theoretically studied the effect of the magnetic field on permittivity and transmittance of a defective one-dimensional photonic crystal structure in UV radiations. Aly *et al.* [28] investigated the effect of the magnetic field on the transmittance of two-dimensional n-doped semiconductor photonic crystals by using the plane wave expansion method. Aly [29] investigated the optical properties of the superconductor-dielectric photonic band gap in ultraviolet radiations. Aly *et al.* [30] investigated the bandwidth of a dielectric and superconductor photonic crystal structure. Aly and Sayed [31] designed a photonic crystal structure to improve light absorption by increasing the optical path length of the incident light inside the absorbing material, which enhances the efficiency of the thin film silicon solar cell. Aly *et al.* [32] investigated the optical properties of a new type of superconductor metamaterial photonic crystals.

In this paper, we study the band structures and the transmission spectra of the one-dimensional periodic structure composed of dielectric (air) and magnetized cold plasma layers with lattice period ten, *i.e.*, $N = 10$. The dielectric and magnetized cold plasma photonic crystals are the right-hand polarization structure, with positive external magnetic field, and the left-hand polarization structure, with negative external magnetic field. The band structure and transmittance response against frequency (GHz) of the right-hand polarization and left-hand polarization structures, with varying the magnetic field, the electron density and the collision frequency of magnetized cold plasma are studied by using the translational matrix method. The tunable band structure of the right-hand polarization and left-hand polarization structures may be used as optical filter and resonance cavity in photonic device applications.

2 Theoretical model

The band gap structure and the transmittance of the considered periodic structure are theoretically calculated by using the well-known simple transfer matrix method (TMM) [33]. A one-dimensional periodic crystal is composed of dielectric (air) and magnetized cold plasma (MCP). The dielectric and magnetized cold plasma photonic crystal is in the form of $(AB)^N$, where A and B represent the dielectric and magnetized cold plasma layers, respectively, and N is the number of lattice periods, as shown in fig. 1. The complex permittvity and permeability of magnetized cold plasma for the magnetized cold plasma layer (B) can be expressed as [18]

$$\varepsilon_B(\omega) = 1 - \frac{\omega_{pe}^2}{\omega^2\left(\left(1 - \frac{i\gamma}{\omega}\right) \mp \frac{\omega_{le}}{\omega}\right)}, \tag{1}$$

with $\mu_B = 1$, where ω, γ and ω_{le} are the angular, effective and gyro-effective collision frequencies.

Here, ω_{pe} is the plasma frequency and is given as

$$\omega_{pe} = \left(\frac{n_e\, e^2}{m\varepsilon_0}\right)^{1/2}, \quad \text{and} \quad \omega_{le} = eB/m, \tag{2}$$

where n_e, m, ε_0, B are the electron density, mass of electron, permittivity in free space, and the external magnetic field, respectively, and e is the electronic charge [11].

The characteristic matrix for the i-th layer is given as

$$M_i = \begin{bmatrix} \cos\gamma_i & -\frac{i}{p_i}\sin\gamma_i \\ -ip_i\sin\gamma_i & \cos\gamma_i \end{bmatrix}, \tag{3}$$

where $\gamma_i = (w/c)n_i d_i \cos\Theta_i$, c is the speed of light in vacuum, Θ_0 is the ray angle inside the i-th layer ($i = A$ and B material), the refractive index of the material $n_i = \sqrt{\mu_i\varepsilon_i}$, $p_i = \sqrt{\frac{\varepsilon_i}{\mu_i}}\cos\theta_i$ and $\cos(\theta_i) = \sqrt{1 - \frac{n_0^2\sin^2\theta_0}{n_i^2}}$, in which n_0 is the refractive index of the air, where the incident wave tends to enter the considered the structure with angle Θ_0.

The characteristic matrix for the considered periodic structure $(AB)^N$, with lattice thickness "d", is given by

$$M(d) = \begin{pmatrix} m_{1,1}\ m_{1,2} \\ m_{2,1}\ m_{2,2} \end{pmatrix}, \tag{4}$$

where $M(d) = (M_A M_B)^N$, M_A and M_B are the characteristics matrix for the layers A and B, respectively. We have considered the M_A and M_B characteristic matrices for the TE wave at incident angle Θ_0 [13].

The transmission coefficient of the multilayer system is calculated by

$$t = \frac{2p_0}{(m_{11} + m_{12}p_s)p_0 + (m_{21} + m_{22}p_s)}, \tag{5}$$

where $p_0 = n_0\cos\Theta_0$ and $p_s = n_s\cos\Theta_s$, n_s is the refractive index of the substrate, whose ray angle is Θ_s.

The transmittance of the multilayer is given by [33]

$$T = \left(\frac{p_s}{p_0}\right)|t|^2. \tag{6}$$

3 Results and discussion

In this work, we have theoretically calculated the band gap structure and the transmittance for a dielectric and magnetized cold plasma periodic structure. The band gap structure and the transmittance of the considered periodic structure against frequency (GHz) are plotted with varying the plasma parameters, like external magnetic field (B), electron density (n_e) and effective collision frequency (γ), with lattice period, *i.e.* $N = 10$, and normal incidence angle, *i.e.* $\Theta_0 = 0^0$. Each parameter of the magnetized cold plasma plays an important role, but the external magnetic field plays a more important role in magnetized cold plasma, due to the positive and negative values of the external magnetic field, when it acts as right-hand and left-hand polarization, respectively. In addition to this, we have calculated all the transmittances corresponding to the band gaps for the dielectrics having refractive index $n_A = 1$ (air) and thickness $d_A = 12\,\text{mm}$; the refractive index of the magnetized cold plasma is taken from eq. (1), and the thickness of the magnetized cold plasma layer is chosen to be 15 mm [15]. The periodic structures of the air/left-hand polarization and air/right-hand polarization are called left-hand polarization and right-hand polarization structures, respectively.

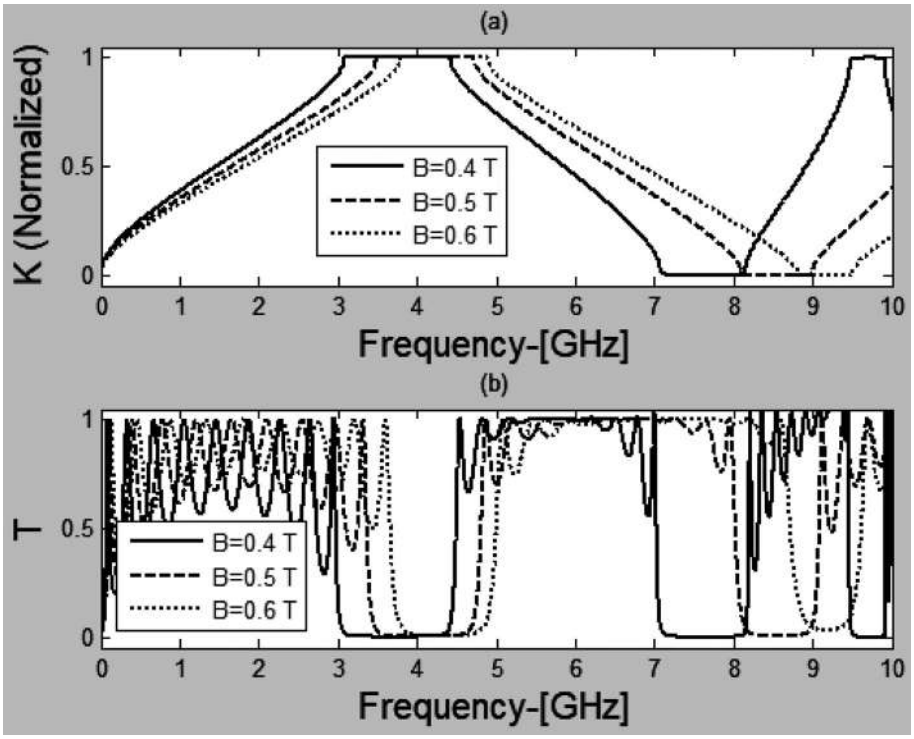

Fig. 2. (a) Dispersion relation and (b) transmittance *versus* frequency plots with varying the magnetic field of magnetized cold plasma for right-hand polarization.

In fig. 2, we have studied the transmittance corresponding to the band gap structure against frequency (GHz) for right-hand polarization with varying the magnetic field of the magnetized cold plasma as $B = 0.4$ tesla, 0.5 tesla and 0.6 tesla, fixing the electron density of the magnetized cold plasma to $n_e = 8 \times 10^{17}/\mathrm{m}^3$, and the effective collision frequency $\gamma = 10^7$ Hz. The band gap structure of the considered periodic structure *versus* frequency (GHz) response shows band gaps at the lower and higher frequency ranges for the different values chosen for the magnetic field. From the band gap structure of the considered photonic crystal *versus* frequency (GHz) curves, with varying the magnetic field, we found two band gaps for the different values of magnetic field. Here, the band edge at the low frequency range does not shift much with the variation in the magnetic field strength, while the band edge at the high frequency is more affected by the magnetic field.

Transmittance corresponding to the band gap of the considered periodic structure also varies simultaneously with shifting the frequency region of the band gap that appears due to the band edge effect. The transmittance *versus* frequency (GHz) response varies at lower as well as higher frequency ranges and the photonic crystal acts as a narrow band tunable filter corresponding to the different values of the magnetic field, *i.e.* $B = 0.4$ tesla, $B = 0.5$ tesla, $B = 0.6$ tesla, as is shown in fig. 2(b).

The band gap structure and transmittance of the left-hand polarization structure *versus* frequency (GHz) curves are drawn for different values of the magnetic field, *viz.* $B = 0.4$ tesla, 0.5 tesla and 0.6 tesla for a fixed plasma density $n_e = 8 \times 10^{17}/\mathrm{m}^3$ and the effective collision frequency $\gamma = 10^7$ Hz, which is shown in fig. 3. The band gaps of the considered periodic structure change at lower and higher frequency ranges. At the low frequency range (0–2.5 GHz), there exists a band gap that is shifted by the change in the values of the magnetic field and also the structure forms a band gap at the higher frequency range (6–7.2 GHz), which shifts with different values of the external magnetic field. The transmittance of the considered periodic structure corresponding to the value of the band gap is calculated and we found that the structure acts as a broadband reflector and a narrow tunable filter at lower (0–2.5 GHz) and higher frequency (6–7.2 GHz) ranges, respectively. From transmittance of the considered periodic structure, we found the left-hand polarization structure as a better broadband reflector or a high pass filter at low frequency at low values of the magnetic field, *i.e.* $B = 0.4$ tesla. The photonic crystal of the left-hand polarization structure acts as a narrow tunable filter for all values of the magnetic field, *i.e.* $B = 0.4$ tesla, 0.5 tesla and 0.6 tesla at higher frequency ranges, which is shown in fig. 3(b).

Similarly, we study the band gap structure and transmittance for the right-hand polarization structure *versus* frequency curves for different values of plasma density, *viz.* $n_e = 8 \times 10^{17}/\mathrm{m}^3$, $12 \times 10^{17}/\mathrm{m}^3$, $16 \times 10^{17}/\mathrm{m}^3$ at a fixed value of the magnetic field $B = 0.6$ tesla and effective collision frequency $\gamma = 10^7$ Hz, as is shown in fig. 4(a). We found that the band gap is shifted towards the lower and higher frequency ranges corresponding to these three values of plasma density for a fixed value of the magnetic field and effective collision frequency. We have calculated the transmittance of the right-hand polarization structure corresponding to the band gap structure for different chosen

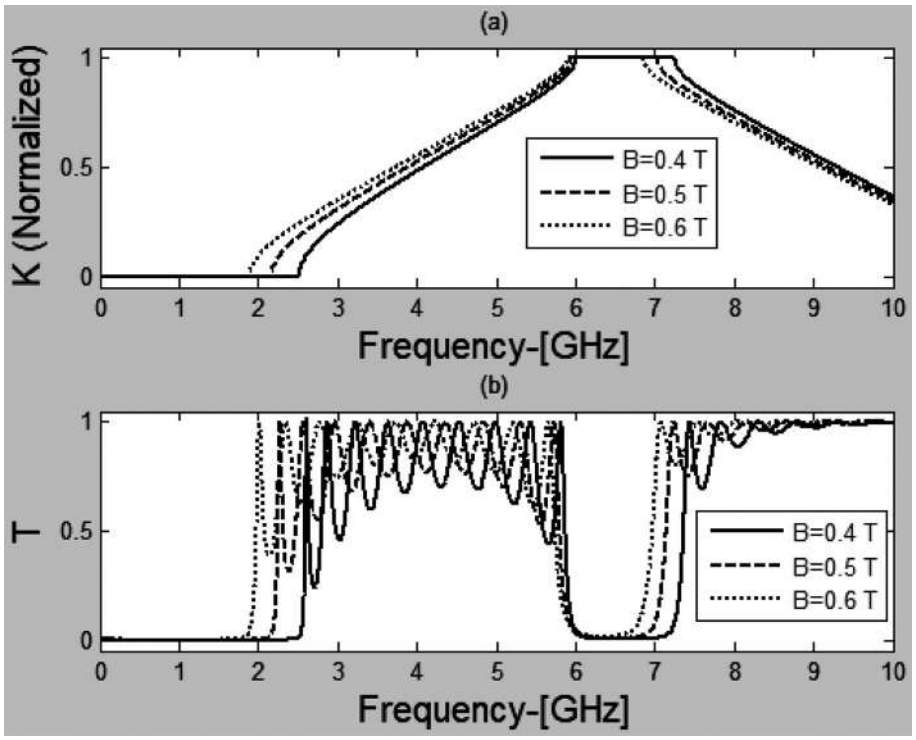

Fig. 3. (a) Dispersion relation and (b) transmittance *versus* frequency plots with varying magnetic field of the magnetized cold plasma for left-hand polarization.

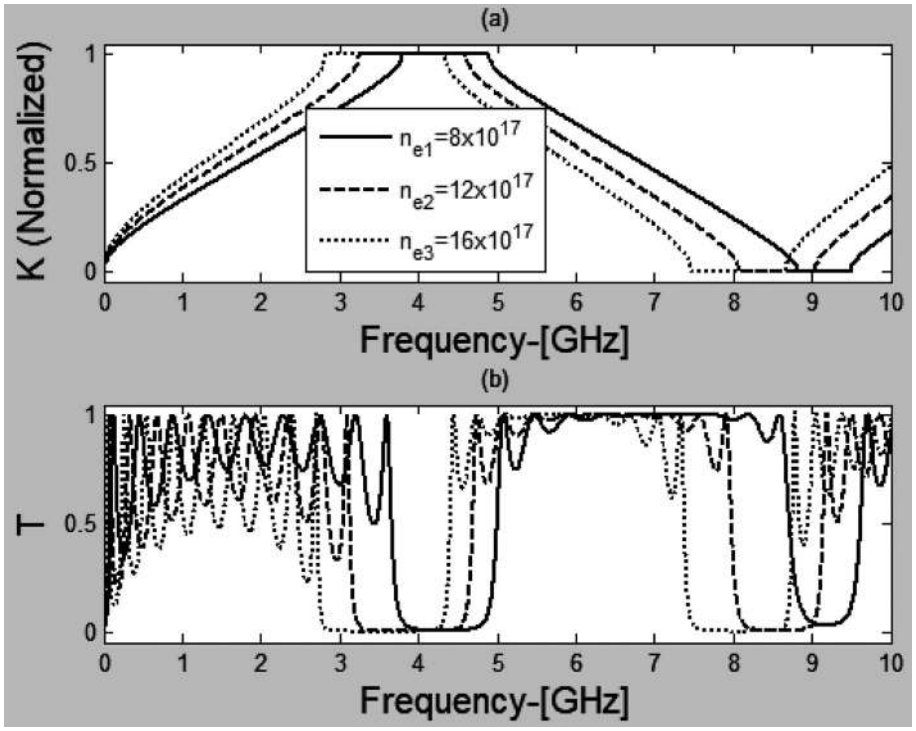

Fig. 4. (a) Dispersion relation and (b) transmittance *versus* frequency plots with varying plasma density of the magnetized cold plasma for right-hand polarization.

values of plasma density, *i.e.*, $n_e = 8 \times 10^{17}/\mathrm{m}^3$, $12 \times 10^{17}/\mathrm{m}^3$, $16 \times 10^{17}/\mathrm{m}^3$ at the fixed magnetic field $B = 0.6$ tesla and effective collision frequency $\gamma = 10^7$ Hz. The transmittance of the right-hand polarization structure also varies for different values of the plasma density and it forms a narrow tunable multichannel filter, which is shown in fig. 4(b).

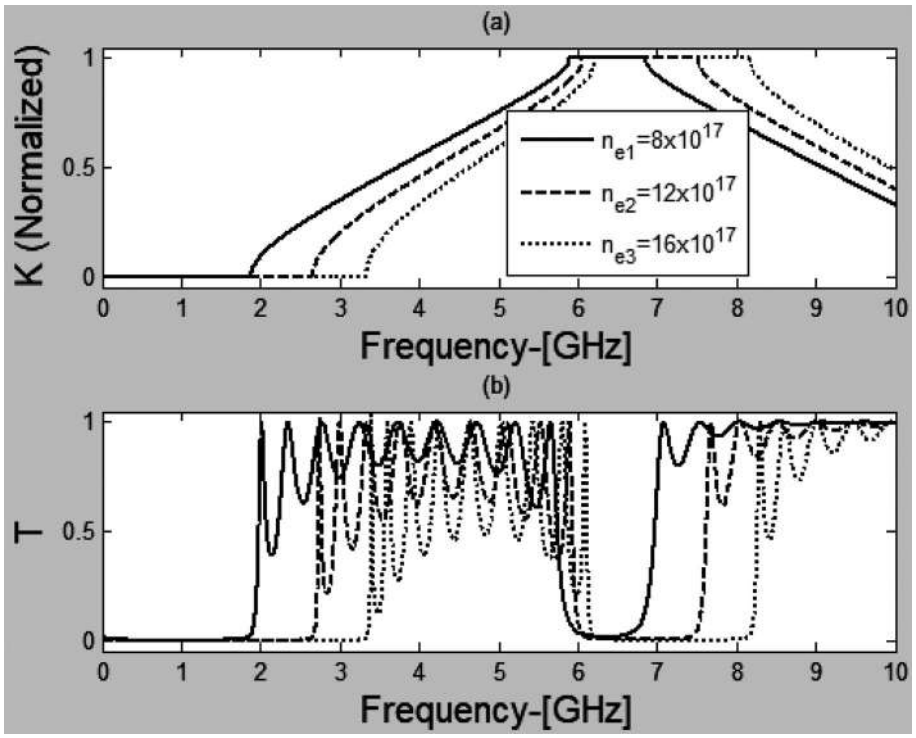

Fig. 5. (a) Dispersion relation and (b) transmittance *versus* frequency plots with varying plasma density of the magnetized cold plasma for left-hand polarization.

Further, the band gap structure and transmittance of the left-hand polarization structure *versus* frequency curves are studied with different values of plasma density $n_e = 8 \times 10^{17}/\mathrm{m}^3$, $12 \times 10^{17}/\mathrm{m}^3$, $16 \times 10^{17}/\mathrm{m}^3$ at a fixed magnetic field as $B = -0.6$ tesla and effective collision frequency $\gamma = 10^7$ Hz, as is shown in fig. 5. It is noticed that the band gap of the considered periodic structure is shifted for lower and higher frequency ranges as we increase the value of plasma density. The transmittance of the left-hand polarization structure exhibits unique results at the lower and higher frequency ranges. Transmittance of the considered periodic structure is zero at the lower frequency range for the different values of plasma density and it acts as a high band reflector or high pass filter, while it forms a tunable narrow band filter for a higher frequency range.

Now, we focus on the band gap structure and transmittance *versus* frequency (GHz) curves with varying effective collision frequency, $\gamma_1 = 1 \times 10^6$ Hz, $\gamma_2 = 5 \times 10^6$ Hz, $\gamma_3 = 1 \times 10^7$ Hz at a fixed magnetic field $B = 0.6$ tesla and electron density of magnetized cold plasma, *viz.* $n_e = 8 \times 10^{17}$ in both right-hand polarization and left-hand polarization structures, as depicted in figs. 6 and 7. For the right-hand polarization, it is observed that the band structure and transmittance do not vary for the different values of the effective collision frequency with fixed magnetic field and electron density of magnetized cold plasma. The shifting in frequencies of band gaps and transmittances of the considered periodic structures are very small and the band gap and transmission spectra exist in the frequency region (3.8–4.9 GHz), which is shown in fig. 6(a).

Similarly, we analyze the band gap structure and transmittance *versus* frequency (GHz) curves with varying the effective collision frequency for the left-hand polarization. Band gap and transmittance of the considered periodic structure with different effective collision frequencies ($\gamma_1 = 1 \times 10^6$, $\gamma_2 = 5 \times 10^6$, $\gamma_3 = 1 \times 10^7$) for fixed magnetic field $B = -0.6$ tesla and electron density ($n_e = 8 \times 10^{17}$) of magnetized cold plasma show very minor effects on band gap or transmittance at lower (0–1.9 GHz) and higher (5.9–6.9 GHz) frequency ranges for the left-hand polarization structure, as is shown in figs. 7(a) and (b).

4 Conclusions

We have theoretically studied the band gap structure and transmittance *versus* frequency response with varying the magnetic field, the plasma density and the effective collision frequency of the magnetized cold plasma for right-hand polarization and left-hand polarization structures. From the above results, we found that the band gap structure of the right-hand polarization and left-hand polarization structures have unique results, where the broadband and tunable filter may be obtained by varying the magnetized cold plasma parameters. We propose a tunable narrow band filter

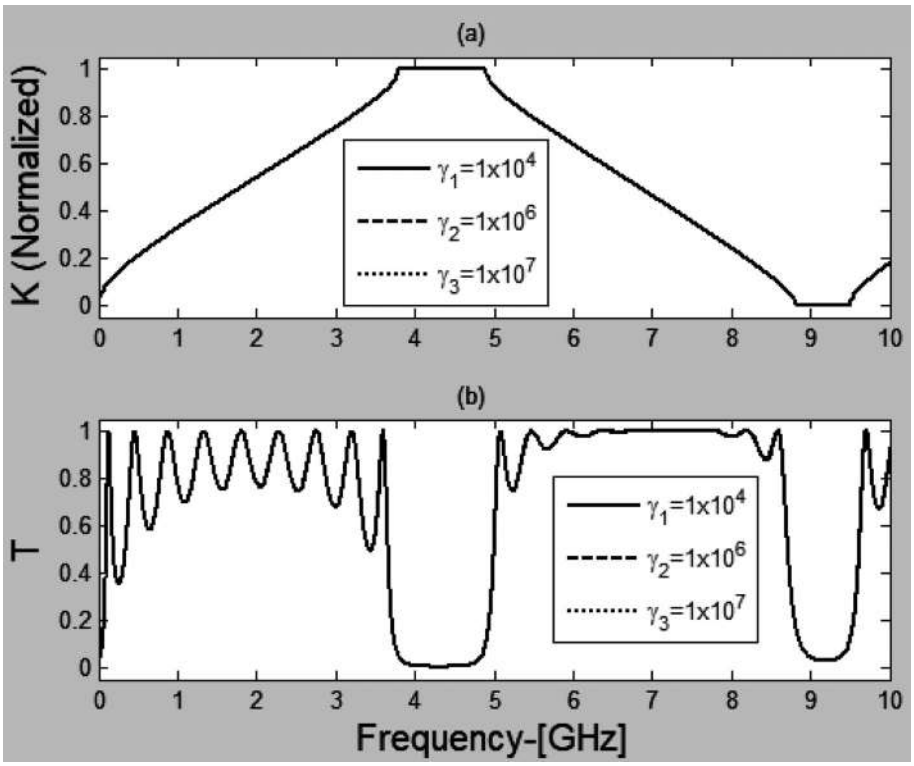

Fig. 6. (a) Dispersion relation and (b) transmittance *versus* frequency plots with varying effective collision frequency of the magnetized cold plasma for right-hand polarization.

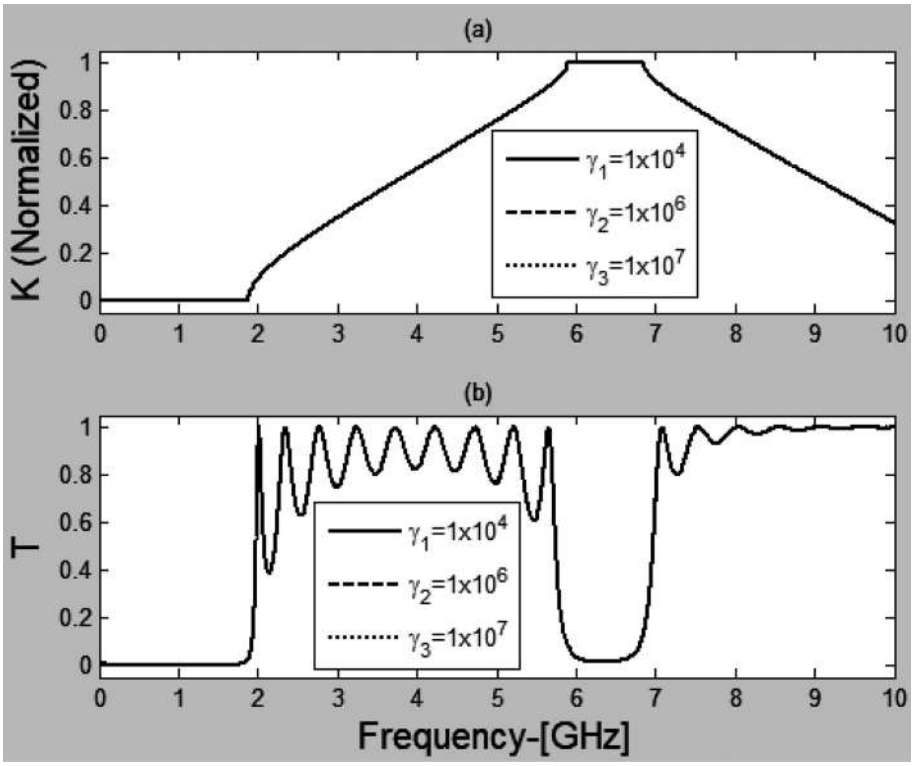

Fig. 7. (a) Dispersion relation and (b) transmittance *versus* frequency plots with varying effective collision frequency of the magnetized cold plasma for left-hand polarization.

and multichannel filter for the right-hand polarization structure for an increased value of the magnetic field, of the magnetized cold plasma, and broadband reflector or high pass filter for the left-hand polarization structure at low value of the magnetic field of the magnetized cold plasma. Besides this, we theoretically propose a design of tunable narrow

band filter for the right-hand polarization structure with different values of electron density of magnetized cold plasma and broadband reflector and high pass filter for the left-hand polarization structure, whose width increases with an increase in the value of electron density of magnetized cold plasma. We have also calculated the band gap structure and transmittance by varying the effective collision frequency for right-hand polarization and left-hand polarization structures where we found that there is no effect of such variation on the band structure. On the basis of our calculated results of the right-hand polarization and left-hand polarization structures, we investigate a new idea for formation of the broadband reflector and narrow tunable filter at lower and higher frequency ranges. Thus, this analysis can be useful in design of tunable photonic devices that can be controlled by changing the parameters of the magnetized cold plasma.

One of the authors, AK, Research Scholar, Department of Physics, Babasaheb Bhimrao Ambedkar University Lucknow, Uttar Pradesh, India, acknowledges UGC, New Delhi for non-NET UGC fellowship.

References

1. V.P. Bykov, Sov. Phys. JETP **35**, 269 (1972).
2. K. Ohtaka, Phys. Rev. B **19**, 5057 (1979).
3. E. Yablonovitch, Phys. Rev. Lett. **58**, 2059 (1987).
4. S. John, Phys. Rev. Lett. **58**, 2486 (1987).
5. J.D. Joannopoulos, R.D. Meade, J.N. Winn, *Photonic Crystals: Molding the Flow of Light* (Princeton University Press, Princeton, 1995).
6. Y. Fink, J.N. Winn, S. Fan, C. Chen, J. Michel, J.D. Joannopoulos, E.L. Thomas, Science **282**, 1679 (1998).
7. T.F. Krauss, R.M. De La Rue, Progr. Quant. Electron. **23**, 51 (1999).
8. D.N. Chigrin, A.V. Lavrinenko, D.A. Yarotsky, S.V. Gaponenko, Appl. Phys. **68**, 25 (1999).
9. K. Sakoda, *Optical Properties of Photonic Crystals* (Springer, Berlin, 2004).
10. X. Gu, X.F. Chen, Y.P. Chen, X.L. Zheng, Y.X. Xia, Y.L. Chen, Opt. Commun. **237**, 53 (2004).
11. S. Massaoudi, A. de Lustrac, I. Huynen, J. Electromagn. Waves Appl. **20**, 1967 (2006).
12. Q.R. Zheng, B.Q. Lin, N.C. Yuan, J. Electromagn. Waves Appl. **21**, 199 (2007).
13. K. Busch, G. von Freymann, S. Linden, S.F. Mingaleev, L. Tkeshelashvili, M. Wegener, Phys. Rep. **444**, 101 (2007).
14. S.V. Gaponenko, *Introduction to Nanophotonics* (Cambridge University Press, Cambridge, 2010).
15. H. Hojo, K. Akimoto, A. Mase, *Conference Digest on 28th International Confereuce on Infrared and Millimeter Waves Otsu* (2003) pp. 347-348.
16. H. Hitoshi, M. Atushi, J. Plasma Fusion Res. **80**, 89 (2004).
17. R. Kumar, *Plasma Photonic Crystal*, in *Photonic Crystals - Innovative Systems, Lasers and Waveguides*, edited by Alessandro Massaro (InTech, 2012).
18. H.G. Booker, *Cold Plasma Waves* (Springer-Verlag, New York, 1984) pp. 23–25.
19. T.C. King, C.C. Yang, P.H. Hseih, T.W. Chang, C.J. Wu, Physica E **67**, 7 (2015).
20. A.H. Aly, H.A. Elsayed, A.A. Ameen, S.H. Mohamed, Int. J. Mod. Phys. B **31**, 1750239 (2017).
21. V. Kumar, K.S. Singh, S.P. Ojha, Progr. Electromagn. Res. M **9**, 227 (2009).
22. X.K. Kong, S.B. Liu, H.F. Jhang, C.Z. Li, Phys. Plasmas **17**, 103506 (2010).
23. A.H. Alyand, D. Mohamed, J. Superconduct. Novel Magn. **28**, 1699 (2015).
24. A. Aghajamali, Appl. Opt. **55**, 6336 (2016).
25. A.H. Aly, H.A. Elsayed, S.A. El-Naggar, J. Mod. Opt. **64**, 74 (2017).
26. A.H. Aly, W. Sabra, H.A. Elsayed, Inter. J. Mod. Phys. B **31**, 1750123 (2017).
27. A.H. Aly, H.A. Elsayed, J. Mod. Opt. **64**, 871 (2017).
28. A.H. Aly, S.A. El-Naggar, H.A. Elsayed, Opt. Express **23**, 15038 (2015).
29. A.H. Aly, in *International Journal of Advanced Applied Physics Research*, Special Issue (2016) pp. 43-47, `https://doi.org/10.15379/2408-977X.2016.04`.
30. A.H. Aly, W. Sabra, H.A. Elsayed, J. Superconduct. Novel Magn. **26**, 553 (2013).
31. A.H. Aly, H. Sayed, J. Nanophoton. **11**, 046020 (2017).
32. A.H. Aly, D. Mohamed, H.A. Elsayed, D. Vigneswaran, J. Superconduct. Novel Magn. `https://doi.org/10.1007/s10948-018-4716-6` (2018).
33. P. Yeh, *Optical Waves in Layered Media* (John Wiley & Sons, New York, 1988).

Indian J Phys (June 2019) 93(6):791–798
https://doi.org/10.1007/s12648-018-1335-9

ORIGINAL PAPER

A tunable broadband filter of ternary photonic crystal containing plasma and superconducting material

A Kumar[1], K B Thapa[1]* and S P Ojha[2]

[1]Department of Physics, School of Physical and Decision Sciences, Babasaheb Bhimrao Ambedkar University, Vidya Vihar, Raebareli Road, Lucknow, UP 226025, India

[2]Department of Physics, Indian Institute of Technology (BHU), Varanasi, UP 221005, India

Received: 02 April 2018 / Accepted: 14 August 2018 / Published online: 15 November 2018

Abstract: This work reports the optical properties of a one-dimensional (1D) ternary periodic structure composed of a dielectric, magnetized cold plasma (MCP) and superconducting material by using well-known simple transfer matrix method. The MCP has considered right-hand and left-hand polarizations having positive (+ B) and negative (− B) transverse magnetic field, respectively. The transmittance of the ternary photonic crystals is analyzed by varying the angle of incidence, the magnetic field, the electron density of the magnetized cold plasma, the temperature of the superconductor, the thickness of magnetized cold plasma and superconducting material for the right-hand and left-hand polarization structures. The transmittance of the ternary photonic crystal containing dielectric, magnetized cold plasma and superconducting material has tunable broadband and narrowband filters for the left-hand and right-hand polarizations, respectively. The magnetized cold plasma layer in the ternary photonic crystal also played an important role to form the tunable gap due to the transverse magnetic field. The analysis of the transmittance of the ternary photonic crystal containing dielectric, magnetized cold plasma and superconducting materials has shown an innovative idea for the formation of the tunable broadband and the narrowband filters.

Keywords: 1D ternary photonic crystal; Magnetized cold plasma; Superconducting material; Tunable broadband and narrowband filters

PACS Nos.: 42.70.Qs-Photonic bandgap materials; 68.65.Ac-Multilayers

1. Introduction

Photonic crystals are artificial dielectric or metallic nanostructures composed of two or more medium in which the dielectric constant varies periodically in space. In 1987, the novel idea of the periodic structure of the dielectric materials was theoretically proposed by Yablonovitch and experimentally observed by John [1, 2]. This type of periodic structure affects the propagation of the electromagnetic wave and is known as photonic crystal (PC). So photonic crystals have a unique feature in which electromagnetic wave does not propagate inside the photonic crystal due to the periodicity of the medium and is called the photonic band gap (PBG). The formation of the PBG due to the periodic media is similar to the electronic band gaps in the solid due to the periodic potentials. Therefore, the periodic structures are used to control the electromagnetic wave propagation owing to the periodicity of the dielectric materials. A few years ago, the researchers focused on superconducting photonic crystal due to its unique behaviors like tenability and negligible loss. The dielectric permittivity of a superconducting material can be tuned with the temperature and the thickness. So, the superconducting photonic crystals have great advantages over metallic and dielectric photonic crystals due to the existence of the tenability parameters [3–24].

The THz transmittance in one-dimensional superconducting nanomaterial dielectric superlattice in many optical applications has been investigated by Aly et al. [25]. Wu et al. studied the band gap extension in one-dimensional ternary metal-dielectric photonic crystal [26]. Jhang investigated the omnidirectional photonic band gap in one-

*Corresponding author, E-mail: khem.bhu@gmail.com

dimensional ternary superconductor dielectric photonic crystal based on a new Thue–Morse aperiodic structure. He demonstrated that the electromagnetic wave does not propagate through the periodic crystal structure below a frequency that is termed as the cutoff frequency [27]. Aly et al. investigated the properties of cutoff frequency in two-dimensional superconducting photonic crystals. They gave a detailed analysis of cutoff frequency where it is needed in the required frequency region for the proper implementation of numerical calculations in many optical applications [28]. Aly and Mohamed reported an analysis of cutoff frequency in a 1D binary superconductor and dielectric photonic crystal. They mentioned that it could be tuned effectively by various parameters of dielectric and superconductor parameters, and their theoretical results could be forwarded to put into applications such as high pass filter and reflector [29]. In addition to this, the theoretical investigations of cutoff frequency in 1D binary superconductor meta-material [30] and superconductor-magnetized cold plasma [31] PCs have been explored in the microwave region. The optical property of 1D all superconducting photonic crystal-comprising pairs of high–high, high–low and low–low refractive indices of the superconductor materials in the visible region has been investigated by Zamani [32]. He has shown in his study that the transmission and reflection spectra of different types of all superconducting photonic crystals are dependent on the temperature and the incident angle. Sreejith has discussed the cutoff frequency in the one-dimensional ternary superconducting photonic crystal [33]. Recently, Aly and Sayed investigated an efficient way to improve the optical property of the pin silicon solar cell by studying the absorption with an anti-reflecting layer [37]. For applications of optical devices, the optical properties of one-dimensional superconductor meta-material photonic crystals by adding two different layers of the semiconductor were investigated by Aly et al. [38]. Recently, Aly et al. also investigated the novel type of smart window using one-dimensional superconductor using nano-metallic photonic crystal [39].

This work reports theoretically that the optical properties of considered ternary periodic structure depend on the parameters of magnetized cold plasma and the superconducting material. Basically, the magnetized cold plasmas form two types of polarizations: (i) right-hand polarization having the positive value of the magnetic field and (ii) left-hand polarization having the negative value of magnetic field. Such right-hand polarization and the left-hand polarization ternary periodic structures are also called the right-hand polarization and left-hand polarization structures. In our calculations, the transmittances of the ternary photonic crystal are studied in detail by varying the incident angle, the magnetic field, the electron density, the temperature and the thicknesses of the magnetized cold plasma and superconducting material. The transmittance properties of considered ternary periodic structure are examined by varying the parameters of the material and by analyzing the transmittance of the ternary periodic structure for a filter application.

2. Theoretical work and methodology

The transmittance of ternary photonic crystal containing dielectric, magnetized cold plasma and high-temperature superconductor ($YBa_2Cu_2O_7$) material is calculated using a simple transfer matrix method [34]. One-dimensional ternary photonic crystal is taken as $(ABC)^N$, where N is a number of the periodicity of the ternary materials; A, B and C are represented dielectric, magnetized cold plasma and superconducting material, respectively. The complex permittivity of the magnetized cold plasma, i.e., layer B, is given as [35],

$$\varepsilon_B(\omega) = 1 - \frac{\omega_{\mathrm{pe}}^2}{\omega^2\left(\left(1 - \frac{i\gamma}{\omega}\right) \mp \frac{\omega_{\mathrm{le}}}{\omega}\right)} \tag{1}$$

with the permeability $\mu_B = 1$ for non-magnetic material; where ω, γ and ω_{le} are the angular, effective and gyro-effective collision frequencies, respectively.

Here, ω_{pe} is the plasma frequency, which is given as [35],

$$\omega_{pe} = \left(\frac{n_e e^2}{m\,\varepsilon_0}\right)^{1/2}, \quad \text{and} \quad \omega_{le} = eB/m; \tag{2}$$

where n_{e}, m, ε_0 are the electron density, the electronic mass, the permittivity in free-space, respectively, and e is the electronic charge [35].

The frequency gap of the dielectric permittivity of the superconducting is close to the metallic material [32, 33]. The dielectric property of the superconductor is dependent on frequency, which can be described by the two fluid models. According to this theory, the relative permittivity of lossless superconducting material, i.e., layer C can be expressed as the following relation [36],

$$\varepsilon_{\mathrm{C}} = \left(1 - \left(\frac{\omega_{\mathrm{th}}^2}{\omega^2}\right)\right) \tag{3}$$

where w_{th} is called the threshold frequency and is given by,

$$\omega_{\mathrm{th}} = \left(\frac{1}{\varepsilon_0 \mu_0 \lambda_{\mathrm{L}}^2}\right) \tag{4}$$

Here λ_{L} is the London penetration depth. The temperature dependence of λ_{L} can be described by,

$$\lambda_L(T) = \left(\frac{\lambda_0}{\sqrt{1-f(T)}}\right) \tag{5}$$

where λ_0 is the London penetration depth at $T = 0$ K. According to Gorter–Casimir model, $f(T)$ is suggested in the following form,

$$f(T) = \left(\frac{T}{T_c}\right)^p \tag{6}$$

where T_c is the transition temperature and T is the operating temperature, and $p = 2$ for high-temperature superconductor and $p = 4$ for low-temperature superconductor [36].

Now, the optical property of the considered structure is calculated by considering the characteristic matrix for considered ternary photonic crystal, i.e., $(ABC)^N$, and the characteristic matrix for ternary layers can be expressed by [34],

$$M(d) = \begin{pmatrix} m_{1,1} & m_{1,2} \\ m_{2,1} & m_{2,2} \end{pmatrix} \tag{7}$$

where $M(d) = (M_A M_B M_C)^N$; N is the periodicity of the photonic crystal, M_A, M_B and M_C are the characteristics matrices of layer A, B and C, respectively.

The characteristics matrix of each layer can be obtained by considering the electric field on each surface. For ternary periodic structure, we have considered three layers with boundary conditions in the x-direction. The electric field in each interface is given by;

$$\vec{E} = \begin{cases} \left(\overrightarrow{E_1} e^{i\overrightarrow{k_1}\cdot\overrightarrow{r}} + \overrightarrow{E_1}' e^{-i\overrightarrow{k_1'}\cdot\overrightarrow{r}}\right) e^{i\omega t}, & -d_A < x < 0; \\ \left(\overrightarrow{E_2} e^{i\overrightarrow{k_2}\cdot\overrightarrow{r}} + \overrightarrow{E_2}' e^{-i\overrightarrow{k_2'}\cdot\overrightarrow{r}}\right) e^{i\omega t}, & 0 < x < d_B; \\ \left(\overrightarrow{E_3} e^{i\overrightarrow{k_3}\cdot\overrightarrow{r}} + \overrightarrow{E_3}' e^{-i\overrightarrow{k_3'}\cdot\overrightarrow{r}}\right) e^{i\omega t}, & d_B < x < d_{B+C}; \end{cases}$$

where k_1, k_2 and k_3 are the propagation vectors corresponding to the dielectric, the magnetized cold plasma and the superconducting material with the above boundary conditions. E_i and $E_i^{'}$ are the incident and the reflected waves where $i = A$, B and C layers. By using Maxwell's equations, we obtain the corresponding magnetic field. The electric and the magnetic fields may be used to the formulation of the characteristics matrix of each layer.

The characteristic matrix M_i for each layer where $i = A$, B and C is calculated for the TE wave at the angle of incidence θ_0 [30].

$$M_i = \begin{bmatrix} \cos\gamma_i & -\frac{i}{p_i}\sin\gamma_i \\ -ip_i\sin\gamma_i & \cos\gamma_i \end{bmatrix}; \tag{8}$$

where $\gamma_i = (w/c)\ n_i d_i \cos\theta_i$, c is the speed of light in vacuum, θ_i is the ray angle inside ith layer with a refractive index as, $n_i = \sqrt{\mu_i \varepsilon_i}, p_i = \sqrt{\frac{\varepsilon_i}{\mu_i}}\cos\theta_i$, and $\cos\theta_i = \sqrt{1 - \frac{n_0^2 \sin^2\theta_0}{n_i^2}}$ in which n_0 is the refractive index of air, where the incidence wave tends to enter the structure. The transmission coefficient of the ternary photonic crystal is calculated by,

$$t = \frac{2p_0}{(m_{11} + m_{12}p_s)p_0 + (m_{21} + m_{22}p_s)} \tag{9}$$

where $p_0 = n_0\cos\theta_0$ and $p_s = n_s\cos\theta_s$, where n_s is the refractive index of the substrate, θ_s is the ray angle. The transmission spectra of the ternary photonic crystal are given by,

$$T = \left(\frac{p_s}{p_0}\right)|t^2| \tag{10}$$

3. Results and discussion

In this work, we have theoretically studied the optical properties of one-dimensional ternary photonic crystal composed of alternating dielectric, magnetized cold plasma and superconducting material by using simple transfer matrix method for right-hand polarization and left-hand polarization [30]. As we know, the magnetized cold plasma demonstrates the right-hand polarization and the left-hand polarization by changing the direction of the magnetic field only, i.e., positive/negative values of the magnetic field. The applied transverse magnetic field also changes the permittivity of the superconducting material and magnetized cold plasma. Due to simple fabrication of the one-dimensional photonic crystal, the transmittance of the right-hand polarization and the left-hand polarization one-dimensional ternary photonic crystal against frequency (GHz) is plotted by varying most valuable parameters: the angle of incidence, the magnetic field, the electron density of magnetized cold plasma, the temperature of superconductor, and the thicknesses of magnetized cold plasma and superconducting materials. The transmittance study gives an informative idea for optical applications in filters.

As shown in Fig. 1, the ternary photonic crystal is $(ABC)^N$ where A, B and C represent the air, the magnetized

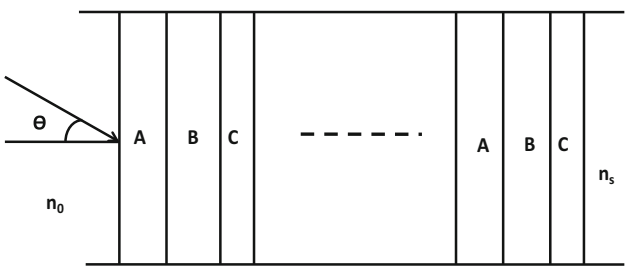

Fig. 1 Schematic diagram of a ternary periodic structure with dielectric (A), magnetized cold plasma (B) and superconductor (C)

cold plasma and superconducting material ($YBa_2Cu_2O_7$) with critical temperature T_c = 92 K and the operating temperature T = 4.2 K, respectively. The thickness of the A, B and C are 18 mm, 18 mm and 80 nm, respectively. The refractive indices of layers A, B and C are $n_A = 1$, $n_B = \sqrt{\varepsilon_B \mu_B}$ and $n_C = \sqrt{\varepsilon_C \mu_C}$, respectively [31, 35, 36]. The periodicity of the lattice (N) is taken as three periods, i.e., $N = 3$.

We calculate the transmittance of the one-dimensional ternary photonic crystal by varying most valuable parameters: the angle of incidence, the magnetic field, the electron density of the plasma, the temperature and the thickness of the magnetized cold plasma and superconducting material. Firstly, we calculate the transmittance of the considered structure by varying the angle of incidence for the right-hand polarization and left-hand polarization structures. The transmittance of the considered ternary photonic crystal against frequency (GHz) with thickness d_A = 18 mm, refractive index $n_A = 1$ (air), external magnetic field B = 0.4T, plasma density $n_e = 12 \times 10^{17}/m^3$, effective collision frequency of magnetized cold plasma $\gamma = 1 \times 10^7$ GHz, transition temperature of high-temperature superconductor ($YBa_2Cu_2O_7$) T_c = 92 K and operating temperature T = 4.2 K by varying incident angles $\theta = 0°$, $\theta = 30°$ and $\theta = 40°$ are studied. The transmittance of the ternary photonic crystal with right-hand polarization material against frequency (GHz) by varying incident angles, $\theta = 0°$, 30° and 40°, is shown in Fig. 2. The zero transmittance at the lower frequency range, 0–1.0 GHz, is due to superconducting behavior inside the structure, and the transmittance at the higher frequency range, 2.3–10.0 GHz, is due to the effect of dielectric behavior of air and magnetized cold plasma material. The transmittance found a negligible shifting for all the angles of incidence at the lower frequency range, i.e., $\theta = 0°$, 30° and 40°. This shows that the incidence angles is independent of the angles at the low frequency because the refractive index of the superconductor does not vary with the angle of incidence. This region acts as a low cutoff frequency for the ternary photonic crystal and has low-pass filter characteristics and may use the low band reflector at the microwave frequency. On the other hand, the transmittance at the higher frequency range for the incident angles $\theta = 0°$, 30° and 40° has shifted toward the higher frequency. Such band acts as a tunable narrowband filter and also uses a multichannel filter by varying the incident angle. As the angle of incidence increases, the band gap also increases at the higher frequency range due to the dielectric behavior of the material as shown in Fig. 2a.

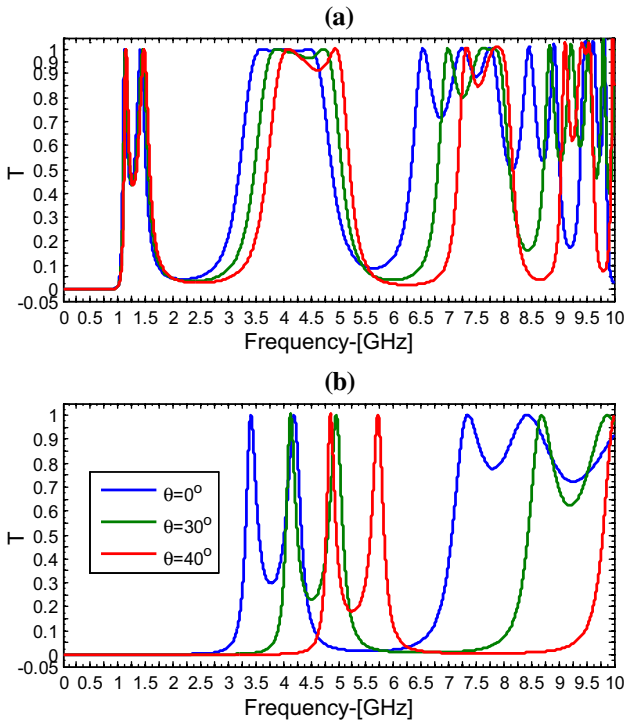

Fig. 2 The transmittance versus frequency by varying angle of incidence for (**a**) right-hand polarization structure and (**b**) left-hand polarization structure

Similarly, the transmittance of the considered ternary photonic crystal against frequency (GHz) with different values of angle of incidences $\theta = 0°$, 30°, 40° for left-hand polarization is studied. In this case, the cutoff frequency for the normal incidence, i.e., $\theta = 0°$ is obtained at 3.2 GHz due to the superconducting layer. The edge of the cutoff frequency shifts toward the higher frequency when the value of incident angles increases due to the effective property of the dielectric material. In the transmittance, the characteristics graph shows that the cutoff frequency becomes 4.5 GHz when the angle of incidence maximum, i.e., $\theta = 40°$. The transmittance of the considered structure at higher frequency range has a huge shift, i.e., 4.5–10 GHz, and obtains a large band gap as shown in Fig. 2b. The left-hand polarization ternary photonic crystal having the large band gap at the low frequency may be used as a broadband reflector or high-pass filter application.

We have compared the transmittance of the right-hand polarization and the left-hand polarization ternary photonic crystals. The left-hand polarization ternary photonic crystal has the better results compared to the right-hand polarization ternary photonic crystal. The cutoff frequency of the left-hand polarization ternary photonic crystal is high in comparison with the right-hand polarization ternary photonic crystal. These studies carried out an informative idea to design a tunable filter which can be tuned by changing the angle of incidence.

As we know, the magnetized cold plasma layer is magnetic field dependent and the superconducting layer, ($YBa_2Cu_2O_7$), is also influenced by the temperature.

Therefore, we have studied the transmittance of the right-hand polarization and the left-hand polarization ternary photonic crystals by varying the magnetic field. The transmittance of the considered ternary periodic structure against frequency (GHz) with the various values of the magnetic field of the magnetized cold plasma, $B = 0.4$T, $B = 0.6$T and $B = 0.8$T, for right-hand polarization, is studied where the wave falls normally, i.e., $\theta = 0°$. The transmittance behavior for the values of magnetic field $B = 0.4$T, $B = 0.6$T, $B = 0.8$T are similar to the previous case when the angle of incidence is varied, but the cutoff band edge is distorted due to change in the gyro-effective frequency. We know that the transmittance is changed due to change in the refractive index. The refractive index of the magnetized cold plasma is dependent on the gyro-effective frequency. So, the refractive index of the right-hand polarization and left-hand polarization ternary photonic crystals is changed due to the applied magnetic field of magnetized cold plasma. Therefore, the transmittance of the ternary photonic crystal with the right-hand polarization material is varied by changing the magnetic field. It means that the permittivity of the magnetized cold plasma is affected only by the applied magnetic field. The cutoff frequency of the right-hand polarization structure increases with increase in the value of magnetic fields shown in Fig. 3a.

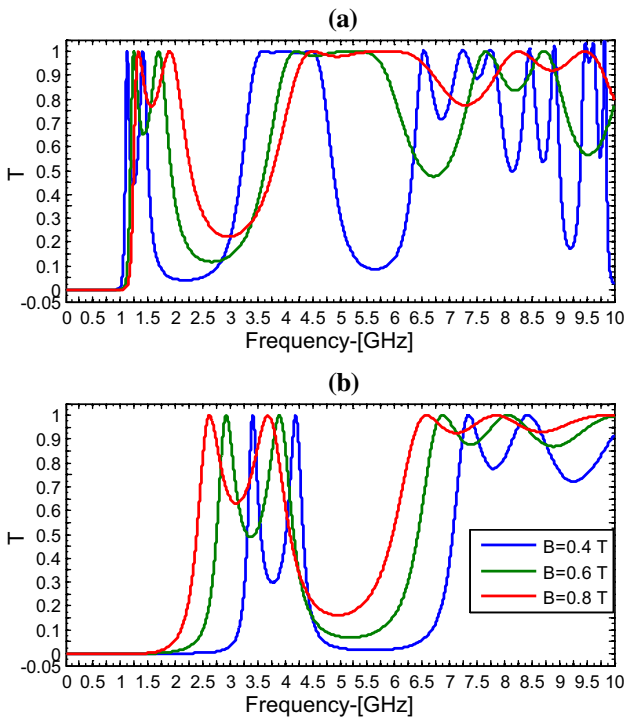

Fig. 3 The transmittance versus frequency by varying magnetic field for (**a**) right-hand polarization structure and (**b**) left-hand polarization structure

Similarly, now we studied the transmittance of considered ternary photonic crystal against frequency (GHz) by varying the magnetic field of magnetized cold plasma for the left-hand polarization, i.e., $B = -0.4$T, $B = -0.6$T, $B = -0.8$T having $\theta = 0°$, $n_e = 12 \times 10^{17}/m^3$ and all parameters same as in the previous calculation. The changed refractive index of the left-hand polarization material is affected by the wave propagation. The transmittance behavior for the left-hand polarization ternary photonic crystal has an opposite trend because the permittivity of the magnetized cold plasma is changed abnormally when the magnetic field applies in the negative direction. The zero transmittance obtains the lowest value for $B = -0.8$T, but this is increased up to 3.2 GHz when the value of the magnetic field decreases as shown in Fig. 3b. The tunable transmittance of the left-hand polarization ternary photonic crystal is obtained by varying the magnetic field. The band gaps at the low frequency, as well as the higher frequency region, are obtained. So, such transmittance behavior of the ternary photonic crystal may be used in the bandpass filter applications.

From Eq. (1), it has been shown that the plasma frequency of the magnetized cold plasma is dependent on the electron density which is next valuable parameter of the magnetized cold plasma and the refractive index of the magnetized cold plasma is dependent upon the plasma frequency. The transmittance of the right-hand polarization and the left-hand polarization ternary photonic crystal is studied by varying the electron density. Now, we focused our study on the transmittance of the considered ternary photonic crystal with right-hand polarization material against frequency (GHz) by varying the values of electron density, i.e., $n_e = 12 \times 10^{17}/m^3$, $16 \times 10^{17}/m^3$ and $20 \times 10^{17}/m^3$. All parameters of the considered structure are same as in the above section. The transmittance of the right-hand polarization ternary photonic crystal at the lower to higher frequency ranges is studied by varying the electron density of the magnetized cold plasma, i.e., $n_e = 12 \times 10^{17}/m^3$, $16 \times 10^{17}/m^3$, $20 \times 10^{17}/m^3$ having the positive magnetic field, i.e., $B = +0.4$T as shown in Fig. 4a. Due to the presence of the superconductor layer, the zero transmittance at the lower frequency range, 0–1.0 GHz, is obtained which is the low cutoff frequency. Such ternary photonic crystal has a low-pass filter characteristic. The cutoff frequency is decreased when the value of electron density of the magnetized cold plasma increases, because of the permittivity of the magnetized cold plasma decreases with increase in the plasma frequency of the magnetized cold plasma.

Similarly, we again studied the transmittance of the left-hand polarization ternary photonic crystal by varying the electron density of the magnetized cold plasma $n_e = 20 \times 10^{17}/m^3$, $16 \times 10^{17}/m^3$, $12 \times 10^{17}/m^3$ having negative

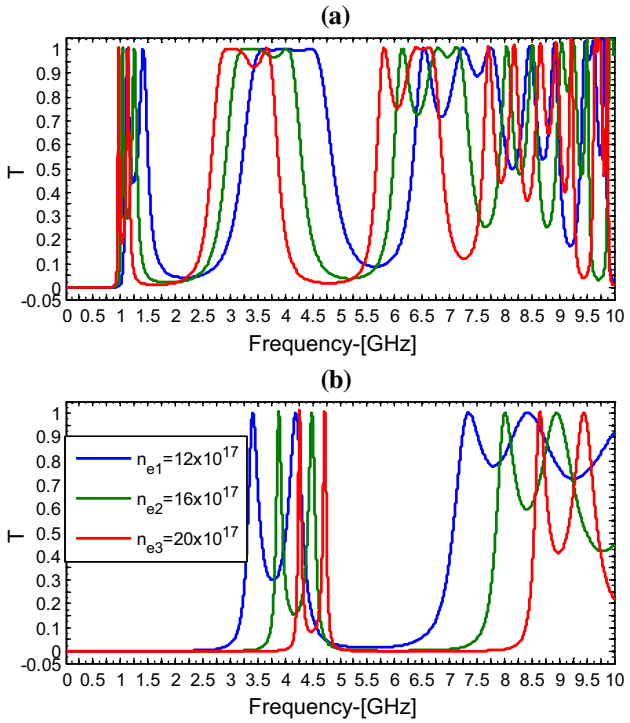

Fig. 4 The transmittance versus frequency by varying electron density of magnetized cold plasma for (**a**) right-hand polarization structure and (**b**) left-hand polarization structure

magnetic field, i.e., $B = -0.4$T. The transmittance at the lower and the higher frequency range is varied due to the effect of electron density of the magnetized cold plasma. The zero transmittance at the lower frequency range is enhanced up to 4.2 GHz when the electron density of magnetized cold plasma increases, i.e., $12 \times 10^{17}/\text{m}^3$, $16 \times 10^{17}/\text{m}^3$, $20 \times 10^{17}/\text{m}^3$ as shown in Fig. 4b. The maximum cutoff frequency is obtained at a maximum value of the electron density of magnetized cold plasma, i.e., $n_e = 20 \times 10^{17}/\text{m}^3$ for the left-hand polarization structure. From Eq. (1), the denominator of permittivity becomes positive when the left-hand polarization material has the negative magnetic field, and the plasma frequency increases with increase in the electron density. Therefore, the permittivity of the magnetized cold plasma is decreased when the value of electron density of the magnetized cold plasma increases. Such band gap of the left-hand polarization ternary photonic crystal region acts as a broadband reflector or a high-pass filter.

The considered ternary photonic crystal has the superconducting material, and this material is affected with different operating temperatures and applied magnetic fields. In this section, the transmittance against frequency (GHz) by varying operating temperature $T_1 = 4.2$ K, 40 K, 150 K of the superconducting material is studied for the right-hand polarization and the left-hand polarization structures. We have taken $YBa_2Cu_2O_7$ material having $T_c = 92$ K, $B = 0.4$T and same parameters as in the above calculations. The transmittance of the right-hand polarization ternary photonic crystal is varied at the lower frequency range due to the effect of superconducting material, but it is not varied at the higher frequency range. So, the effective transmittance at the high frequency shows only due to the effect of dielectric behavior of the air and the magnetized cold plasma materials. The cutoff frequency of the ternary photonic crystal is very sensitive for the operating temperature. It shows that the cutoff frequency is decreased for the operating temperature below the critical temperature, i.e., $T = 4.2$ K, 40 K. But the transmittance is increased due to the effect of the magnetic field in the superconducting material when the operating temperature is larger than the critical temperature, i.e., $T = 150$ K, Fig. 5a.

Similarly, the transmittance of the left-hand polarization ternary photonic crystal against frequency (GHz) by varying operating temperature $T = 4.2$ K, 40 K, 150 K, at magnetic field $B = -0.4$T is studied having the same parameters. The transmittance behavior of the left-hand polarization ternary photonic crystal is not changed compared to the right-hand polarization ternary photonic crystal but the zero transmittance at the lower frequency range is found at 3.2 GHz frequency as shown in Fig. 5b. It means that the transmittance of the considered left-hand

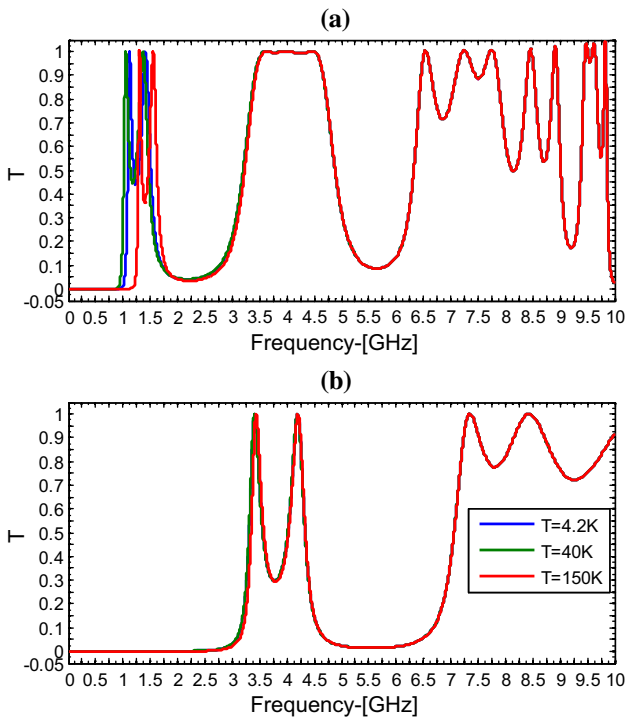

Fig. 5 The transmittance versus frequency by varying temperature of superconductor for (**a**) right-hand polarization structure and (**b**) left-hand polarization structure

polarization ternary photonic crystal is not affected by varying the temperatures. The left-hand polarization ternary photonic crystal may act as a broadband reflector having the cutoff frequency 3.2 GHz.

In this section, we studied the transmittance against frequency (GHz) by varying the thickness of the magnetized cold plasma for right-hand polarization and left-hand polarization as shown in Fig. 6. The transmittance against frequency (GHz) by varying the thickness of the superconducting material for right-hand polarization/left-hand polarization is shown in Fig. 7. The transmittance against frequency (GHz) for the right-hand polarization is studied by varying the thickness of the magnetized cold plasma, i.e., 18, 22 and 26 mm having $B = 0.4\text{T}$ and $n_e = 12 \times 1017/\text{m}^3$, as shown in Fig. 6a. The cutoff frequency for the right-hand polarization ternary photonic crystal with the superconducting material is decreased with increase in the thicknesses of the magnetized cold plasma material, i.e., 0.0–1.0 GHz. The transmittance at the higher-frequency region has obtained large variation due to the effect of the thickness of the magnetized cold plasma layer.

Similarly, the transmittance of the considered ternary periodic the left-hand polarization ternary photonic crystal against frequency (GHz) is studied by varying the thickness of the magnetized cold plasma with the same parameters as earlier calculations. The cutoff frequency of the considered left-hand polarization ternary photonic crystal has an

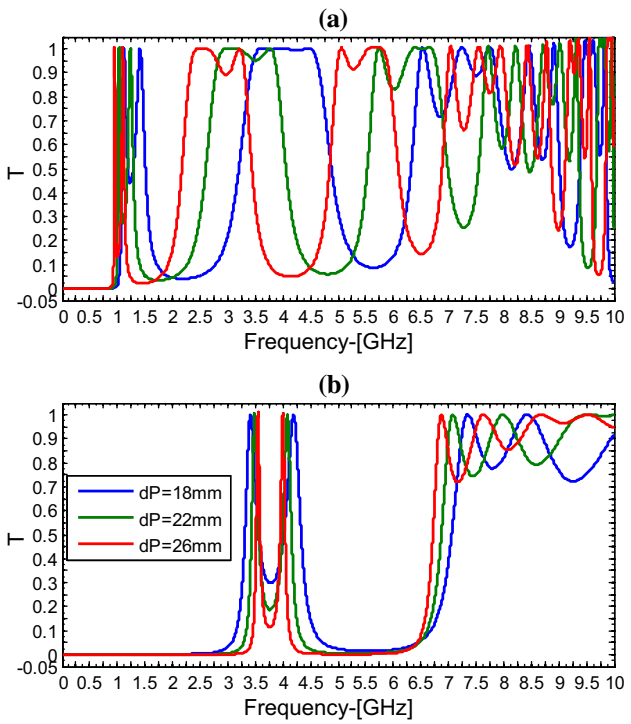

Fig. 6 The transmittance versus frequency by varying thickness of magnetized cold plasma for (**a**) right-hand polarization structure and (**b**) left-hand polarization structure

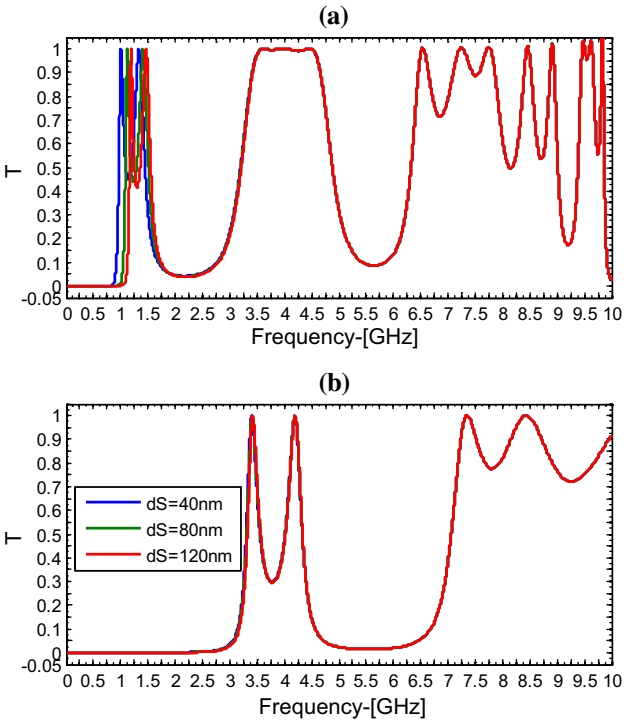

Fig. 7 The transmittance versus frequency by varying thickness of superconductor for (**a**) right-hand polarization structure and (**b**) left-hand polarization structure

opposite trend for the lower-frequency region to the higher-frequency region, i.e., the transmittance at the lower frequency range, 0–3.4 GHz, is increased with increase in the thickness of the magnetized cold plasma material but the transmittance at the higher frequency range is decreased with increase in the thickness of the magnetized cold plasma material as shown in Fig. 6b. In between these frequencies, a low-value transmittance is obtained that is independent of the thicknesses of the magnetized cold plasma material. It may be used as a narrowband filter application.

Now, we studied the transmittance against frequency (GHz) with different values of the thickness of the superconducting layer, i.e., 40 nm, 80 nm and 120 nm and other parameters are same as in previous calculation. The transmittance at the lower frequency range has varied only due to the effect of the thickness of the superconducting material as shown in Fig. 7a. However, the transmittance at the higher-frequency region is constant for all thicknesses. The cutoff frequency of the right-hand polarization ternary photonic crystal is slightly changed. The large cutoff frequency is found when the thickness of the superconducting material is 120 nm. The cutoff frequency of the superconducting material is increased with increase in the thickness of the superconducting material.

Similarly, the transmittance of the considered cutoff frequency for the left-hand polarization material is studied

by varying thickness of the superconducting material, i.e., 40 nm, 80 nm and 120 nm as shown in Fig. 7b. The transmittance of the left-hand polarization ternary photonic crystal is independent of the thickness of the superconducting material. The study of transmittance of the left-hand polarization ternary photonic crystal reveals that the transmittance characteristics by varying thickness of the superconducting material having dielectric nature when the magnetic field is applied in reversed direction, i.e., $B = -4$T. This result is similar to the right-hand polarization ternary photonic crystal having the same temperature as shown in Fig. 5b.

4. Conclusions

In this work, we studied theoretically the transmittance of the considered ternary photonic crystal against frequency (GHz) by varying the angle of incidence, the magnetic field, the electron density of the magnetized cold plasma, the temperature and the thickness of the magnetized cold plasma for the right-hand polarization/the left-hand polarization structure. The optical properties of the right-hand polarization and the left-hand polarization ternary photonic crystals are affected by the effective parameters of the magnetized cold plasma and the superconducting material. The transmittance of the left-hand polarization ternary photonic crystal has found the better results compared to the transmittance of the right-hand polarization ternary photonic crystal due to the presence of the superconducting layer that is influenced by the temperature and the magnetic field itself. The large band gap of the left-hand polarization ternary photonic crystal may be used as the broadband reflector or high-pass filter applications. The superconducting layer has played the important role to form the band gap of the ternary photonic crystal. However, the tunable transmittance of the right-hand polarization ternary photonic crystal has also been obtained by varying parameters of the magnetized cold plasma. Such a structure may be used as a tunable filter. On the basis of our calculated results, we proposed an innovative idea to design the broadband reflector or the high-pass filter and the narrow tunable filter of the ternary photonic crystal containing the magnetized cold plasma and the superconducting material under certain the transverse magnetic field and the operating temperature.

Acknowledgements One of the authors, Asish Kumar, Research Scholar, Department of Physics, Babasaheb Bhimrao Ambedkar University (A Central University) Lucknow, acknowledges UGC, New Delhi, for non-NET UGC fellowship.

References

[1] E Yablonovitch *Phys. Rev. Lett*. **58** 2059 (1987)
[2] S John *Phys. Rev. Lett.* **58** 2486 (1987)
[3] J D Joannopolos Johnson R D Meade and J N Winn *Photonic crystals: Molding the flow of light, Princeton*. New Jersey: Princeton University Press (2007)
[4] E Centeno B Guizal D Felbacq *J. Opt. A* **1(5)** L10 (1999)
[5] B Temelkuran M Bayindir E Ozbay R Biswas M M Sigalas G K Tuttle M Ho *J. Appl. Phys.* **87** 603 (2000)
[6] Y B Chen C Zhang Y Y Zhu S N Zhu N B Ming *Mater. Lett.* **55** 12 (2002)
[7] T V Murzina, F Y Sychev E M Kim, E I Rau, S S Obydena, O A Aktsipetrov M A Bader G Marowsky *J. Appl. Phys.* **98**, 123702 (2005)
[8] P St. J Russell *J. Light wave Technol.* **24** 4729 (2006)
[9] Z Qiang W Zhou R A Soref *Opt. Exp*. **15** 1823 (2007)
[10] B Curtin R Biswas V Dalal *Appl. Phys. Lett.* **95** 231102 (2009)
[11] T Ergin T Benkert H Giessen M Lippitz *Phys. Rev. B* **79** 245134 (2009)
[12] P Rani Y Kalra R K Sinha *Opt. Commun*. **298** 227 (2013)
[13] C Caër, S Combrié, X Le Roux, E Cassan, A De Rossi *Appl. Phys. Lett.* **105** 121111 (2014)
[14] R Kakimi M Fujita M Nagai M Ashida T Nagatsuma *Nat. Photonics* **8** 657 (2014)
[15] N M Dsouza V Mathew *Appl. Opt*. **54** 2187 (2015)
[16] J N Dash R Jha J Villatoro S Dass *Opt. Lett.* **40** 467 (2015)
[17] X Xiao, W Wenjun, L Shuhong, Z Wanquan, Z Dong, D Qianqian, G Xuexi, Z Bingyuan *Optik-Int. J. Light Electron Opt.* **127** 135 (2016)
[18] H M Lee J C Wu *J. Appl. Phys.* **107** 09E149 (2010)
[19] W H Lin C J Wu T J Yang S J Chang *Opt. Express* **18** 27155 (2010)
[20] P Athe S Srivastava *J. Supercond. Novel Magn*. **28** 2331 (2015)
[21] J Wu, J Gao *J. Supercond. Novel Magn*. **28** 1971 (2015)
[22] M Upadhyay, S K Awasthi, L Shiveshwari, S N Shukla, S P Ojha *J. Supercond. Nov Magn.* **28** 1937 (2015)
[23] A H Aly, H T Hsu, T J Yang, C J Wu, C K Hwangbo *J. Appl. Phys.* **105** 083917 (2009)
[24] A H Aly, A Mehaney, S A El-Naggar *J. Supercond. Nov Magn*. **30** 2711 (2017)
[25] A H Aly, S W Ryu, H T Hsu and C J Wu, *Materials Chem. Phys.* **113** 382 (2009)
[26] C J Wu Y H Chung and B J Syu *Progress In Electromagnetics Research* (PIER) **110** 81 (2010)
[27] H F Jhang *J. Supercond. Nov. Magn*. **27** 41 (2014)
[28] A H Aly H A Elsayed S A El Naggar *J. Mod. Opt.* **61** 1064 (2014)
[29] A H Aly D Mohamed *J. Supercond. Nov. Magn.* **28** 1699 (2015)
[30] A H Aly A Aghajamali H A Elsayed M Mobarak *Physica C: Superconductivity and its Applications* **528** 5 (2016)
[31] A Aghajamali *Appl. Opt*. **55** 6336 (2016)
[32] M Zamani *Physica C* **520** 42 (2016)
[33] K P Sreejith *Physica C* **540:** 44-47 (2017)
[34] P Yeh *Optical Waves in Layered Media. New York: Wiley* (1988)
[35] H G Booker *Cold Plasma Waves. New York: Springer*, **23** (1984)
[36] M Tinkham *Introduction to Superconductivity, Courier Corporation, USA* (1996)
[37] A H Aly H Sayed *Surf. Rev. Lett.* **25(8)** 1850103 (2017).
[38] A H Aly D Mohamed H A Elsayed D Vigneshwaran *J. Supercond. Nov. Magn*. (2018) https://doi.org/10.1007/s10948-018-4628-5
[39] A H Aly A A Ameen D Vigneshwaran *J. Supercond. Nov. Magn*. (2018) https://doi.org/10.1007/s10948-018-4716-6

Optical and Quantum Electronics (2019) 51:355
https://doi.org/10.1007/s11082-019-2070-y

Multichannel filter application of a magnetized cold plasma defect in periodic structure of ZnS/TiO_2 materials

Asish Kumar[1] · **Khem B. Thapa**[1]

Received: 20 April 2019 / Accepted: 10 October 2019 / Published online: 19 October 2019

Abstract
In this article, transmission spectra of multilayer structure of zinc sulfide (ZnS) and titanium dioxide (TiO_2) with defect of magnetized cold plasma (MCP) have been calculated theoretically by using characteristics transfer matrix method. The transmission spectra versus frequency have been analyzed for symmetric and asymmetric structure. Due to have a multiple band gaps in the asymmetric structure, we have taken the asymmetric structure for analysis with the parameters of MCP and the thicknesses of the dielectric materials. It is well known that magnetized cold plasma is an abnormal material because the permittivity changes with applied external magnetic field, and shows tunable photonic band gap for permittivity of the MCP. Now, the transmission spectra of the asymmetric structure versus frequency by inserting one or two magnetized cold plasma layer were analyzed with the variation of incident angles, the parameters of MCP, and the thicknesses of ZnS and TiO_2 material. The analyzed transmission spectra of asymmetric structure with the variation of electron density, thicknesses of dielectric materials were obtained better results with defect of two plasma layers as compare to the defect of one layer of plasma. These obtained results reveal that the defect of two magnetized cold plasma layers of one dimensional asymmetric structure of ZnS, TiO_2 may be used for the tunable multichannel filter at microwave region.

Keywords Zinc sulfide (ZnS) · Titanium oxide (TiO_2) · Magnetized cold plasma (MCP) · Defect MCP multilayer structure

1 Introduction

Photonic crystals (PCs) are periodic structure of nanostructures and microstructure in which the optical constant of two or more than two medium varied in the space. First time, Yablonovitch (1987) and John (1987) proposed the origin of photonic band gap. Presently, photonic crystals are more attractive in research community due to its abnormal band gap properties. Photonic band gap (PBG) is the unique properties of photonic crystal. The

✉ Khem B. Thapa
khem.bhu@gmail.com

[1] Department of Physics, School of Physical and Decision Sciences, Babasaheb Bhimrao Ambedkar University, Lucknow, U.P 226025, India

photonic band gap is produced when the electromagnetic wave propagates through the periodic structure with a certain frequency which frequency does not propagate and create a frequency gap is known as photonic band gap. The wave propagation inside the periodic structure depends on the unique property of material i.e. refractive index, unit cell, the filling fraction, frequency and dimensionality, etc. (Joannopolos et al. 1995). The PBG material has the great application in research and technology because it can be used to control and manipulate the flow of electromagnetic wave. The one-dimensional photonic crystals (1-DPCs) are the simplest structures because the direction of the wave propagation in one dimension, and the 1-DPC can be easily fabricated using the modern thin film technology. Presently, 1-DPCs have lots of applications in the different directional field of optics: optical engineering, photonic device, optical filter; resonance cavity, laser application, high-reflecting omni-directional mirror, and optoelectronic circuit (Fink et al. 1998; Krauss and De La Rue 1999; Chigrin et al. 1999; Sakoda 2004; Gu et al. 2004; Massaoudi et al. 2006; Zheng et al. 2007; Busch et al. 2007; Gaponenko 2010).

Plasma is a hot ionized gas consisting of equal number of positively charged ions and negatively charged electrons. The characteristics properties of plasma are different from those of the ordinary neutral gases. A non-thermal plasma or cold plasma or non-equilibrium plasma is plasma that is not in thermodynamic equilibrium because temperature of electron is much hotter than the temperature of heavy species like ions and neutrals. Now, plasma has been introduced in photonic crystals to create the tunable plasma photonic band gap at microwave region. One-dimensional multilayer periodic structure of thin plasma and dielectric materials is known as plasma photonic crystal (PPC). Therefore, the plasma photonic crystal becomes an active research area in field of photonics. Plasma material has lots of potential applications and perform plasma photonic band gap, which is similar to periodic structure of dielectric material (Hojo et al. 2003; Hitoshi and Atushi 2004; Kumar 2012). Plasma photonic crystal displays strong spatial dispersion resulting in the appearance of electromagnetic band gap structure (Kong et al. 2010a; Zhang et al. 2011a, b). At the same year, some experiments about one dimensional and two dimensional plasma photonic crystals had also been done by the Sakai research group (Sakaguchi et al. 2007; Sakai et al. 2005, 2007). The plasma photonic band gap can be also controlled by the variable parameters of plasma material. Some previous years, magnetized cold plasma had attracted to lots of researchers due to abnormal behavior. If the external magnetic field is introduced in plasma photonic crystal then a new kind of photonic crystal generates is called magnetized cold plasma. The MCP has one extra variable in the presence of magnetic field, called gyro-effective frequency. MCP has unique property that the wave propagates in positive and negative direction due to effect of applied magnetic field (Booker 1984; King et al. 2015; Aly et al. 2017a). The magnetized plasma photonic crystals are more interesting properties comparison to conventional plasma photonic crystals (Feng and Kong 2012). The magnetized plasma materials exhibit tunable photonic band gaps. So the adhesive materials with plasma are considered for possible fabrication of multilayer structure with magnetized cold plasma material because the multilayer structure with magnetized cold plasma material has abnormal optical properties. Kumar et al. (2009) have investigated the dispersion relation, reflection spectra of the periodic structure of dielectric and magnetized cold plasma material. Narrow and tunable filters of the similar structure with defect of magnetized cold plasma had suggested by Kong et al. (2010b). Aly and Mohamed (2015) recommended the transmission spectra of 1-DPC of the superconducting material and dielectric material for the applications of band pass filter. The transmittance property of magnetized cold plasma-superconductor periodic multilayer structure had proposed by Aghajamali et al. (2016) for the applications in reflectors. Aly and Sayed (2017) designed

the periodic structure to enhance the electromagnetic wave absorption by varying the optical length of the electromagnetic wave propagate inside the absorbing material which used to enhance the efficiency of silicon solar cell device. Aly et al. (2018) proposed an idea for the optical properties of a new type of superconductor and semiconductor meta-material photonic crystals. The transmittance property of one dimensional periodic structure of defective photonic crystal had done and analyzed that defect of photonic band gap at the central wavelength vary with variation angle of incidence in ultraviolet region by Aly and El Sayad (2012). The transmittance of one dimensional defective photonic crystal structure had studied, and analyzed the tunability of one dimensional periodic structure based on Faraday Effect (Aly and ElSayad 2016). Optical properties of one dimensional defective photonic crystal containing nanocomposite material of silver (Ag) as a defect layer had analyzed in UV region with varying other parameters by Aly et al. (2017b). Transmittance properties of two types of one-dimensional periodic structures and the optical properties of meta-material superconductor photonic band gap with/without defect layer analyzed by Aly (2009, 2018). Aly (2012) had also analyzed the metal-dielectric periodic structure and defect mode characterizations. Kumar and Thapa (2018) and Kumar et al. (2018a) recommended the optical property of one-dimensional photonic crystal of negative photonic crystal with the defect of plasma material and also analyzed for silicon and silicon dioxide periodic structure with defect of plasma material. Kumar et al. (2018b) also proposed the transmittance property of one-dimensional dielectric magnetized cold plasma periodic structure for optical applications. Kumar et al. (2019) also analyzed the transmittance of ternary periodic multilayer structure of dielectric, plasma and superconductor for the application tunable reflector applications. Recently, tunable multichannel filter had designed using one dimensional photonic crystal incorporating uniaxial meta-material at microwave region (Kazempour 2019). On the basis of reviewing these research papers, we have found several ideas related to tunable narrowband filter applications at microwave region. On the other hand, we have chosen one-dimensional periodic structure for analyzing tunable narrowband filter due to cheap and easy to fabricate the devices.

In this work, we study and analyze the transmittance versus frequency (GHz) of one-dimensional periodic structure of ZnS and TiO_2 layers with defect magnetized cold plasma (MCP) for symmetric and asymmetric structures using transfer matrix method (TMM) and Bloch's wave. The optical constant of MCP material is tuned with variables parameters of the plasma. Therefore, we calculate the transmittance of MCP defective photonic crystal with variation of incident angle, electron density magnetic field and thickness of ZnS and TiO_2 material. Besides this, we calculate and compare the transmittance of the considered structures with one and two defect MCP layers. The transmittance versus frequency of considered periodic multilayer structures analyze for potential application in tunable multichannel filter at microwave region.

2 Theory and methodology

The band gap, transmission spectra, reflection spectra and absorption spectra of 1-DPC are calculated using transfer matrix method (TMM) (Yeh 1988; Ward and Pendry 1996). The concept of computational studies of Maxwell's equations in complex geometries encounters in periodic structure calculations have lots of difficulties when several length scales of periodic structures occurs, such as the wavelength of light in free space and skin depth in metal. These difficulties are remedied by using an adaptive system which expands

or contracts length scale as need. Here, we show that moving general transformation is equivalent to renormalizing of the electric permittivity and magnetic permeability of the material. This simplifies theory was also given by Yeh (1988) and Ward and Pendry 1996) pioneering work for the refraction and geometry of the Maxwell's equations attached. For our calculations, we have taken symmetric and asymmetric structure where $(AB)^N$ and $(AB)^{N/2}(BA)^{N/2}$ are symmetric and asymmetric structure. The asymmetric structure with defect of two magnetized cold plasma layers is $(AB)^{N/2}(CC)(BA)^{N/2}$ form, where A, B and C shows the zinc sulfide (ZnS) and titanium dioxide (TiO_2), and MCP layers (Lee and Yao 2003; Kong et al. 2010c; Palik 1998; Cai and Shalaev 2010) as shown in the Fig. 1.

Now, the optical constant of magnetized plasma layer (C) has a complex permittvity followed by;

$$\varepsilon_c(\omega) = 1 - \frac{\omega_p^2}{\omega\left(\left(1 + \frac{i\gamma}{\omega}\right) \mp \frac{\omega_{le}}{\omega}\right)} \mu_c = 1 \tag{1}$$

where ω is angular frequency, γ is effective collision frequency, and ω_{le} is gyro-effective frequency). The ω_p is plasma frequency which is given by;

$$\omega_p = \left(\frac{n_e e^2}{m \varepsilon_0}\right)^{1/2} \tag{2}$$

where n_e, m, ε_0, and e are electron density, mass of electron, permittivity in free space, electronic charge of the plasma material respectively.

The expression of gyro-effective frequency (ω_{le}) is given as;

$$\omega_{le} = \left(\frac{eB}{m}\right) \tag{3}$$

where e, B, and m are the electronic charge, applied external magnetic field and mass of electron of the plasma, respectively (Booker 1984). Here, plasma material is taken as a dielectric materials with μ = 1. In our calculation the electron collision frequency or the value of damping is so negligible; the imaginary part of ε (ω) has not so effective in the calculations which has included in the revised manuscript. The ω and γ are angular frequency of incident wave and damping frequency or electron collision frequency of the plasma respectively. The γ is the property of the MCP where ω is the property of the interacted waves.

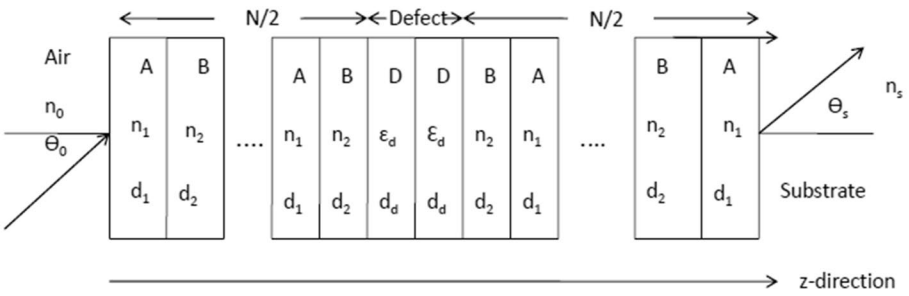

Fig. 1 Schematic diagram of 1-DPC with defect of two magnetized cold plasma

Therefore, ω and γ have lots of difference in the nature. The suffix le is used for gyro-electric frequency of the MCP.

On the basis of transfer matrix method, the optical properties of the finite structure can be analyzed by considering the characteristic matrix M_i for the transverse electric mode at wave angle Θ_0 from free space to a 1-DPC structure as shown in the Fig. 1 (Yeh 1988; Ward and Pendry 1996).

$$M_i = \begin{bmatrix} \cos\gamma_i & -\frac{i}{p_i}\sin\gamma_i \\ -ip_i\sin\gamma_i & \cos\gamma_i \end{bmatrix} \tag{4}$$

and $\gamma_i = \left(\frac{\omega}{c}\right) n_i\, d_i\, \cos\theta_i$, where c is speed of light in vacuum, θ_i is ray angle at surface ith layer with refractive index $n_i = \sqrt{\mu_i\,\varepsilon_i}$, and impedance $p_i = \sqrt{\frac{\varepsilon_i}{\mu_i}}\cos\theta_i$ and angle $\cos\theta_i = \sqrt{1 - \frac{n_0^2\sin^2\theta_0}{n_i^2}}$ in which n_0 is the optical constant of the free space. Using this characteristic matrix (M_i), we can construct the matrix for finite symmetric, asymmetric and defective asymmetric structure with the unit cell length d, which is given by;

$$M(d) = \begin{pmatrix} m_{1,1} & m_{1,2} \\ m_{2,1} & m_{2,2} \end{pmatrix} \tag{5}$$

where $M(d) = \left(M_A\, M_B\right)^N$ for symmetric, $M(d) = \left(M_A\, M_B\right)^{N/2}\left(M_B\, M_A\right)^{N/2}$ for asymmetric and $M(d) = \left(M_A\, M_B\right)^{N/2}(CC)\left(M_B\, M_A\right)^{N/2}$ for defective asymmetric. The characteristic matrix M_A, M_B and M_C are the characteristics layer A (ZnS), B (TiO_2) and C (MCP), respectively.

The transmission coefficient of the considered periodic structure is calculated by Yeh (1988), Ward and Pendry (1996);

$$t = \left| \frac{2p_0}{(m_{1,1} + \frac{m_{1,2}}{p_0}) + (m_{2,1}\, p_0 + m_{2,2})} \right| \tag{6}$$

where $p_0 = n_0\cos\theta_0$ and $p_s = n_s\cos\theta_s$, n_s is the optical constant of air substrate, Θ_s is the incident angle at air substrate. The transmission spectra of the periodic multilayer is followed by-

$$T = \left(\frac{p_s}{p_0}\right)|t|^2 \tag{7}$$

Using Eqs. (6) and (7), we can calculate the transmittance of the finite symmetric, asymmetric and defective asymmetric structure with suitable thicknesses and refractive indices of the layer A (ZnS), B(TiO_2) and C (MCP) at specific frequency range.

3 Results and discussion

In this section, transmittance characteristics of symmetric and asymmetric 1D periodic structures of zinc sulfide (ZnS) and titanium dioxide (TiO_2) are analyzed using transfer matrix method (TMM). The transmittance of considered defect periodic structure is analyzed by inserting the one and two plasma layers in the symmetric and the asymmetric

structure. The parameters for ZnS material are $\varepsilon_A = 6.25$, $\mu_A = 1$, $d_A = 0.0188$ mm, and TiO_2 material are $\varepsilon_B = 5.05$, $\mu_B = 1$, $d_B = 0.0375$ mm (Lee and Yao 2003; Kong et al. 2010c; Palik 1998; Cai and Shalaev 2010). The parameters for magnetized cold plasma (MCP) material are taken from Booker (1984) that is $\varepsilon_c(\omega) = 1 - \frac{\omega_p^2}{\omega\left(\left(1+\frac{i\gamma}{\omega}\right)\mp\frac{\omega_{le}}{\omega}\right)}$ $\mu_c = 1$ where ω (angular frequency), γ (effective collision frequency) and ω_{le} (gyro-effective frequency) (Booker 1984). The ω_p plasma frequency is $\omega_p = \left(\frac{n_e e^2}{m\varepsilon_0}\right)^{1/2}$ where n_e (electron density), m (mass of electron), ε_0 (permittivity in free space), e is electronic charge. The expression of gyro-effective frequency is given as; $\omega_{le} = \left(\frac{eB}{m}\right)$ where e, B, and m are the electronic charge, magnetic field and mass of electron, respectively (Booker 1984). The value of parameters for MCP material is electric charge, $e = 1.6 \times 10^{-19}$ C, permittivity in free space, $\varepsilon_0 = 8.854 \times 10^{-12}$ m^{-3} Kg^{-1} s^4 A^2, external magnetic field, B = 0.4 T, mass of electron, $m = 9.11 \times 10^{-31}$ Kg, electron density of magnetized plasma,$n_e = 3.54 \times 10^{16}/m^3$, and $\gamma = 1 \times 10^7$ Hz (Booker 1984).

Using these parameters with TMM, transmittance of one-dimensional periodic structure of ZnS and TiO_2 material is analyzed in symmetric and asymmetric form as shown in Fig. 2. The transmittance of the symmetric structure shows a large bad gap as shown in the Fig. 2a. Similarly, transmittance of the asymmetric structure is analyzed which shows that the band gap divides into two bands due to asymmetricarrangement as shown in Fig. 2b. The band width of the defective asymmetric structure increases in comparison to the symmetric structure due to existing defect mode. The sharp defect transmission peak of the asymmetric structure is used in many applications like filters and laser resonators etc. Further, we focus on the study of asymmetric structure with defect of one or two defect layers of magnetized cold plasma with variation of incident angle and plasma parameters.

As we know that optical property of material changes by changing of refractive index of material as well as incident angle. The variation of incident angle plays key role for change

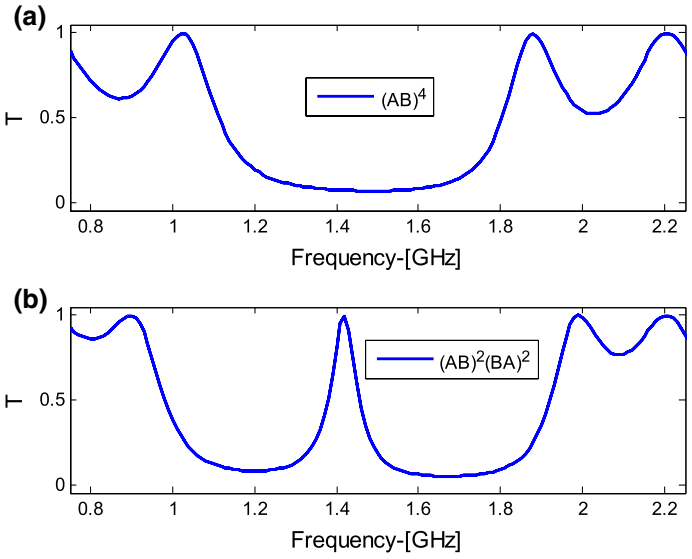

Fig. 2 Transmission spectra **a** symmetric periodic structure, **b** asymmetric periodic structure versus frequency

in the optical property of the considered defective periodic structure. Hence, the transmittance of asymmetric 1-DPS with zinc sulfide and titanium dioxide material with defect of MCP is analyzed on variation of incident angle θ = 0°, θ = 10°, θ = 20° as shown in Fig. 3. Figure 3a shows the transmittance of one dimensional periodic structure inserted one defect layer of magnetized cold plasma with variation of incident angle θ = 0°, θ = 10°, θ = 20°. The figure is depicted that defect transmission peaks and band gaps are shifted towards the higher frequency for increase the value of incident angles and also forms multiband filter.

Similarly, the transmittance of one-dimensional periodic structure with defect of two magnetized cold plasma materials with variation of incident angles have studied. The transmittance of considered periodic structure versus frequency is analyzed with variation of incident angle θ = 0°, θ = 10°, θ = 20° as shown in Fig. 3b. The figure is also depicted that the obtained transmittance is shifting towards the higher frequency that also forms multiband due to composite behavior of dielectric and plasma material. The transmittance shows that the large shifting in transmittance obtains for corresponding to the large value of incident angle θ = 20°. These obtained results may act as tunable multichannel filters at microwave region as shown Fig. 3b. This result can be compared with meta-material superconductor based with and without defect layer (Aly and Mohamed 2018), and analyzed the defect peak which is shifted at higher frequency when incident angle increases but multichannel behavior did not show for the structure composed with meta-material superconductor. They had used periodic structure of double negative (DNG) material and high temperature superconducting material (Hg1223) with lattice period N = 8 with inserted dielectric (SiO_2) as a defect material that is very complicated in the fabrication (Aly and Mohamed 2018). Therefore, we have proposed a very simple adhesive material ZnS/TiO_2 material with defect of MCP material with lattice period N = 4, which is very simple for fabrication. Another work, Aly et al. (2017a) had also suggested a periodic structure of dielectric (quartz) and dielectric (air) with defect of magnetized plasma material and studied optical

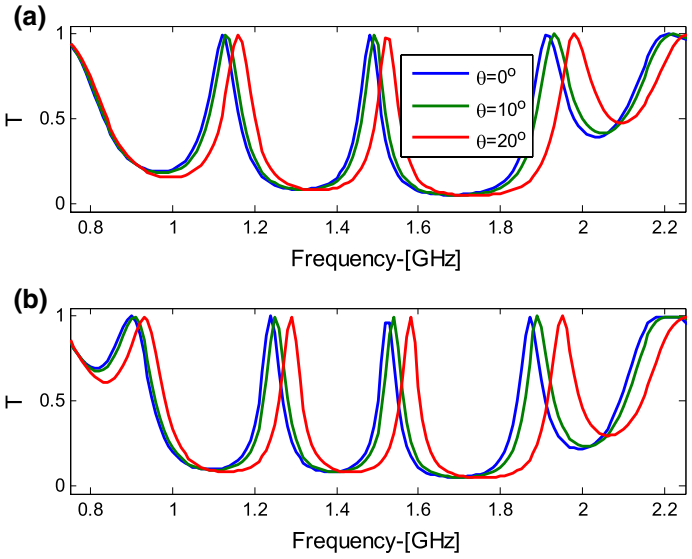

Fig. 3 Transmission spectra versus frequency of the 1-DPS of ZnS and TiO_2 with variation of incident angle θ = 0°, θ = 10°, θ = 20° for **a** one layer of magnetized cold plasma defect, **b** two layers of magnetized cold plasma defect

properties at higher frequency region with varying incident angle, thickness of dielectric material and also varying the plasma parameters for the applications of narrowband filters. Our calculations for transmittance of one dimensional asymmetric structure of zinc sulfide (ZnS), titanium dioxide (TiO_2) with defect of two magnetized cold plasma layers are found better for the applications of multichannel filter having tenability property.

Further, the magnetized cold plasma has an important parameter is electron density. The electron density can change the plasma frequency and plays a key role in change the refractive index of MCP. As the number of particles per unit volume increases the electron density of plasma increases. Similar way, the electron density of plasma increases the plasma frequency increases and optical constant vary corresponds to electron density. The transmittance versus frequency (GHz) of periodic multilayer structure of zinc sulfide and titanium dioxide with defect of one and two layer of magnetized cold plasma as shown in Fig. 4. The transmittance of the structure with defect of one layer of magnetized cold plasma versus frequency was analyzed on variation of varying electron density $n_e = 1.54 \times 10^{16}/m^3$, $n_e = 3.54 \times 10^{16}/m^3$, $n_e = 5.54 \times 10^{16}/m^3$ as shown in Fig. 4a. Transmittance versus frequency with varying electron density $n_e = 1.54 \times 10^{16}/m^3$, $n_e = 3.54 \times 10^{16}/m^3$, $n_e = 5.54 \times 10^{16}/m^3$ is shifted towards the lower frequency when the electron density increases due to the value of refractive index of plasma material decreases. Similarly, the transmittance with defect of two magnetized cold plasma layer are analyzed on variation of different value of electron density $n_e = 1.54 \times 10^{16}/m^3$, $n_e = 3.54 \times 10^{16}/m^3$, $n_e = 5.54 \times 10^{16}/m^3$ and transmission peak shown slightly high and shifted towards the lower frequency when the electron density increases and optical constant of plasma material changes. Therefore, the electric permittivity of magnetized cold plasma material changes due to the electron density as shown in Fig. 4b. The obtained results of the transmittance show as tunable multichannel filter at microwave region.

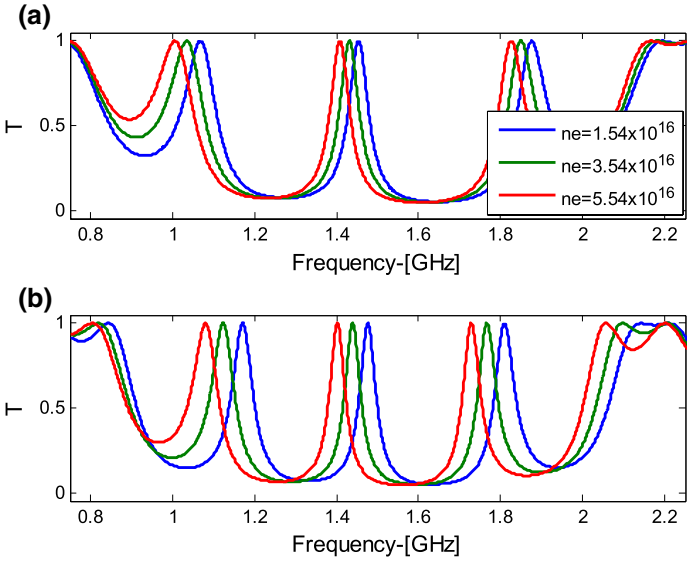

Fig. 4 Transmission spectra versus frequency of the one-dimensional periodic structure of ZnS and TiO_2 with varying $n_e = 1.54 \times 10^{16}/m^3$, $n_e = 3.54 \times 10^{16}/m^3$, $n_e = 5.54 \times 10^{16}/m^3$ of **a** one layer of magnetized cold plasma defect, **b** two layers of magnetized cold plasma defect

The electric permittivity of the magnetized cold plasma can change by the external magnetic field because the gyro-effective frequency is dependent on the magnetic field. The external magnetic field changes the refractive index of the MCP. It means that the transmittance of periodic structure containing plasma is also varied with magnetic field in the MCP. Applied external magnetic field shows an abnormal behavior due to positive and negative value, exhibit right hand polarization and left hand polarization, respectively. Therefore, we have studied the transmittance of periodic structure of zinc sulfide and titanium dioxide with inserted one and two defect layers of magnetized cold plasma on variation of the applied external magnetic field, B = 0.3 T, B = 0.4 T, B = 0.5 T, as shown in Fig. 5a, b, respectively. Transmittance of one-dimensional periodic structure versus frequency with variation of external magnetic field have been analyzed that the transmission peak shifted towards the higher frequency due to effect of optical constant magnetized cold plasma material. As the magnetic field increases then each band is shifted towards the higher frequency corresponding to the value of magnetic field as shown in Fig. 5a.

Similarly, transmittance of one-dimensional periodic structure with defect of two layer of magnetized cold plasma is inserted and shown the abnormal behavior in transmittance of the structure due to the large effect of plasma material. The shifted transmission peaks have found high due to twice times of thickness of plasma material. The changed optical behavior of material changes corresponds to the magnetic field on the plasma material as shown in Fig. 5b. This shows that tunable multichannel filter is obtained by external magnetic field for microwave devices. These results also compare a novel tunable filter featuring defect mode of TE wave from one dimensional photonic crystal doped by magnetized plasma found that the dispersion relation and transmittance spectra of dielectric (SiO_2) and dielectric (air) material periodic structure. Transmittance spectra versus frequency

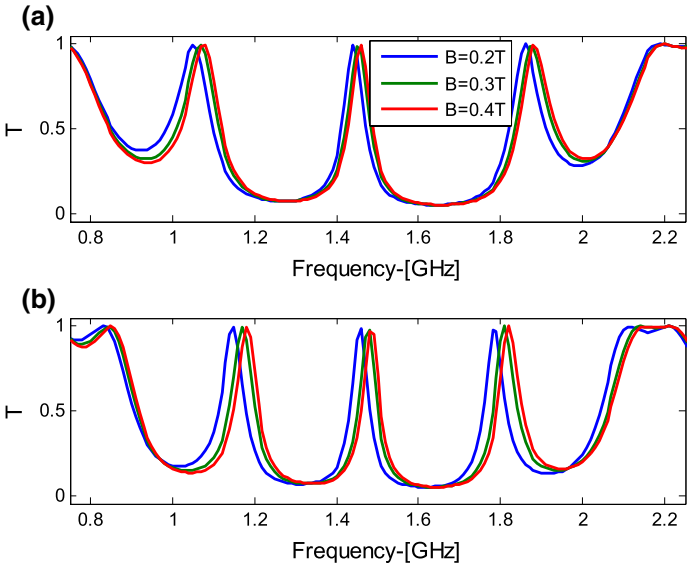

Fig. 5 Transmission spectra versus frequency of the one-dimensional periodic structure of ZnS and TiO_2 with varying B = 0.3 T, $B = 0.4$ T, $B = 0.5$ T of **a** one layer of magnetized cold plasma defect, **b** two layers of magnetized cold plasma defect

analyzed with defect of magnetized plasma on the variation of magnetic field, plasma density and electron density of MCP and found application in tunable filter (Kong et al. 2010b).

As we have been analyzed that the defect transmission peak for two magnetized plasma layer is more variation than the defect transmission peak for one magnetized plasma layer. So, transmittance versus frequency (GHz) of one-dimensional periodic structure of ZnS and TiO_2 materials have analyzed with the variation of thickness of ZnS material with same data. The transmittance property of the considered asymmetric periodic structure with defect of one layer of MPC is studied with variation of different value of thicknesses of ZnS i.e. dA = 0.0188 mm, dA = 0.0208 mm, dA = 0.0228 mm. The transmittance does not change but it is shifted towards lower frequency on increase the value of thickness of ZnS which shown in Fig. 6a and the corresponding 2D image Fig. 6b and 2D image data is verified.

Similarly, transmittances of the considered asymmetric structure with two layers of magnetized cold plasma versus frequency (GHz) have analyzed with the variation of thickness of ZnS material dA = 0.0188 mm, dA = 0.0208 mm, dA = 0.0228 mm which is shown in the Fig. 7a. The transmittance of the considered defect structure is tuned for corresponding thickness of ZnS material where it goes to lower frequency on increase the value of thickness of ZnS material. The multiple bands of the structure are controlled by the thickness of the ZnS material and may be used in multichannel tunable filter as predicted in 2D image plot as shown in Fig. 7b.

Now the transmittancesof one-dimensional defective periodic structure of incorporated the one layer of magnetized cold plasma in asymmetric periodic structure versus frequency (GHz) with variation of thickness of titanium oxide material have analyzed. The transmittance varies with increase the value of thickness of titanium oxide material i.e.dB = 0.0375 mm, dB = 0.0395 mm, dB = 0.0415 mm. The transmittance is shifted again towards the lower value of frequency on increase the value of thicknesses as shown in Fig. 8a and corresponding transmittance results is plotted the 2D image plot for same data as shown Fig. 8b.

In the similar way, the transmittance property of one-dimensional asymmetric periodic structure with defect of two layers magnetized cold plasma versus frequency has

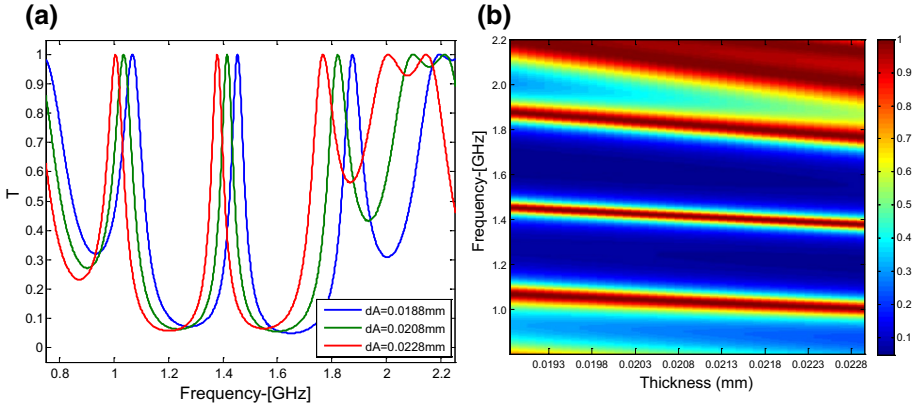

Fig. 6 **a** Transmittance versus frequency with variation of thickness of ZnS material and **b** 2D image plot of frequency versus variation of thickness of ZnS material

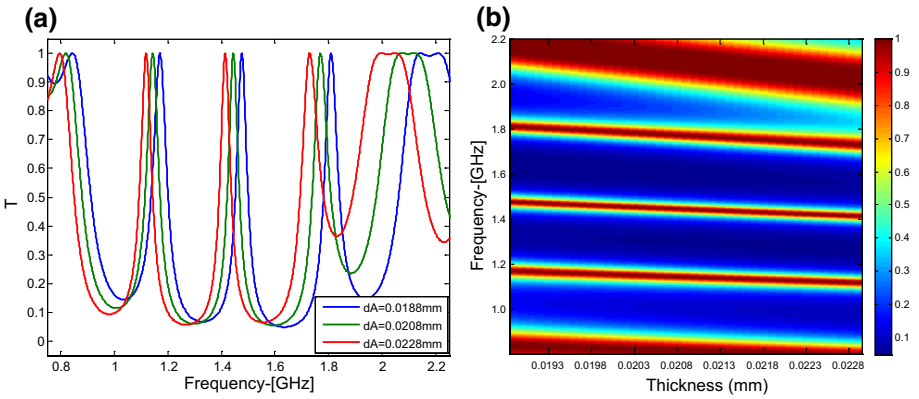

Fig. 7 **a** Transmittance versus frequency with variation of thickness of ZnS material, **b** 2D image plot of frequency versus variation of thickness of ZnS material

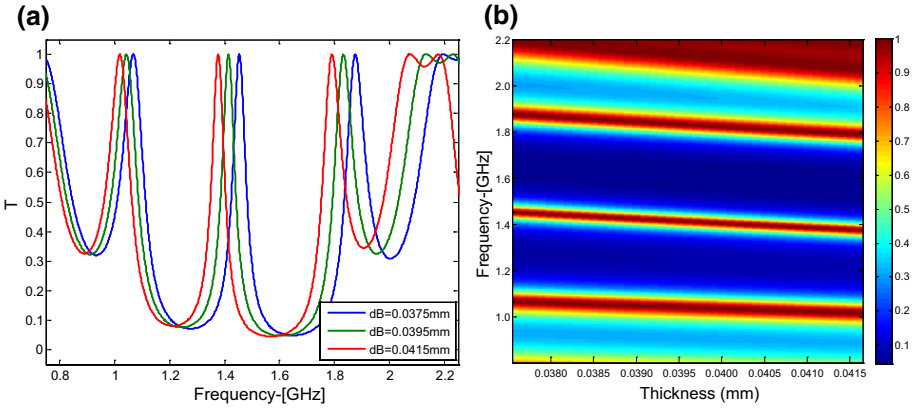

Fig. 8 **a** Transmittance versus frequency with variation of thickness of TiO_2 material, **b** 2D image plot of frequency versus variation of thickness of TiO_2 material

analyzed. The transmittance has obtained same results with large number of multiple transmittance peaks which varies with the value of thickness of titanium oxide material i.e. $dB = 0.0375$ mm, $dB = 0.0395$ mm, $dB = 0.0415$ mm as shown in Fig. 9a and corresponding 2D image plot is shown in Fig. 9b. These results are also compared with the work of Aly et al. (2017a) where they had suggested that defect of magnetized plasma material in the periodic structure of dielectric (quartz) and dielectric (air) and transmittance had found possible result at higher frequency region with varying thickness of dielectric material for the applications of narrowband filters. But our calculated results are found better for the applications of multichannel filter.The variations of thickness of the materials are considered in our calculations, becausethe thickness of dielectric material and the volume ratio of nanocomposite material change the optical property of one-dimensional defective photonic crystal with defect material (Aly et al. 2017b).

From above calculations, the transmittances of the considered asymmetric structures with defect MCP have predicted that such defect structure with plasma layers have

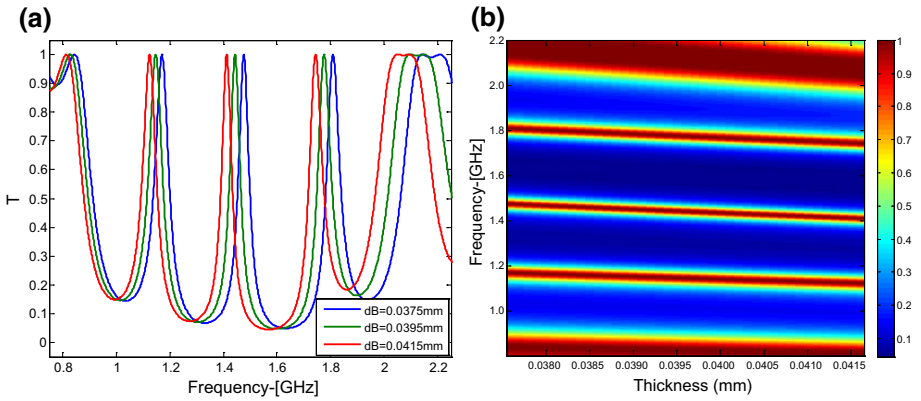

Fig. 9 **a** Transmittance versus frequency with variation of thickness of TiO_2 material, **b** 2D image plot of frequency versus variation of thickness of TiO_2 material

multichannel transmission defect peaks. These defect transmission peaks are increased when the MCP defect increases. Besides this, we have also predicted that these defect transmission peaks are also varied with the thickness of the ZnS and TiO_2 material.

4 Conclusion

The transmittance of symmetric and asymmetric one dimensionalperiodic structure containing zinc sulfide and titanium dioxide with one or two defect of magnetized cold plasma layerversus frequency (GHz) wereanalyzed. The transmittance of the asymmetric one dimensional periodic structure containing zinc sulfide and titanium dioxide with one or two defect of magnetized cold plasma layer was analyzed with variation of incident angles, electron densities, magnetic fieldsof the magnetized cold plasma material and thickness of the ZnS and TiO_2 material. The transmittance of two MCP layer inserted in asymmetric periodic structure with variation of electron density of plasma as well as thickness of ZnS and TiO_2 material found better response as comparison to one layer defect in same periodic structure. These calculated results of the transmittanceare suggested that the asymmetric one dimensional periodic structure containing zinc sulfide and titanium dioxide with two defects of magnetized cold plasma layers may be a simple and innovative idea to fabricate the tunable multichannel filter at microwave region.

Acknowledgements Asish Kumar, Research Scholar, Department of Physics, Babasaheb Bhimrao Ambedkar University (A Central University) Lucknow, acknowledges to UGC, New Delhi for Non-Net UGC fellowship.

References

Aghajamali, A.: Transmittance properties in a magnetized cold plasma and superconductor periodic multilayer. Appl. Opt. **55**, 6336–6340 (2016)

Aly, A.H.: The transmittance of two types of one-dimensional periodic structures. Mater. Chem. Phys. **115**(1), 391–394 (2009)

Aly, A.H.: Metal dielectric periodic structure and defect characterizations. J. Comput. Theor. Nanosci. **9**(12), 2045–2051 (2012)
Aly, A.H., El Sayad, H.A.: Defect mode properties of one dimensional photonic crystal. Phys. B **407**(1), 120–125 (2012)
Aly, A.H., ElSayad, H.A.: Tunability of one dimensional photonic crystals based on Faraday Effect. J. Mod. Opt. (2016). https://doi.org/10.1080/09500340.2016.1265676
Aly, A.H., Mohamed, D.: BSCCO/$SrTi_{O3}$one dimensional superconducting photonic crystal for many applications. J. Supercond. Nov. Magn. **28**, 1699–1703 (2015)
Aly, A.H., Mohamed D. The optical properties of meta-material superconductor photonic band gap with/without defect layer. J. Supercond. Nov. Mag.1–6 (2018)
Aly, A.H., Sayed, H.: Enhancement of the solar cell based on the nanophotonic crystals. J. Nanophotonics **11**(4), 046020 (2017)
Aly, A.H., Elsayed, H.A., Ameen, A.A., Mohamed, S.H.: Tunable properties of one dimensional photonic crystal that incorporate a defect layer of magnetized cold plasma. Int. J. Mod. Phys. B **31**, 1750239-9 (2017a)
Aly, A.H., ElSayad, H.A., Malek, C.: Optical properties of one dimensional defective photonic crystal containing nanocomposite material. J. Nonlinear Opt. Phys. Mater. **26**(1), 1750008-8 (2017b)
Aly, A.H., Ameen, A.A., Mohamed, HS., Elsayed, H.A., Singh, MR.: One dimensional metallo superconductor photonic crystals as a smart window. J. Supercond. Nov. Magn. **32**(8), 2313–2318 (2018). https://doi.org/10.1007/s10948-018-4978-z
Booker, H.G.: Cold Plasma Waves, pp. 23–25. Springer, New York (1984)
Busch, K., Freymann, G., von Linden, S., Mingaleev, S.F., Tkeshelashvili, L., Wegener, M.: Periodic nanostructures for photonics. Phys. Rep. **444**, 101–202 (2007)
Cai, W., Shalaev, W.: Optical Metamaterials: Fundamental and Applications. Springer, New York (2010)
Chigrin, D.N., Lavrinenko, A.V., Yarotsky, D.A., Gaponenko, S.V.: Observation of total omni-directional reflection from a one-dimensional dielectric lattice. Appl. Phys. **68**, 25–28 (1999)
Feng, Z.H., Kong, X.K.: Photonic band gap in one dimensional magnetized plasma photonic crystals with arbitrary magnetic declination. Phys. Plasma **19**, 122103–122115 (2012)
Fink, Y., Winn, J.N., Fan, S., Chen, C., Michel, J., Joannopoulos, J.D., Thomas, E.L.: A dielectric omnidirectional reflector. Science **282**, 1679–1682 (1998)
Gaponenko, S.V.: Introduction to Nanophotonics. Cambridge University Press, Cambridge (2010)
Gu, X., Chen, X.F., Chen, Y.P., Zheng, X.L., Xia, Y.X., Chen, Y.L.: Narrowband multiple wavelengths filter in aperiodic optical super lattices. Opt. Commun. **237**, 53–58 (2004)
Hitoshi, H., Atushi, M.: Dispersion relation of electromagnetic wave in one dimensional plasma photonic crystal. J. Plasma Fusion Res. **80**(2), 89–90 (2004). https://doi.org/10.1585/jspf.80.89
Hojo, H., Akimoto K., MaseA. In: Conference Digest on 28th International Conference on Infrared and Millimeter Waves Otsu, pp. 347–348 (2003)
Joannopolos, J.D., Meade, R.D., Winn, J.N.: Photonic Crystals: Molding the Flow of Light. Princeton University Press, Princeton (1995)
John, S.: Strong localization of photons in certain disordered dielectric super lattices. Phys. Rev. Lett. **58**, 2486–2489 (1987)
Kazempour, B.: design of tunable multichannel filter in a one dimensional photonic crystal incorporating uniaxial meta-material at microwave frequency. Opt. Appl. **49**, 1–26 (2019)
King, T.C., Yang, C.C., Hseih, P.H., Chang, T.W., Wu, C.J.: Analysis of tunable photonic band gap structure in an extrinsic plasma photonic crystal. Phys E **67**, 7–11 (2015). https://doi.org/10.1016/j.physe.2014.11.001
Kong, X.K., Yang, H.W., Liu, S.B.: Anamalous dispersion in one dimensional plasma photonic crystals. Optik (Jena) **121**(20), 1873–1876 (2010a)
Kong, X.K., Liu, S.B., Jhang, H.F., Li, C.Z.: A novel tunable filter featuring defect mode of the TE wave from one-dimensional photonic crystals doped by magnetized plasma. Phys. Plasmas. **17**, 103506 (2010b)
Kong, X.K., Liu, S.B., Jhang, H.F., Li, C.Z.: Am. Inst. Phys. **17**, 103506 (2010c)
Krauss, T.F., De La Rue, R.M.: Photonic crystals in the optical regime: past, present and future. Progress. Quant. Electron. **23**, 51–96 (1999)
Kumar, R.: In: Massaro, A. (ed.), Plasma Photonic Crystal (Photonic Crystals—Innovative Systems, Lasers and Waveguides. InTech (2012)
Kumar, A., Thapa, K.B.: Study of optical property of defect mode in one dimensional double negative photonic crystal with plasma. Adv. Sci. Eng. Med. **10**, 1–5 (2018)
Kumar, V., Singh, K.S., Ojha, S.P.: Band structure, reflection properties and abnormal behaviour of one-dimensional plasma photonic crystals. Prog. Electromagn. Res. M **9**, 227–241 (2009)

Kumar, A., Singh, P.P., Thapa, K.B. A new idea for broadband reflector and tunable multi-channel filter of one dimensional symmetric photonic crystal with magnetized cold plasma defects. In: AIP Conference Proceedings, vol. 1953, p. 60043 (2018a)
Kumar, A., Kumar, N., Thapa, K.B.: Tunable broadband reflector and tunable narrowband filter of a dielectric and magnetized cold plasma photonic crystal. Eur. Phys. J. Plus **133**, 250 (2018b)
Kumar, A., Thapa, K.B., Ojha, S.P.: A tunable broadband filter of ternary photonic crystal containing plasma and superconducting material. Indian J. Phys. **93**(6), 791–798 (2019)
Lee, H.Y., Yao, T.: Design and evaluation of omni-directional one dimensional photonic crystals. J. Appl. Phys. **93**, 819 (2003)
Massaoudi, S., de Lustrac, A., Huynen, I.: Properties of metallic photonic band gap material with defect at microwave frequencies: calculation and experimental verification. JEMWA **20**(14), 1967–1980 (2006)
Palik, E.D.: Handbook of Optical Constants of Solids. Academic Press limited, London (1998)
Sakaguchi, T., Sakai, O., Tachibana, K.: J. Appl. Phys. **101**, 073305 (2007)
Sakai, O., Kishimoto, Y., Yachibana, K.: J. Phys. D Appl. Phys. **38**, 431 (2005)
Sakai, O., Sakaguchi, T., Tachibana, K.: J. Appl. Phys. **101**, 073304 (2007)
Sakoda, K.: Optical Properties of Photonic Crystals. Springer, Berlin (2004)
Ward, A.J., Pendry, J.B.: Refraction and geometry in Maxwell's equations. J. Mod. Opt. **43**(4), 773–794 (1996)
Yablonovitch, E.: Inhibited spontaneous emission in solid-state physics and electronics. Phys. Rev. Lett. **58**, 2059–2062 (1987)
Yeh, P.: Optical Waves in Layered Media. Wiley, New York (1988)
Zhang, H.F., Liu, S.B., Kong, X.K.: Analysis of the properties of tunable prohibited band gaps for two dimensional unmagnetized plasma photonic crystals under TM-modes. Acta Phys. Sin. **60**, 055209 (2011a). http://wulixb.iphy.ac.cn/CN/article/downloadArticleFile.do?attachType=PDF&id=18400 (**in Chinese**)
Zhang, H.F., Liu, S.B., Kong, X.K.: Defect mode properties of two dimensional unmagnetized plasma photonic crystals with line defect under TM-mode. Acta Phys. Sin. **60**, 025215 (2011b). http://wulixb.iphy.ac.cn/CN/article/downloadArticleFile.do?attachType=PDF&id=18019 (**in Chinese**)
Zheng, Q.R., Lin, B.Q., Yuan, N.C.: Characteristics and applications of a noval compact spiral electromagnetic band gap (EBG) structures. J. Electromagn. Waves Appl. **21**, 199–213 (2007)

Journal of Magnetism and Magnetic Materials 489 (2019) 165371

Contents lists available at ScienceDirect

Journal of Magnetism and Magnetic Materials

journal homepage: www.elsevier.com/locate/jmmm

Research articles

Enhancement of absorption property of one-dimensional ternary periodic structure containing plasma based hyperbolic material for the application of microwave devices

Asish Kumar, Khem B. Thapa*, Anil K. Yadav

Department of Physics, School of Physical and Decision Sciences, Babasaheb Bhimrao Ambedkar University, Lucknow 226025, U.P., India

ARTICLE INFO

Keywords:
Hyperbolic meta-material
Plasma
Multilayer structure
Enhanced absorption
Tunable absorber based microwave device

ABSTRACT

This work reports a theoretical analysis of the absorption properties of a one-dimensional ternary periodic structure of dielectric, silicon dioxide and hyperbolic materials using well-known simple transfer matrix method (TMM). The hyperbolic material is a composite material of dielectric and plasma materials in which the optical constants of hyperbolic material have been studied by considering the effective medium theory. The relative permittivity of hyperbolic material has been studied with the variation of filling fraction and the electron collision frequency. The absorption of ternary periodic structure was studied with varying incident angle, in which the maximum absorption is found at incident angle 80°. Therefore, we have studied the absorption spectra of the considered periodic structure with variation of filling fraction, electron collision frequency, and thickness of dielectric material where the incident angle is constant at 80° for the maximum absorption. In this particular case, we have obtained the enhanced absorption spectra for ternary periodic structure in comparison to other angle of incidence at low normalized frequency. However, zero absorption for the same structure is obtained at the high normalized frequency range that exhibits a band gap. Now, the enhanced absorption of the considered structure has been studied with variation of filling fraction, electron collision frequency and thickness of dielectric material. We have obtained that the enhanced high absorption at the low microwave frequency may be used as a sensor, detector, logic gate; and the absorption band gap at the high microwave frequency range may as tunable absorber based microwave devices.

1. Introduction

As we know that the photonic crystals are artificial dielectric, metallic or plasma nanostructures composed of two or more medium in which the dielectric constant varies periodically in the space. The novel idea of the periodic nano-structure of materials is to have photonic band gap that was experimentally observed by Yablonovitch, and theoretically proposed by John [1,2] in the same year. The photonic band gap (PBG) has unique features of the photonic crystals in which electromagnetic wave doesn't propagate in the periodic structure [3–5]. The periodic structure of the dielectric materials affects the electromagnetic wave propagation due to PBG, which is analogous to the electron propagation inside the periodic potential. Such photonic band gap plays an important role in optical applications [6–9]. The study of periodic structure of the different materials is led to a roadmap for optical metamaterials, and the study of optical metamaterial is given a very informative and potential application in different field of the science [10].

The hyperbolic metamaterials (HMMs) are an anisotropic medium, which exhibits the hyperbolic shape of the dispersion relation at terahertz (THz), optical and near-infrared frequency regions. Hyperbolic material has a lot of potential applications including negative refraction, an optical waveguide, and imaging hyper lens [11–15]. Recently, a novel implementation of HMMs at the far-infrared frequency has been proposed with the compositions of the stacked graphene sheets separated by thin dielectric layer and it has a super absorber for near fields. Such HMMs are also used to enhance the decay rate of emitters near its surface for designing efficient and innovative absorbers [16,17]. Hyperbolic meta-material has dual behavior like metallic and dielectric. In metallic behavior, large number of free electrons are present parallel to the direction of propagation, so it has high reflectance and absorption. On other hand, the dielectric behavior of HMMs has less number of free electrons which propagate in the direction of propagation and hence it behaves like dielectric and also has high transmission. Thus, the

* Corresponding author.
E-mail address: khem.bhu@gmail.com (K.B. Thapa).

https://doi.org/10.1016/j.jmmm.2019.165371
Received 22 November 2018; Received in revised form 18 March 2019; Accepted 27 May 2019
Available online 30 May 2019
0304-8853/

hyperbolic materials are also known as type I (metallic) and type II (dielectric) material. In theoretical characterization of the epsilon near zero, epsilon near pole plays an important role in propagation wave spectrum. Epsilon near zero always occurs in the direction of wave propagation and epsilon near pole always exists in that region in which no free electron motion occurs [18–23].

In recent years, the absorption based optical devices have been paid attention by the scientists and the researchers in the field of science and technology. The absorption of HMMs is very high and varied with the variable parameters. So, there are several researchers who have contributed their works to develop the innovative idea for the HMMs. The tunable absorption of composed graphene sheets that are separated by using thin dielectric layer was studied at near infrared frequency. A homogenization formula for the multilayer structure using the surface conductivity theory has been proposed by Oatham et al. [24]. A novel implementation of the dual-gated tunable absorption of the graphene-based hyperbolic material for optical gate applications was investigated by Ning et al. [25]. The spectral characteristic of nanostructure hyperbolic material based UV- absorber in ultraviolet region of electromagnetic spectrum was investigated by Baqir et al. [26] by considering the periodically arranged assembly of gold nanostrips.

The new research based on the concept of grating coupled hyperbolic meta-materials as multiband perfect absorber was investigated by Sreekanth et al. [27] at spanning frequencies from microwave to visible frequencies. A new structure of N-doped Si/Si hyperbolic meta-material integrated with subhole Si grating was proposed and the absorption of the structure had worked as Si based HMM for mid IR super absorber. The absorption of proposed structure can have tuned with the grating parameter [28]. The dielectric singularity in the anisotropic permittivity response of the possibility of HMM was presented where a transition point of inverted but coexisting anisotropies was obtained at a specified wavelength due to the particular design of the multilayer structure and possessing different optical properties which is depending on the investigated frequency [29]. A hyperbolic dispersion of the photonic multilayer waveguide with the layers of dielectric and meta-materials had different geometric waveguides when a long range propagation of Plasmon and phonon polariton at the dielectric HMM interfaces. The performance of the waveguide with hexagonal boron nitride in the range possessed the hyperbolic dispersion. The absorption of the waveguides with natural hyperbolic properties have the higher lengths compared to metal based HMM waveguides which was proposed by Babicheva et al [30]. The optical properties of quantum dipole emitters coupled to hyperbolic meta-material nanoresonators had been proposed using semi analytical quasi normal mode.

An informative idea about the hyperbolic meta-material nano-resonators for developing the poor single photons was investigated by Axelrod et al. [31] The measurement and simulation of the polarization dependent Purcell factor for the microwave fishnet material was investigated by Rustomji et al. [32] The low threshold spaser based on deep sub-wavelength spherical hyperbolic material cavities was investigated by Wan et al. [33] The tunable mid-IR focusing of Indium Arsenide (InAs) based semiconductor hyperbolic material was analyzed by Desouky et al. [34]. The experimental demonstration of angle-independent gap in the one-dimensional photonic crystal containing layered hyperbolic materials and dielectrics at visible wavelengths was investigated by Wu et al. [35]. The near perfect broadband absorption of hyperbolic meta-materials was investigated by Riley et al. [36]. The controlled near-infrared surface Plasmon polariton dispersion of the hyperbolic material was investigated by Luk et al. [37].

After reviewing all these papers, we have proposed a HMM with dielectric and plasma material. In this article, we have analyzed the perpendicular and parallel permittivity of the hyperbolic meta-material with variation of filling fraction and electron collision frequency. Based on simple transfer matrix method, the absorption properties of ternary periodic structure are studied with variation of incident angle, electron collision frequency of plasma, filling fraction and thickness of the dielectric material. Firstly, we have studied the absorption of ternary periodic structure against normalized frequency with varying angle of incidence i.e. $\theta = 0°$, $\theta = 20°$, $\theta = 40°$, $\theta = 60°$, $\theta = 80°$. Then, we have studied the optical properties of the ternary periodic structure, especially absorption, by choosing other parameters filling fraction, electron collision frequency and thickness of dielectric of a material with keeping fixed incident angle $\theta = 80°$. Such absorption property of the periodic structure is very important for designing absorption based devices like logic gate, electromagnetic switch, sensor, photodetector, and microwave absorber. We have also proposed to design the tunable absorber for microwave devices composed of the hyperbolic material at higher frequency range.

2. Theoretical model

The absorption spectra of the one-dimensional ternary periodic structure of dielectric, SiO_2 (Silicon dioxide), and hyperbolic metamaterials are calculated by using a simple transfer matrix method and Bloch' function [38]. The hyperbolic material is the composite material of dielectric (air) and plasma-material [39]. One-dimensional ternary periodic structure is taken as $(ABC)^N$, where N is the number of the unit cell of ternary periodic structure; A, B and C are dielectric (air), SiO_2 and hyperbolic material layer, respectively, as shown in Fig. 1.

The dielectric permittivity and magnetic permeability of dielectric (air) and silicon dioxide material are taken as-

$$\varepsilon_{die} = \mu_{die} = 1 \ , \quad \text{and } \varepsilon_{SiO_2} = 2.2, \ \mu_{SiO_2} = 1$$

The hyperbolic material is a composite of dielectric and plasma material where the complex permittivity of plasma is given as [39];

$$\varepsilon_{plasma}(\omega) = 1 - \frac{\omega_p^2}{\omega\left(\left(1 + \frac{i\gamma}{\omega}\right)\right)} \tag{1}$$

with the permeability, $\mu_{plasma} = 1$ i.e. non-magnetic material; where ω and γ is the angular frequency and effective collision frequency, respectively. Here, $\omega_{pe}\omega_{pe}\omega_{pe}\omega_p$ is the plasma frequency which is given as [40],

$$\omega_p = \left(\frac{n_e e^2}{m\varepsilon_0}\right)^{1/2} \tag{2}$$

The concept of material of the hyperbolic behavior originates from the optics of crystals. In such media, the constitutive relations connecting the electric displacement, **D**, and the magnetic induction, **B**, to the electric and magnetic fields **E** and **H** can be written as-

$$\bar{D} = \varepsilon_0 \bar{\bar{\varepsilon}} E \tag{3}$$

$$\bar{B} = \mu_0 \bar{\mu} H \tag{4}$$

where ε_0, μ_0 are the electric permittivity and magnetic permeability in vacuum and $\bar{\bar{\varepsilon}}$, $\bar{\mu}$ are relative permittivity and relative permeability tensors. In the present work, we consider non magnetic media $\bar{\mu}$ simply reduces to the unit tensor. Upon diagonalization, $\bar{\bar{\varepsilon}}$ assumes the forms

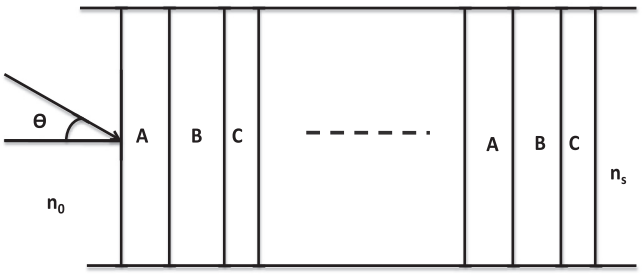

Fig. 1. Schematic diagram of one-dimensional dielectric, silicon dioxide, and hyperbolic material ternary periodic structure.

and the hyperbolic material is an anisotropic medium with uniaxial dielectric tensor components that were approximated as follows [18]

$$\bar{\bar{\varepsilon}} = \begin{bmatrix} \varepsilon_{xx} & 0 & 0 \\ 0 & \varepsilon_{yy} & 0 \\ 0 & 0 & \varepsilon_{zz} \end{bmatrix} \tag{5}$$

in a Cartesian frame of reference oriented along the so called principal axes of the crystal. The three diagonal components are all positive and in general depend on the angular frequency ω; the termed biaxial, when $\varepsilon_{xx} \neq \varepsilon_{yy} \neq \varepsilon_{zz}$, uniaxial when $\varepsilon_{xx} = \varepsilon_{yy} \neq \varepsilon_{zz}$ and becomes isotropic when $\varepsilon_{xx} = \varepsilon_{yy} = \varepsilon_{zz}$.

To determine the dispersion relation of light in a medium described by Eq. (5), let us consider the following two Maxwell's equations in the absence of source:

$$\nabla \times E = -\frac{\partial B}{\partial t} \tag{6}$$

$$\nabla \times H = \frac{\partial D}{\partial t} \tag{7}$$

where **D** and **B** are as in the Eqs. (3) and (4), respectively. The plane wave expressions for both fields can be given by $E = E_0 e^{i(\omega t - k.r)}$ and $H = H_0 e^{i(\omega t - k.r)}$ where k is wave vector. By inserting the **D** and **B** in the Eqs. (6) & (7), we obtain

$$k \times E = \omega \mu_0 H \tag{8}$$

$$k \times H = -\omega \varepsilon_0 \bar{\bar{\varepsilon}} E \tag{9}$$

By taking curl of the k and substitution of Eq. (8) into Eq. (9), the Eigen value problem of electric field;

$$k \times (k \times E) + \omega^2 \mu_0 \varepsilon_0 \bar{\bar{\varepsilon}} E = 0 \tag{10}$$

This can be developed in the matrix form and also called the dispersion relation-

$$\begin{bmatrix} k_0^2\varepsilon_{xx} - k_y^2 - k_z^2 & k_x k_y & k_x k_z \\ k_x k_y & k_0^2\varepsilon_{yy} - k_x^2 - k_y^2 & k_y k_z \\ k_x k_z & k_y k_z & k_0^2\varepsilon_{zz} - k_x^2 - k_y^2 \end{bmatrix} \begin{bmatrix} E_x \\ E_y \\ E_z \end{bmatrix} = 0 \tag{11}$$

where $k_0 = \frac{\omega}{c}$ is the magnitude of wave vector and $c = \frac{1}{\sqrt[2]{\varepsilon_0 \mu_0}}$ the speed of light in vaccum. We now focus on the hyperbolic media, with optical axis oriented along the z direction, $\varepsilon_{xx} = \varepsilon_{yy} = \varepsilon_\perp$ and $k_\perp = \sqrt{k_x^2 + k_y^2}$. The imposition of nontrivial solution to Eq. (11) leads to the dispersion relation [18]:

$$(k_\perp^2 + k_z^2 - \varepsilon_\perp k_0^2)\left(\frac{k_\perp^2}{\varepsilon_{zz}} + \frac{k_z^2}{\varepsilon_\perp} - k_0^2\right) = 0 \tag{12}$$

In the above Eq. (12) have two terms, one of them equal to zero and correspond to spherical behavior and an ellipsoidal iso-frequency surface in the k-space, the first term describes the wave polarized the xy-plane (ordinary or TE waves); second terms correspond to the wave polarized in the plane containing the optical axis (extraordinary waves or TM waves).

The condition changes substantially if we assume an extreme anisotropy, namely when one between $\varepsilon_\perp$ and ε_{zz} is negative. Media with such an optical signature are termed an indefinite from the point of view of mathematics [41], since their permittivity tensor represents an indefinite non-degenerate quadratic form, and exhibits a number of unconventional properties. Permittivity components with an opposite sign result in hyperbolical iso-frequency surface for the extraordinary polarization and hence the physical denomination hyperbolic material. As consequences, waves with arbitrarily large wave vector retain a propagating nature while in isotropic materials they become evanescent due to the bounded iso-frequency contour [42]. The choice $\varepsilon_\perp > 0$, $\varepsilon_{zz} < 0$ correspond to a twofold hyperboloid, and the hyperbolic medium is called dielectric (with reference its behavior in xy-plane) [43] or Type I (metallic); [44] the choice $\varepsilon_\perp < 0$ and $\varepsilon_{zz} > 0$ describes a one fold hyperboloid, namely a metallic or Type II (dielectric) medium.

In our calculation, we have considered $\varepsilon_{xx} = \varepsilon_\perp$, $\varepsilon_{yy} = \varepsilon_{zz} = \varepsilon_{||}$, $\varepsilon_{||}$ and $\varepsilon_\perp$ are the parallel and perpendicular component of relative permittivity, respectively, which can be calculated by effective medium theory. So, $\varepsilon_{||}$ and $\varepsilon_\perp$ can be approximated as [45];

$$\varepsilon_{||} = \frac{\varepsilon_{die}\varepsilon_{plasma}(d_{die} + d_{plasma})}{\varepsilon_{die}d_{plasma} + \varepsilon_{plasma}d_{die}} \tag{13}$$

$$\varepsilon_\perp = \frac{d_{die}\varepsilon_{die} + d_{plasma}\varepsilon_{plasma}}{d_{die} + d_{plasma}} \tag{14}$$

where d_{die}, d_{plasma} are the thicknesses of considered dielectric and plasma material, respectively and ε_{die} and ε_{plasma} are the electric permittivity of considered dielectric material and plasma material, respectively. The filling fraction $f = \frac{d_{plasma}}{d_{HM}}$ is the volume percentage of plasma in a unit cell or period, dielectric layer and a plasma layer with thickness d_{die} and d_{plasma} and permittivity's ε_{die} and ε_{plasma}. For transverse magnetic (TM) wave propagation in the structure, the spatial dispersive curve can be performed as,

$$\frac{k_{zz}^2}{\varepsilon_{xx}} + \frac{k_{xx}^2}{\varepsilon_{zz}} = k_0^2 \tag{15}$$

If the product of perpendicular and parallel permittivity is less than zero it always shows the dispersive curve is hyperbolic behavior ($\varepsilon_\perp \varepsilon_{||} < 0$), and the product of perpendicular and parallel permittivity is greater than zero, the dispersive curve is shown elliptical ($\varepsilon_\perp \varepsilon_{||} > 0$) [46,47].

The characteristic matrix of then one-dimensional ternary periodic structure i.e. $(ABC)^N$ is expressed as [38]

$$M(d) = \begin{pmatrix} m_{11} & m_{12} \\ m_{21} & m_{22} \end{pmatrix} \tag{16}$$

where $M(d) = (M_A M_B M_C)^N$; N is the number of unit cell, M_A, M_B, and M_C are the characteristics matrices of layers dielectric (A), silicon dioxide (B), and hyperbolic material (C), respectively.

The characteristic matrix M_i for each layer of the periodicity of the ternary structure is calculated for the transverse magnetic (TM) wave at the angle of incidence θ_0 from vacuum to a one-dimensional photonic crystal (PC) structure [38].

$$M_i = \begin{bmatrix} \cos\gamma_i & -\frac{i}{p_i}\sin\gamma_i \\ -ip_i\sin\gamma_i & \cos\gamma_i \end{bmatrix} \tag{17}$$

where $\gamma_i = \left(\frac{\omega}{c}\right) n_i d_i \cos\theta_i$, c are the speed of light in vacuum, θ_i is the ray angle inside i^{th} layer with the refractive index as, $n_i = \sqrt{\mu_i \varepsilon_i}$, $p_i = \sqrt{\frac{\mu_i}{\varepsilon_i}}\cos\theta_i$ and $\cos\theta_i = \sqrt{1 - \frac{n_0^2 \sin^2\theta_0}{n_i^2}}$ in which n_0 is the refractive index of air, where the incidence wave tends to enter the structure.

The characteristic matrix of each layer can be obtained by considering the electric field on each surface. For ternary periodic structure, we have considered three layers in the x-direction. The electric field distribution in each interface is given by;

$$\vec{E} = \begin{cases} (\vec{E}_1 e^{i\vec{k}_1.\vec{r}} + \vec{E}'_1 e^{-i\vec{k}'_1.\vec{r}})\, e^{i\omega t}, & -d_A < x < 0; \\ (\vec{E}_2 e^{i\vec{k}_2.\vec{r}} + \vec{E}'_2 e^{-i\vec{k}'_2.\vec{r}})\, e^{i\omega t}, & 0 < x < d_B; \\ (\vec{E}_3 e^{i\vec{k}_3.\vec{r}} + \vec{E}'_3 e^{-i\vec{k}'_3.\vec{r}})\, e^{i\omega t}, & d_B < x < d_{B+C}; \end{cases} \tag{18}$$

where k_1, k_2, and k_3 are the propagation wave vector corresponding to the dielectric, silicon dioxide and hyperbolic material respectively with the above boundary conditions. By using Maxwell's equations, we obtain the corresponding magnetic field. The electric and magnetic field may use to the formulation of the Eq. (18) at each interface.

The transmission coefficient of the ternary photonic crystal is calculated by,

$$t = \left| \frac{2p_0}{\left(m_{11} + \frac{m_{12}}{p_0}\right) + (m_{21}p_0 + m_{22})} \right| \tag{19}$$

where $p_0 = n_0 \cos\theta_0$ and $p_s = n_s \cos\theta_s$, n_s is the refractive index of the substrate, θ_0 is the ray angle.

The transmission spectra of the ternary photonic crystal are given by [38],

$$T = \left(\frac{p_s}{p_0}\right) |t|^2 \tag{20}$$

The reflection coefficient of the one-dimensional ternary periodic structure containing dielectric, silicon dioxide, and hyperbolic material is calculated by-

$$r = \left| \frac{m_{11} + \frac{m_{12}}{p_0} - m_{21}p_0 - m_{22}}{\left(m_{11} + \frac{m_{12}}{p_0}\right) + (m_{21}p_0 + m_{22})} \right| \tag{21}$$

where $p_0 = n_0 \cos\theta_0$ and $p_s = n_s \cos\theta_s$, n_s is the refractive index of the air, whose ray angle is θ_i. The reflection spectra or reflectance of the one-dimensional photonic crystal containing dielectric, silicon dioxide, and hyperbolic material is given by;

$$R = |r|^2 \tag{22}$$

The absorption spectra of the one-dimensional ternary periodic structure of dielectric, silicon dioxide, and hyperbolic material are calculated by the equation;

$$A = 1 - R - T \tag{23}$$

3. Results and discussion

In this article, we first discuss about the optical constant of the hyperbolic meta-material, and then optical property of the ternary periodic structure. The perpendicular and parallel permittivity of hyperbolic meta-material against normalized frequency ($\frac{\omega}{\omega_p}$) is theoretically analyzed by varying filling fraction, electron collision frequency using Eqs. (13) & (14). As we discussed earlier that the hyperbolic material has specific property like filling fraction ($f = \frac{d_{plasma}}{d_{HM}}$) due to the property of composite materials of dielectric and plasma, and the electric permittivity of the HMM is an anisotropic property.

The material C is a hyperbolic meta-material (HMM) in our ternary periodic structure which is composed with two materials of plasma and air dielectric [48,49]. The HMM has $d_{HM} = d_{plasma} + d_{die(air)} = 2mm$ and $f = \frac{d_{plasma}}{d_{HM}}$ with a thickness of the plasma material $d_{plasma} = 0.2mm$, plasma frequency $\omega_p = 28.4 \times 10^9$. The dielectric of the air is $\varepsilon_{die(air)} = \mu_{die(air)} = 1$. The permittivity of hyperbolic material varies along perpendicular and parallel directions, studied using Eqs. (13) & (14). As we know that the hyperbolic material property is purely depending upon the dispersion relation of relative permittivity. The dispersion relation shows that the product of perpendicular and parallel permittivity is less than zero then the dispersive curve shows the hyperbolic behavior having the metallic behavior ($\varepsilon_\perp \varepsilon_{||} < 0$). On the other hand, the dispersion relation shows that the product of perpendicular and parallel permittivity obtains greater than zero; the dispersive curve shows dielectric behavior ($\varepsilon_\perp \varepsilon_{||} > 0$). We plot the relative permittivity against normalized frequency that shows hyperbolic behavior for parallel and perpendicular permittivity in a particular range of the frequency.

The real and the imaginary part of parallel permittivity of hyperbolic material are plotted using Eq. (13) which are shown in Fig. 2 and analyzed. The real part of parallel permittivity against normalized frequency increases on increasing the value of filling fraction. The value of permittivity is negative at a certain range of frequency after that it is positive corresponding to the value of filling fraction. The real part of parallel permittivity is obtained the negative at a certain normalized frequency 0.30, 0.43, 0.55, 0.63, 0.71 corresponding to the value of filling fraction f= 0.1, f= 0.2, f= 0.3, f= 0.4, f= 0.5 respectively, as shown in Fig. 2(a). Similarly, the imaginary part of parallel permittivity has found the same behavior but it has purely negative value and is also shifted towards the higher frequency on increase the value of filling fraction comparison to real permittivity. The imaginary part of parallel permittivity is negative at a certain normalized frequency 0.51, 0.63, 0.72, 0.82, 0.88 for corresponding to the value of filling fraction f= 0.1, f= 0.2, f= 0.3, f= 0.4, f= 0.5 respectively, as shown in Fig. 2(b). The real and the imaginary part of perpendicular permittivity of hyperbolic material have plotted using Eq. (14), which is shown in Fig. 3 and analyzed. The real part of perpendicular permittivity decreases on increase the value of filling fraction, and finds the blue shift. The real part of perpendicular permittivity is negative at a certain normalized frequency range 0.26–1.00, 0.43–1.00, 0.48–1.00,

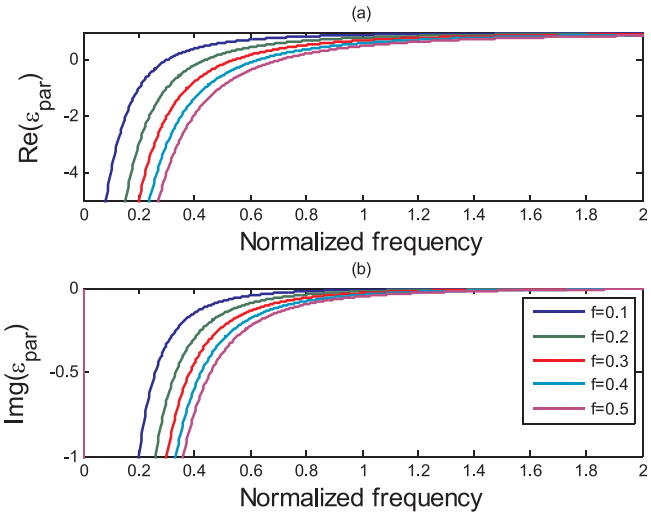

Fig. 2. (a) Real part of $\varepsilon_{||}$ for different value of filling fraction against normalized frequency, (b) Imaginary part of $\varepsilon_{||}$ for different value of filling fraction versus normalized frequency.

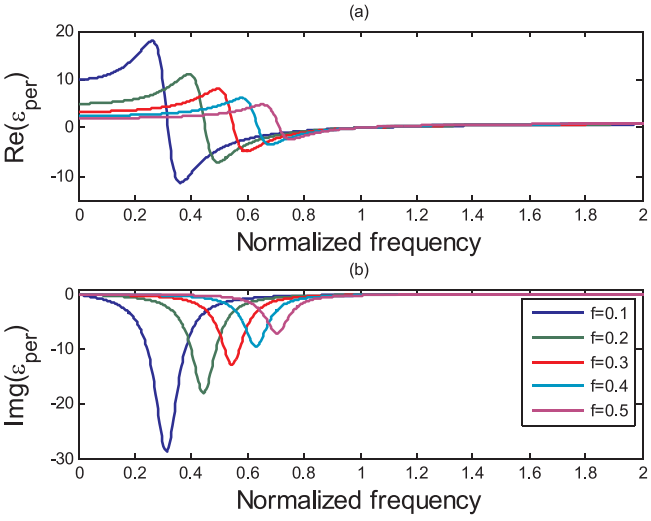

Fig. 3. (a) Real part of $\varepsilon_\perp$ for different value of filling fraction against normalized frequency, (b) Imaginary part of $\varepsilon_\perp$ for different value of filling fraction against normalized frequency.

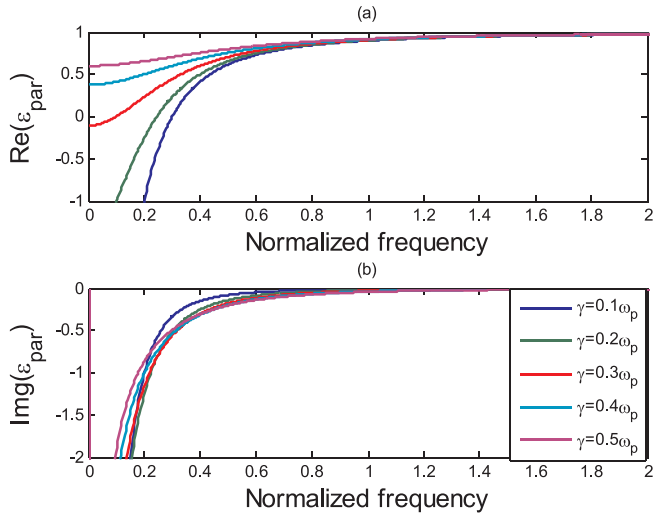

Fig. 4. Real part of $\varepsilon_{||}$ for different value of electron collision frequency, γ against normalized frequency, (b) Imaginary part of $\varepsilon_{||}$ for different value of electron collision frequency, γ against normalized frequency.

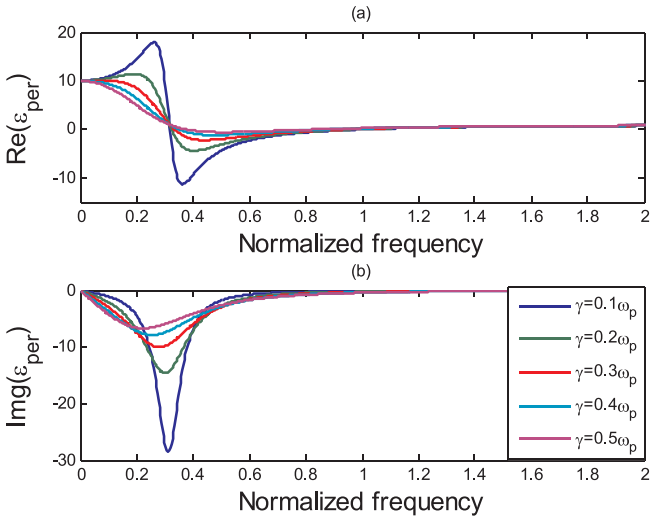

Fig. 5. Real part of $\varepsilon_{\perp}$ for different value of electron collision frequency, γ against normalized frequency, (b) Imaginary part of $\varepsilon_{\perp}$ for different value of electron collision frequency, γ against normalized frequency.

0.62–1.00, 0.66–1.00 for the value of filling fraction f= 0.1, f= 0.2, f= 0.3, f= 0.4, f= 0.5 respectively, as shown in Fig. 3(a). Moreover, the imaginary part of the perpendicular permittivity shifts towards higher frequency on increases the value of filling fraction. The imaginary part of perpendicular permittivity is negative at a certain normalized frequency range 0.00–1.00, 0.02–1.00, 0.04–1.00, 0.06–1.00, 0.07–1.00 for the value of filling fraction f= 0.1, f= 0.2, f= 0.3, f= 0.4, f= 0.5 respectively, as shown in Fig. 3(b).

Further, we have analyzed the real and the imaginary part of parallel permittivity against normalized frequency with the variation of electron collision frequency. The real part of parallel permittivity is decreased on increasing normalized frequency; it is also found the blue shift. The real part of parallel permittivity is negative at a certain normalized frequency 0.30, 0.24, 0.10 for corresponding to the value of electron collision frequency $\gamma = 0.1\omega_p$, $\gamma = 0.2\omega_p$, $\gamma = 0.3\omega_p$ as shown in Fig. 4(a). The imaginary part of parallel permittivity is decreased on increasing the value of electron collision frequency and is shown blue shift. The imaginary part of parallel permittivity is negative at a certain normalized frequency 0.75, 0.95, 1.05 for different electron collision frequency $\gamma = 0.1\omega_p$, $\gamma = 0.2\omega_p$, $\gamma = 0.3\omega_p$ respectively, as shown in Fig. 4(b).

In last calculation, the real and the imaginary part of perpendicular permittivity with variation of electron collision frequency are analyzed as shown in Fig. 5. The real part of perpendicular permittivity decreases on increase of electron collision frequency; it also behaves as a blue shift. The real part of perpendicular permittivity is negative at a certain normalized frequency 1.10, 0.99, 0.96, 0.91, 0.85 for the value of electron collision frequency $\gamma = 0.1\omega_p$, $\gamma = 0.2\omega_p$, $\gamma = 0.3\omega_p$, $\gamma = 0.4\omega_p$, $\gamma = 0.5\omega_p$, respectively, as shown in Fig. 5(a). The imaginary part of the permittivity increases on increasing the value of electron collision frequency which shows the red shift. The imaginary part of perpendicular permittivity is negative at a certain normalized frequency 0.99, 1.21, 1.35, 1.50, 1.60 for corresponding to the value of electron collision frequency $\gamma = 0.1\omega_p$, $\gamma = 0.2\omega_p$, $\gamma = 0.3\omega_p$, $\gamma = 0.4\omega_p$, $\gamma = 0.5\omega_p$, respectively, as shown in Fig. 5(b). These studies show that the perpendicular and the parallel permittivity of the considered material play the main role for the hyperbolic behavior because the permittivity affects the dispersion relation of the material.

Therefore, the absorption property of the ternary periodic structure containing HMMs against normalized frequency is studied for TM mode for corresponds to the parallel permittivity. The absorption property of the ternary periodic structure is calculated using simple transfer matrix method with variation of incident angle, filling fraction, electron collision frequency as well as the thicknesses of dielectric (A) material. The ternary periodic structure is the composite material of the three materials ABC, where A = air, B= SiO_2 and C = hyperbolic meta-material (HMM). The parameters for dielectric (A) and SiO_2 (B) materials are taken as $\varepsilon_{die} = 1$, $d_{die} = 2.8$mm, $\varepsilon_{SiO_2} = 2.2$, $d_{SiO_2} = 3$mm, $\mu_{die} = \mu_{SiO_2} = 1$, $\theta_0 = 0°$, and number of unit cell i.e. N = 10.

First of all, we have calculated the absorption of the ternary periodic structure against normalized frequency with varying the incident angles $\theta = 0°$, $\theta = 20°$, $\theta = 40°$, $\theta = 60°$, $\theta = 80°$ having electron collision frequency $\gamma = 0.1\omega_p$ and filling fraction f = 0.1 where normalized frequency is $\frac{\omega}{\omega_p}$. The wave incident on the multilayer structure is originated the band structure due to the fundamental property of the interfaces. So, we have obtained the increase absorption spectra against normalized frequency when the incident angle increases, and it is achieved the maximum absorption at 0.14 normalized frequencies due to effective behavior of relative permittivity. The absorption spectra continuously decrease above the 0.15 normalized frequencies due to the multi-reflection inside the interfaces. Above this frequency, the absorption band gaps are formed between 1.0 and 1.5 normalized frequency ranges. The study shows that the absorption of the considered structure has obtained the better absorption for $\theta = 80°$ as shown in Fig. 6.

Now we have focused our study on the absorption of the ternary periodic structure at the angle of incidence $\theta = 80°$ by varying the most valuable parameters: filling fraction, electron collision frequency and thickness of dielectric material. The filling fraction (f) is an important parameter which defines how much volume of the material occupied in the hyperbolic meta-material. So, we have analyzed the absorption of the ternary periodic structure against normalized frequency at $\theta = 80°$ with variation of filling fraction f= 0.1, f= 0.2, f= 0.3, f= 0.4, f= 0.5 with constant parameters: collision frequency $\gamma = 0.1\omega_p$ and thickness of the dielectric $d_{die} = 2.8$ mm, and silicon dioxide $d_{SiO_2} = 3$ mm, and hyperbolic meta-material $d_{HM} = d_{plasma} + d_{die(air)} = 2$ mm, respectively. The absorption spectra shifts from lower to higher frequency, and obtain the maximum absorption on increase the value of filling fraction. The 100% absorption is found at 0.19 normalized frequencies for f= 0.2 has metallic behavior, and also shows red shift. After that the absorption spectra for the normalized frequency continuously decrease for the different values of filling fraction. The absorption spectra again shift toward lower to the higher frequency as the filling fraction increases. The 90% absorption is found for f= 0.5 due to highly metallic behavior

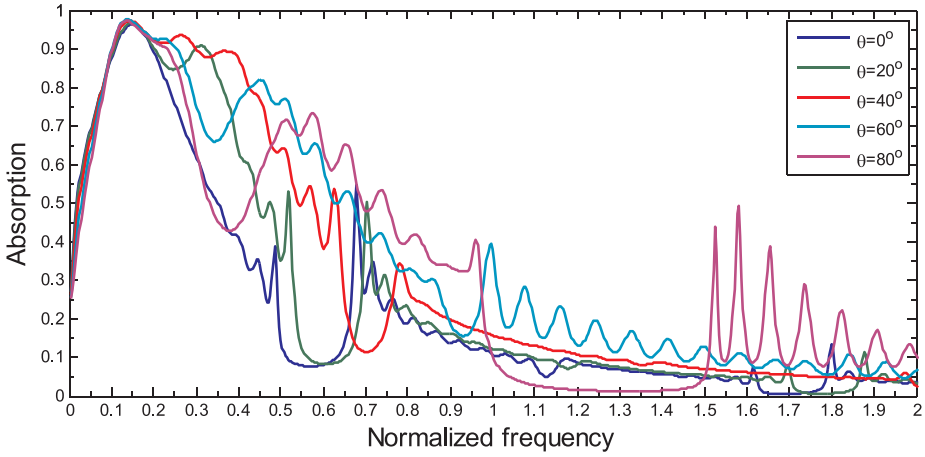

Fig. 6. Absorption of multilayer structure at different value of incident angle against normalized frequency.

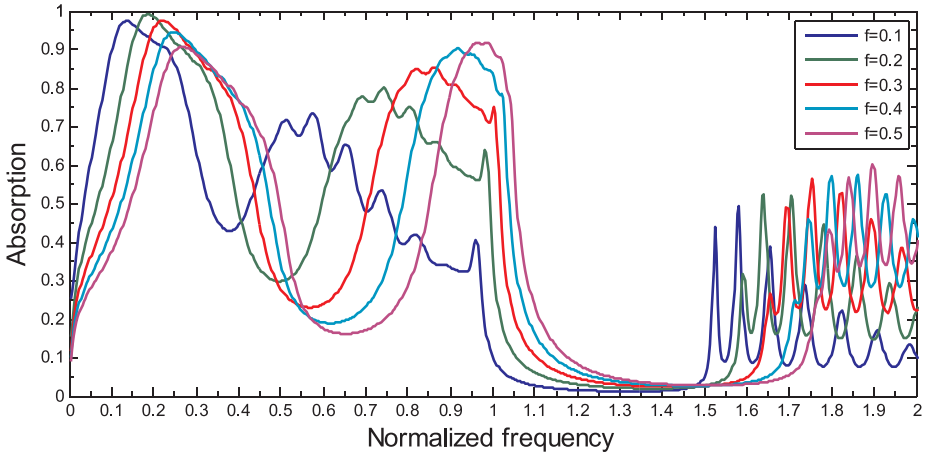

Fig. 7. Absorption of multilayer structure at different value of filling fraction against normalized frequency.

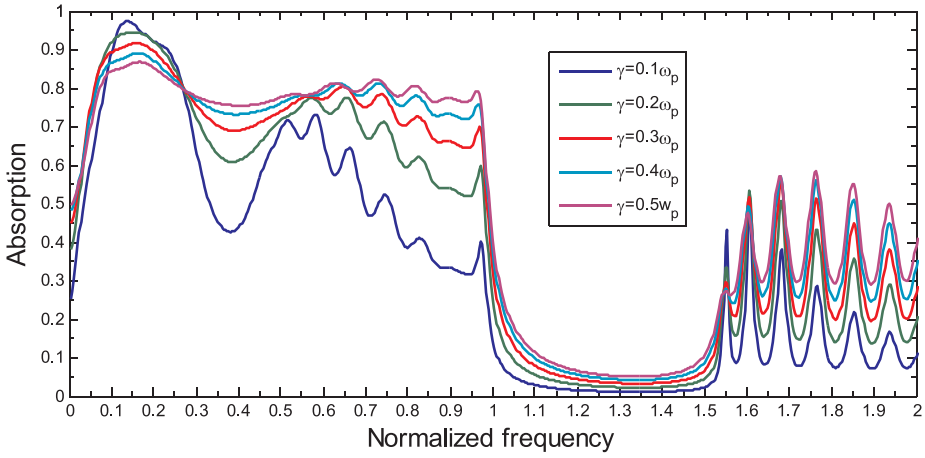

Fig. 8. Absorption of multilayer structure at a different value of collision frequency against normalized frequency.

and also obtained an absorption band in 1.00–1.50 range as shown in Fig. 7. The study shows that the absorption of the structure containing HMMs has very informative results for designing the absorption-based devices in microwave region.

Similarly, we have also studied the absorption of the structure by variation of the electron collision frequency $\gamma = 0.1\omega_p$, $\gamma = 0.2\omega_p$, $\gamma = 0.3\omega_p$, $\gamma = 0.4\omega_p$, $\gamma = 0.5\omega_p$, with f= 0.1 and $\theta = 80°$ having other parameters constant as in the above section. The absorption spectra against normalized frequency shift towards the higher normalized frequency for increase the value of electron collision frequency, but the 98% absorption found at 0.13 normalized frequencies for $\gamma = 0.1\omega_p$. The 80% absorption is achieved for $\gamma = 0.5\omega_p$ due to high absorption of the plasma that shows the metallic behavior of the HMMs. Further, the absorption spectra have found nearly zero absorption at 1.0–1.5 normalized frequency and formed an absorption band with large variation of band edges.

After this band range, the absorption is slightly increased as the value of electron collision frequency increases. The absolutely zero

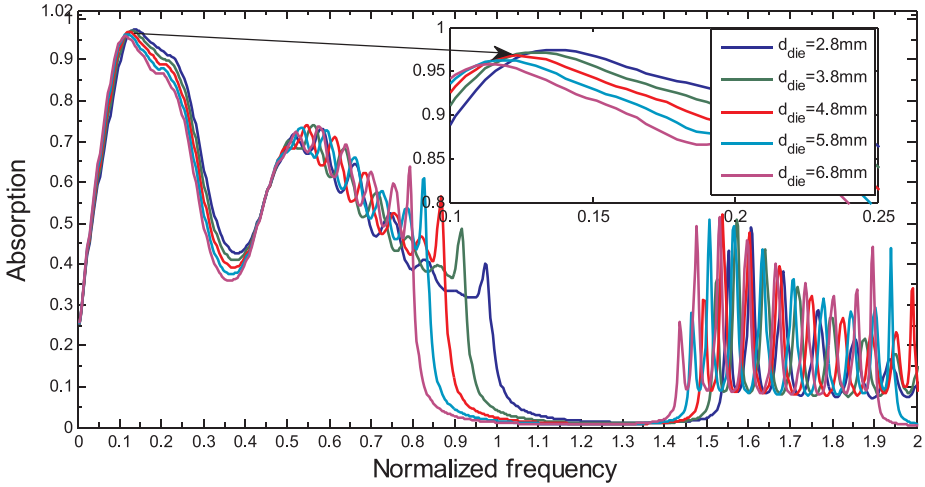

Fig. 9. Absorption of multilayer structure at different value of the thickness of the dielectric material against normalized frequency.

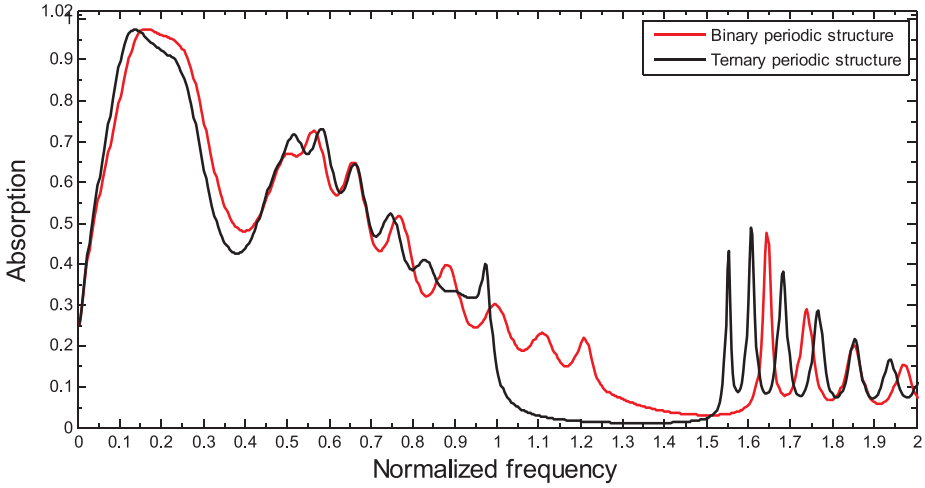

Fig. 10. Comparison of absorption of multilayer structure for binary structure $(BC)^N$ (red) and ternary structure $(ABC)^N$ (black). (For interpretation of the references to colour in this figure legend, the reader is referred to the web version of this article.)

absorption band gaps are formed for $\gamma = 0.1\omega_p$ having maximum absorption at 1.40, as shown in Fig. 8. We conclude that the absorption of the structure may be used to design the sensor as well as detector at low frequency range, and tunable absorber at band edges at high frequency range.

Again we have focused on another parameter that is thickness of A material. As we know that thickness of the dielectric (A) material of the periodic material affects the band gap structure. The absorption of the ternary periodic structure against normalized frequency is studied with variation of thickness of dielectric material $d_{die} = 2.8\,mm$ $d_{die} = 3.8\,mm$ $d_{die} = 4.8\,mm$ $d_{die} = 5.8\,mm$ $d_{die} = 6.8\,mm$ with fixed $\theta = 80°$, $\gamma = 0.1\omega_p$ and f= 0.1. The absorption spectra of ternary periodic structure against normalized frequency shift from higher to lower normalized frequency as thickness increases and acts as the blue shift. The 98% absorption is achieved at 0.13 normalized frequencies for lowest value of dielectric thickness, which is predicted from Fig. 9. The maximum absorption shifts from higher frequency to lower frequency on increase the thickness of dielectric material which clearly shown in the inset plot corresponding to the value of dielectric thickness $d_{die} = 2.8\,mm$ $d_{die} = 3.8\,mm$ $d_{die} = 4.8\,mm$ $d_{die} = 5.8\,mm$ $d_{die} = 6.8\,mm$. The absorption decreases continuously and become 40% for $d_{die} = 6.8mm$. The absorption spectra for above 0.4 normalized frequencies increases and it becomes 0.75%. The absorption spectra continuously decreases above 0.5 frequencies, and form a band gap in between the frequency range of 0.85–1.55, as shown in Fig. 9. Such absorption with variation of the thickness of dielectric may be applicable for absorption-based devices at microwave region.

In the last calculations, we have compared our calculated results of absorption of ternary periodic structure with binary periodic structure containing HMMs for $\theta = 80°$ $\gamma = 0.1\omega_p$ and f= 0.1, having other parameters are same as previous calculations, which is shown in Fig. 10. The binary structure is $(BC)^N$ where, B= SiO_2, C= HMM and the ternary structure is $(ABC)^N$ where A= Dielectric (air) B= SiO_2 and C= HMM. We have analyzed the absorption for both structures, and obtained the same absorption at low frequency range, and a band gap is obtained only for ternary periodic structure at higher frequency range. So our calculated results reveal that the absorption of ternary periodic structure is found to be better result than the absorption of binary periodic structure for low to high frequency ranges.

4. Conclusion

In this article, parallel and the perpendicular permittivity of hyperbolic meta-material were analyzed theoretically with the variation of filling fraction and effective collision frequency. The study shows that the real part of the parallel and the perpendicular permittivity of hyperbolic meta-material have the metallic and dielectric behaviors at certain frequency range. Using these concepts of the HHMs, the absorption of one-dimensional ternary periodic structure containing dielectric, silicon dioxide and hyperbolic material were studied with

varying incident angle, filling fraction, electron collision frequency as well as the thicknesses of dielectric (A) material. All absorption properties were calculated by using the well-known simple transfer matrix method. First, we calculated the absorption of the considered structure with varying the angles of incidence (θ). The calculated absorption has shown the maximum value at $\theta = 80°$. In this continuation, we were also studied the absorption of considered ternary periodic structure with varying the other parameters like filling fraction, electron collision frequencies and thicknesses of dielectric material while the incident angle is $\theta = 80°$. The study shows that the 100% tunable absorption was found due to the filling fraction of the hyperbolic meta-material and the metallic nature of effective permittivity of the hyperbolic material. The study of the absorption property of the ternary periodic structure containing hyperbolic materials are very innovative results to design the optical switch, logic gate, sensor as well as the absorber at microwave region. In addition to this, the study of optical property of the ternary periodic structure containing HMMs has investigated the highest absorption property for application of the microwave devices. In our best knowledge our group has performed such calculations first time, and carried out the interesting result of the absorption of one-dimensional ternary periodic structure with a composite of dielectric, silicon dioxide and hyperbolic material.

Acknowledgment

One of the authors, Asish Kumar, Research Scholar, Department of Physics, Babasaheb Bhimrao Ambedkar University (A Central University) Lucknow, acknowledges to UGC, New Delhi for UGC fellowship.

Appendix A. Supplementary data

Supplementary data to this article can be found online at https://doi.org/10.1016/j.jmmm.2019.165371.

References

[1] E. Yablonovitch, Inhibited spontaneous emission in solid-state physics and electronics, Phys. Rev. Lett. 58 (1987) 2059.
[2] S. John, Strong localization of photons in certain disordered dielectric super lattices, Phys. Rev. Lett. 58 (1987) 2486.
[3] J.D. Joannopolos, Johnson, R.D. Meade, J.N. Winn, Photonic Crystals: Molding the Flow of Light, Princeton Univ. Press, Princeton, NJ, USA, 2007.
[4] E. Centeno, B. Guizal, D. Felbacq, Multiplexing and demultiplexing with photonic crystals, J. Opt. A1 (5) (1999) L10.
[5] B. Temelkuran, M. Bayindir, E. Ozbay, R. Biswas, M.M. Sigalas, G.K. Tuttle, M. Ho, Photonic crystal based resonant antenna with a high directivity, J. Appl. Phys. 87 (2000) 603.
[6] A. Kumar, K.B. Thapa, Study of optical property of defect mode in one dimensional double negative photonic crystal with plasma, Adv. Sci. Eng. Med. 10 (2018) 1–5.
[7] A. Kumar, P.P. Singh, K.B. Thapa, A new idea for broadband reflector and tunable multi-channel filter of one dimensional symmetric photonic crystal with magnetized cold plasma defects, AIP Conf. Proc. 1953 (2018) 060043.
[8] A. Kumar, N. Kumar, K.B. Thapa, Tunable broadband reflector and tunable narrowband filter of a dielectric and magnetized cold plasma photonic crystal, Eur. Phys. J. Plus 133 (2018) 250.
[9] A. Kumar, K.B. Thapa, S.P. Ojha, A tunable broadband filter of ternary photonic crystal containing plasma and superconducting material, Indian J. Phys. (2018) 1–8, https://doi.org/10.1007/s12648-018-1335-9.
[10] A.M. Urbas, Z. Jacob, L.D. Negro, N. Engeta, A.D. Broadman, P. Egan, A.B. Khanikaev, V. Menon, M. Ferrera, N. Kinsey, C.D. Vault, J. Kim, V. Shalaev, A. Boltasseva, J. Valentine, C. Pefeiffer, A. Grbic, E. Narrimanov, L. Zhu, S. Fan, A. Alu, E. Poutrina, N.M. Litchnitsir, M.A. Noginov, K.F. Macdonald, E. Plum, X. Liu, P.F. Nealey, C.R. Kagan, C.B. Murray, D.A. Pawlak, I.I. Smolyaninov, V.N. Smolyaninov, D. Chanda, Roadmap on optical meta-materials, J. Opt. 18 (2016) 093005.
[11] D.R. Smith, D. Schuring, Electromagnetic wave propagation in media with indefinite permittivity and permeability tensors, Phy. Rev. Lett. 90 (2003) 077405.
[12] I.V. Iorsh, I.S. Mukhin, I.V. Shadrivov, P.A. Belov, Y.S. Kivshar, Hyperbolic metamaterials based on multilayer graphene structures, Phys. Rev. B 87 (2013) 075416.
[13] N. Engeta, R.W. Ziolkowski, A positive future for double-negative metamaterials, IEEE Trans. Microw. Theory Tech. 53 (2005) 1535–1556.
[14] K.V. Sreekanth, A. De Luca, G. Strangi, Negative refraction in graphene-based hyperbolic meta-materials, Appl. Phys. Lett. 103 (2013) 023107.
[15] Y. He, S. He, X. Yang, Optical field enhancement in nanoscale slot waveguides of hyperbolic metamaterials, Opt. Lett. 37 (2012) 2907–2909.
[16] T. Zhang, L. Chen, X. Li, Graphene-based tunable broadband hyperlens for far-field subdiffraction imaging at mid-infrared frequencies, Opt. Express 21 (2013) 20888–20899.
[17] C. Guclu, S. Campionee, F. Capolino, Hyperbolic metamaterial as super absorber for scattered fields generated at its surface, Phys. Rev. B 86 (2012) 205130.
[18] L. Ferrari et al., Hyperbolic material and their applications, Progress in quantum electronics, 2014.
[19] P. Shekhar, J. Atkinson, and Z. Jacob, Hyperbolic metamaterials: fundamentals and applications, 1:14 (2014).
[20] D. Korobekin, B. Neuner III, C. Fietz, N. Jegeneyes, G. Ferro, G. Shvets, Measurement of the negative refractive index of sub diffraction waves propagating in a indefinite permittivity medium, Opt. Exp. 18 (22) (2010) 22734.
[21] S. Molesky, C.J. Dewalt, Z. Jacob, High temperature epsilon near zero and epsilon near pole meta-material emitters for thermophotovaltaics, Opt. Exp. 21 (S1) (2013) A96.
[22] A. Alu, M.G. Silverinha, A. Salendrino, N. Engeta, Epsilon near zero metamaterials and electromagnetic sources: tailoring the radiation phase pattern, Phys. Rev. B 75 (15) (2007) 155410.
[23] M. Silverinha, N. Engeta, Tunneling of electromagnetic energy through sub-wavelength channels and bends using epsilon near zero metamaterials, Phys. Rev. Lett. 97 (15) (2007) 157403.
[24] M.A.K. Othman, C. Guclu, F. Capolino, Graphene-based tunable hyperbolic metamaterials and enhanced near-field absorption Opt, Express 21 (2014) 7614.
[25] R. Ning, S. Liu, H.F. Zhang, Z. Jiao, Dual-gated tunable absorption in graphene-based hyperbolic metamaterial, AIP Adv. 5 (2015) 067106.
[26] M.A. Baqir, P.K. Chaudhary, Hyperbolic meta-material based UV absorber, IEEE Photonics Technol. Lett. (c) (2017) 1041–1135.
[27] K.V. Sreekanth, M. Elkabbash, Y. Alapan, A.R. Rasheed, U.A. Gurkan, G. Strangi, A multiband perfect absorber based on hyperbolic meta-material, Sci. Rep. 6 (2016) 26272.
[28] M. Desouky, A.M. Mahmoud, M.A. Swillam, Silicon based mid-IR super absorber using hyperbolic metamaterial, Sci. Rep. 8 (2018) 2036.
[29] V. Caliguiri, A.D. Luca, Metal-semiconductor oxide extreme hyperbolic meta-material for selectable canalization of wavelength, J. Phys. D Appl. Phys. 49 (2016) 08LT01.
[30] V.B. Babicheva, Long range propagation of Plasmon and phonon polaritons in hyperbolic meta-material waveguides, J. Opt. 19 (2017) 124013.
[31] S. Axelrod, M.K. Dezfouli, H.M.K. Wong, A.S. Helmy, S. Hughes, Hyperbolic metamaterial nanoresonator make a poor single photons, Phys. Rev. B. 95 (2017) 155424.
[32] K. Rustomji, R. Abdeddaim, C.M. de Streke, B. Kuhulmey, S. Enouch, Measurement and simulation of the polarization dependent Purcell factor in a microwave fishnet meta-material, Phys. Rev. B 95 (2017) 035156.
[33] M. Wan, P. Gu, W. Liu, Z. Wang, Low threshold spaser based on deep sub-wavelength spherical hyperbolic meta-material cavities, Appl. Phys. Lett. 110 (2017) 031103.
[34] M. Desouky, A.M. Mahmoud, M.A. Swillam, Tunable mid-IR focusing in InAs based semiconductor based hyperbolic metamaterials, Sci. Rep. 7 (2017) 15312.
[35] F. Wu, G. Lu, C. Xue, H. Jiang, Z. Guo, M. Zheng, C. Chen, G. Du, H. Chen, Experimental demonstration of angle independent gaps in one dimensional photonic crystal containing layered hyperbolic meta-materials and dielectric at visible wavelengths, Appl. Phys. Lett. 112 (2018) 041902.
[36] C.T. Riley, Joseph S.T. Smalley, Jeffrey R.J. Brodie, Y. Fainman, D.J. Sirbulyand, Z. Liu, Proc. Natl. Acad. Sci. (PNAS) 7 (6) (2017) 114.
[37] T.S. Luk, I. Kim, S. Campione, S.W. Howell, G.S. Subramania, R.K. Grubbs, I. Brener, H.T. Chen, S. Fan, M.B. Sinclair, Near infrared surface Plasmon polariton dispersion control with hyperbolic metamaterials, Opt. Exp. 21 (9) (2013) 11107.
[38] P. Yeh, Optical Waves in Layered Media, John Wiley & Amp; Sons, New York, 1988.
[39] Z. Jiao, R. Ning, Y. Xu, J. Bao, Tunable angle absorption of hyperbolic metamaterials based on plasma photonic crystals, Phys. Plasma 23 (2016) 063301.
[40] H.G. Booker, Cold Plasma Waves, 23 Springer-Netherlands, New York, 1984.
[41] D.R. Smith, D. Schurig, "Electromagnetic wave propagation in media with indefinite permittivity and permeability tensors, Phys. Rev. Lett. 90 (2003) 077405.
[42] L. Novotny, B. Hecht, Principles of Nano-optics, Principles of Nano-Optics, Cambridge University Press, New York, 2012.
[43] S. Ishii, A.V. Kildishev, E. Narimanov, V.M. Saleav, V.P. Drachev, Subwavelength interference pattern from volume Plasmon polaritons in a hyperbolic medium, Laser Photonics Rev. 7 (2013) 265.
[44] C.L. Cortes, W. Newman, S. Molesky, Z. Jacob, Quantum nanophotonics using hyperbolic meta-materials, J. Optics 14 (2012) 063001.
[45] W. Zhu, F. Xiao, M. Kang, D. Sikdar, M. Premratne, Tunable terahertz left hand metamaterials based on multilayer graphene dielectric composite, Appl. Phys. Lett. 104 (2014) 051902.
[46] C. Guclu, S. Campinone, F. Capolino, Hyperbolic meta-material as super absorber for scattered fields generated at its surface, Phys. Rev. B 86 (2012) 205130.
[47] E.E. Narimanov, Photonic hypercrystals, Phys. Rev. X 4 (2014) 041014.
[48] Y. Xiang, X. Dai, J. Guo, H. Jhang, S. Wen, D. Tang, Critical coupling with graphene based hyperbolic meta-material, Sci. Rep. 4 (2014) 5483.
[49] O. Kidwai, S.V. Zhukovosky, J.E. Sipe, Effective medium approach to planer multilayer hyperbolic meta-materials: strengths and limitations, Phys. Rev. A 85 (2012) 053842.

Advances in Photonic Crystals and Devices

Edited by
Narendra Kumar
Bhuvneshwer Suthar

CRC Press
Taylor & Francis Group
Boca Raton London New York

CRC Press is an imprint of the
Taylor & Francis Group, an **informa** business

9

Tunable Broadband Reflector Using a One-Dimensional Photonic Crystal Containing Metamaterial with Symmetrically Introduced Magnetized Cold Plasma Defect

Asish Kumar, Khem B. Thapa, Narendra Kumar, and Anil K. Yadav

CONTENTS

9.1 Introduction

Photonic crystals (PCs) are artificial periodic nanostructures and microstructures containing dielectric, metallic, superconductor, and plasma materials, where the refractive index changes periodically in space. In 1987, PCs were experimentally introduced by Yablonovitch and theoretically proposed by John in the same year (John 1987; Yablonovitch 1987). Such kind of periodic structures affects the propagation of electromagnetic (EM) wave and produces bandgaps due to the periodicity of the materials. It is similar to the motion of an electron in the semiconductor material, which produces electronic bandgaps due to the periodic potentials. The wave propagation inside the periodic structure depends upon frequency of incident EM wave. Frequencies that are allowed to propagate are known as modes, and groups of allowed frequency modes constitute bands. In contrast, forbidden frequency ranges are called photonic bandgaps (PBGs), which are also known as Bragg's gaps because they are originated from the Bragg scattering in the periodic structures (Fink et al. 1998; Chigrin et al. 1999; Wu et al. 2003; Aghajamali et al. 2016).

In 1968, Veselago et al. theoretically predicted that electric permittivity and magnetic permeability of the materials are the fundamental characteristics, and they determine the propagation of EM waves in the matter (Veselago et al. 1968). The materials are called metamaterials or negative index materials (NIMs) or double-negative (DNG) materials, which have simultaneously negative values of the electric permittivity and the magnetic permeability. However, if both the electric permittivity and the magnetic permeability of the material are positive, then it is known as double-positive (DPS) material. According to

A New Idea for Broad Band Reflector and Tunable Multichannel Filter of One Dimensional Symmetric Photonic Crystal with Magnetized Cold Plasma Defects

Asish Kumar[1], Prabal P. Singh[2] and Khem B. Thapa[1*]

[1]*Department of Applied Physics, School for Physical Sciences*
Babasaheb Bhimrao Ambedkar University, Vidya Vihar, Raebareli Road, Lucknow
[2]*Department of Physics, University Institute of Engineering & Technology*
Chhatrapati SahuJi Maharaj University, Kalyanpur, Kanpur

[1*)] Corresponding author: khem.bhu@gmail.com
[1)] Another author: kumar2013asish@gmail.com
[2)] Another author: pratapprabal82@yahoo.com

ABSTRACT. The optical properties of one-dimensional periodic structure composed by SiO_2 and dielectric (air) layers with asymmetric and symmetric forms studied. The transmittance for symmetric periodic defective structure analyzed by introducing one, two, three layers of magnetized cold plasma (MCP) in one-dimensional periodic structure. We found better result for symmetric defect of three layer of the MCP compare to the other defective structures. On the basis of our calculated results, we proposed a new idea for broadband reflector at lower frequency range as well as the multichannel filter at higher frequency range.

INTRODUCTION

The precursor works of Yablonovitch and John in 1987 flush a new idea in the field of photonic crystals (PCs) [1, 2]. The study of photonic crystals has become popular and continues to be more excited for the optical community till today. The essential physics of photonic crystals has unique property due to a band gap and such structures are called as photonic band structure (PBS). The PBS is analogous to the electronic band structure (EBS) in solids. Photonic crystals have received emerging attention in the field of solid state and optical physics due to exhibition of many unique features [2, 3]. The photonic band gap (PBG) prohibits the propagation of an electromagnetic wave of certain frequency through it or the periodic structures. Different periodic materials have been admitted to study and design tunable PBG materials. The propagation of electromagnetic waves (EMW) inside the photonic crystal depends on the several parameters like refractive index, contrast, incident wave, refractive index of material etc. The allowed frequency inside the photonic crystal is known as mode and group of all allowed frequency modes are formed allowed bands. On the other hand, the frequency modes are not allowed is called as Photonic Band Gaps (PBGs) [4, 5]. In recent years, plasma PCs has attracted considerable attention due to their tunable characteristics, which is a periodic arrangement of alternating thin plasma and dielectric material like vacuum. Plasma photonic band gap (PPBG) is obtained due to the periodicity of thin plasma and dielectric materials. Plasma photonic band gap is tuned by the various parameter of plasma like plasma density; effective collision frequency and thickness of plasma layer [6-8]. Recently magnetized cold plasma has attracted having external magnetic field as an extra parameter is called gyro-effective frequency. The gyro-effective frequency depends upon applied magnetic fields of the magnetized cold plasma. The right hand polarization (RHP) and left-hand polarization (LHP) MCP has negative and positive value of the gyro-effective frequency respectively. The behavior of refractive index of magnetized cold plasma (MCP) shows unusual due to the tunable parameters: external magnetic field, electron density and effective collision frequency. So, all metal or dielectric material of the photonic crystal may be replaced by plasma for better controlled optical properties

2nd International Conference on Condensed Matter and Applied Physics (ICC 2017)
AIP Conf. Proc. 1953, 060043-1–060043-4; https://doi.org/10.1063/1.5032774
Published by AIP Publishing. 978-0-7354-1648-2/$30.00

IOP Publishing Journal of Physics: Condensed Matter
J. Phys.: Condens. Matter **32** (2020) 325701 (13pp) https://doi.org/10.1088/1361-648X/ab858f

Metamaterial-plasma based hyperbolic material for sensor, detector and switching application at microwave region

Asish Kumar[1], Narendra Kumar[2], Girijesh N Pandey[3], Devendra Singh[1] and Khem B Thapa[1,4]

[1] Department of Physics, School of Physical and Decision Sciences, Babasaheb Bhimrao Ambedkar University (A Central University), Lucknow226025, India
[2] Department of Physics, SLAS, Mody University of Science and Technology, Lakshmangarh 332311, Sikar, India
[3] Department of Applied Physics, Amity Institute of Applied Sciences, Amity University, Noida 201303, India

E-mail: khem.bhu@gmail.com and kbthapa@bbau.ac.in

Received 2 January 2020, revised 15 March 2020
Accepted for publication 1 April 2020
Published 15 May 2020

Abstract

Superconductor-plasma based hyperbolic material (SPHM) and meta-material-plasma based hyperbolic materials (MPHM) are the plasma based composite hyperbolic materials. Using the effective medium theory, the permittivity of SPHM and MPHM has been investigated. Perpendicular and parallel permittivities, real and imaginary part, versus normalized frequency have been analyzed with variation of filling fraction of composite hyperbolic material. The optical properties of one-dimensional ternary periodic structure (1DTPS) containing Si, SiO_2 and SPHM or MPHM have been studied using the well-known simple transfer matrix method and Bloch's function. The absorption spectra of 1DTPS containing plasma based hyperbolic material have been analyzed with the variation of incident angle, electron collision frequency of plasma and filling fraction of the composite materials. By studying absorption property of 1DTPS, the absorption spectra of MPHM were found to yield better results compared to the absorption spectra of SPHM. The calculations reveal that meta-material-plasma based hyperbolic material may be used to design the sensor, detector and switching applications at microwave region.

Keywords: plasma based hyperbolic material, SPHM, MPHM, ternary periodic structure and microwave devices

(Some figures may appear in colour only in the online journal)

1. Introduction

The fundamental phenomenon of optics is wave interference that is concerned with electromagnetic (EM) wave propagation in the material. The propagating phase of the EM wave plays an important role for wave interferences in periodic structure. By analysis of phase at the interface of materials, the wave interference property of two dielectric mediums is determined. Photonic crystals (PCs) are artificially designed periodic nanostructures of dielectric, metal, plasma, graphene etc. The PCs are made of two or more than two media with periodic variation of optical constants in space. In 1987 first time, the existence of photonic band gap (PBG) in periodic nano-structure was theoretically suggested by John [1] and was experimentally proposed by Yablonovitch [2]. These PCs prohibit the certain frequency ranges of propagating EM wave, which are commonly referred as photonic band gap (PBG) materials [3–5]. The PBGs find the fascinating applications in absorbers [6], waveguides [7], optical fibers [8], lasers [9], cavities [10], and many others applications [11–16]. The periodic

[4] Author to whom any correspondence should be addressed.

Tunable optical properties of hyperbolic meta-material

Asish Kumar[1], Khem B. Thapa[1]* and Girijesh N. Pandey[2]

[1]Department of Physics, School of Physical and Decision Sciences, *BabasahebBhimraoAmbedkar University, Lucknow-226025 (U.P.), India*

[2]Department of Applied Physics, Amity Institute of Applied Sciences, *Amity University, Sector- 125, Express Highway, Noida (U.P.) India.*

*Email: khem.bhu@gmail.com

Abstract: In this communication, the reflection, transmission and absorption spectra of one-dimensional multilayer periodic structure with alternating traditional dielectric, silicon dioxide (SiO_2) and hyperbolic meta-materials (HMMs) are analyzed using well-knowntransfer matrix method (TMM). The HMM is considered thecompositematerialsofplasma and dielectric.The reflection, transmission and absorption spectrum of the considered structure at the normal incidentareinvestigated by varying effective collision frequency of the plasma. Such periodic structure may be used to design the optical devices.The calculated result reveals that the absorption spectrum at a lower frequency is found a large gapdue tohavelarge effective collision frequencyof the plasma.

INTRODUCTION

Hyperbolic meta-material (HMM) is a composite material having filling fraction (f). These are an anisotropic mediumexhibits a hyperbolic shape of the dispersion relation at the terahertz (THz), optical and near-infrared frequency regions. HMMs have a lot of potential applications in the field of optics including negative refractions,opticalwaveguides and imaging hyper lens [1-5]. The absorption of HMMs has been studied in the last several yearsdue to their abnormal behavior. For example,a novel implementation of HMMs at the far-infrared frequency is composed of the stacked graphenesheets separated by a thin dielectric layer, and has a superabsorber for near fields. The HMMs have also used to enhance the decay rate of emitters near its surface for designing the efficient and innovative absorbers [6-8].The dual-gated tunable absorption in graphene-based hyperbolic meta-material and hyperbolic meta-material based UV absorber have analyzed for optical applications by several groups[9, 10].Further, other groups have also investigated themultiband perfect absorber based on hyperbolic meta-materials and silicon-based mid-IR super absorber [11, 12].

Theory: The characteristics matrix for a stacked layer of the photonic crystalis formulated using transfer matrix method (TMM)[13]. The HMM is an anisotropic medium with uni-axial dielectric tensor components [14].The reflection, transmission and absorption properties of the periodic structure with HMMs are calculated by: $M(d) = (M_A M_B M_C)^6 = \begin{pmatrix} M_{11} & M_{12} \\ M_{21} & M_{22} \end{pmatrix}$, where the d= thickness of the unit cell. The reflection and transmission coefficients are:

$t = \dfrac{2p_0}{(M_{11} + M_{12}/p_0 + M_{21}p_0 + M_{22})}$ and $r = \dfrac{(M_{11} + M_{12}/p_0 - M_{21}p_0 - M_{22})}{(M_{11} + M_{12}/p_0 + M_{21}p_0 + M_{22})}$. The absorption spectrum is given as

$A = 1 - R - T$, where $T = \left(\dfrac{p_s}{p_0}\right)|t|^2$ and $R = |r|^2$. The characteristic matrix for a stackedsingle layer is given by;

Advances in Basic Science (ICABS 2019)
AIP Conf. Proc. 2142, 050002-1–050002-3; https://doi.org/10.1063/1.5122368
Published by AIP Publishing. 978-0-7354-1885-1/$30.00

Broadband Reflector of 1D Photonic Crystal Containing TiO_2/SiO_2 Material at Visible Region

Asish Kumar[1], Pawan Singh[1], Krishan Pal[1], Narendra Kumar[2] and Khem B. Thapa[1*]

[1]*Department of Physics, School of Physical and Decision Sciences, Babasaheb Bhimrao Ambedkar University, Lucknow 226025, India*
[2]*Department of Physics, School of Sciences, Mody University of Science and Technology, Lakshmangarh 332311, Sikar, India*

[*]Email: khem.bhu@gmail.com

Abstract. Using the transfer matrix method (TMM) and Bloch function, the optical property of 1D photonic crystal of titanium dioxide (TiO2) and silicon dioxide (SiO2) material was theoretically analyzed. The dispersion curve versus wavelength (nm) study shows that lower band edge varies with increase in angle of incidence, and the structure offers a huge bandwidth. On comparing the dispersion curves and the reflection spectra for the considered structure, they are found to be in the same wavelength band. From the study of the reflection spectra with increase in incident angle, we find a blue shift at visible range with a huge bandwidth, and hence the structure may be used as a broadband reflector. Due to advanced development in the thin film technology, the obtained results may be useful to design the photonic devices of titanium dioxide (TiO2) and silicon dioxide (SiO2) material at visible region of electromagnetic spectrum.

Keywords: Photonic crystal, TiO_2 and SiO_2 material, broadband reflector, photonic devices, thin film technology

INTRODUCTION

The periodic structure of nanostructures and microstructure of two or more than two optical constant medium in the space has the interference of the wave at each surface is called Photonic Crystal (PC). Such PC has one of the unique properties called photonic band gap (PBG) and PBG can use to control the electromagnetic wave (photons) propagation in the materials. The origin of PBGs was first time experimentally and theoretically analyzed by Yablonovitch and John in the year 1987 [1, 2]. The PBG material has the great application in research and technology because PBG control and manipulate the flow of electromagnetic wave through the medium. The PBG of the periodic structure depends on refractive index, unit cell, filling fraction of the material, frequency and dimensionality etc. [3]. One-dimensional photonic crystal (1D-PC) is most popular in the thin film technology due to ease fabrication and have a lots of applications in optical engineering, photonic device, optical filter; resonance cavity, laser application, high-reflecting omnidirectional mirror, and optoelectronic circuit etc. [4–8]. The periodic structure of the different refractive index materials affects the photon propagation due to different PBG, and such PBG plays a crucial role in optical applications [9-12].

THEORETICAL METHODOLOGY

The dispersion curve and the reflection spectra are theoretically calculated by well known TMM and Bloch's function [13]. In this paper we have considered one-dimensional periodic crystal which is composed with titanium dioxide (TiO_2) and silicon dioxide (SiO_2) material. The photonic crystal containing TiO_2 and SiO_2 is in the periodic

3rd International Conference on Condensed Matter and Applied Physics (ICC-2019)
AIP Conf. Proc. 2220, 020068-1–020068-4; https://doi.org/10.1063/5.0002138
Published by AIP Publishing. 978-0-7354-1976-6/$30.00

Article

Advanced Science, Engineering and Medicine
Vol. 10, 1–5, 2018
www.aspbs.com/asem

Study of Optical Property of Defect Mode in One-Dimensional Double Negative Photonic Crystal with Plasma

Asish Kumar and Khem B. Thapa*

Department of Applied Physics, School for Physical Sciences, Babasaheb Bhimrao Ambedkar University, Vidya Vihar, Lucknow

The optical property of one-dimensional meta-photonic crystal with defect magnetized cold plasma has studied theoretically. The meta-photonic crystal is the periodic structure of double negative (DNG) and double positive (DPS) materials. A double negative material has unusual behavior due to negative refractive index of the material. The defect structure of the meta-photonic crystal is considered by sandwiched a plasma material in a symmetry/asymmetry way of the DNG-DPS periodic structure where plasma is the function of magnetic field as well as electron density. The optical properties of the meta-photonic crystal with defect plasma material is changed when the parameters of the plasma is changed. The transmission of the defect plasma meta-photonic crystal is obtained very high when the effective value of an external magnetic field is $B = 0.8$ T. The calculated results of the defect plasma meta-photonic crystal show a tunable narrow band filter at the microwave frequency region.

Keywords: Photonic Crystals, Meta-Material, Tunable Narrow Band Filter.

1. INTRODUCTION

Photonic crystals (PCs) are artificial or metallic dielectric periodic structures in which the refractive index of material varies periodically in one, two and three-dimensional spaces. In 1987 Yablonovitch experimentally introduced the PCs and John explained theory of the PCs in the same year.[1, 2] Such PCs affect the propagation of electromagnetic wave (photon) that is analogous to the periodic potential of the semiconductor material that affects electron motion, which is significantly produced the allowed and forbidden energy bands. The propagation of photons in periodic crystal structures is depending on the frequency. The allowed frequency range of the photons travel in the periodic structures of the dielectric materials are known as modes, and groups of all allowed modes form bands. The frequency range where photon doesn't allow through the periodic structures is known as Photonic Band Gaps (PBGs). This type of photonic band gap is also called Bragg gaps because they are formed due to Bragg scattering.[3–5] In 1968, Veselago predicted theoretically that the electric permittivity and magnetic permeability of the material is a fundamental property that tells about the unusual behavior of the electromagnetic wave propagation in matter due to double negative material (DNG). Double negative (DNG) materials are those materials in which the electric permittivity and magnetic permeability simultaneously negative. The periodic structures of the meta-material and dielectric materials are called meta-photonic crystals (Meta-PCs). The most important property of DNG material is that it has negative value of refractive index. DNG materials have two types one type is left handed and other type is right handed materials. Left Handed Material (LHM), in which the permittivity and the permeability are simultaneously less than zero. Right handed material (RHM) is a material in which the permittivity and the permeability are simultaneously greater than zero. Kramers-Kronig relation explain that meta-material not only dispersive as well as lossy materials.[6–8] The electric permittivity and magnetic permeability of meta-material have a complex value, due to complex

*Author to whom correspondence should be addressed.

Analysis of the Impact of Graphene Coating on Reflectivity of a Silicon Substrate for Optoelectronic Devices

Narendra Kumar[1, a)], Anisha Kumari Poonia[1], Asish Kumar[2], Khem B. Thapa[2], Girijesh N. Pandey[3], and Bhuvneshwer Suthar[4]

[1]*Department of Physics, Mody University of Science and Technology, Lakshmangarh 332311, India*
[2]*Department of Physics, Babasaheb Bhimrao Ambedkar University, Lucknow 226025, India*
[3]*Department of Applied Physics, Amity University, Noida 201303, India*
[4]*Department of Physics, MLB Govt. College, Nokha 334803, Bikaner, India*

[a)]Corresponding author: nkumar.mu.in@gmail.com

Abstract. In this work, we analyze the effect of graphene coating on reflectivity of a silicon substrate. First, the reflectance of a thin layer of silicon, a thin film without graphene coating, is computed. Thereafter, by applying the transfer matrix method, the reflectance of silicon substrate with a monolayer graphene coating is determined. We compare the reflectance plots of the Si substrate in different cases of graphene coatings and some important insights are drawn. Comparing the reflectance spectra plotted in different cases, we infer that graphene coating effectively reduces the reflectance of silicon substrate, which is in a good agreement with the results obtained experimentally by some of the investigators. Such an antireflection coating of graphene, for the specified parameters in the analysis, can be used in efficiency enhancement of solar cells and photodiodes, and may also introduce innovative applications in design of other silicon-based optoelectronic devices.

Keywords: graphene, thin film, silicon substrate, anti-reflection coating, solar cell

INTRODUCTION

It is now well-known that graphene was being produced and existed in small quantities in pencils from the earlier centuries, and there have been similar applications of graphite too. Sporadic attempts to study graphene were begun in 1859, while such a wonder material received a considerable attention since 2004 when a single atomic carbon layer was first measurably produced and isolated by Andre Geim and Kostya Novoselov. Further, researchers around the globe have theorized about graphene in the recent decades [1-3]. Graphene is an allotropic form of carbon having a two-dimensional hexagonal lattice at atomic-scale dimension with a honeycomb crystal structure in which there exist two carbon atoms in each unit cell and one atom forms each vertex [2]. Graphene is the basic structural element of other allotropes of carbon, namely graphite, charcoal, fullerenes, and carbon nanotubes (CNTs). Nowadays, explosive investigations are being made on the basis of existing theoretical descriptions regarding its composition, structure and properties. Graphene has fascinating electronic, mechanical and optical properties, and is found to be highly sensitive to photons and electrons. The theoretical and experimental evidences prove that graphene is stronger, more flexible and highly conducting in nature, and can show a wide range of applications in optoelectronic devices as well as in nanoelectronics [4-5].

To study the optical properties of a graphene sheet, we choose a 0.4-1.6 nanometer thick graphene coated on silicon (Si) substrate having thickness in micro range. In this work, we calculate the refractive index of graphene using its optical conductivity, whereas the refractive index of Si is taken 3.5. First, the reflection from silicon substrate, considering it as thin film without graphene coating, is determined. Further, we apply the transfer matrix method (TMM) to plot the reflection spectra of graphene coated silicon substrate with varying the thickness of the graphene

3rd International Conference on Condensed Matter and Applied Physics (ICC-2019)
AIP Conf. Proc. 2220, 020038-1–020038-6; https://doi.org/10.1063/5.0001390
Published by AIP Publishing. 978-0-7354-1976-6/$30.00